Electrophysiological Investigation of Some Mechanisms Underlying Muscarinic Agonist-Induced Epileptiform Activity Observed in Immature Rat Olfactory Cortical Brain Slices, *In Vitro.*

A thesis submitted in part fulfilment of the University of London for the award of Doctor of Philosophy in Medicine (Pharmacology)

by

Ben Whalley B. Pharm. (Hons.), M. R. Pharm. S.

Department of Pharmacology

The School of Pharmacy

29-39 Brunswick Square

London

WC1N 1AX

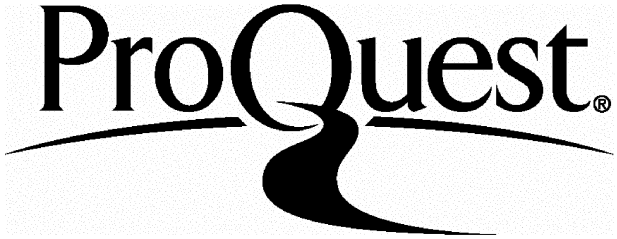

There are no innocent bystanders.

W. S. Burroughs

Dedication

To my daughters, Georgia Helice and Amber Renée and in memory of my grandfather, Dr. H. K. Whalley.

Acknowledgements

I would like to thank my supervisor, Dr. Andrew Constanti for his unfailing support, advice and help during the last three years. Without his decision to take me on as a student and his irrepressible desire to impart knowledge, I know I would undoubtedly be poorer in many more ways than I can imagine.

My eternal thanks, as always, go to my partner, Sam and my children, Louis, Georgia and Renée without whose support I would never have reached the end of this piece of work.

My thanks also to Dr. E. M. Williamson, without whose efforts on my behalf, I would never have had the opportunity to begin a PhD let alone finish one.

I would also like to thank the members of the Department of Pharmacology for all of the suggestions, insights and advice that seemed to come at the most uncannily opportune moments. Special thanks go to Dr. M. Postlethwaite and Dr. J. Boorman for tea, talk and, of course, indispensable scientific advice.

Finally, my thanks go to my family and friends; you all know who you are and although you probably know that I couldn't have finished this piece of work without your support, you may not know how grateful I am for it. My thanks, always.

Abstract

The properties and mechanisms underlying the muscarinic acetylcholine receptor (mAChR) agonist-induced epileptiform bursting phenomenon seen in immature rat piriform cortex slices *in vitro* were investigated using 'sharp' intracellular recording. In accordance with a previous report, mAChR agonist-induced epileptiform activity occurred regularly in immature slices, but never in adult preparations; moreover, the magnitude of paroxysmal depolarising shifts, burst duration and incidence of bursts induced in the presence of the muscarinic agonist oxotremorine-M (OXO-M; 10 μM) were found to be inversely related to animal age. Burst incidence was also higher at the anterior and posterior (compared with median) regions of the immature piriform cortex. A range of anti-epileptic drugs were screened for their ability to abolish the OXO-M-induced bursting behaviour. Based on their postsynaptic effect, the descending order of potency was: topiramate >carbamazepine >felbamate =gabapentin >lamotrigine >phenobarbitone; the order based on their ability to reduce afferent synaptic transmission was: felbamate >lamotrigine >topiramate >gabapentin >phenobarbitone. The ability of the acetylcholinesterase inhibitor neostigmine to mimic the effects of OXO-M in immature slices was also assessed; although epileptiform bursting was not induced, several changes in neuronal and synaptic excitability were observed (blocked by atropine) that suggest a possible role for the endogenous cholinergic system in epileptogenesis in this brain area. A significant presynaptic endogenous 'cholinergic tone' within the slices was also confirmed using paired-pulse synaptic analysis.

The presynaptic effects of OXO-M on excitatory synaptic potentials (EPSPs) evoked from adult and immature slices by afferent (lateral olfactory tract: LOT) or intrinsic fibre stimulation were also examined and the results confirmed with paired-pulse analysis. Significant differences between the responsiveness of adult and immature preparations, pertinent to epileptogenesis, were found: *e.g.* in immature slices, LOT afferent-evoked EPSPs in OXO-M showed a prolonged depolarizing phase, *all or nothing* behaviour and superimposed spike firing ($GABA_BR$-mediated inhibition was also reduced), while intrinsic fibre-evoked excitatory synaptic transmission showed only *inhibition*; this inhibition was mediated by M1-type mAChRs in the adult, but M2-type mAChRs in immature slices. Synaptic responses showing epileptiform characteristics were also found to occur more frequently in the anterior and posterior

regions of the piriform cortex; the median region thus appears to act as a buffer to overexcitability.

Possible differences in $GABA_AR$-mediated inhibitory postsynaptic potentials (IPSPs) and their sensitivity to OXO-M in adult and immature slices that could contribute to muscarinic epileptiform activity were also examined. Thus, isolated IPSPs evoked in immature preparations were smaller than those evoked in adults, and mAChR-mediated IPSP suppression was also greater in immature slices; additionally, adult and immature IPSPs evoked in the anterior and posterior regions of the slice were smaller than those evoked in the median region. As with EPSPs, presynaptic muscarinic inhibition was mediated by M2 mAChRs in immature slices, but M1 mAChRs in adults; results were confirmed using paired-pulse analysis. The effect of rostro-caudal lesions between piriform cortical layers I and II (apical) or layer III and the endopiriform nucleus (basal) were examined in adult and immature slices. Neither lesion had any effect upon evoked EPSPs, depolarizing effects of OXO-M or epileptiform bursting. However, the slow post-stimulus afterdepolarization (sADP), normally induced in OXO-M, was absent in adult but not immature lesioned slices. Interestingly, the gap junction blockers carbenoxolone and octanol disrupted muscarinic epileptiform activity and also diminished the evoked sADP in immature slices.

In conclusion, the present work has demonstrated that a number of critical physiological, pharmacological and regional differences exist between the excitatory and inhibitory synaptic systems, presynaptic muscarinic sensitivity and gap junction connectivity of adult and immature piriform cortex, which contribute towards the increased susceptibility of this brain area to epileptiform events in the immature animal.

Table Of Contents

Chapter 1:
Introduction

1.1 Foreword

Approximately 1% of the world's population (~50 million people) are affected by epilepsy (Laidlaw *et al.*, 1988), a serious neurological disorder that typically manifests as spontaneous convulsions ('fits') and/or a loss of consciousness. These symptoms are caused by the appearance of abnormal electrical seizure discharges, characterized by episodic high frequency firing of impulses by a group of neurones within the brain as a result of an imbalance between excitatory and inhibitory synaptic processes; such seizures typically begin (and may stay) in a specific area and/or spread to other regions of the brain, including passage from one hemisphere to another (Ebert *et al.*, 1995); (Applegate & Samoriski, 1993). The specific cellular, molecular and genetic mechanisms underlying the many different forms that comprise this disorder are still relatively poorly understood, although over the years, a large number of animal models of epilepsy have been developed in an attempt to reproduce the seizure discharges seen in clinical cases and as a means of developing more effective antiepileptic agents (Fisher, 1989).

A previous report from our laboratory described an *in vitro* model of epileptiform activity, recorded intracellularly from deep pyramidal neurones, seen following muscarinic acetylcholine receptor (mAChR) activation by the mAChR agonist, oxotremorine-M (OXO-M) in immature, but not adult, transverse piriform cortical brain slices (Postlethwaite *et al.*, 1998a). Although some of the basic characteristics of this muscarinic bursting phenomenon have previously been reported (Libri *et al.*, 1998; Postlethwaite *et al.*, 1998a), the developmental differences underlying its occurrence, its usefulness as a model of epileptiform behaviour, its comparability with other models of epileptiform activity (in this brain area and others) and any implications it may have upon our understanding of the structure, function and development of the piriform cortex have yet to be investigated. Consequently, the principal purpose of this present study was to further investigate this phenomenon, using standard 'sharp' intracellular electrophysiological recording and pharmacological manipulation methods in an attempt to answer the questions posed above.

1.2 The physiology of the mammalian piriform cortex

The piriform (primary olfactory) cortex of normal, healthy mammals is understood to be responsible for the assimilation of odour-encoded information into learning and memory (Wilson & Bower, 1989). Since animals are routinely exposed to new odours and odour has previously been shown to be a better memory cue than any other sense

(Chu & Downes, 2000), this area of the brain is considered to be an excellent area for research into learning and associative memory function (Dade *et al.*, 2002; Hasselmo *et al.*, 1992). Additionally, with critical relevance to the present investigation, these functions have not only been shown to undergo muscarinic cholinergic modulation in this brain area (Barkai & Hasselmo, 1997; Saar *et al.*, 2001), but also require the presence of intrinsic oscillatory networks (Chabaud *et al.*, 1999) for effective function of associative memory, a requirement that has previously been shown to predispose some brain areas to epileptogenesis (Draguhn *et al.*, 2000; Liljenstrom & Hasselmo, 1995; Loscher & Ebert, 1996).

1.2.1 Location and gross structure of the piriform cortex

The mammalian piriform cortex is a phylogenically old structure, located bilaterally towards the rostral end of each side of the cerebral cortex, near the junction with the temporal cortex (Fig. 1.1) (Loscher & Ebert, 1996). Afferent fibres of the lateral olfactory tract (LOT), arising from mitral cell bodies, join the piriform cortex with the olfactory bulbs and differentiate nontopographically across the surface of the piriform cortex, making this the largest area in the cortex to receive direct input from the LOT without thalamic intermediation (Saar *et al.*, 1999). Significant to this present study, the sole source of cholinergic innervation to the piriform cortex has been shown, using acetylcholinesterase staining techniques, to arise from the nucleus of the diagonal band (Eckenstein *et al.*, 1988; Saper, 1985) and diffuse extensively upon reaching layers II and III of the piriform cortex (Zimmer *et al.*, 1999) where four (M1-M4) mAChR subtypes have been shown to be abundantly expressed (Buckley *et al.*, 1988). The piriform cortex also receives afferent inputs from a number of other brain areas, such as dopaminergic inputs from the substantia nigra-ventral tegmental area (Fallon *et al.*, 1983), serotonergic inputs from the raphe nuclei (Chabaud *et al.*, 1999) and catecholaminergic inputs from the locus coeruleus (Datiche & Cattarelli, 1996a). The piriform cortex is a laminar structure (Fig. 1.2), comprising three principal layers (with the underlying endopiriform cortex sometimes termed 'layer IV' (Tseng & Haberly, 1989a; Tseng & Haberly, 1989b)) that may be clearly visualised under a microscope (Haberly & Behan, 1983; Haberly, 1983; Haberly & Feig, 1983), making the preparation especially well suited to electrophysiological recording from individual layers and/or electrically stimulating specific synaptic inputs in those layers (Hori *et al.*, 1988). As with other parts of the cortex, the principal neurones of the piriform cortex are pyramidal, characterized by long apical and basal dendritic trees and located in large

numbers in the densely packed layer II and in smaller numbers in the more diffusely populated layer III (Haberly, 1983; Haberly & Feig, 1983). In addition to the principal pyramidal cell type, a further nine other cell types have been identified (primarily in layer III), including aspiny inhibitory interneurones (Protopapas & Bower, 3 A.D.). Each layer of the piriform cortex has previously been demonstrated to serve a number of specific functions and to contain unique neuronal populations (Fig. 1.2): Layer Ia contains the termini of afferent fibres of the LOT that stimulate the apical dendrites of deep and superficial pyramidal neurones and inhibitory interneurones located in layer II, which in turn synapse with pyramidal neurones, giving rise to a feed-forward inhibitory circuit.

Layer Ib predominantly carries association (1.2.3.2) fibres that comprise the cortico-cortical connections arising from the basal dendrites of primarily superficial (and some deep pyramidal) cells and intrinsic (1.2.3.3) fibres that arise from the basal dendrites of the pyramidal neurones in layers II and III and pass in either a rostral or caudal direction and provide modulatory excitatory stimuli as part of a feed-back (caudo-rostral) or feed-forward (rostro-caudal) circuit. It is the intrinsic fibre system and its complex network of feed-forward and feedback modulation of pyramidal cell responses that allows the piriform cortex to show features of associative memory (Hasselmo & Bower, 1993). Layer I also contains ~50% of the inhibitory interneurones found in the piriform cortex that are activated either following stimulation by the LOT or association fibres (Loscher *et al.*, 1998). Layer II contains the densely packed cell bodies of superficial pyramidal neurones, the basal dendrites of which synapse with either the apical dendrites or soma of deep or superficial pyramidal neurones, pass up through layer II to join the intrinsic fibre system in layer Ib or synapse with inhibitory interneurones in layers II or III. The inhibitory interneurones present in layer II represent ~5% of the total inhibitory interneurone population present within the piriform cortex. Layer III contains ~15% of the total interneurones present in the piriform cortex that are activated by synapses arising from the basal dendrites of deep and superficial pyramidal neurones in layers II and III. Significantly, layer III also contains 'deep' pyramidal neurones from which the majority of recordings in this present study were made. The apical dendrites of this neurone-type pass through all three layers towards the pial surface where they are stimulated by LOT afferents. The basal dendrites of the deep pyramidal neurones either synapse with the interneurones located in layer III or pass into layer Ib to join the association fibre system (Haberly & Bower, 1984; Haberly &

Price, 1978). The characteristics of the principal cell types listed here are described in the next section and their connectivity in Section 1.2.3.

1.2.2 Properties of the principal cell types found in the piriform cortex

The principal neurone types found in the piriform cortex have previously been categorized, by a number of studies, according to their morphology and responsiveness to electrical stimulation and exposure to a number of pharmacological agents, including mAChR agonists (Ekstrand *et al.*, 2001a; Hoffman & Haberly, 1991a; Libri *et al.*, 1994; Protopapas & Bower, 3 A.D.; Tseng & Haberly, 1989a; Tseng & Haberly, 1989b). The key results obtained in these studies from each cell type (according to the classification of Libri *et al.*, 1994) are summarised below and were used to identify recorded cells in the present study.

1.2.2.1 Deep pyramidal (type 1) neurones

Deep pyramidal neurones were termed type 1 cells in a comprehensive study comparing the neuronal morphology of the principal cell types to muscarinic responsiveness in the piriform cortex (Libri *et al.*, 1994). This report found this cell type only in Layer III of the piriform cortex, typically with a pyramidal-shaped cell body, a thick spiny, apical dendrite orientated towards the pial surface (that characteristically bifurcated ~50 μm from the soma and reached into layer I) and a highly branched basal dendritic tree. These deep pyramidal cells were shown to have a typical resting membrane potential of ~–85 mV, a membrane input resistance of ~40 MΩ and to exhibit a slow after-hyperpolarization (sAHP; revealed as an underlying slow outward tail current, I_{AHP} under voltage clamp conditions) following a long depolarizing stimulus (+2 nA; 1.6 s) that, in the presence of the mAChR agonist, OXO-M (10 μM) or the metabotropic-glutamate receptor (mGluR) agonist, trans-ACPD (50 μM), was replaced by a slow after-depolarization (sADP; accompanied by an underlying slow inward tail current, I_{ADP}). Additionally, these cells responded with a sustained membrane depolarization, repetitive firing and significantly increased membrane input resistance in the presence of either agonist (Constanti & Libri, 1992), whilst the OXO-M-induced epileptiform activity previously reported in immature slices from this brain area was recorded solely from this deep pyramidal cell type (Postlethwaite *et al.*, 1998a). Furthermore, these cells have also been shown to drive persistent epileptiform excitatory postsynaptic potentials (EPSPs) recorded in superficial pyramidal neurones (see below) (Hoffman & Haberly, 1991b) and have been shown to exhibit variable amplitude, long latency EPSPs,

characteristic of epileptogenic cells (Tseng & Haberly, 1989d; Tseng & Haberly, 1989c). It was this cell type that was recorded from in the majority of experiments described in the present work.

1.2.2.2 Non-pyramidal (type 2) neurones

Cells defined as type 2 by Libri *et al.* are typically found in layers II - III of the piriform cortex and were found to be very morphologically varied, unlike the deep and superficial pyramidal cell types. They were also found to lack the single dominant apical dendrite and broadly diffuse basal dendritic tree that are characteristic of deep and superficial pyramidal neurones (Protopapas & Bower, 2000). Consequently, the only common characteristics reported for these cells were an ovoid (~15 μm diameter) soma and a broadly branching dendritic tree, limited to within layer III, giving these neurones a fusiform or bipolar appearance (Libri *et al.*, 1994). A separate study, physiologically characterising these non-pyramidal neurones that populate layer III, found this cell type to exhibit numerous, highly branched smooth beady dendrites and proposed this cell type to represent a population of inhibitory interneurones (Protopapas & Bower, 2000). This cell type was found to have a similar resting potential, membrane input resistance and responsiveness to depolarizing and hyperpolarizing electrotonic stimuli as cells previously characterised as being deep pyramidal neurones, although spikes elicited following depolarizing electrotonic stimuli from these interneurones were frequently characterised by an early fast after-hyperpolarization not seen in either deep or superficial pyramidal cells (Libri *et al.*, 1994). However, although the responses of these neurones to depolarizing and hyperpolarizing electrotonic stimuli in the presence of 10 μM OXO-M and the consequent changes in membrane input resistance and resting membrane potential were found to be similar to those elicited from deep pyramidal neurones, Libri *et al.* found that a smaller sADP (in comparison to that evoked from type 1 cells) could be evoked from these cells following a long depolarizing stimulus train.

1.2.2.3 Superficial pyramidal (type 3) neurones

Superficial pyramidal neurones are found in the densely populated layer II of the piriform cortex and were termed type 3 cells by Libri *et al.* They are distinguishable by their location and pyramidal cell bodies (15-30 μm) surmounted by a short apical dendrite directed towards the pial surface, whilst conversely, the basal dendritic trees of these cells are truncated and less branched in comparison to the apical dendritic trees

(Haberly & Behan, 1983; Haberly, 1983; Haberly & Feig, 1983). The membrane input resistance of superficial pyramidal neurones was found to be significantly lower than that of deep pyramidal or interneuronal cells, although the resting membrane potential was comparable with the other two cell types. The application of positive electrotonic stimuli through the recording microelectrode has been shown to elicit spike pre-potentials early in the evoked spike train, indicative of more than one spike initiation site in the cell, possibly at an apical *'bifurcation trigger zone'* (Libri *et al.*, 1994). This report also showed that when a long stimulus was applied to this cell type, held close to firing threshold potential, little or no sAHP could be elicited. It has been proposed that this characteristic may be due to a relative lack of voltage-activated Ca^{2+} channels in this cell type (Tseng & Haberly, 1989a), thereby also explaining the absence of an sADP in these cells when the same stimulus was applied in the presence of a muscarinic agonist (Libri *et al.*, 1994). In the presence of muscarinic agonists, superficial pyramidal neurones were found to depolarize only very slightly, showing no repetitive firing or sADP (in response to a long depolarizing stimulus train) (Libri *et al.*, 1994). Interestingly, despite the fact that the deep layers of the piriform cortex have been shown to be responsible for the initiation of epileptiform activity (Loscher & Ebert, 1996), the neurones most exhaustively investigated in this brain area are superficial pyramidal neurones that show very few pro-convulsive responses or characteristics (Hasselmo & Bower, 1990; Hasselmo & Bower, 1991; Hasselmo & Bower, 1992; Tang & Hasselmo, 1994).

1.2.2.4 The slow post-stimulus after-depolarization (sADP)

The usual response of most recorded olfactory cortical neurones to a prolonged depolarizing stimulus is a *slow afterhyperpolarization* (sAHP) associated with an increase in membrane conductance; this after-potential has been shown to be associated with a calcium-dependent K^+ conductance and is reversibly decreased (Constanti & Sim, 1987a) and replaced by a slow *afterdepolarization* (sADP) following mAChR activation in susceptible cells (Constanti & Bagetta, 1991). Although the intracellular experiments of Krnjevic *et al.* where acetylcholine (Ach) was iontophoretically-applied to cat cortical neurones *in vivo*, were the first to demonstrate a transformation of a sAHP to a sADP following mAChR activation (Krnjevic *et al.*, 1971), it was some time before further investigations of the sADP were performed. Subsequently, a post-stimulus sADP was discovered during intracellular recordings from cat sensorimotor cortical cells in the presence of the mAChR agonist, muscarine. This sADP was found to also

replace a sAHP and was characterised by repetitive firing that occurred at the peak of the post-stimulus depolarization (Schwindt *et al.*, 1988) and was found to be dependent on Ca^{2+} entry into the cell during the sustained depolarizing stimulus. It was initially suggested that the movement of Cl^- ions from the recording microelectrode may have contributed to the generation of this sADP, however this was subsequently disproved using impermeant anions in the recording microelectrode, leaving the ionic mechanisms underlying the sADP still unclear. Soon afterwards, the first voltage *and* current clamp study of an sADP was made using piriform cortical brain slices and the mAChR agonist, OXO-M (Constanti & Bagetta, 1991). The sADP was found to be expressed only in certain neuronal populations located in layer III of the piriform cortex in the presence of a mAChR agonist and following a long depolarizing stimulus (+2 nA; 1.6 s) applied to the cell held close to firing threshold potential (~-70 mV in deep pyramidal neurones) (Constanti *et al.*, 1993). Subsequent experiments by the same group further subdivided the cells into those capable or not capable of exhibiting a sADP (Section 1.2.2.1, 1.2.2.2 & 1.2.2.3) (Libri *et al.*, 1994). In addition to a mAChR-induced sADP being found in these cells, a sADP with similar characteristics was also recorded following metabotropic glutamate receptor (mGluR) activation in the same cell type in this brain area (Constanti & Libri, 1992). Additionally, a slow inward tail current, measured using the 'hybrid' voltage clamp technique (Lancaster & Adams, 1986) and termed the I_{ADP}, has been shown to underlie the piriform cortical sADP (Constanti *et al.*, 1993). This mAChR-induced slow after-depolarization, its underlying slow inward tail current and the associated increase in postsynaptic excitability have been suggested to arise as a result of a slow Ca^{2+}-dependent *blockade* of a novel K^+ current at membrane potentials positive to -60mV in the presence of mAChR or mGluR agonists; accordingly, the input conductance at the peak of the sADP was found to be *decreased* rather than increased (Libri *et al.*, 1997). It is notable that although this current has been shown to be *Ca^{2+}-dependent*, it is not *Ca^{2+}-mediated* (Constanti & Libri, 1992). The proposed modulation of K^+ flux underlying the sADP is supported by its sensitivity to external K^+ channel blockers such as tetraethylammonium (TEA), tetrabutylammonium (TBA) or 4-aminopyridine (4-AP) (Constanti & Bagetta, 1991) and also its blockade following the application of caffeine, which is known to affect Ca^{2+} channels and consequently, K^+ channel activity (Postlethwaite *et al.*, 1998a).

The sADP cannot be elicited by a single action potential, but requires the application of repeated depolarizing stimuli to evoke it, with the duration and amplitude

of the sADP being dependent upon the applied stimulus size and duration (in addition to being agonist concentration dependent (Constanti & Bagetta, 1991)). The amplitude of the sADP has also been shown to diminish as the membrane potential is artificially shifted towards the threshold potential (by the injection of positive current through the recording microelectrode). The sADP was not generated by the addition of the K^+ channel blockers Ba^{2+}or Cs^+ to the external bathing medium, indicating that mAChR (or mGluR) activation was necessary for its generation, rather than just requiring a simple depolarization of the membrane potential and a decrease in background K^+ leak conductance, although interestingly, in the presence of a mAChR agonist, Ba^{2+} does increase the magnitude of the elicited I_{ADP} (Constanti & Bagetta, 1991). The role of Ca^{2+} in sADP generation was first suggested by the fact that the Ca^{2+}channel blockers, Cd^{2+} and Mn^{2+}, blocked the generation of an sADP in rat association cortical cells (Andrade, 1991); this report suggested that the sADP elicited here resulted from the activation of a Ca^{2+}-dependent cation non-selective channel associated with mAChR activation, which contrasts with the mechanism subsequently proposed by Constanti & Libri to explain sADP generation in the piriform cortex (Constanti & Libri, 1992). sADPs have also been seen in a number of other different cerebral neurone types such as hippocampal pyramidal cells (Gahwiler, 1984), septal neurones (Hasuo & Gallagher, 1990) and Layer V cells of the frontal cortex (Araneda & Andrade, 1991). Despite the fact that these reports have all described similar (but not identical) sADPs that all share common features, a number of the results do not suggest that the same underlying mechanisms are responsible for their generation.

Ca^{2+} has previously been inconsistently implicated in the generation of the sADP following the observation that the sADP was diminished in a bathing medium containing the Ca^{2+} channel blocker, Cd^{2+}, whilst the K^+ channel blocker, Cs^+ did not affect the sADP (Constanti *et al.*, 1993). As a consequence of these sometimes conflicting results, it has been proposed that, in the piriform cortex, mAChR activation may *'prime'* (Constanti *et al.*, 1993) a background K^+ conductance to become sensitive to changes in intracellular Ca^{2+} concentrations. When a long depolarizing stimulus is applied to a neurone, Ca^{2+} floods the cell and the now Ca^{2+}-sensitive, background K^+ conductance is deactivated. Post-stimulus, as the cell begins to return to a resting state, Ca^{2+}levels slowly begin to return to their resting values and the blocking effect of Ca^{2+} upon the K^+ conductance diminishes. Despite this hypothesis and the fact that the sADP and its underlying tail current are clearly sensitive to external Ca^{2+} concentrations, the

role of intracellular Ca^{2+} in the cortical sADP generation is still not entirely clear and other possible underlying mechanisms (e.g. an *increase* in a rectifying non-specific cationic conductance [CAN] (Haj-Dahmane & Andrade, 1998; Haj-Dahmane & Andrade, 1999)) have not been entirely excluded.

1.2.3 Synaptic connectivity of the piriform cortex

By virtue of its laminar organisation, the synaptic circuitry of the piriform cortex has previously been demonstrated to possess a highly organised structure, with different fibre and cell types located in specific layers (Fig. 1.2; Section 1.2.2) (Haberly & Bower, 1984; Haberly & Presto, 1986; Rodriguez & Haberly, 1989). A typical excitatory postsynaptic potential/inhibitory postsynaptic potential (EPSP/IPSP) complex elicited, *in vitro*, following local electrical stimulation of the slice preparation and recorded by an intracellular microelectrode from a deep pyramidal piriform cortical neurone exhibits a number of well characterised features; a fast excitatory component of the EPSP, mediated by the neurotransmitter, glutamate, released from synaptic terminals and acting on NMDA and non-NMDA glutamatergic receptors precedes the early, fast component of the IPSP produced by γ-aminobutyric acid (GABA) released onto $GABA_AR$s mediating Cl^- channels. This fast IPSP component is followed by a longer, slow IPSP arising from GABA acting on pertussis toxin-sensitive $GABA_BR$s mediating K^+-channels (Malcangio *et al.*, 1995). In EPSP/IPSP complexes recorded from deep piriform cortical neurones, the fast $GABA_AR$-mediated component of the IPSP has been found to reverse at a membrane potential of ~-50 mV whilst the slow $GABA_BR$-mediated component of the IPSP has been shown to disappear without a clear reversal at ~-90 mV (Libri *et al.*, 1996).

1.2.3.1 Lateral olfactory tract afferents

The principal excitatory afferent input to the mammalian piriform cortex arises from lateral olfactory tract (LOT) fibres originating from mitral cells (Haberly & Price, 1977) in the olfactory bulbs. It is these connections that caused the piriform cortex to be referred to as the *'primary olfactory'* cortex since it receives the largest direct input from the olfactory bulbs of any brain area (Johnson *et al.*, 2000). These afferents are principally found in layer Ia of the piriform cortex, appearing most densely at the anterior end and spread in a rostro-caudal direction, parallel to the pial surface of the brain, towards the posterior end of the of the piriform cortex (Fig. 1.2). The bundled afferent LOT fibres, the number of which gradually decrease rostro-caudally, branch

frequently giving rise to LOT axons that descend into layers Ib and II, perpendicular to the surface of the piriform cortex (Haberly & Behan, 1983). It is here that LOT afferents synapse with distal portions of the apical dendrites of superficial and deep pyramidal cells (Fig. 1.3), and interestingly, it has been shown that whilst each LOT axon typically only synapses with a single superficial pyramidal cell, these axons form di- or polysynaptic connections with each deep pyramidal neurone (Biedenbach & Stevens, 1969). Consequently, deep pyramidal cells receive greater excitatory input from the LOT, an observation that may have significant implications upon the epileptiform events seen in immature deep, but not superficial pyramidal cells (Ekstrand *et al.*, 2001b; Hoffman & Haberly, 1991a; Postlethwaite *et al.*, 1998a).

1.2.3.2 Association fibres

Another significant excitatory synaptic system found within the piriform cortex is the association fibre system that comprises the cortico-cortical connections arising from the basal axons of primarily superficial (and some deep pyramidal) cells. These axons typically pass upwards through layers II (and III) into layer Ib where they travel either rostrally or caudally, parallel to LOT afferents (in layer Ia) and the pial surface of the brain, before leaving the piriform cortex for other brain regions such as the pre-frontal cortex, amygdala, entorhinal and perirhinal cortices (Luskin & Price, 1983). It has been shown that these axons, although branching rarely in the piriform cortex, are highly branched upon egressing and can, in principle, traverse an entire cerebral hemisphere, arborizing in a number of brain areas associated with behavioural, memory, emotive and cognitive processes illustrating the pervasive influence of odour response upon these 'higher' brain processes. Additionally, a comparison of synaptic bouton distribution has shown that association fibres make a small number of synapses with a very large (>1000) number of cells and possess few specialized terminal regions, instead displaying boutons distributed over the entire extent of each axon (Johnson *et al.*, 2000), an observation that is, interestingly, comparable with the structure of a number of artificial neural networks (Hasselmo & Barkai, 1995). These cortico-cortical connections are spatially distributed to a great degree that strongly contrasts with the structure commonly seen in primary sensory areas responsible for the integration of inputs arising from the non-chemical senses, such as the primary auditory, visual and somatosensory cortices, that tend to have an ordered, columnar structure. Additionally, the piriform cortex is the only sense-interpretion/integration area of the brain containing ascending afferents that are *not* mediated by a secondary area prior to reaching higher

brain areas. It has been suggested that the structure of the piriform cortex and the manner in which it connects with higher brain areas indicate that rather than *'extracting and refining specific stimulus features'*, it *'plays a role in linking the combinatorial representations of odorant structure that constitute the olfactory code, and in associating olfactory and other forms of information'* (Johnson *et al.*, 2000), concomitant with associative memory function (Haberly & Bower, 1989).

1.2.3.3 Intrinsic fibres

The final excitatory synaptic system of fundamental significance within the mammalian piriform cortex is composed of intrinsic fibres. This comprises excitatory fibres arising from the basal axons of superficial and deep pyramidal cells that do not go on to form the association fibre system, but instead travel either rostrally or caudally within layers II and III before rising towards the pial surface to synapse with the proximal portions of the apical dendrites of other superficial or deep pyramidal cells (Fig. 1.3) of the piriform cortex (Haberly & Price, 1978; Luskin & Price, 1983; Price, 1973). These connections are divided into two subsystems, a feed-forward (if passing rostro-caudally) system and a feed-back (if travelling caudo-rostrally) system within the piriform cortex (Haberly & Price, 1978) and consequently remain distinct from either the afferent (layer Ia) and association (layer Ib) fibre systems described previously (Litaudon *et al.*, 1997). Of the two identified intrinsic subsystems, the rostro-caudal, feed-forward system has been shown to comprise approximately twice the number of fibres as comprises the caudo-rostral system (Datiche & Cattarelli, 1996b). The intrinsic fibre system has also been proposed to play a role in the distribution of excitatory stimuli originating from LOT afferents and has consequently been proposed to play a temporal role in information processing and possibly stabilising spatial patterns of olfactory coding within the piriform cortex (Litaudon *et al.*, 1997).

1.2.3.4 Inhibitory synaptic connections within the piriform cortex

Excitatory fibres, originating from the LOT and intrinsic fibre systems, arise from the axon collaterals of deep and superficial pyramidal neurones as described previously and synapse with non-pyramidal GABA-ergic inhibitory interneurones that are known to be present within all three layers of the piriform cortex (Satou *et al.*, 1982; Satou *et al.*, 1983a; Satou *et al.*, 1983b). These interneurones then exert their inhibitory effect upon the same deep or superficial pyramidal neurones that are also stimulated by LOT and intrinsic fibres, thereby forming feed-forward and feed-back inhibitory pathways. It has been suggested that the intrinsic fibre system may also play a role in the modulation of

feed-back inhibitory processes in the piriform cortex (Barkai *et al.*, 1994), whereby association fibres arising from pyramidal neurone axon collaterals stimulate interneurones that, in turn inhibit the pyramidal neurones from which the axons arose. A number of studies have investigated the characteristics and distribution of inhibitory interneurones within the piriform cortex using both electrophysiological (Satou *et al.*, 1982; Satou *et al.*, 1983a; Satou *et al.*, 1983b) and immunocytochemical staining techniques (Haberly *et al.*, 1987; Loscher *et al.*, 1998). These studies found and confimed that the majority of GABA-ergic neurones were located within layer I (~50%) of the piriform cortex with ~5% and ~15% found in layers II and III respectively. Another report (Kapur *et al.*, 1997a) showed that fast $GABA_AR$-mediated inhibition was dendritically generated in the piriform cortex and that the circuits responsible for this inhibition, in the apical dendritic and somatic regions, were independent of one another. This divergence of fast inhibitory synaptic processes within the piriform cortex was confirmed by a study that identified distinct subpopulations of interneurones within the piriform cortex (Ekstrand *et al.*, 2001a) in an arrangement similar to that described in the rat auditory cortex (Aramakis *et al.*, 1997), cat visual cortex (Tamas *et al.*, 1997), rat neocortex (Thomson *et al.*, 1996) and hippocampus (Traub *et al.*, 1987; Vu & Krasne, 1992). Consequently, the inhibitory circuit set up by an individual interneurone is dependent not only upon whether the downstream synapsed pyramidal neurone is as yet unstimulated or not, but also upon the origin of the excitatory input initially stimulating the inhibitory interneurone. This permits the creation of complex feed-back and feed-forward inhibitory synaptic circuits within the piriform cortex, with inhibitory effects upon pyramidal cells being exerted by inhibitory interneurones as a consequence of either excitatory stimulation of the pyramidal cell (feed-back inhibition) or as a result of afferent fibre stimulation of the interneurone, exerting an inhibitory effect upon the pyramidal neurone prior to the arrival of the afferent excitatory stimulus at the pyramidal neurone (feed-forward inhibition).

1.2.3.5 Differences in pharmacological responsiveness of excitatory synaptic systems in the piriform cortex

The distinct laminar organisation of the principal excitatory fibre systems of the piriform cortex (Fig. 1.3) has permitted a number of studies to be performed that have examined whether any pharmacological differences in responsiveness exist between these fibre systems by using stimulating electrodes placed in specific areas of the piriform cortex to preferentially stimulate particular fibre systems and consequently

elicit postsynaptic potential complexes (EPSPs/IPSPs). From a functional point of view, variations in fibre system responsiveness to different modulators provides the piriform cortex with further flexibility to respond to changes in its input and output. One such study of particular significance to the present work demonstrated that presynaptic mAChR-mediated suppression of excitatory synaptic transmission (caused by inhibiting the release of glutamate from presynaptic terminal boutons (Constanti & Bagetta, 1991) was specific to intrinsic, but not afferent excitatory synaptic transmission in the rat piriform cortex (Hasselmo & Bower, 1992). However, this investigation only described a disparity in the presynaptic cholinergic sensitivity of terminals synapsing onto *superficial* and *not deep* pyramidal piriform cortical neurones, thereby limiting the usefulness of the study in explaining possible synaptic mechanisms that might underlie the mAChR-agonist-induced epileptiform bursting phenomenon seen in immature deep pyramidal piriform cortical neurones (Postlethwaite *et al.*, 1998a). However, despite this limitation, the results of their report clearly demonstrated a possible role for the intrinsic cholinergic innervation in the rat piriform cortex in selectively suppressing intrinsic fibre-mediated excitatory synaptic transmission and were appropriately in accordance with the observation that cholinergic innervation to the piriform cortex only reaches as far as layers II and III (containing intrinsic fibres), but not into layer I, containing afferent fibres (Zimmer *et al.*, 1999).

Additionally, the same group that demonstrated cholinergic modulation of intrinsic excitatory synaptic transmission also demonstrated that intrinsic, but not afferent excitatory synaptic transmission was suppressed by the presynaptic action of the $GABA_BR$ agonist, baclofen (Tang & Hasselmo, 1994). In contrast to this reported specificity of intrinsic fibre-mediated excitatory synaptic transmission to modulation by cholinergic or $GABA_B$-ergic agents, suppression of afferent, but not intrinsic excitatory synaptic transmission was produced by the glutamatergic agonist, 2-amino-4-phosphonobutyric acid (4-APB) (Hasselmo & Bower, 1991). From these reports it is clear that a number of different interrelated systems are involved with presynaptic modulation of both afferent and intrinsic excitatory synaptic transmission within the piriform cortex, which is, in turn, complemented by the laminar organisation of these fibre systems. Since intrinsic fibres typically synapse with their target pyramidal cells at a point more proximal to the soma and afferent fibres synapse at more distal points, it is clear that suppression of intrinsic, but not afferent excitatory synaptic transmission, of the type described by Hasselmo *et al.* (1991), and following mAChR activation, would stabilise the soma of the target neurone (due to suppression of intrinsic synaptic

transmission), whilst not affecting dendritic sensitivity to afferent excitatory inputs (due to the lack of suppression of afferent synaptic transmission). When the implications of this layer-selective suppression of excitatory synaptic transmission, either by cholinergic or $GABA_B$-ergic mechanisms, upon the neural circuitry in this area are considered together, it is clear that the observed shift in dominance from intrinsic to afferent input would permit synapsed pyramidal cells to preferentially accept information from afferent inputs rather than intrinsic, modulatory inputs. Overall, this would enhance responses to new (afferent) stimuli rather than to existing, entrenched (intrinsic) pathways and consequently, new sensory stimuli are given a greater probability of affecting the neural circuitry than the (inhibited) modulatory stimuli arising from existing pathways, a factor considered vital to the modification, modulation and maintenance of associative memory function (Barkai & Saar, 2001; Hasselmo & Bower, 1993; Loscher & Ebert, 1996; Patil & Hasselmo, 1999).

1.3 The piriform cortex as an epileptogenic area

The piriform cortex is a brain area that is known to be particularly prone to limbic epileptiform events, a susceptibility that has previously been demonstrated by a number of studies both *in vivo,* in kindled seizure investigations (Hoffman & Haberly, 1996a; Loscher & Ebert, 1996) and to a lesser extent, *in vitro*, in response to pharmacological or electrical stimulation (Hoffman & Haberly, 1989a) (Ekstrand *et al.*, 2001b; Postlethwaite *et al.*, 1998a). Additionally, the majority of seizures that may be induced in the piriform cortex, using a variety of techniques, all manifest themselves as complex partial seizures, the most common seizure type of the human epilepsies (Loscher & Ebert, 1996). When this well documented ease of seizure induction, the variety of seizure induction methods available and the characterization of induced seizures as being highly pertinent to the most prevalent human epilepsies are all taken together, it is clear that models of epileptiform behaviour utilising this brain area represent very valuable analytical and diagnostic tools, critically useful in improving our understanding of epilepsy and in testing and screening potential anticonvulsants. Postulated and proven reasons for the susceptibility of the piriform cortex to seizure generation are numerous; for example, in kindling experiments, interictal discharges characteristic of epileptiform activity, have been consistently shown to originate in the piriform cortex, regardless of the original point of the kindling focus. Additionally, the piriform cortex has been shown to possess the most seizure prone neural circuits of any limbic brain area and is the brain area most damaged following seizure induction in the

rat amygdala or hippocampus, with such damage being characterised by induction of the immediate-early gene, *c-fos*, astrogliosis and the loss of GABA-ergic neurones (Loscher & Ebert, 1996).

Of the *in vitro* models of epileptform behaviour in the piriform cortex, seizures may be induced by using a number of chemical means, all of which achieve burst induction by either reducing inhibitory limitations or increasing excitatory factors (or indeed by simultaneously changing both aspects). Candidate proconvulsants in this brain area take the form of agents such as the mGluR agonist, *trans*-ACPD (that increases excitation by acting upon non-NMDA-gated ion channels) (Constanti & Libri, 1992), penicillin (Yamauchi *et al.*, 1989), picrotoxin, 4-aminopyridine (4-AP), OXO-M (Postlethwaite *et al.*, 1998a) or tetraethylammonium (TEA) (Velisek *et al.*, 1995), all of which have been shown to induce seizures in the piriform cortex. In conclusion, both clinical and experimental investigations have suggested that, like other mammalian limbic structures, the piriform cortex shows a low threshold for chemical or electrical seizure induction, but also possesses a unique association fibre system that is not only highly directional (Haberly & Price, 1978) but also efficiently links a very large number of other brain areas (Litaudon & Cattarelli, 1994), thereby making it a unique locus from which seizure activity can originate and may, to a certain extent account for the overall susceptibility of the temporal lobe to epileptiform bursting (Loscher & Ebert, 1996).

1.4 Historical development of the piriform cortex slice preparation

The use of *in vitro* piriform cortical brain slices for initially, extracellular and later intracellular and patch clamp electrophysiological investigations of the neuronal circuitry, cellular responses and seizure characterisation within this brain area first began with slices prepared from the guinea pig. The tangentially-cut ('*surface*') slice preparation was initially used as part of the development of extracellular recording techniques (Yamamoto & McIlwain, 1966) (Richards & Sercombe, 1968) (Harvey *et al.*, 1974). Subsequently, *in vivo* intracellular experiments were carried out using the oppossum (Haberly, 1973) and cat (Biedenbach & Stevens, 1969) piriform cortices which led, in turn, to the development of *in vitro* intracellular recording techniques that used slices prepared from the guinea pig piriform cortex (Scholfield, 1978c; Scholfield, 1978b; Scholfield, 1978a). It was these pioneer *in vitro* intracellular investigations that provided the first data describing the electrical membrane properties, current-voltage relationships and synaptic responses of piriform cortical neurones, such as the relatively

high resting membrane potential (~-85 mV) of cells found in this brain area, under these conditions. Additionally, it was noted that EPSPs elicited following repeated stimulation of LOT afferents were smaller than EPSPs elicited following a single stimulus to the LOT, indicating the presence of strong feed-forward and feed-back inhibitory pathways in effect within this area. Subsequently, these pioneering results obtained by Scholfield have been further refined and explored and consequently a detailed body of knowledge describing the structure of the piriform cortex and its afferent, efferent and intrinsic synaptic connections has now been assembled. Finally, sufficient electrophysiological data has been accumulated describing piriform cortical cellular responses to enable a partial computer neuronal model of this brain area to be constructed (Wilson & Bower, 1989). This model has permitted greater understanding of the links between behaviour at a cellular level and macroscopic processes such as learning and memory within this brain area. However, the role of the deep pyramidal neurones (and their synaptic connections) found in layer III of the piriform cortex, have yet to be addressed and integrated into this or any other model. Consequently, although the model has described a working simulation of the associative memory function predicted for the piriform cortex (Barkai *et al.*, 1994; Haberly & Bower, 1989; Hasselmo & Bower, 1993), it does not simulate any of the induced seizure states that have been previously reported (Hoffman & Haberly, 1991a; Postlethwaite *et al.*, 1998a). Accordingly, it would be of particular interest to incorporate the existing data, describing the responses of recorded deep pyramidal neurones (Libri *et al.*, 1994; Protopapas & Bower, 2000) together with the new data presented in this report, into this model thereby providing not only a more complete neuronal model of the mammalian piriform cortex but also the possibility to simulate the experimentally-observed observed seizure states seen in this brain area. Such a refined model could then prove to be a useful analytical tool for gaining a better understanding of the mechanisms that underlie such seizure activity.

Finally, the choice of the slice preparation, determined by the plane in which the brain tissue is cut, has been demonstrated to be of considerable importance (Hori *et al.*, 1988). In most slice studies, it is clearly desirable to leave as much of the fibre systems described previously (Section 1.2.3) as intact as possible in order to retain as much physiological significance in the subsequent *in vitro* experiments. Although initial electrophysiological investigations of the piriform cortex utilised tangential brain slices hand-cut from the surface of the brain with a bow-cutter and guide (Yamamoto & McIlwain, 1966), later investigations used slices cut perpendicular to the pial surface

(Bower & Haberly, 1986; Constanti & Sim, 1987b). Slices of this type had the clear advantage of permitting the investigator access not only to a large area of the pyramidal neurone layer targeted for recording (since the plane of the cut ran parallel to the long axis of these cells), but also permitted separate stimulation of the different fibre systems within the slice (Hori *et al.*, 1988). However, perpendicularly cut slices such as these may be prepared following a cut severing or running parallel to the LOT (parasagittal or transverse respectively), the choice of which has obvious implications upon the usefulness of the slice for the investigation of synaptic responses (Demir *et al.*, 2001). Consequently, in this present study, the parasagittal (running parallel to the LOT) slice preparation (Libri *et al.*, 1994) was used since it permitted easy access to deep pyramidal neurones and maintained, to a greater degree, the integrity of the fibre systems mentioned. This was particularly important, since one of the main objectives of the present study was to determine the degree of local excitatory and inhibitory synaptic influence upon mAChR agonist-induced epileptiform burst firing in the immature slice preparation (Postlethwaite *et al.*, 1998a).

1.5 A comparison of some common approaches used to study epileptogenic mechanisms

The models that have been used to date in the experimental study of epileptogenesis may be broadly divided intotwo categories describing those using *in vivo* and *in vitro* techniques. Of the *in vivo* techniques, the majority have been kindling models (Goddard, 1967) (Racine *et al.*, 1991) that take advantage of what has previously been termed the *'kindling response'*, where low intensity electrical stimuli are applied to the brain areas that comprise the limbic system, such as the amygdala. Initially, this does not result in seizure activity but, after a number of days, these low-level repetitive stimuli do produce permanent recurrent seizure activity, thus mimicking (to some extent) the clinical epileptogenic process (Mosh & Ludvig, 1988). The mechanism(s) by which this phenomenon occurs is still not fully understood, although it is believed that processes similar to those that cause long-term potentiation (LTP; a process closely linked to NMDA receptor activity causing increased overall excitability in affected areas) in areas such as the hippocampus may be involved (Malinow *et al.*, 1988) (Andreasen *et al.*, 1989).

Of the variety of *in vitro* models that have been used, those most frequently utilised are brain slice models. The brain area that has been most intensely studied in this way thus far, has been the hippocampus since it provides a limbic area of study with

an easily visualized laminar structure permitting accurate cellular impalements in specific areas and cell-types (Turski *et al.*, 1989) and also exhibits seizure behaviour that may be easily characterised in response to many of the chemical proconvulsants described previously (Section 1.3). Consequently, since piriform cortical slices, particularly in the form of the transverse slice preparation (Section 1.4), share the majority of the features, such as laminar organisation and susceptibility to proconvulsants, described above, they too are very well suited to the study of epileptogenesis.

1.6 Pharmacological characterization, coupling and function of central muscarinic acetylcholine receptors (mAChR)

mAChRs have previously been shown to mediate the majority of the excitatory (and inhibitory) effects of acetylcholine (ACh) within the mammalian central nervous system (CNS) (Krnjevic, 1986). In the early 1980s, an investigation using the mAChR antagonist, pirenzepine, (Hammer *et al.*, 1980) demonstrated that it was not possible for a single type of mAChR to be wholly responsible for all of the observed actions of ACh upon CNS tissues. By 1988, three distinct mAChR subtypes had been determined and characterized by their responses to antagonists such as pirenzepine and 4-diphenylacetoxy-N-(2-chloroethyl) piperidine hydrochloride (4-DAMP), and classified as M1, M2 and M3 (Mitchelson, 1988). The subsequent application of molecular biological techniques has since revealed the existence of five different genes that code for mAChR subtypes (Parker *et al.*, 1991; Vilaro *et al.*, 1990a), that have been found to be natively expressed as the subtypes M1-M5. The pharmacological and functional categorization of these mAChR subtypes has been hindered by a lack of sufficiently selective agonists with which to elicit responses mediated solely by a single mAChR subtype. This has resulted in a situation where the detailed elucidation of mAChR subtype role and function has become dependent upon receptor selectivity profiles constructed using antagonists of *varying specificity* for all mAChR subtypes. Additionally, the use of transfected cell lines to express homogenous mAChR populations may have provided somewhat misleading results, since a single receptor subtype may not necessarily be coupled to a *single* effector mechanism (as is the case in transfected cells), but may, natively, be coupled to *multiple* second messenger systems (Parker *et al.*, 1991). Comparisons of the data so far collected that have reported mAChR antagonist specificity and potency (Caulfield, 1993) have revealed differences of up to three fold for results obtained for individual antagonists from different research

groups, demonstrating that it is considerations such as these that impose additional obstacles before investigators trying to identify mAChR subtypes responsible for the manifestation of particular phenomena. One reason that has been proposed for the lack of antagonist specificity for mAChRs is the existence of an allosteric site on the M2 mAChR subtype that is modified by a number of ligands such as gallamine and methoctramine. These ligands have also been shown to have affinity for the ACh binding site on the mAChR and consequently, the effect of these antagonists is likely to be comprised of a combination of allosteric and competitive mechanisms depending upon the ligand type and concentration. Consequently, the variations seen in response to such mAChR antagonists may be accounted for by the difference in antagonist action upon these two sites (Levey *et al.*, 1992).

1.6.1 mAChR profiling by antagonist type

Despite the problems inherent in the use of a number of the mAChR antagonists available for determining mAChR subtypes, investigators have succeeded in characterising the various mAChR subtypes according to their responses to the partially selective antagonists available. Thus, the M1 mAChR subtype has been shown to have a high affinity for the mAChR antagonist, pirenzepine and a low affinity for the mAChR antagonist, AF-DX-116. However both the M1 and M4 mAChR subtypes have a similar affinity for pirenzepine and consequently, the mAChR antagonist, himbacine has been frequently used to differentiate between possible M1 or M4 mAChR-mediated responses, since himbacine has been shown to have a higher affinity for the M4 mAChR subtype. Thus, pirenzepine is typically used to differentiate between the M1, M2, M3 and M5 mAChR subtypes in conjunction with the mAChR antagonist methoctramine as a confirmatory antagonist, due to its higher affinity for the M2 mAChR subtype over the M1 mAChR subtype (Caulfield & Brown, 1991). The M2 mAChR subtype displays a high affinity for methoctramine and a low affinity for pirenzepine. However, as previously stated, methoctramine has an allosteric effect at concentrations greater than 1μM, a property that may be detrimental to the accuracy of characterization studies performed (Waelbroeck *et al.*, 1990). The M3 mAChR subtype has a high affinity for 4-DAMP and para fluoro hexahydrosiladifenidol (pFHHSiD) and a low affinity for pirenzepine (Caulfield, 1993). Finally, the M4 mAChR subtype has a moderate affinity for pirenzepine and a high affinity for himbacine. Within this particular mAChR subtype, differences between antagonist affinities are not great and consequently the M4 mAChR subtype remains the hardest of the four natively expressed mAChR subtypes to

characterize. New mAChR antagonists, such as zamifenacin, more specific for the M4 mAChR subtype, are being investigated and may provide more effective characterization tools in due course (Caulfield & Brown, 1991). The M5 mAChR subtype still, to a certain extent, remains a putative mAChR subtype since it has, as yet, only been expressed in transfected cell lines, such as CHO cells, although m5 mRNA has been shown to exist in the hippocampus, substantia nigra pars compacta, ventral tegmental area, lateral habenula and ventromedial hypothalamic nucleus (Vilaro *et al.*, 1990b). Consequently, the result of m5 activation is as yet unknown and characterization by antagonist profiling is therefore currently incomplete (Dorje *et al.*, 1991).

1.6.2 Distribution of mAChRs within the mammalian CNS

Determining the distribution (and localisation) of mAChR subtypes within different brain tissues has historically proven difficult, due to a lack of specific probes. Consequently, binding studies using radiolabelled forms of known mAChR antagonists such as ^{3}H-pirenzepine have been most frequently performed (Buckley, 1990). More effective and specific studies have subsequently been carried out using polyclonal antibodies raised against the third intracellular loop of the mAChR receptor, known to be the least conserved domain within the mAChR family, and has consequently provided the greatest degree of differentiation between the known subtypes (Levey *et al.*, 1991) (Dorje *et al.*, 1991). A number of tissue types have now been examined using this technique and, pertinent to this present study, it has been shown that the M1, M2 and M4 mAChR subtypes are expressed in significant numbers in the olfactory bulbs, olfactory tubercle and piriform cortex of the adult rat (Caulfield, 1993).

1.6.3 Biochemical mechanisms affected by mAChR activation

It is generally understood that agonist activation of mAChRs results in coupling of the receptor to a heterotrimeric G-protein, leading to activation of the GDP-bound G_{α} subunit of the G-protein through loss of GDP, binding of GTP, uncoupling of the receptor/β-γ complex and dissociation of the agonist. The activated G_{α} subunit may then stimulate an enzyme, generate a second messenger or directly interact with an ion channel (Birnbaumer *et al.*, 1990). However, another report has suggested that activation of some effector mechanisms may occur via the β-γ complex thereby affecting the enzymes phospholipase-C or adenylyl cyclase (Kobayashi *et al.*, 1990). It has also been shown (Hulme *et al.*, 1990) that the third intracellular loop, termed i3, of

the mAChR is critical to G-protein coupling function since experiments exchanging the i3 section of the M2 mAChR subtype with that of the M3 mAChR produce a different G-protein-mediated effect (Levey *et al.*, 1992). Additionally, G-proteins can have a reciprocal action upon the mAChR themselves where G-protein activation may lead to phosphorylation of the mAChR itself, thus modulating its activity in the absence of any external influence (Haga & Haga, 1990). The M1, M3 and M5 mAChR subtypes have previously been shown to *stimulate* the enzyme phospholipase-C (PLC) via a pertussis toxin-insensitive G-protein, whilst the M2 and M4 mAChR subtypes typically *inhibit* the enzyme adenylate cyclase (AC) via a pertussis toxin-sensitive G-protein (Levey *et al.*, 1992). Again, the effector mechanism coupled to the receptor ultimately determines the result of receptor activation and the above separation of the systems to which the subtypes are coupled should not be taken as an absolute indication of function, since G-protein coupling has been shown to vary considerably from tissue to tissue (Hulme *et al.*, 1990).

Considering the typical G-protein couplings described above, activation of the M1, M3 or M5 mAChR subtypes resulting in the G-protein mediated (Katz *et al.*, 1992) activation of PLC has been shown to lead to the hydrolysis of membrane bound phosphatidylinositol 4,5 bisphosphonate, releasing inositol-1,4,5-trisphosphate (IP_3) and diacylglycerol (DAG) (Henzi & MacDermott, 1992). The release of intracellular IP_3 results in the release of Ca^{2+} from IP_3 sensitive intracellular stores responding to IP_3 receptors on the cytoplasmic side of the store's surface (Hulme *et al.*, 1990). It has been proposed that this action may be self-limiting since increased intracellular Ca^{2+} levels reduce the affinity of IP_3 for the IP_3 receptors on the surface of the stores (Ferris & Snyder, 1992). The exact mechanism by which Ca^{2+} is released is as yet unknown (although the initial phase is known to be mediated by IP_3), this is then followed by a *'plateau'* phase where Ca^{2+} levels are maintained by the influx of extracellular Ca^{2+} into the cell (but not via voltage-gated Ca^{2+} channels). This plateau phase may exist to replenish intracellular stores depleted by IP_3 stimulated Ca^{2+} release during the initial phase and may also be facilitated by IP_3 (Putney, Jr. *et al.*, 1989). Interestingly, the activation of mAChRs has been suggested to cause the opening of Ca^{2+} channels producing the Ca^{2+} influx during this latter plateau phase (Felder *et al.*, 1992).

1.6.4 Functional effects following mAChR activation

It is known that all four of the natively expressed mAChR subtypes (m1-m4) are expressed in the mammalian cortex (Buckley *et al.*, 1988; Vilaro *et al.*, 1990a) and the

presence of cholinergic pathways within the CNS has been well documented and has been particularly well illustrated in studies of the pathway from the septum to the hippocampus (Cole & Nicoll, 1984). Here, a specific cholinergic slow excitatory postsynaptic potential (EPSP) (and associated underlying current) has been studied and shown to be sensitive to the anticholinesterase, physostigmine and the mAChR antagonist, atropine. The consensus view is that the postsynaptic actions of ACh typically only arise under conditions of high neurotransmitter concentration generated by repeated high frequency stimulation, thus making them of particular interest within the area of epilepsy where burst firing creates conditions such as these. Membrane depolarization, as a result of mAChR activation, has also been demonstrated in a number of cell types and tissues (Brown *et al.*, 1997) such as the locus coeruleus (Egan & North, 1985), substantia nigra, ventral tegmentum (Lacey *et al.*, 1990), the hippocampal CA1 region (Pitler & Alger, 1990), amygdaloid pyramidal cells (Washburn & Moises, 1992), nucleus accumbens (Uchimura & North, 1990) and the piriform cortex (Postlethwaite *et al.*, 1998a) and is generally due to a decrease in K^+ conductance and mediated by the M1 mAChR subtype, although in some tissues the remaining mAChR subtypes may also be involved. mAChRs have also been shown to be expressed *presynaptically* in neurones of the CNS where they act not only as autoreceptors, inhibiting the release of ACh from cholinergic presynaptic boutons, but also inhibit the release of other neurotransmitters such as glutamate and GABA (Starke *et al.*, 1989). Studies using antagonist profiling techniques have suggested that mAChR-mediated modulation of ACh release is likely to be mediated by the M2 mAChR subtype (Caulfield, 1993), whilst the mAChRs affecting the release of other neurotransmitters have been shown to be principally mediated by the M1 mAChR subtype (Raiteri *et al.*, 1984) and decreased glutamate release (Marchi & Raiteri, 1989), with the M2 mAChR subtype causing decreased GABA release being an exception (Raiteri *et al.*, 1990). Prior studies have reported difficulties in precisely determining the mechanisms involved in mAChR-mediated presynaptic modulation of neurotransmitter release due to the probability, in brain slice preparations particularly, that the effects seen are likely to be composed of a direct agonist effect and indirect effects upon connecting neuronal links. Thus far, it has been suggested that presynaptic mAChR activation may lead to a reduction in the opening of voltage-gated Ca^{2+} channels, involved in neurotransmitter release, although the possibility that modulation may be mediated by a presynaptic increase in K^+ conductance still remains (Scholz & Miller, 1992). A clear example of such modulation of synaptic transmission by different

mAChR subtypes was reported in interconnected cultured cortical cells, where ACh was shown to suppress both inhibitory and excitatory postsynaptic potentials. Here, EPSP suppression was found to be modulated by the M4 mAChR subtype whilst IPSP suppression was found to be mediated by the M1 mAChR subtype (Kimura & Baughman, 1997).

1.6.5 mAChR-mediated modulation of neuronal ionic currents

The activation of mAChRs has previously been shown to also modulate a number of significant postsynaptic cellular membrane currents such as the M-current ($I_{K(M)}$). This is a non-inactivating, voltage-gated K^+ current that switches on slowly at membrane potentials more positive than –70 mV (Brown & Adams, 1980) and acts to oppose depolarizing influences upon the cell at resting potential. It has been demonstrated in sympathetic neurones, the hippocampus, the piriform cortex and spinal cord neurones (North, 1989a) and is reversibly inhibited following mAChR activation, allowing easier depolarization and action potential firing by affected neurones (Adams *et al.*, 1982; Dutar & Nicoll, 1988a). In addition to the M-current, mAChRs also affect the K^+ leak conductance ($I_{K(LEAK)}$) (Womble & Moises, 1992), a membrane potential independent non-inactivating K^+ conductance that reverses at the K^+ equilibrium potential (E_K). It is inactivated following mAChR activation and its modulation has been attributed to the M1 mAChR subtype since its inhibition is potently anatagonised by pirenzepine (North, 1989b). Another current affected by mAChR activation is the Ca^{2+}-activated K^+ conductance, $I_{K(Ca)}$ that underlies the slow post-stimulus afterhyperpolarization tail current (or I_{AHP}), a K^+ conductance activated by increased intracellular Ca^{2+} concentrations arising from Ca^{2+} influx through voltage-gated Ca^{2+} channels, operating during action potentials and leading to hyperpolarization. mAChR agonists have been shown to reversibly inhibit this current leading to more frequent cell firing during a depolarizing stimulus (decreased spike accommodation). Since this current is activated by Ca^{2+}, it has been suggested that $I_{K(Ca)}$ may be a consequence of I_{Ca} (see below). The M1 (and possibly M4) mAChR subtypes have been implicated in the modulation of this current (Galligan *et al.*, 1989). A number of studies have also reported hyperpolarizations in response to muscarinic stimulation (McCormick & Prince, 1986) (Egan & North, 1985) and this effect has been proposed to be due to increased K^+ conductance, similar to that produced by ACh in cardiac pacemaker cells. Studies thus far have shown that this effect is likely to be a result of activation of mAChR subtypes other than M1 or M4 (Egan & North, 1985) (McCormick & Prince, 1986) since it is

demonstrably pertussis toxin (PTX) sensitive. mAChR agonists have been shown to inhibit voltage-gated Ca^{2+} currents (I_{Ca}) in sympathetic, parasympathetic and CNS neurones (Caulfield, 1993). An inhibition that has been shown, using antagonist profiling techniques and mRNA Northern blots, to be M2 (Allen & Brown, 1993) or M4 (Caulfield & Brown, 1991) mAChR subtype-mediated. Finally, the fast, transient outward current (I_A), the fast, inward rectifying current ($I_{K,IR}$) (Brown, 1990)) and some inward calcium currents (Gahwiler & Brown, 1987; Scanziani *et al.*, 1995) are also affected following mAChR activation.

1.6.6 Muscarinic responses in the piriform cortex

As previously stated, the presence of mAChRs in the mammalian brain has been known for some time and binding studies have shown that they are present at both presynaptic and postsynaptic locations (Weinstock, 1997). The slow depolarizing effect following mAChR activation in the cortex was also reported a long time ago, since the early experiments using iontophoretic techniques to apply ACh directly onto the cortex in cats, *in vivo*, showed a distinct, long duration, excitatory response (Krnjevic, 1986). This characteristically slow muscarinic response was subsequently confirmed using *in vitro* intracellular recording techniques, and shown to be associated with a slow decrease in resting membrane potential, an increase in input resistance and an intense neuronal discharge (McCormick & Prince, 1986). These effects were originally considered to be due to a decrease in resting K^+ conductance but subsequent studies have shown that cortical mAChR activation suppresses a number of different cellular ionic currents (Section 1.6.5). Additionally, some cortical neurones exhibit a slow, post-stimulus after-depolarization (sADP; Section 1.2.2.4) following a train of action potentials in the presence of a mAChR agonist. In the olfactory cortex, the sADP is believed to be mediated by an underlying calcium-sensitive potassium current ($I_{K(ADP)}$) that can be resolved using the *'hybrid'* voltage clamp technique (Constanti *et al.*, 1993; Lancaster & Adams, 1986). This phenomenon is considered important in sustaining the muscarinic agonist-induced depolarization seen in piriform cortical deep pyramidal neurones (Constanti & Bagetta, 1991; Libri *et al.*, 1994), but its contribution to the muscarinic agonist-induced epileptiform bursting seen in immature deep olfactory pyramidal cells is still unclear (Postlethwaite *et al.*, 1998a).

1.6.7 Juvenile onset epilepsy and the characteristics defining mAChR agonist-induced epileptiform discharges in immature, deep pyramidal piriform cortical neurones

A significant proportion of the human epilepsies initially manifest whilst the brain is still developing (Bocti *et al.*, 2003; Cowan, 2002; Klein *et al.*, 2003), and a number, such as infantile spasms, only manifest during specific developmental stages (Kellaway *et al.*, 1979). A number of animal models also exhibit specific developmental periods of heightened seizure susceptibility (Johnston, 1996); it is thus clear that there is a significant requirement for well documented, well understood *in vivo* and *in vitro* models of epileptiform behaviour with a juvenile onset, in order to provide a more comprehensive framework around which further research into their causes and treatments may be based. Consequently, the *in vitro* model of mAChR agonist-induced epileptiform bursting described in immature deep pyramidal cells of the piriform cortex, (Postlethwaite *et al.*, 1998a) represents a potentially useful tool to improve our understanding of the factors influencing juvenile seizure states. In adult deep pyramidal neurones of the rat piriform cortex, using conventional intracellular recording techniques, the application of the mAChR agonist, OXO-M typically results in a sustained membrane depolarization, onset of repetitive firing, increased membrane input resistance and the appearance of a slow post-stimulus sADP. Critically, in the same slice preparation taken from immature animals (postnatal days 14-24), the changes in membrane potential, membrane input resistance and sADP generation produced by OXO-M remained the same as in the adult, but repetitive firing was replaced by *'spontaneous rhythmic epileptiform activity'* (Postlethwaite *et al.*, 1998a). Additionally, EPSPs elicited following stimulation by a bipolar stimulating electrode situated in layer II/III were found to be suppressed following mAChR activation in the adult slice preparation, but were conversely *prolonged* in the immature preparation. These novel responses elicited from the immature preparation were all abolished or reduced on application of the fast Na^+ channel bloker tetrodotoxin (TTX), the mAChR antagonists, atropine or pirenzepine, the glutamate antagonists CNQX (non-NMDA receptor) or DL-APV (NMDA receptor), or the sedative barbiturate, pentobarbitone, whilst conversely, application of the $GABA_AR$ antagonist, bicuculline was found to facilitate epileptiform burst firing and the prolongation of excitatory synaptic transmission (Postlethwaite *et al.*, 1998a). However, despite this basic pharmacological profiling of the bursting phenomenon in this report, the elucidation of a definitive underlying mechanism for its generation remained elusive. One of the principal aims of the present study is to

determine what developmental change(s) could be occurring in the immature piriform cortex that could be contributing towards its heightened susceptibility towards mAChR-induced epileptiform bursting.

1.6.8 The apparently contradictory effects of mAChR activation in the mammalian cortex; suppressed synaptic transmission yet increased postsynaptic excitability

The mammalian cortex is known to be innervated by a dense population of cholinergic fibres arising from the basal forebrain; however, this innervation is diffuse in nature and has little postsynaptic density (Eckenstein *et al.*, 1988) indicating a predominantly presynaptic role, where mAChR activation suppresses both inhibitory and excitatory synaptic potentials (Hasselmo & Bower, 1992; Williams & Constanti, 1988a). This fact, coupled with observations from electrophysiological experiments that mAChR activation typically produces a sustained postsynaptic depolarization in a number of different cortical cell types (Caulfield, 1993) portrays the cortical role of ACh in a somewhat contradictory light; a cell will be depolarized, by the direct postsynaptic action of ACh upon muscarinic AChRs, increasing excitability, but the presynaptic action of ACh will also inhibit synaptic transmission between these cells. This inhibitory effect of ACh upon synaptic transmission has also been demonstrated as being dependent upon the synaptic input source to the cell; inputs to the neocortex, arising from intracortical connections have been shown to be inhibited preferentially to extracortical inputs (Gil *et al.*, 1997), an interesting parallel to the results obtained in studies of similar behaviour in the piriform cortex (Section 1.2.3.5) described previously (Hasselmo & Bower, 1992). This selective mAChR-mediated modulation of synaptic inputs allows the brain to allot new sensory stimuli a greater probability of affecting the neuronal circuitry (the postsynaptic excitability of which has simultaneously been increased) than stimuli from existing pathways. Consequently, it is reasonable to suggest that a breakdown of the presynaptic inhibitory action of ACh, but not the postsynaptic excitatory role could give rise to a positive feedback loop within the relevant neuronal circuitry that may manifest as epileptiform behaviour.

1.7 Age-related changes in the piriform cortex and their effect upon pharmacological responses

Practically all mammalian neural systems show progressive developmental changes from birth into old age (Milburn & Prince, 1993), (Gaiarsa *et al.*, 1995), (Gaiarsa *et al.*, 1994), (Araki *et al.*, 1996) and consequently it was not unexpected to find such changes

occurring throughout the cortex. It has previously been shown that the density of mAChRs changes most rapidly postnatally in the medulla pons, with a slower rate of development occurring in the cortex, basal ganglia and hippocampus (Hohmann *et al.*, 1985; Kuhar *et al.*, 1980). It has also been found that mAChR agonist affinity for mAChRs also changes postnatally (Soreq *et al.*, 1982), illustrated by the rat cerebellum undergoing a 20 fold increase in affinity for ACh in the 30 days following birth. This change in affinity is also accompanied by changes in the cellular localization of mAChRs (Rotter *et al.*, 1979), where mAChRs have been found in larger numbers in the granular layer than in the Purkinje or molecular layers. Additionally, it was also found that the neonatal destruction of cerebellum granular cells resulted in a massive increase in mAChR affinity for ACh by the 12^{th} postnatal day (Soreq *et al.*, 1982) and mAChRs have also been found to develop in patches in the basal ganglia of neonatal rats (Rotter *et al.*, 1979) which only become more evenly distributed by postnatal day 10. Additionally, the mechanisms governing ACh breakdown also show developmental variation, as illustrated by the observation that although cholinesterase-rich regions are seen in neonatal cats, they disappear to be replaced by a more uniform distribution as the animal matures (Graybiel *et al.*, 1981). Interestingly, two different mAChR types have been isolated from the rat olfactory bulb and cortex, one of which has a high affinity for agonist and larger molecular weight, whilst the other has a lower affinity for agonist and a smaller molecular weight (Large *et al.*, 1986). At birth, the receptor types are found in equal proportions, but this changes as the animal matures until only the larger molecular weight, higher affinity type remains. A process similar to this has also been noted in the human foetal brain, where three different mAChR types have been found that eventually achieve an equilibrium by birth (Large *et al.*, 1985). mAChR density has also been shown to increase at a variable rate postnatally, independent of whether the area developing is designated to become a highly cholinergic area or not. For example, the rat cortex and midbrain are known to exhibit a high density of mAChRs and have been shown to develop faster than the cerebellum, that exhibits a lower density of mAChRs (Egozi *et al.*, 1986). It has also been found that the expression of mAChRs and acetylcholinesterase activity are controlled by two distinct, unconnected mechanisms in young animals, where expression is modulated according the development of necessary cholinergic pathways, whilst acetylcholinesterase activity was found to be independent of this (Egozi *et al.*, 1986). Since epileptiform behaviour is generally understood to arise from an imbalance between neural inhibitory and excitatory mechanisms (Loscher & Ebert, 1996), it is clear from these examples of

developmental change in the cholinergic systems described above could give rise to such imbalances. Changes in receptor localisation, the affinity of mAChRs for ACh, variability in mAChR expression rates in different areas and also changes associated with acetylcholinesterase activity all describe neural systems that exist in a more dynamic state than the adult animal, thereby making it more prone to seizure generation. At present, it cannot be definitively stated which area of developmental change may give rise to the mAChR agonist-induced epileptiform behaviour seen in the immature, but not adult piriform cortical slice preparation (Postlethwaite *et al.*, 1998a). Any variations in the characteristics of the sADP between adult and immature deep pyramidal piriform cortical neurones are also due consideration alongside variations in burst incidence since that has also been clearly demonstrated to be mAChR-mediated. Consequently, when considering developmental variations in burst firing and sADP generation, it is changes in mAChR population density and proportional numbers of different mAChR subtypes in young animals that are of particular interest, since mAChR populations have been shown to reach adult levels by the 28th postnatal day (Tice *et al.*, 1996). In addition to the fact that the overall number of mAChRs present, or of a particular subtype, or indeed the proportion of mAChR subtypes present may change developmentally, the function of the mAChRs themselves may change, resulting in changes in the effector mechanisms to which they are coupled and therefore changes in the consequential cellular effect following their activation. It has been demonstrated that the M2 and M4 mAChR subtypes increase in number in rats postnatally to the fourth postnatal week (Tice *et al.*, 1996), a change that would obviously affect cellular responses following mAChR activation in young animals (Kimura & Baughman, 1997). Phosphoinositol turnover is another system that has previously been linked with mAChR function in the cortex and has also been shown to change developmentally (Gonzales & Crews, 1984), whilst another second messenger system also worthy of consideration is cyclic-AMP, since it is known that adenylate cyclase levels decrease with increasing age, suggesting an increased tendency towards excitability in younger animals (Araki *et al.*, 1995).

1.8 Gap junction function and distribution

Since the first report describing electrotonic junctions in the giant motor synapse of the crayfish (Furshpan & Potter, 1959), considerable effort has been invested in understanding the molecular structure, functions and purposes of electrotonic (gap junction-mediated) transmission (Bruzzone, 2001). Gap junctions are formed by two

linked connexons, each of which comprises a proteinaceous cylinder with a central hydrophilic channel composed of hexamers of connexin (Cx) proteins. The linked connexons are ~2 nm in diameter and, with their ends aligned, form a functional channel linking two proximal cells and permitting not only cytoplasmic continuity but also the passage of ionic current and small molecules between the cells (Li *et al.*, 2001). Open gap junction channels have also been shown to significantly increase synchronous activity between linked neurones by virtue of their gap junction-mediated electrotonic coupling. Consequently, an upregulation of such coupling has previously been proposed as a possible mechanism by which epileptiform activity might be generated and/or synchronised (de Curtis *et al.*, 1998). A number of details describing gap junction expression in the mammalian CNS have been experimentally determined, with the gap junction proteins Cx43, 32, 26 and 36 all having been characterised in CNS neurones (Condorelli *et al.*, 1998) and interestingly, the gene found to code for connexin-36 is located in an area linked to a form of familial epilepsy (Belluardo *et al.*, 1999). These studies have found that connexin protein expression is not only cell and brain region specific, but, most critical to this present investigation, also developmentally specific (Li *et al.*, 2001). Gap junctions have been shown to exist (in adult and immature rats) in both the olfactory bulbs (Reyher *et al.*, 1991) and cortex (Teubner *et al.*, 2000) and are known to play a significant role in high-frequency network oscillations (Maier *et al.*, 2002) and the onset and maintenance of epileptiform activity in a number of brain areas, such as the adult guinea pig piriform cortex (de Curtis *et al.*, 1998), adult and immature rat hippocampus (Traub *et al.*, 2002; Uusisaari *et al.*, 2002), adult rat dentate gyrus (Schweitzer *et al.*, 2000) and adult rat amygdala (Elisevich *et al.*, 1998). In human epilepsies, gap junctions have been linked to complex partial (Elisevich *et al.*, 1997a), intractable (Lee *et al.*, 1995), mesial temporal lobe (Fonseca *et al.*, 2002) and other seizures (Li *et al.*, 2001; Naus *et al.*, 1991). These findings have led to gap junction blockers being proposed as potential anticonvulsants (Margineanu & Klitgaard, 2001). Given that the mechanism underlying mAChR agonist-induced epileptiform bursting in the immature piriform cortex is still unknown, it remains a reasonable proposition that changes in gap junction expression or function may play a role in this phenomenon.

1.9 Aims and objectives of the present work

1. The principal aim of this thesis project was to identify and investigate the mechanism(s) underlying the previously reported mAChR agonist-induced epileptiform burst firing phenomenon (Postlethwaite *et al.*, 1998a). This was done using conventional 'sharp' intracellular recordings made from deep pyramidal neurones in transverse slices of rat piriform cortex, taken from both adult and immature (P+14 to P+30) rats. Although the specific approaches used in this investigation changed slightly as a result of data obtained from ongoing experiments, the original objective of the project remained the same and consequently, the following areas were investigated in detail:
2. A comparison of the electrophysiological properties and muscarinic responsiveness of both adult and immature piriform cortical neurones in order to confirm the results of prior reports and satisfactorily identify targeted cell types.
3. An examination of a larger population sample of neurones exhibiting mAChR agonist-induced burst firing in order to more accurately characterise the bursting phenomenon.
4. A determination, using anticholinesterases, of whether sufficient endogenous cholinergic 'tone' existed in the piriform cortical slice preparation to induce epileptiform behaviour without the use of a mAChR agonist.
5. A comparison of afferent and intrinsic excitatory synaptic transmission in both the adult and immature piriform cortical slice preparations in control conditions and in the presence of a mAChR agonist. Muscarinic receptor subtype-specific antagonists were also used to identify the presynaptic mAChR subtypes responsible for the developmental variation in effects following mAChR activation.
6. The same comparison as in (4) was also performed upon pharmacologically-isolated fast, $GABA_AR$-mediated synaptic transmission.
7. A confirmation of the presynaptic nature of the mAChR-induced effects on synaptic transmission in (4) and (5) using standard paired-pulse stimulation techniques.
8. The use of gap junction blockers in order to investigate any possible involvement of electrotonic transmission in the mAChR agonist-induced epileptiform bursting phenomenon.
9. The use of microlesions to isolate specific areas of the slice preparation and thereby remove certain synaptic inputs/outputs, in order to determine their role in generating/sustaining the bursting phenomenon.

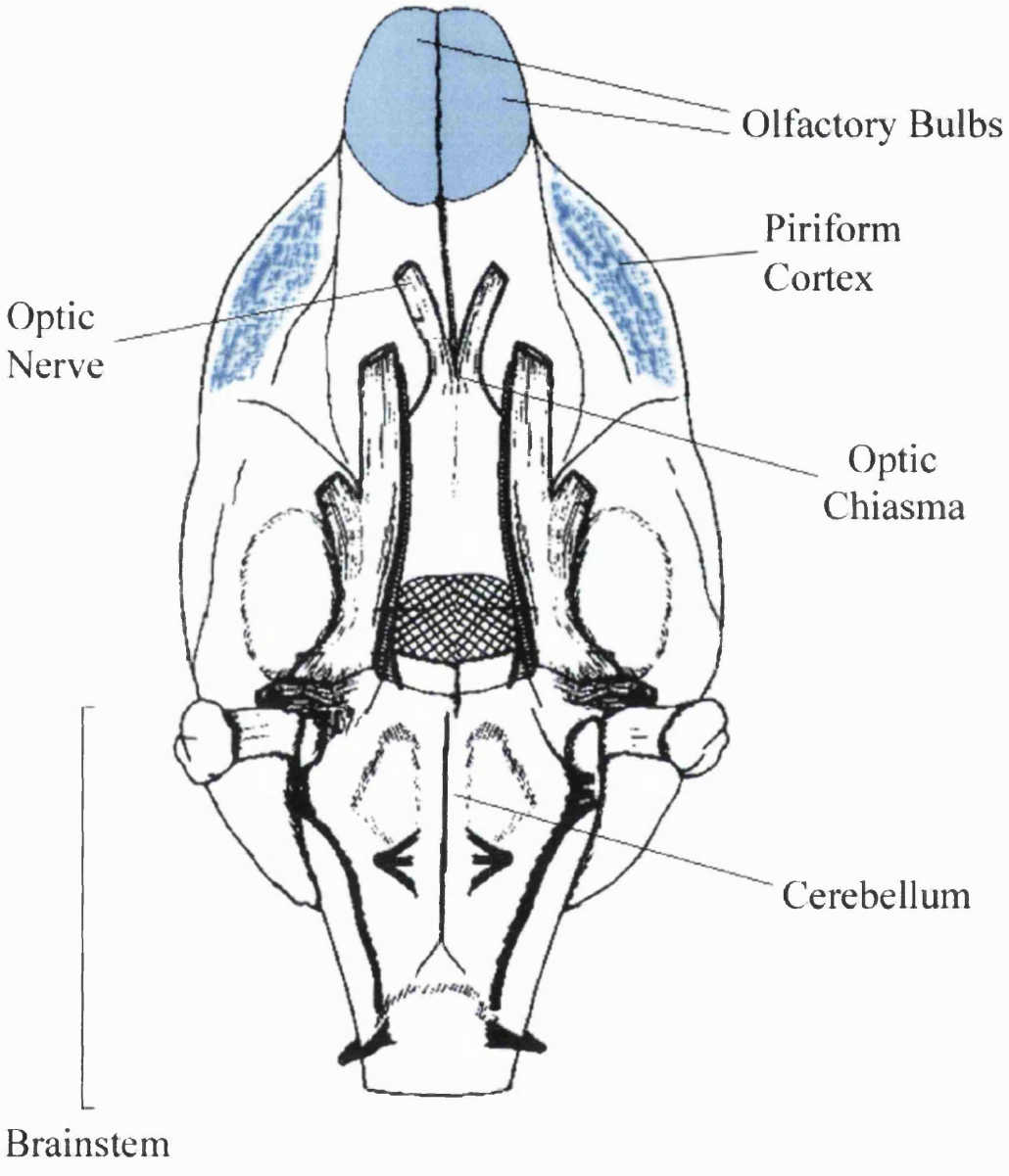
Olfactory Bulbs
Piriform Cortex
Optic Nerve
Optic Chiasma
Cerebellum
Brainstem

Figure 1.1

Figure 1.1

The location of the piriform cortex (shaded area) of the rat, seen from the underside of the brain (Modified from (Olds, 1979)).

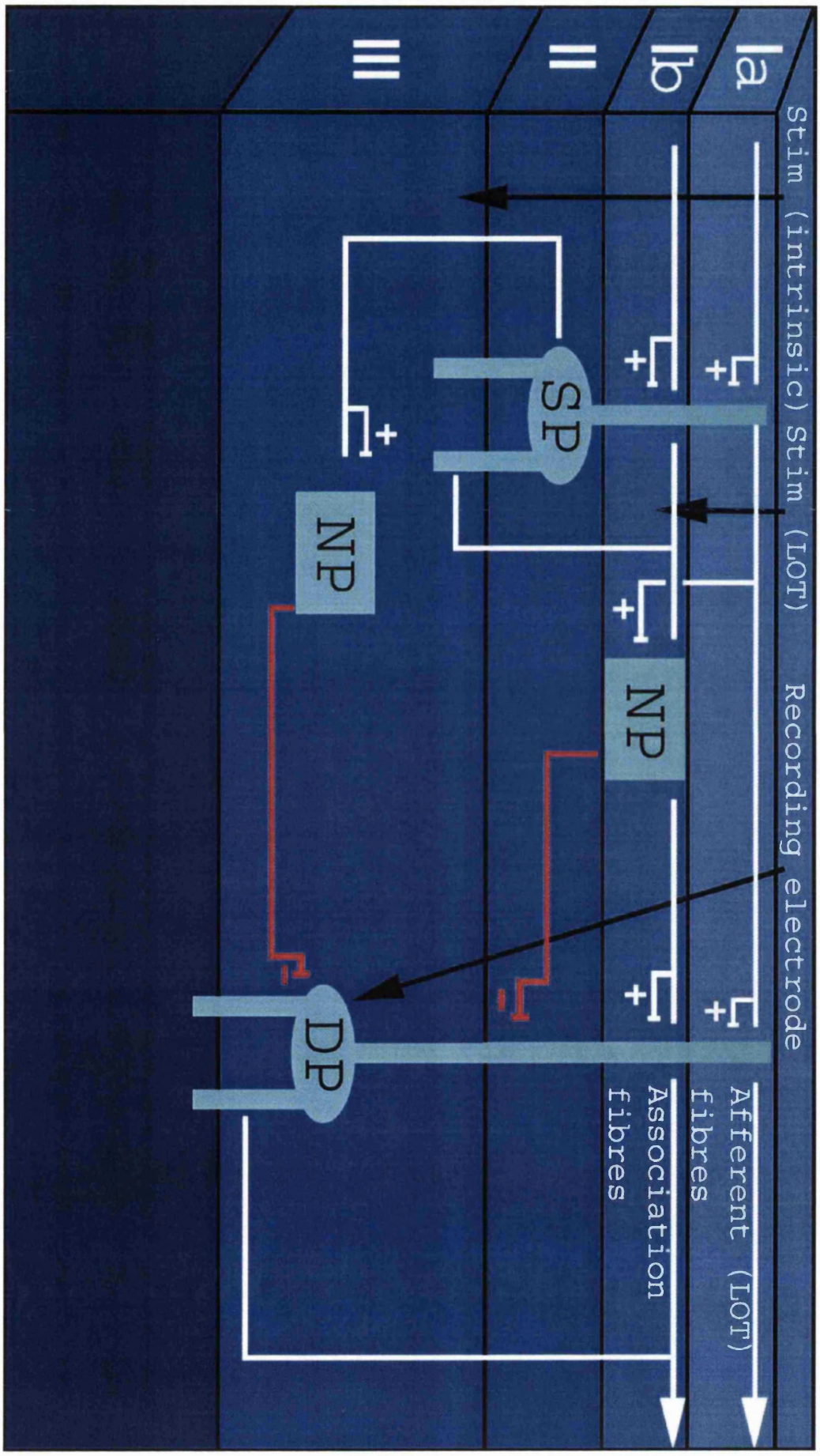
Stim (intrinsic)
Stim (LOT)
Recording electrode
Ia
Ib
II
III
SP
NP
NP
DP
Afferent (LOT) fibres
Association fibres

Figure 1.2

Figure 1.2

A simplified diagrammatical representation of the principal cell types and their synaptic connection in the transverse piriform cortical brain slice preparation used in this present study. The relative positions of deep pyramidal neurones (**DP**), superficial pyramidal neurones (**SP**) and non-pyramidal interneurones (**NP**) are shown, together with the positions of the two bipolar stimulating electrodes (in layers I and II/III) used to elicited postsynaptic potentials and the locations of the afferent and association fibre systems. Excitatory synaptic connections are shown in **white** and inhibitory synaptic connections are shown in **red**. Afferent fibres of the lateral olfactory tract (**LOT**), carrying odour-encoded information stimulate the apical dendrites of (deep (**DP**) and superficial (**SP**)) pyramidal neurones and non-pyramidal inhibitory interneurones (**NP**; that synapse with pyramidal neurones, setting up feed-forward inhibition). The stimulated pyramidal neurones in turn, stimulate inhibitory interneurones (that consequently synapse with the same or other pyramidal neurones, setting up feed-back inhibition) and/or other pyramidal neurones via the **intrinsic** (intracortical) **and association** (cortico-cortical) **fibre systems** that arise primarily from the basal dendrites of the pyramidal neurones. (Representation adapted from (Hasselmo & Bower, 1992).)

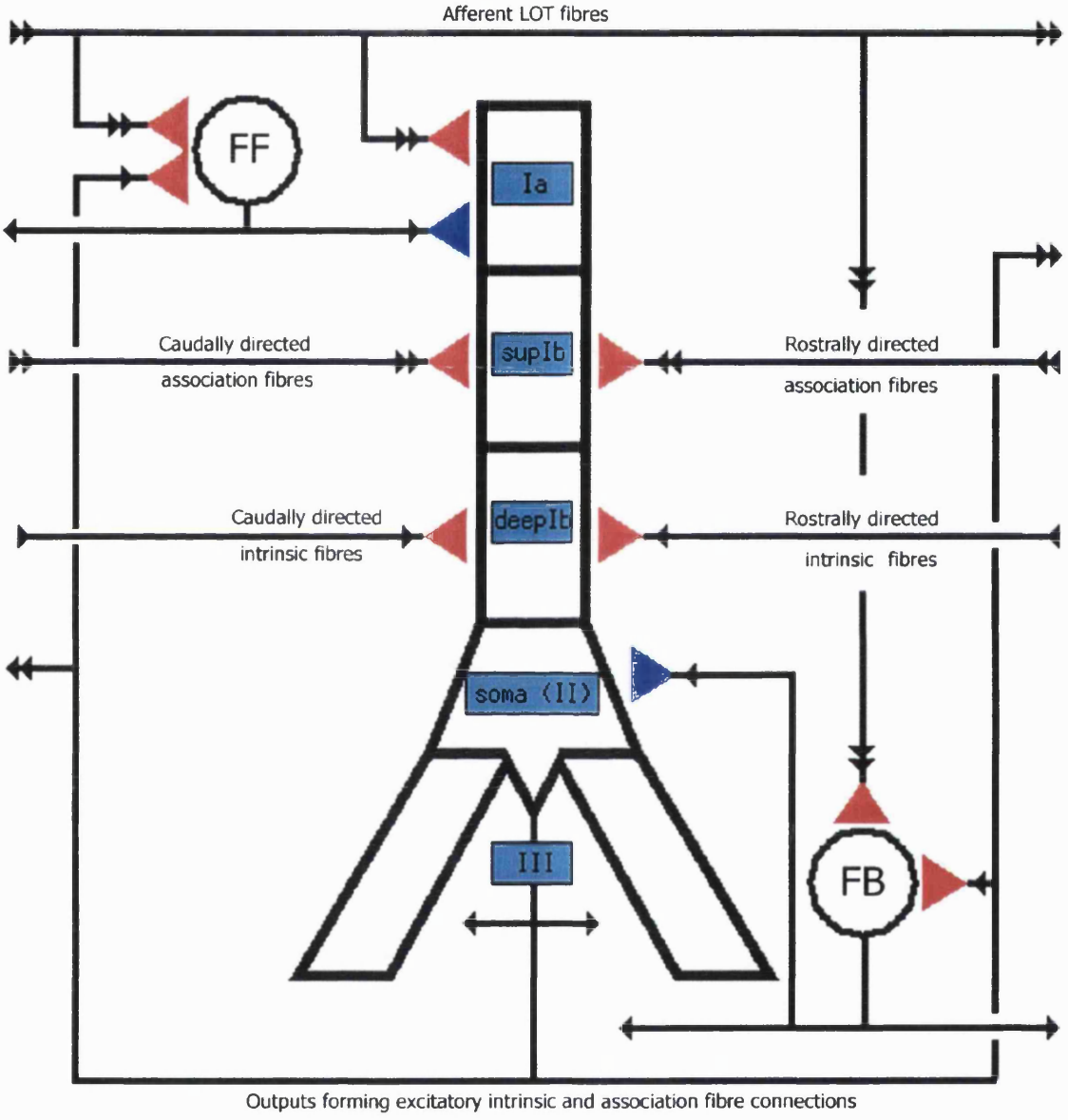
Afferent LOT fibres
FF
Ia
supIb
deepIb
Caudally directed
association fibres
Rostrally directed
association fibres
Caudally directed
intrinsic fibres
Rostrally directed
intrinsic fibres
soma (II)
III
FB
Outputs forming excitatory intrinsic and association fibre connections

Figure 1.3

Figure 1.3

A simplified diagrammatical representation of the principal excitatory and inhibitory synaptic connections affecting deep and superficial pyramidal neurones of the mammalian piriform cortex. The compartmentalisation of the pyramidal cell displays the location of the respective parts of the cell within the laminar structure of the piriform cortex and the locations of the synaptic connections it receives. Legend: **Red** triangles indicate excitatory synapses, **blue** triangles indicate inhibitory synapses. **Ia** – layer Ia; **supIb** – superficial layer Ib; **deepIb** – deep layer Ib; **II** – layer II; **III** – layer III; **FF** – feed-forward inhibition; **FB** – feed-back inhibition. Arrowed lines indicate the direction of synaptic transmission. Adapted from http://www.bbb.caltech.edu/GENESIS/illtuts/piriform.html (Wilson & Bower, 1989).

Chapter 2:
Materials & Methods

2.1 Olfactory cortex brain slice preparation

Rostrocaudal piriform cortical brain slices were prepared from adult (P>40) and immature (P+14 to P+25) Sprague-Dawley rats (of either sex) that included the afferent inputs from the lateral olfactory tract (LOT) and the underlying cell layers to be recorded from (Fig. 1.2), as previously described in the methods of Constanti (Constanti & Sim, 1987a). The animals were first anaesthetised with halothane (May & Baker, Dagenham, U.K.) and rapidly decapitated with sharp secatueurs (or scissors, in the case of immature animals). All procedures were performed in accordance with Home Office regulations as set out in the Animals (Scientific Procedures) Act 1986. Immediately following decapitation, the brain was carefully exposed by removal of the skull and meninges (from the lambda to the bregma) with forceps. The olfactory bulbs were then separated from the brain and the optic nerves severed, each with a single scalpel cut and the brain removed from the skull with a spatula onto a piece of filter paper moistened with Kreb's solution and placed over a cooled inverted Petri dish. The brain was then bisected longitudinally with a razor blade to separate the two hemispheres. One hemisphere was placed in oxygenated ice cold Kreb's (for later slicing) and from the other, a rectangular block of tissue was cut containing the areas of interest detailed above. The block of tissue was then mounted on the teflon stage of a Campden Vibroslice-752M tissue cutter (Fig. 2.3B; Campden Instruments, U.K.) and affixed using cyanoacrylate glue (Loctite Ltd, Cheshire, U.K.). The stage and tissue were transferred to the tissue cutter bath containing ice cold (4°C) oxygenated Kreb's solution where ~450 μm thick slices were cut, along the axis of the lateral olfactory tract and perpendicular to the pial surface of the brain (Figs. 1.2 & 2.3B).

The slices were carefully transferred by glass pipette from the tissue cutter bath to a suitable vessel containing oxygenated Kreb's and stored at 32°C. Slices were left to recover and stabilise for 30 minutes to 1 hour after cutting before transferral to the recording chamber. The composition of the modified Kreb's solution used was (mM): NaCl 118; KCl 3; $NaHCO_3$ 25; $MgCl_2.6H_2O$ 1; $CaCl_2$ 2.5 and D-glucose 11. All drug solutions were continuously bubbled with 95% O_2: 5% CO_2 and maintained at a pH of 7.4. All reagents for the preparation of Kreb's solution were obtained from BDH (BDH, U.K.)

2.2 Maintenance of brain slices during recording

The methods used for brain slice maintenance during recording in this study were based upon those described by Constanti (Constanti *et al.*, 1993; Constanti & Sim, 1987a; Postlethwaite *et al.*, 1998a). Following recovery, and for recording purposes, slices

were carefully transferred by glass pipette to the recording chamber, illuminated from below by a Schott KL1500-T fibre optic light, held in place between two nylon meshes and superfused at ~10 ml min^{-1} (bath fluid exchange period of ~30 seconds) with modified Kreb's constantly maintained at 29-30°C and monitored by a temperature probe (Figs. 2.1 & 2.2B). The Kreb's solution was circulated through the system with a Watson-Marlow peristaltic pump (Falmouth, UK) from an external reservoir that was maintained at room temperature and continuously oxygenated. The pump (Fig. 2.3A) fed Kreb's through fine polythene tubing via a perspex bubble trap (Fig. 2.3A; preventing bath fluid level changes caused by the peristaltic pump), through the thermostatically controlled heater (Fig 2.3A) and into the recording chamber. The same pump removed Kreb's from the recording chamber via an outlet pipe that exited either into waste or recirculated into the reservoir container, depending upon experimental circumstances.

2.3 Electrophysiological recording

2.3.1 Microelectrode preparation

Intracellular recording electrodes were prepared from GC100F-15 glass capillary tubes (1.0 mm outer diameter, 0.58 mm inner diameter, with inner filament; Clark Electromedical Instruments (Pangbourne, Reading, UK)) using a Narashige PN-30 electrode puller (Narashige, Japan; Fig. 2.4) and were filled with 4 M potassium acetate (Kac adjusted to pH 7.4 with glacial acetic acid; for recording from slices from adult animals) or 2 M KAc (for recording from slices from immature animals). Different electrolyte concentrations were used as previous studies have shown that higher (>2M Kac) concentrations have a detrimental effect upon the health of the impaled neurone (Libri *et al.,* 1998). Initial tip resistances for the electrodes ranged from 40-60 MΩ (for 4 M KAc filled electrodes) or 50-80 MΩ (for 2 M KAc filled electrodes). Microelectrodes not within these ranges were routinely discarded.

2.3.2 Amplifier modes and apparatus used in recording

Microelectrodes were connected to an Axoclamp 2A (Fig. 2.2A; Axon Instruments, Foster City, CA.) current-voltage preamplifier, via an Axon HS-2L headstage unit (Fig. 2.2B) with the recording circuit being completed by a hand-made bath electrode consisting of a silver/silver chloride pellet (Clark Electromedical Instruments; Fig. 2.1B). The amplifier permitted recordings in current clamp, discontinuous current clamp (DCC) or single electrode voltage clamp (SEVC) modes. The most commonly used

recording technique (and the method most frequently used in these experiments) was current-clamp, whereby the potential (and changes in potential) inside the cell were measured. This technique is also frequently referred to as 'bridge' or 'voltage-follower' mode, the former in reference to the technique's use of a standard electrical Wheatstone bridge in its circuitry.

2.3.3 Current clamp recording

The microelectrode was attached to a unity gain buffer amplifier (Fig. 2.5A) via a silver/silver chloride-coated wire. The input resistance of the FET operational buffer amplifier was many orders of magnitude larger than that of the microelectrode and cell (~10 GΩ). Accordingly, the output of the amplifier followed the changes in cellular potential and the attachment of a current source to the input of the buffer amplifier (Fig. 2.6A) permitted current injection into the cell through the microelectrode, since the high resistance of the amplifier negated current flow in any other direction. Thus current commands could be applied to depolarize or hyperpolarize the recorded cell via the single recording microelectrode. However, this arrangement does not permit measurement of accurate cellular potential changes, since the passage of current waveforms through the microelectrode (necessary to record changes in potential) would result in corresponding artifactual potential changes across the microelectrode resistance. Thus, the resulting potential changes become combined in the output signal and cannot be easily separated from one another (i.e. $\Delta V_p = \Delta V_m + \Delta V_e$). In order to surmount this problem, the addition of another differential amplifier allows a scaled fraction (proportional to V_e) of the input current to be subtracted from the microelectrode potential (Fig 2.5Bi) leaving the output accurately representing the membrane potential. Calibration of this circuit was achieved experimentally by the application of brief repetitive current pulses (-0.25 nA; 17 Hz) through the microelectrode, whilst submerged in the bath solution. The bridge balance control was then adjusted until the steady-state pulse response was eliminated (Fig 2.5Aii) and the circuit 'balanced'. The microelectrode resistance could then be determined from the readout of the bridge balance control and the output values provided by the amplifier known to be correct. This value would ideally be in the range 40 – 80 MΩ. The addition of a resistor and another differential amplifier (in series to the circuit shown in Fig 2.6A), produced the circuit shown in Fig. 2.7A which permitted the monitoring of any voltage changes, since such changes were simply proportional to the current flowing across the resistor.

2.3.4 Discontinuous Current Clamp (DCC) recording

Some recordings made in this series of experiments required the injection of high amplitude current steps (e.g. for evoking the tail currents I_{AHP} and I_{ADP}; see section 2.5.2), a situation that would, in 'bridge' mode, cause considerable microelectrode rectification. In order to prevent this, these recordings were made in DCC mode whereby the tasks of voltage recording and current injection are performed by the same microelectrode operating on a 'timesharing' basis (Fig 2.8A). When in DCC mode, the microelectrode potential is passed to a sample-and-hold amplifier, the scaled output of which is passed to a differential amplifier where the microelectrode potential is compared to the command voltage. When the circuit is in a 'current passing' state (as illustrated by the switch states in Fig. 2.8A), the amplifier output is passed to the current source, the output of which is injected into the cell, where the output amplitude is proportional to the input received by the current source. When the circuit is switched from 'current passing' to a 'voltage recording' state (i.e. when both switches in Fig. 2.8 are switched to their alternate positions), the microelectrode potential naturally decays towards the membrane potential, at which point the microelectrode potential is measured and the circuit switched to a 'current passing' state, repeating the cycle. Calibration of the circuit is achieved by adjustment of the microelectrode capacitance neutralization on the amplifier to produce a smooth electrotonic potential in response to a 7 ms; 0.25 nA negative current pulse (the sampling frequency was typically 2-3 kHz at a 30% duty cycle). This setting was then rechecked by comparison to the electrotonic potential generated in response to the same stimulus in 'bridge' mode.

2.3.5 Data acquisition

Current and voltage data output from the amplifier was viewed using a Tektronix 5111A storage oscilloscope (Beaverton, Oregon, USA) and captured and analysed via a Digidata 1200 analog to digital interface (Axon Instruments, Foster City, CA.) installed in a PC (733MHz Viglen Contender-P3/700, Viglen Ltd., U.K.) using pCLAMP6.0.1 (Axon Instruments, Foster City, CA.) software (which was also used for post-experimental, off-line analysis) running in DOS mode under Microsoft Windows 98SE (Microsoft, Richmond, VI, USA). Records of real-time current and voltage changes were also made on a Gould RS3200 ink jet chart recorder (Gould, Cleveland, Ohio, USA).

2.4 Impalement of cells

The recording electrode was manually lowered with a Prior 83346 micromanipulator (Prior, UK) onto the surface of the slice, almost perpendicular to the plane upon which the slice rested, in the piriform layer II-III area (Fig. 1.2), as close as possible to the stimulating electrodes (determined visually from observation through a Nikon SMZ-1 binocular stereomicroscope (Nikon, Japan)). Cells were routinely impaled in 'bridge' mode by slowly advancing the electrode tip through the slice (Fig. 2.2B) until a negative deflection of the recorded potential was observed, indicating that the tip of the electrode was in contact with the soma of a cell. A very brief, large positive current step was then passed into the cell through the electrode tip by means of the 'positive clear' facility of the preamplifier, allowing the electrode tip to penetrate the soma. Alternatively, a high frequency oscillatory current could be passed through the microelectrode by manually switching from 'bridge' mode to SEVC mode (with full feedback gain applied) causing a large increase in capacitance compensation and an oscillation in the compensation circuit of the amplifier. The former method was more commonly used in this series of experiments. Immediately following impalement by either of the methods above, negative current was applied lowering the membrane potential to ~-80 mV in order to facilitate *'sealing'* of the cell membrane. The negative current was slowly removed as the cell hyperpolarized following impalement and sealing of the cell membrane around the microelectrode occurred (with the bridge balance adjusted if necessary to accommodate changes in microelectrode resistance). Cells impaled in this way usually settled within 3 to 10 minutes to a typical resting membrane potential of –80 to –85 mV, with this criterion being one of those used to determine the suitability of a cell for recording.

2.5 Measurements made from recorded neurones

2.5.1 Electrotonic properties

The electrotonic properties of cells were recorded following application of positive and negative current pulses of 0.25–1.25 nA amplitude; 160 ms duration; 2 s interval. Positive electrotonic potentials produced firing in the recorded cell when the positive pulse applied was sufficient to raise the membrane potential above the threshold for spike firing, the amplitude of which allowed confirmation of the resting membrane potential to be made (spike amplitude is considered to include an 'overshoot' of ~20 mV from 0 mV). Negative electrotonic potentials (routinely elicited in DCC mode in

order to minimise microelectrode rectification), allowed the input resistance of the cell to be calculated (using negative stimuli producing deflections of ≤20 mV; according to Ohm's law) and any rectifying cellular currents observed. Repeated (~0.5 Hz; 0.25 nA) negative electrotonic pulses were routinely applied throughout all experiments (unless otherwise noted) to continuously monitor changes in input resistance. Finally, most cells in layers II and III of the piriform cortex could be physiologically categorized and identified (Section 1.2.2) following the application of electrotonic pulses that elicited the characteristic cellular responses that enabled their identification and classification (Libri *et al.*, 1994).

2.5.2 Measurement of slow membrane currents

As previously mentioned, recordings that required a large amplitude 'priming' injection of current were performed in DCC mode. Measurement of the slow after-hyperpolarizing (I_{AHP}) and after-depolarizing (I_{ADP}) currents, underlying the slow afterhyperpolarization (sAHP) and slow afterdepolarization (sADP) respectively, were made using a combination of DCC and voltage clamp modes, termed the 'hybrid clamp' technique (Constanti *et al.*, 1993; Lancaster & Adams, 1986). To elicit these currents, a large depolarizing stimulus (+2 nA for 1.6 s) was applied to the cell whilst balanced in DCC mode (with a relatively low clamp feedback gain to avoid causing electrode oscillation) whilst the membrane potential was held close to the threshold potential for the cell (by application of positive holding current), which produced a sustained spike train. At the end of the stimulus train, the amplifier was manually switched to SEVC mode, and the cell voltage clamped at a preset potential (usually -70 mV) a few millivolts below firing threshold potential, revealing the deactivation of the current underlying the afterhyperpolarization or afterdepolarization.

2.5.3 Recording of synaptic events

2.5.3.1 Synaptic stimulating electrodes

Two bipolar stimulating electrodes, each composed of two twisted 45 μm (25 μm inner core diameter; 20 μm insulator thickness) diameter nichrome wires (insulated along their length, except at the tips and mounted on a micromanipulator; Fig. 2.1B) were attached to a Digitimer DS2 (Digitimer Ltd., Welwyn Garden, UK) isolated stimulus generator that delivered stimuli of 5 to 20 V in amplitude and 0.2 ms duration to elicit synaptic responses. The stimulus amplitude was determined by the distance of the

stimulating electrodes from the recorded cell and the type of experiment being performed (see below). All synaptic events were recorded in 'bridge' mode.

2.5.3.2 Placement of stimulating electrodes

In early experiments, a single stimulating electrode was placed in layers Ib to II (Fig. 1.2) to stimulate intrinsic and afferent fibres simulataneously. However, in later experiments, two stimulating electrodes of the same type were used; one placed near the pial surface in layer Ia and the other within layer II/III in order to independently stimulate either the LOT or intrinsic fibres respectively (Hasselmo & Bower, 1990; Hasselmo & Bower, 1992). Accurate placement of the stimulating electrodes in the appropriate layers was possible visually since the laminar segregation of the piriform cortex made layer Ia clearly distinguishable (by its greater opacity) from layer Ib, particularly in its upper, myelinated area. Additionally, the presence of a glial cell rich area between layer Ia and layer Ib allowed clear visual distinction between these layers, whilst the opacity of layer Ib also allowed accurate placement of the second electrode into the less opaque layer II (Price, 1973; Price & Sprich, 1975).

2.5.3.2 Excitatory- and inhibitory- postsynaptic potentials

When eliciting excitatory- and inhibitory postsynaptic potentials (EPSPs and IPSPs), recorded cells were usually held at -90 mV by applying steady negative current and varying stimulus strengths applied to produce a range of EPSP/IPSP complexes from subthreshold (not eliciting an action potential) to suprathreshold (eliciting an action potential) depending on the experiment being performed. When examining the effects of agonists and antagonists on excitatory synaptic transmission and comparing their effects upon different (LOT or intrinsic) inputs using two stimulating electrodes, it was necessary to elicit responses that satisfied the following requirements:

- A large enough stimulus strength to elicit a reproducible and characteristic EPSP/IPSP complex.
- A small enough stimulus strength to elicit subthreshold responses of <40% suprathreshold amplitude, since stimuli producing EPSPs of greater amplitude than this have been shown to produce postsynaptic effects that would affect the results (Saar *et al.*, 1999). Additionally, lower EPSP amplitudes produce only monosynaptic effects (Hasselmo & Bower, 1990). This approach also reduced the probability that a drug or change in environment would produce a potentiation resulting in a suprathreshold response.

- A stimulus strength of appropriate amplitude to produce the optimum measurable change in amplitude on application of drug.
- Stimulus strengths that produced *responses of identical amplitude* for both LOT and intrinsic fibre stimulation in control conditions. Different stimulus strengths applied to LOT and intrinsic stimulating electrodes were routinely used to elicit the same amplitude response from the recorded cell since the stimulating electrodes were varying distances from the cell.

These criteria allowed the observation of the presynaptic actions of some drugs and quantitatively accurate comparisons of those actions upon different inputs to be made. Each stimulus was repeated five times and a minimum interval of 30 s allowed between each stimulus, with the total response duration being measured from the stimulus artefact to a return to baseline. Additionally, repeats of all stimuli were performed at the end of each experiment to ensure that there had been no change in threshold level for each input. All figures showing traces of synaptic potentials are composite averages of at least 3 consecutive traces unless otherwise indicated.

2.5.3.3 Isolation of fast IPSPs

In order to determine the effect of a number of drugs upon the fast inhibitory ($GABA_A$-mediated) component of the EPSP/IPSP complex, this part of the IPSP response was isolated pharmacologically. This was achieved by the selective blockade of excitatory (glutamatergic) and 'slow' inhibitory ($GABA_B$-mediated) transmission by application of 10 μM DL-APV, 20 μM CNQX and 1 μM CGP-52432 (Table 2.1) followed by depolarization of the cell by application of positive current through the microelectrode (in DCC mode to reduce rectification). The cell would repetitively fire on application of the depolarizing current until eventual adaptation occurred and a steady membrane potential of ~-40 mV was achieved, at which point the amplifier was switched back to 'bridge' mode and recordings of the fast IPSP component were made. As with the elicitation of EPSPs (see section 2.5.3.2), the same criteria to achieve comparable IPSPs were applied and adhered to.

2.5.3.4 Paired-pulse facilitation and inhibition

Analyses of the presynaptic effects of a number of drugs were also made by means of a paired-pulse protocol (Chapters 4 and 5). A preparatory stimulus was applied to the cell through a stimulating electrode followed by an identical stimulus applied a specified time period later (50-500 ms; the inter-stimulus interval (ISI)) and the effect of the time

period variation upon the amplitude of the second evoked potential observed. Results were plotted as paired-pulse ratio (second pulse amplitude (P2)/first pulse amplitude (P1)) *vs.* ISI. The paired-pulse protocol was applied to both EPSPs and isolated IPSPs, following the protocols set out for the individual elicitation of each.

2.6 Lesioning of slices

In order to further determine the contribution of specific inputs to the muscarinic bursting behaviour observed in the immature piriform cortex (see Section 2.5.3), the slice preparations were lesioned using an FST10055-12 optical microscalpel (Fine Science Tools, Vancouver, Canada) (Lian *et al.*, 2001). Two lesion types were made; one along the boundary of layer Ib/II (Fig. 2.9A; effectively separating the LOT from the rest of the preparation and severing the distal apical dendrites of the superficial and deep pyramidal cells) and the other at the boundary of layer III and the lower endopiriform nucleus (layer IV (Hoffman & Haberly, 1993a); 2.9B; severing the basal dendrites and axons of the deep pyramidal cells and any synaptic inputs to layer II/III arising from the endopiriform nucleus). The lesions made were through the entire thickness and entire width of the slice, leaving no tissue connecting the two sections being separated. Slices were lesioned after placement in the recording bath and were then left to recover and stabilise for a minimum of 40 minutes. A stimulating electrode was routinely placed in the section of the slice that was separated from the recorded cell in order for test stimuli to be applied to confirm the physical and electrical separation of that area from the area being recorded from.

2.7 Preparation and application of drugs

All drugs used and associated information are listed in Table 2.1.

All drugs were introduced to the preparation by exchange of the control Kreb's superfusion medium for the same medium containing a known concentration of added drug stock. The drugs were made up freshly by dilution of previously prepared stock solutions. These stocks were prepared by dissolution of the drug in distilled water at known concentration and storing at 8°C (or frozen at –20°C, if unstable in solution) and brought to room temperature just prior to dilution in Kreb's.

Water-insoluble drugs were dissolved in dimethylsulfoxide (DMSO; RMM 78.13; Sigma, UK) or ethanol where the final concentration of DMSO or ethanol did not exceed 0.01% in the bath perfusion medium. Control experiments were peformed to

determine whether there was any effect from application of these solvents upon the tissue preparation and no changes were observed.

Measurements were taken prior to any application of drug (control), after 3-30 minutes drug superfusion and after a minimum period of 40 minutes washout with the control medium. In this manner, each neurone was able to serve as its own control by providing data before, during and after drug application. The majority of drugs exerted their effects within a few minutes of application, however some drugs such as the gap junction blockers used and anticholinesterases required longer to attain their maximal effect. The duration of application in such cases is individually noted in the results.

2.8 Histology and intracellular staining of recorded cells

In this study, a methylene blue staining technique was used to confirm that the cells recorded from were of the presumed physiological type and located in the appropriate region of the piriform cortex.

2.8.2 Methylene blue staining

In order to study and identify the gross morphological characteristics of the piriform cortical slice preparation used in these experiments, slices were stained using the Terry's methylene blue technique (Terry, 1922). A number of 30-150 μm slices were cut from tissue as previously described (see Section 2.1) and fixed in 4 % paraformadehyde and 0.2% picric acid in 0.15 M phosphate buffer solution (as described in Section 2.8.1) prior to staining. The working methylene blue staining solution was routinely freshly prepared by combining 6 ml of 1% $^{w}/_{v}$ methylene blue stock (1 g methylene blue dissolved in 100 ml d.H_20) and 6 ml of 1% potassium carbonate stock (1 g potassium carbonate in 100 ml d.H_20) to 30 ml with d.H_20, boiled over a flame (for exactly 2 min 30 s) and cooled under running water. Any water lost in boiling was replaced by addition of distilled water to a total volume of 30 ml after cooling. Slices were rinsed in distilled water then each was teased with a brush onto individual glass slides. Excess water was drained from the slide (the sections not allowed to dry) and the slice covered with a small amount of working methylene blue solution for 3-5 seconds (the duration varied depending upon the thickness of the slice). The stain was drained from the slide, rinsed in distilled water and the tissue transferred to a clean slide and examined while still wet. The best images were obtained from freshly prepared slides although permanently fixed slides could be produced by

allowing the stained tissue to dry for 10-15 minutes before fixing with xylene and coverslipped.

Photographs of both neurobiotin and methylene blue stained sections were taken using a JVC KY-F55B '3 Colour' camera mounted on a Nikon Microphot-FXA microscope (Nikon, Japan) and captured using PaintShop Pro (Jasc Software, USA) running on a Viglen PC (Viglen, UK).

2.9 Data analysis and statistical treatment of results

2.9.1 General statistical analyses

As previously stated, data were permanently recorded on a chart recorder trace and a personal computer. Statistical significance was generally determined by use of a two-tailed Student's paired t-test, unless data were presented as percentage change versus control for comparison of two independent populations (e.g. adult *vs.* immature) in which case statistical differences were assessed using a Wilcoxon rank sum (Mann-Whitney) test for two independent samples.

2.9.2 Comparability of burst discharges

To establish the degree of comparability and consistency of the burst discharges in any given experiment, the percentage coefficients of variation (SD/mean} expressed as a percentage) of the burst duration (CV_d) and interburst interval (CV_i) were measured as previously described by (Postlethwaite *et al.*, 1998b). Means of these values were calculated to provide global values of CV_d and CV_i.

2.10 Abbreviations

Some common abbreviations used in this thesis.

Abbreviation	Meaning	Units (if applicable)
4-AP	2-amino-4-phosphonobutyric acid	
4-DAMP	4-diphenylacetoxy-N-methylpiperidine methiodide	
A_1	Unity gain operational buffer amplifier	
A_2	Current source amplifier	
A_3	Series current amplifier	
AC	Adenylate cyclase	
ACh	Acetylcholine	
AED	Anti-epileptic drug	
AMPA	α-amino-3-hydroxy-5-methyl-isoxazole	
APC	Anterior piriform cortex	
AT	*Area tempestas*	
Ca^{2+}	Calcium ion	
C_{in}	Input capacitance	pF
Cl^-	Chloride ion	
CNQX	6-cyano-7-nitroquinoxaline-2,3-dione	
CNS	Central nervous system	
C_w	Capacitance of the microelectrode wall	pF
DL-APV	DL-amino-5-phosphonovaleric acid	
DMSO	Dimethylsulfoxide	
EPSP	Excitatory postsynaptic potential	
$GABA_BR$	$GABA_B$ receptor	
GAT-1	Gamma-amino-butyric acid transporter-1	
GT	Transconductance circuit gain	
I	Current	nA
I_{cmd}	Command current	nA
I_m	Current through recorded cell	nA
IPSP	Inhibitory postsynaptic potential	
K^+	Potassium ion	
LOT	Lateral olfactory tract	

LTP	Long term potentiation	
mAChR	Muscarinic acetylcholine receptor	
mGluR	Metabotropic glutamate receptor	
MPC	Median piriform cortex	
Na^+	Sodium	
nAChR	Nicotinic acetylcholine receptor	
NMDAR	N-methyl-D-aspartate receptor	
OXO-M	Oxotremorine-M	
PC	Piriform cortex	
pFHHSiD	p-fluoro-hexahydro-sila-difenidol	
PLC	Phospholipase-C	
PPC	Posterior piriform cortex	
PPF	Paired-pulse facilitation	
PPI	Paired-pulse inhibition	
R_o	Output resistor	Ω
R_p	Resistance across the microelectrode	MΩ
TEA	Tetraethylammonium	
trans-ACPD	trans-aminocyclopentane-1,3- dicarboxylic acid	
V_{cmd}	Command voltage	mV
V_e	Potential across microelectrode	mV
V_i	Output potential	mV
V_m	Potential across the cell membrane	mV
V_{ms}	Value of V_m when sampled	mV
V_p	Total potential across microelectrode	mV

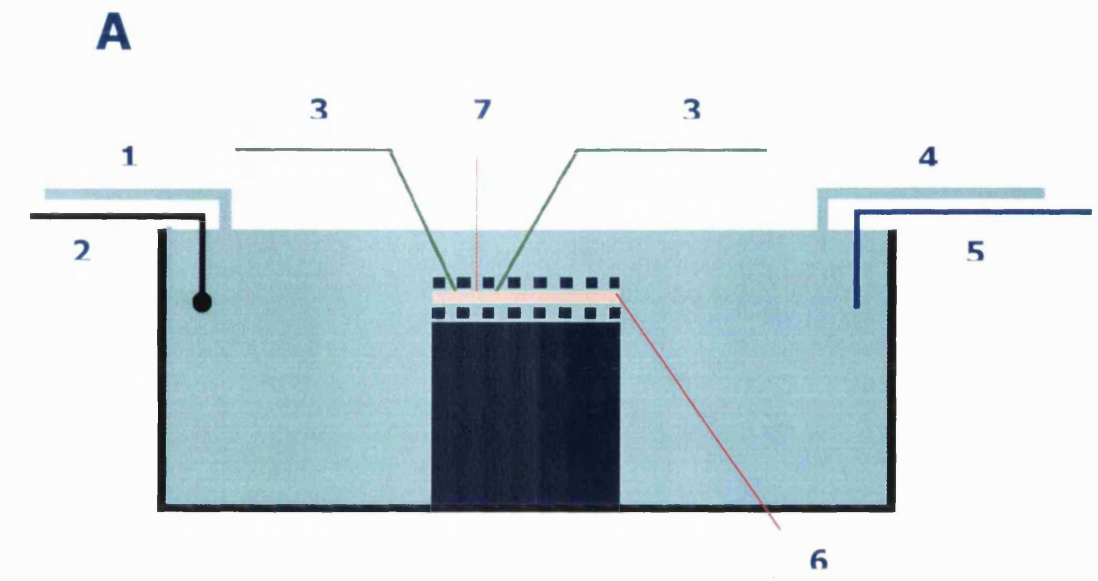

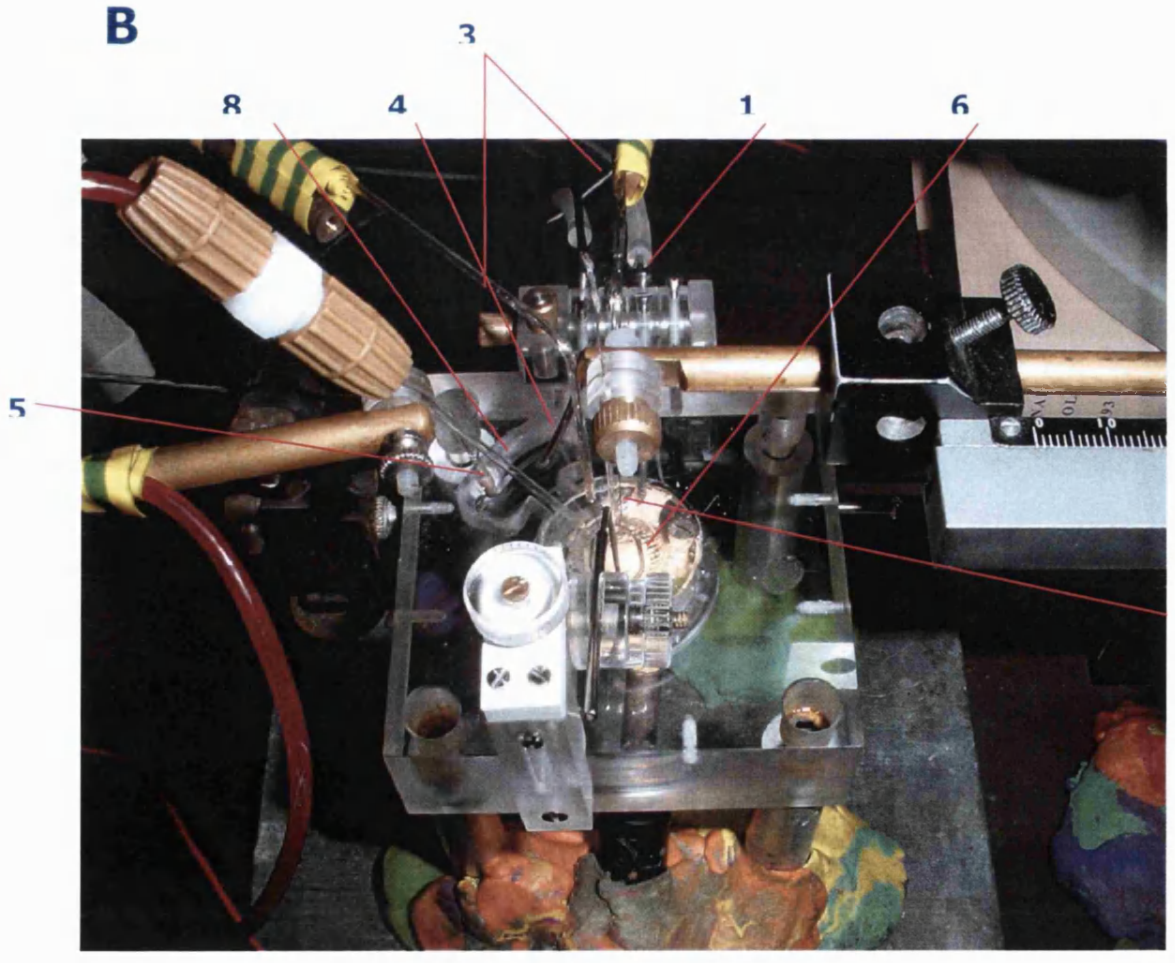

Figure 2.1

Figure 2.1.

A. Schematic illustration of brain slice recording bath. **B.** Photograph of brain slice recording bath. [1] – Kreb's inlet; [2] – Temperature sensor*; [3] – Stimulating electrodes; [4] – Kreb's outlet; [5] – Ag/AgCl bath (reference/ground) electrode; [6] – Brain slice held between two nylon meshes; [7] – Recording microelectrode; [8] – Patch electrode for focal drug application (not used in these experiments). ***N.B.** The temperature sensor is not shown in (**B**) as it was situated at the heater block on this particular recording rig.

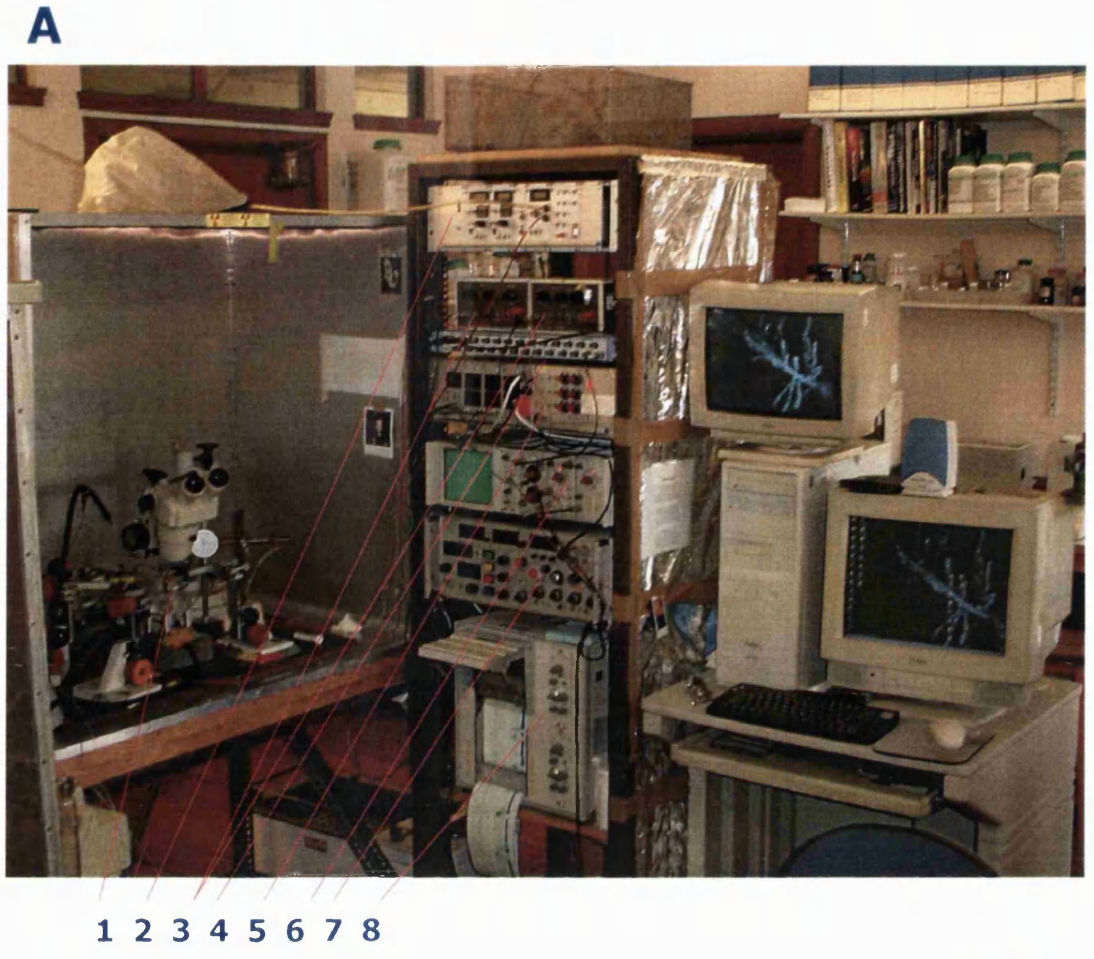

Figure 2.2

Figure 2.2

A. Photograph of the intracellular recording rig used in these experiments. [1] – Recording bath; [2] – Spritzer pump (for pressure application of drugs); [3] – External stimulators; [4] – Analogue to digital converter; [5] – Signal generator; [6] – Storage oscilloscope; [7] – Axoclamp 2A preamplifier; [8] – Chart recorder. **B.** Overhead view of recording bath. [1] – Micromanipulator holding recording electrode; [2] – Fibre optic light illuminating the recording bath from below; [3] – Axon HS-2L headstage.

A

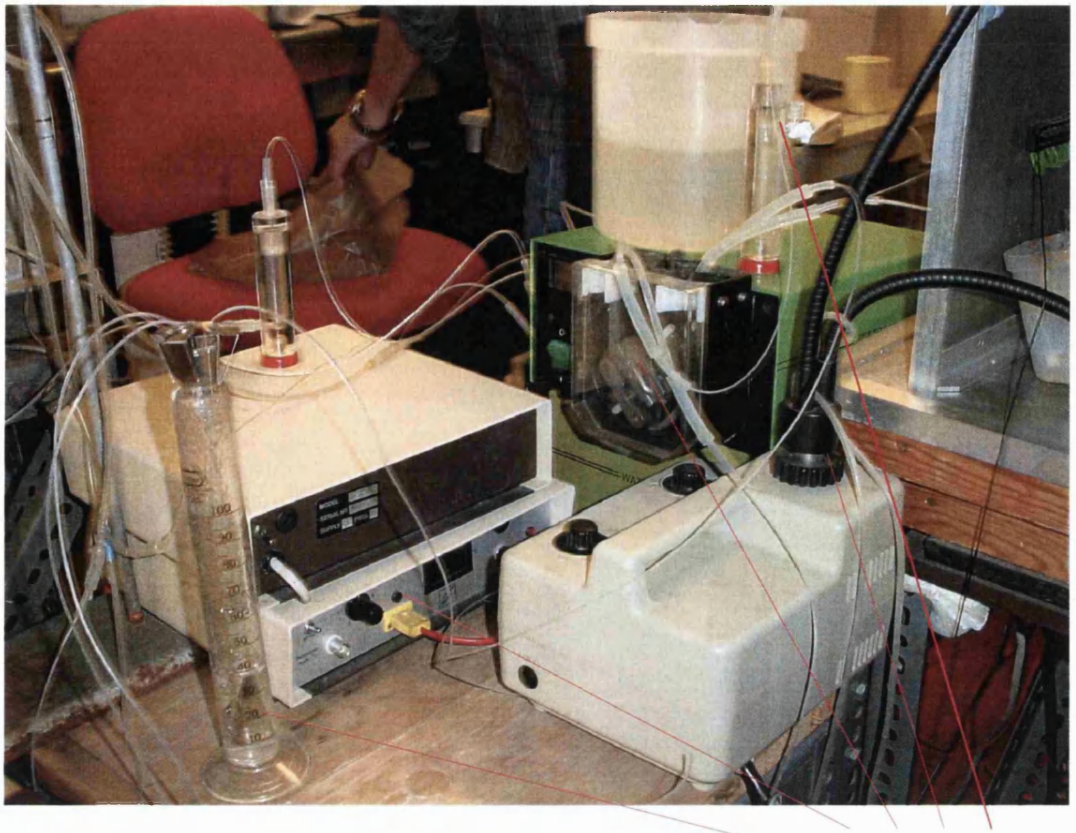

B

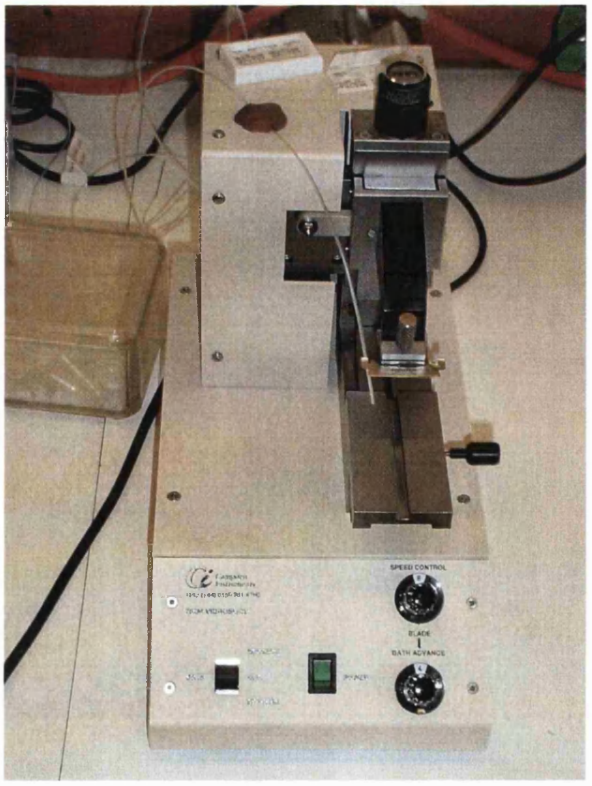

Figure 2.3

Figure 2.3

A. Photograph showing Krebs reservoir [1], Kreb's heater [2], peristaltic pump [3], fibre optic illumination for the recording bath [4] and bubble trap [5]. **B.** Camden Vibroslice-752M used for cutting olfactory cortical brain slices.

A

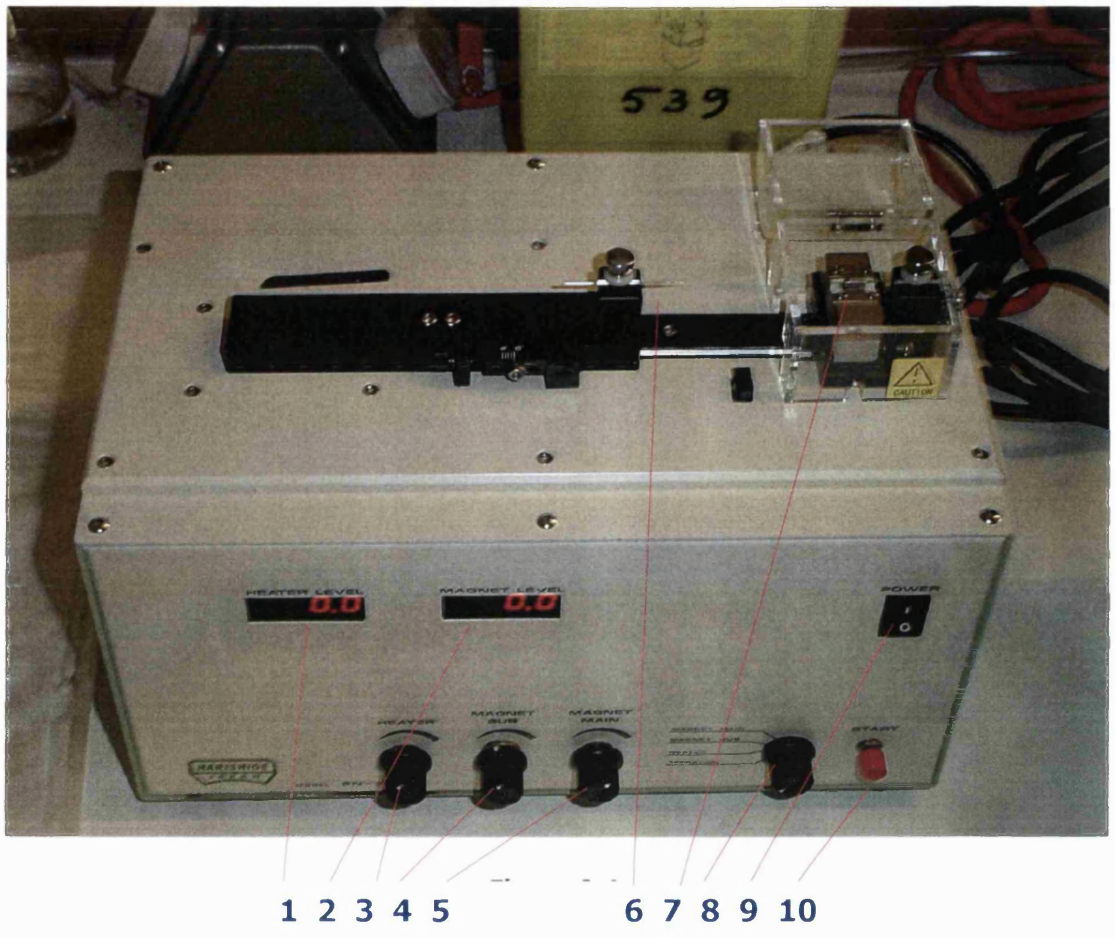
539
HEATER LEVEL
0.0
MAGNET LEVEL
0.0
POWER
HEATER
MAGNET BUR
MAGNET MAIN
START
CAUTION
1 2 3 4 5
6 7 8 9 10

Figure 2.4

Figure 2.4

A. Photograph of the Narashige PN-30 microelectrode puller used in these experiments. [1] – Heater level indicator; [2] – Magnet level indicator; [3] – Heater adjustment; [4] – Sub-magnet adjustment; [5] – Main magnet adjustment; [6] – Microelectrode; [7] – Heating element; [8] – Parameter selector switch; [9] – Power switch; [10] – Start pull switch.

A

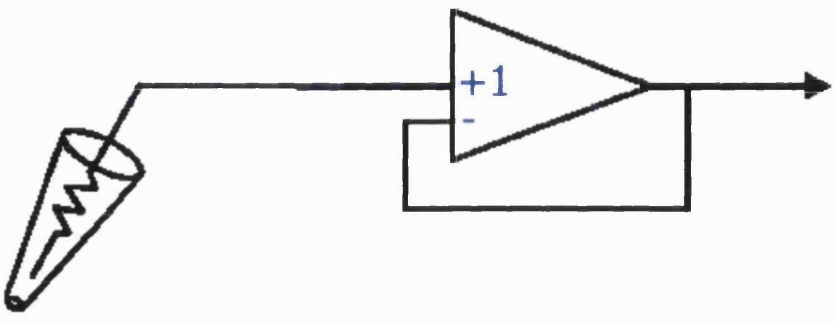

B

i

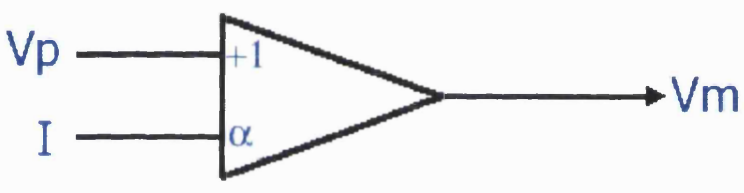

$$Vp = Vm + IRp$$

ii

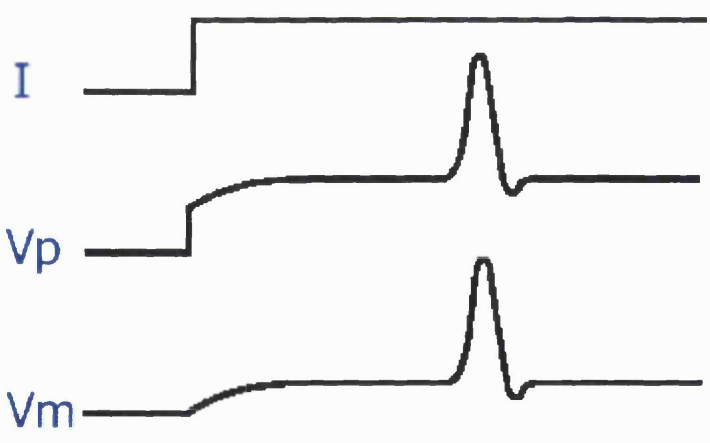

Figure 2.5

Figure 2.5

A. Circuit diagram illustrating the unity gain operational buffer amplifier as used in the Axoclamp HS-2L headstage. **B. i.** Circuit diagram illustrating the circuit used to create a 'bridge balance'. **ii.** Example traces showing the effect of a rapid change in potential.

Key:

R_p Resistance across the microelectrode (MΩ)

V_p Total potential across microelectrode (mV)

V_m Potential across the cell membrane (mV)

I Current (nA)

Figures adapted from the Axon Guide (Axon Instruments, CA., USA).

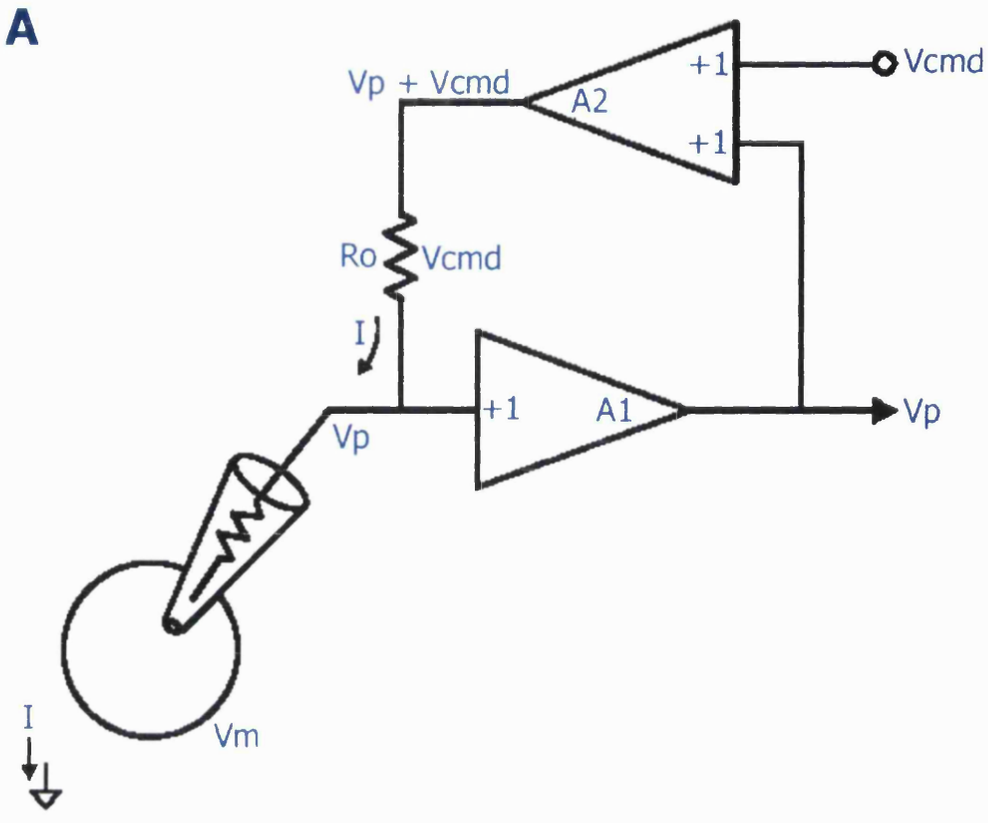

Figure 2.6

Figure 2.6

A. Circuit diagram showing the attachment of a current source to a buffer amplifier as shown previously (Fig. 2.5A).

Key:

V_p	Total potential across microelectrode (mV)
V_m	Potential across the cell membrane (mV)
I	Current (nA)
A_1	Unity gain operational buffer amplifier
A_2	Current source amplifier
V_{cmd}	Command voltage (mV)
R_o	Output resistor

Figures adapted from the Axon Guide (Axon Instruments, CA., USA).

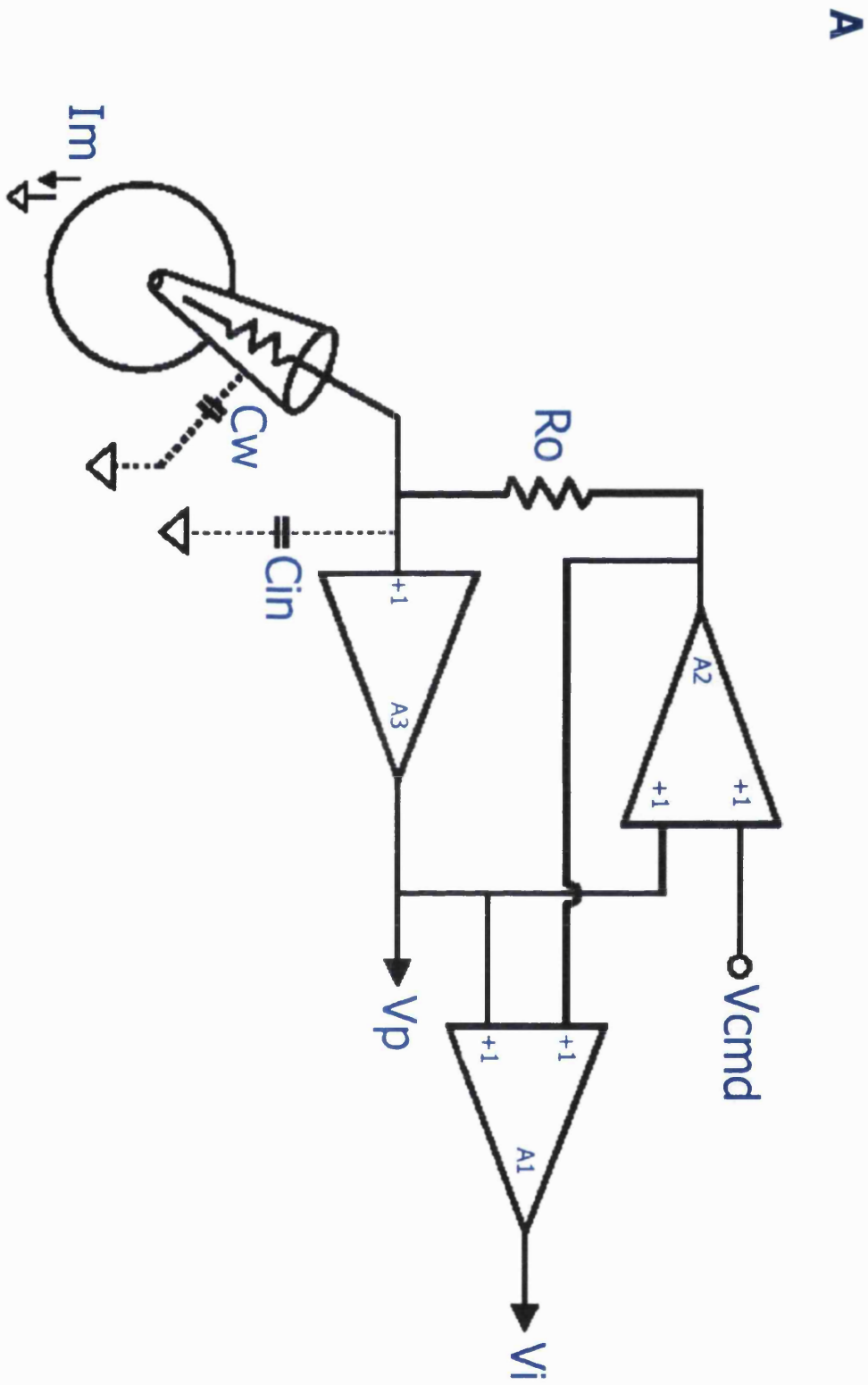

Figure 2.7

Figure 2.7

A. Circuit diagram showing a series current amplifier connected to the buffer and current source circuit shown in Figs. 2.5A and 2.6A.

Key:

V_p	Total potential across microelectrode (mV)
A_1	Unity gain operational buffer amplifier
A_2	Current source amplifier
A_3	Series current amplifier
V_{cmd}	Command voltage (mV)
R_o	Output resistor
V_i	Output potential (mV)
C_w	Capacitance of the microelectrode wall (pF)
C_{in}	Input capacitance (pF)
I_m	Current through recorded cell (nA)

Figures adapted from the Axon Guide (Axon Instruments, CA., USA).

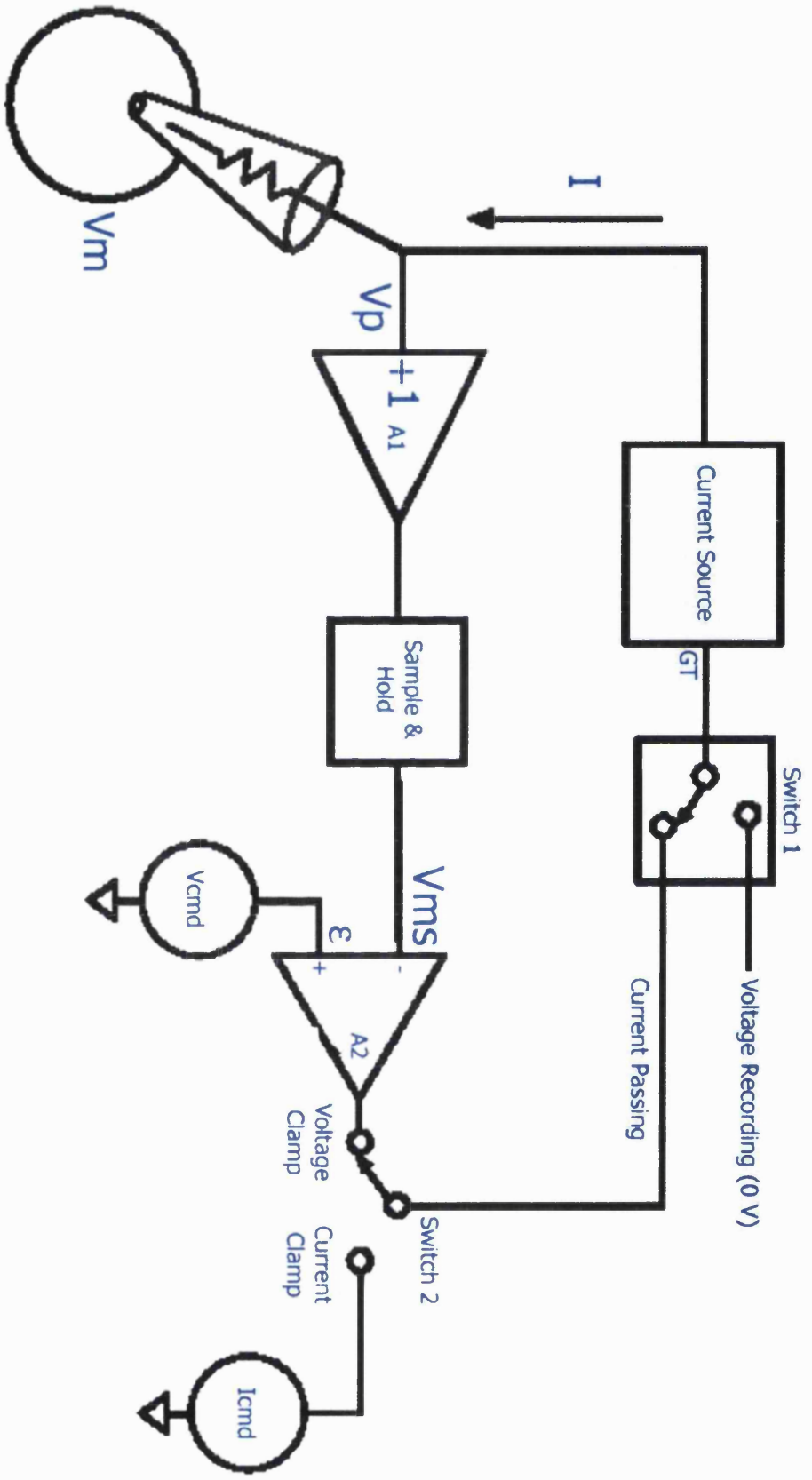
A
Vm
I
Vp
+1
A1
Current Source
GT
Sample &
Hold
Switch 1
Vcmd
ε
Vms
+
-
A2
Voltage Recording (0 V)
Current Passing
Voltage
Clamp
Switch 2
Current
Clamp
Icmd

Figure 2.8

Figure 2.8

A. Circuit diagram illustrating a discontinuous current clamp.

Key:

V_p	Total potential across microelectrode (mV)
V_m	Potential across the cell membrane (mV)
I	Current (nA)
A_1	Unity gain operational buffer amplifier
A_2	Current source amplifier
V_{ms}	Value of V_m when sampled (mV)
GT	Transconductance circuit gain

Figures adapted from the Axon Guide (Axon Instruments, CA., USA).

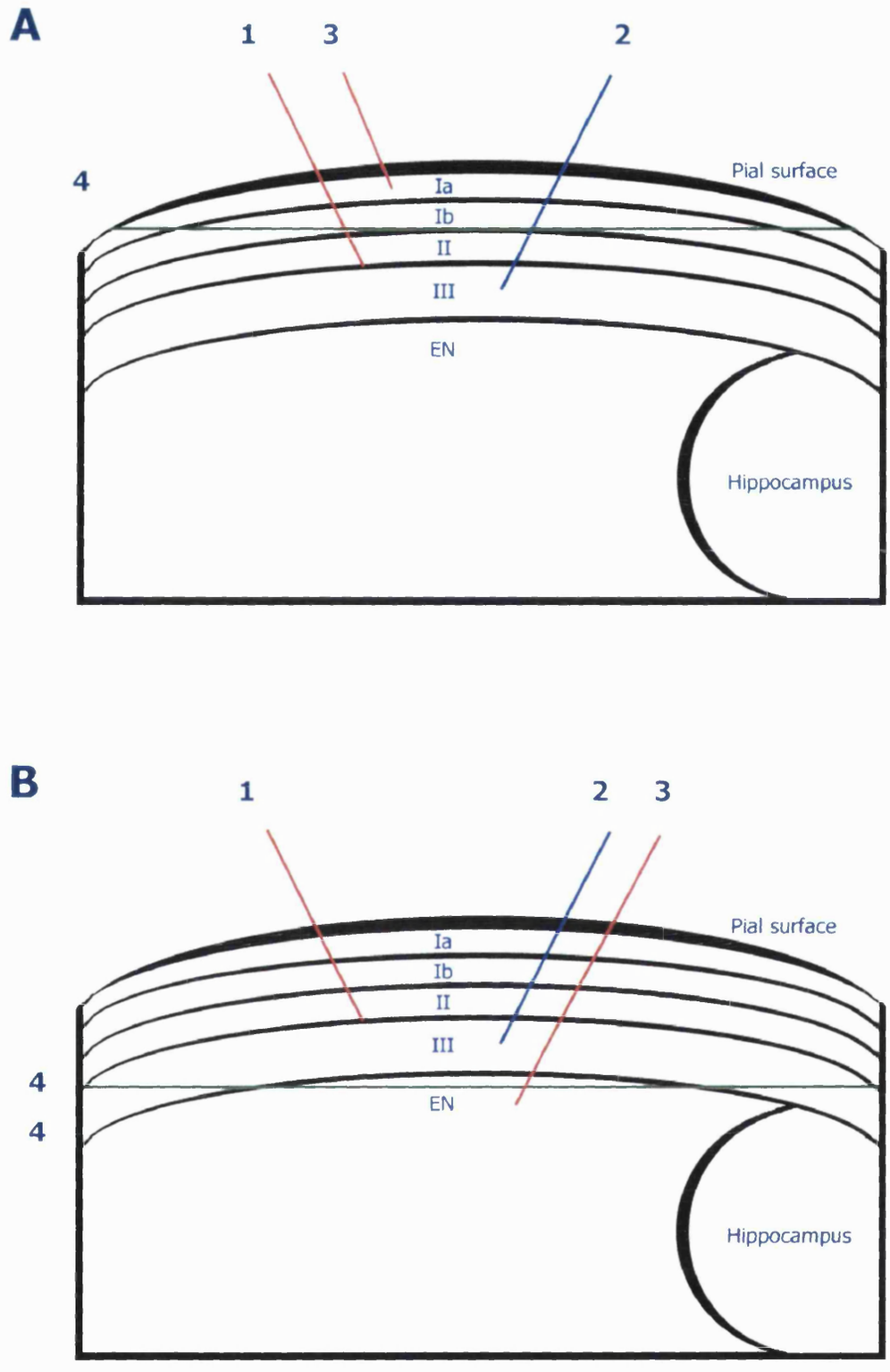
A
1
3
2
4
Pial surface
Ia
Ib
II
III
EN
Hippocampus
B
1
2
3
Pial surface
Ia
Ib
II
III
4
EN
4
Hippocampus

Figure 2.9

Figure 2.9

A. Illustration of an 'apically' lesioned piriform cortical slice showing layer I separated from the rest of the preparation.

B. Illustration of an 'basally' lesioned piriform cortical slice showing the endopiriform nucleus separated from the rest of the preparation.

Legend: [1] – Stimulating electrode; [2] – Recording microelectrode; [3] – Stimulating electrode (placed in the lesioned area and used to confirm effective lesioning of this area of tissue away from the area being recorded from); [4] – Lesion. [EN] – Endopiriform nucleus/piriform cortical layer IV. Legend applies to both illustrations.

Table 2.1 Drugs used.

Drug Name	Abbreviation	Relative Molecular Mass (RMM)	Action/Effects	Solvent for Stocks	Source
Oxotremorine-M methiodide	OXO-M	322.2	Non-selective mAChR agonist	d.H_2O	Semat Ltd., UK.
Neostigmine methylsulphate	NEO	334.4	Anticholinesterase	d.H_2O	Sigma Ltd., UK.
Atropine sulphate	ATR	694.8	Non-selective mAChR antagonist	d.H_2O	Sigma Ltd., UK.
(-)-Bicuculline methiodide	BIC	509.3	$GABA_A$ antagonist	d.H_2O	Sigma Ltd., UK.
Pirenzepine dihydrobromide	PZ	424.3	M1 mAChR antagonist	d.H_2O	Sigma Ltd., UK.
Telenzepine dihydrobromide	TZ	443.4	M1 mAChR antagonist	d.H_2O	Sigma Ltd., UK.
AFDX-116	AFDX	421.5	M2 mAChR antagonist	DMSO	Sigma Ltd., UK.
Methoctramine tetrahydrochloride	MET	728.8	M2 mAChR antagonist	d.H_2O	Sigma Ltd., UK.
Carbenoxolone hemisuccinate	CBX	614.7	Gap junction blocker	DMSO	Sigma Ltd., UK.
Octanol	OCT	130.2	Gap junction blocker	d.H_2O	Sigma Ltd., UK.
Felbamate dicarbamate	FBM	238.2	Anticonvulsant	Ethanol	Sigma Ltd., UK.
Phenobarbitone sodium	PBN	254.2	Anticonvulsant	d.H_2O	Sigma Ltd., UK.
Gabapentin	GPN	171.2	Anticonvulsant	d.H_2O	Sigma Ltd., UK.
Carbamazepine	CBZ	236.3	Anticonvulsant	Ethanol	Sigma Ltd., UK.
Topiramate	TPM	339.0	Anticonvulsant	d.H_2O	Sigma Ltd., UK.
Lamotrigine	LTG	256.0	Anticonvulsant	d.H_2O	Sigma Ltd., UK.
dl-amino-5-phosphonovaleric acid	DL-APV	197.13	NMDA glutamate receptor antagonist	Sodium hydroxide	Tocris Cookson Ltd., Bristol, UK.
6-cyano-7-nitroquinoxaline-2,3-dione	CNQX	232.2	Non-NMDA glutamate receptor antagonist	DMSO	Tocris Cookson Ltd., Bristol, UK.
CGP-52432	CGP-52432	384.2	$GABA_BR$ antagonist	d.H_2O	Sigma Ltd., UK.
Spironolactone	N/A	416.6	Mineralocorticoid antagonist	d.H_2O	Sigma Ltd., UK.
Distilled water	d.H_2O	16.0	N/A	N/A	N/A

Table 2.1

Chapter 3:

Comparison of electrophysiological properties and muscarinic responsiveness of adult and immature piriform cortex neurones

3.1 Introduction

This section of the present study was primarily concerned with investigating the electrophysiological properties and muscarinic responsiveness of deep pyramidal neurones in adult and immature piriform cortical (PC) brain slices and developing the ability to characterize and identify such neurones by their responses to injected current, thereby building upon existing knowledge of this brain area and its susceptibility to epileptiform activity. A number of groups (Constanti & Galvan, 1983; Libri *et al.*, 1994; Scholfield, 1978c) have extensively characterized the electrotonic responses and morphological properties of the main neurone types found in the adult piriform cortex (Section 1.2.2), prior knowledge of which has permitted the identification of recorded neurone types by their electrotonic responses and firing properties in the present experiments. This area of the brain is also known to be highly susceptible to epileptogenesis (Piredda & Gale, 1985); thus, spontaneous epileptiform activity develops following the application of the muscarinic agonist, oxotremorine-M (OXO-M; 10 μM) in the immature (but not adult) rat piriform cortical slice preparation (Postlethwaite *et al.*, 1998a). Consequently, the main neurone types encountered (characterized by a number of notable phenomena, some of which were found to vary with age) are described and illustrated below. The responses of both adult and immature neurones following mAChR activation were also studied and compared with previous reports (see specific sections for references) and attempts made to elucidate the mAChR subtype responsible for the postsynaptic events and epileptiform activity. Histological staining of whole piriform cortical sections was also performed upon tissues obtained from both adult and immature animals in order to determine whether any gross developmental differences in cell morphology could be seen (Section 3.7). Additionally, a number of commonly used anti-epileptic drugs (AEDs; Section 3.5) were tested for activity against mAChR agonist-induced epileptiform bursting observed in the immature PC slice preparation (Postlethwaite *et al.*, 1998a) in an attempt to further understand the mechanisms underlying this behaviour. Finally, we were interested to establish whether endogenous ACh, arising from cholinergic nerve terminals in the slice preparation, was able to produce effects similar to those seen following the application of OXO-M when an acetylcholinesterase inhibitor was present in the bathing medium.

3.2 Comparison of electrotonic responses recorded from adult and immature neurones in the rat piriform cortex

It was of interest to assess the basic electrotonic membrane properties of adult and immature piriform cortical neurones under our present recording conditions, to serve as a comparison with those previously published by our laboratory (Libri *et al.*, 1994; Postlethwaite *et al.*, 1998a) and others (Haberly, 1983; Haberly & Bower, 1984; Harvey *et al.*, 1974; Hasselmo & Bower, 1992; Protopapas & Bower, 2000; Scholfield, 1978c; Tseng & Haberly, 1989b; Tseng & Haberly, 1989d) in which the same neurone types were recorded. Stable (2-3 hour) intracellular recordings were obtained from a total of 399 piriform cortical neurones from either adult (P>40; 98 neurones) or immature (P+14 to P+25; 301 neurones) rat brain slices. All piriform cortical neurones encountered had a relatively negative resting membrane potential (–80 to –85 mV), which permitted an easy assessment of impalement stability, electrode seal and overall health of the impaled neurone. Each impaled neurone had a minimum stable resting potential of at least –75 mV and a control input resistance >20 MΩ; neurones deviating from these parameters were routinely discarded. The basic, electrical membrane properties of the three different neurone types (deep (type 1), interneuronal (type 2) and superficial (type 3)) recorded from adult and immature rat brain slices are summarised in Table 3.1 and were found to be comparable with the definitions described by Libri *et al.* (Libri *et al.*, 1994). The only significant difference between the neurone types investigated was that the mean input resistance of adult (25 ± 1.9 MΩ; n=7) or immature (25 ± 1.4 MΩ; n=17) presumed superficial neurones was found to be significantly smaller that the respective values for presumed deep pyramidal (adult: 44 ± 2.1 MΩ; n=86; immature 46 ± 1.8 MΩ; n=266) or presumed interneuronal (adult: 41.4 ± 2.2 MΩ; n=5; immature 40.9 ± 2.5 MΩ; n=18) cells. There were no statistically significant differences between the resting potential, input resistance or directly evoked, action potential amplitude recorded from adult or immature cells, of the *same* type, in this study, although immature neurones did display a trend towards lower resting membrane potentials than adult neurones (Table 3.1).

3.2.1 Presumed deep pyramidal neurones (Type 1)

Recordings from 266 immature and 86 adult presumed deep (Type 1 (Libri *et al.*, 1994)) pyramidal neurones were made in the course of this investigation. Typical recordings obtained from adult (P>40) and immature (P+17) presumed deep pyramidal neurones are shown in Fig. 3.1A. Unlike superficial pyramidal neurones, both adult and

immature deep cells demonstrated only weak accommodation of spike firing in response to large depolarizing stimuli (0 to +1.2 nA). Additionally, at potentials negative to -100 mV, a fast inward rectification (shown by 1; Fig. 3.1A and appearing as a 'sag' of the electrotonic potential (Constanti & Galvan, 1983)) was elicited in response to hyperpolarizing stimuli of increasing amplitude (up to 2 nA). This rectification, proportional to the amplitude of the hyperpolarizing stimulus, gave rise to a non-linear current-voltage relation (Fig. 3.2) and was seen in both adult (55 %) and immature (59 %) neurones. The difference between the peak potential (peak of the 'sag') and the steady state electrotonic potential was found to be slightly, but significantly larger ($P<0.05$; Students' t-test) in the immature (3.8 ± 0.7%, following a -1.2 nA stimulus) than the adult (2.1 ± 0.9%, following a -1.2 nA stimulus) preparation (Fig. 3.2). Following large negative stimuli, a rebound depolarization was observed (shown by 6; Fig. 3.1A), in 74 % of immature (but not adult) deep pyramidal neurones. Associated with this, immature deep pyramidal neurones exhibited a characteristically slow inward rectification in response to increasingly large hyperpolarizing stimuli (shown by 2; Fig. 3.1A); this slow rectification was never seen in adult neurones, consistent with the reports of Sciancalepore and Constanti (1998). Apart from this difference in inward rectification, the firing patterns in response to current stimulation, were essentially similar for both adult and immature neurones (Fig. 3.1A). Application of a long depolarizing stimulus train (+2 nA; 1.6 s; 2.5.2) to the neurone (held at –70 mV in DCC mode) revealed a characteristic slow after-hyperpolarizing potential (sAHP; Fig. 3.3B) and in 'hybrid' voltage clamp mode, the underlying outward tail current (I_{AHP}; Fig. 3.3D). No significant difference in the magnitude or time course of the sAHP (or its underlying outward tail current) in adult and immature deep pyramidal neurones was observed in the present study ($P>0.05$; Students' t-test; Table 3.2).

3.2.2 Presumed interneurones (non-pyramidal; Type 2)

A total of 18 immature and 5 adult piriform cortical presumed interneurones (Type 2) (Libri *et al.*, 1994) were recorded from. Figure 3.1B shows examples of the electrotonic responses of adult (P>40) and immature (P+19) interneurones. In the same manner as the deep pyramidal neurones, interneurones demonstrated weak spike accommodation in response to depolarizing stimuli, (unlike superficial neurones; Fig. 3.1C). Interneurones, like deep pyramidal neurones, also exhibited fast inward rectification (Fig. 3.1B) as displayed by deep pyramidal neurones in response to hyperpolarizing stimuli (Fig. 3.1A). However, the frequency with which this rectification appeared was

lower in adult (33%) than immature cells (68%). Also notable was the presence of a fast afterhyperpolarization (fAHP) following each spike (shown by 5 in Fig. 3.1B), a feature characteristic of previously identified guinea-pig piriform cortical interneurones (Libri *et al.*, 1994). Application of a long depolarizing stimulus (+2 nA; 1.6 s) to recorded interneurones also elicited a sAHP (Fig. 3.5B) and I_{AHP} (Fig. 3.5D) tail current comparable, but significantly smaller than those seen in deep pyramidal neurones (I_{AHP} amplitude: 50 ± 11.1% smaller; $P<0.01$; Students' t-test). No significant differences ($P>0.05$; Students' t-test) were observed between adult and immature recordings of the sAHP or I_{AHP} evoked by comparable current steps (Table 3.2) in interneurones.

3.2.3 Presumed superficial pyramidal neurones (Type 3)

A total of 17 immature and 7 adult presumed superficial (Type 3) (Libri *et al.*, 1994) pyramidal neurones were recorded from. These neurones were all located in the compact layer II (Fig. 3.31A (4)) and consequently were not routinely recorded from, but are described here, as their reliable identification was required to eliminate them from later experiments. Figure 3.1C compares the electrotonic responses of adult (P>40) and immature (P+21) presumed superficial type 3 pyramidal neurones. Considerably greater accommodation and fractionation of spike firing compared to that seen in deep pyramidal and interneuronal cells can be clearly seen in both adult and immature neurones (shown by 3; Fig. 3.1C) coupled with the absence of a strong post-stimulus afterhyperpolarization (shown by 4; Fig. 3.1C) following long depolarizing stimuli. A strong outward rectification was also observed in response to depolarizing stimuli and the presence of a fast inward. In addition to the differences in firing properties displayed by superficial neurones, the input resistance of the neurones sampled was significantly smaller than both deep ($P<0.01$; Students' t-test) and interneuronal ($P<0.05$; Students' t-test) cells (Table 3.1). Application of a long depolarizing stimulus train (+2 nA; 1.6 s) failed to elicit either a sAHP (Fig. 3.7B) or any underlying tail current (Fig. 3.7D) as previously found by Libri *et al.* (Libri *et al.*, 1994).

3.3 The postsynaptic effects of mAChR activation by oxotremorine-M (OXO-M) on piriform cortical neurones

OXO-M was bath-applied and the postsynaptic responses of the previously described principal neurone types of the piriform cortex observed in adult and immature cells. OXO-M elicited varied responses dependent upon the neurone type being recorded as previously reported (Constanti *et al.*, 1993; Krnjevic, 1986; Libri *et al.*, 1994;

Postlethwaite *et al.*, 1998a). However, although the OXO-M-induced epileptiform activity seen in the immature slice preparation has previously been described in some detail, no reports have so far been published investigating the specific developmental differences that give rise to this phenomenon. A comparison of the postsynaptic effects of OXO-M, upon the principal cells types in the piriform cortex at a number of ages, may provide additional evidence to explain the observed epileptiform bursting phenomenon.

3.3.1 Comparison of postsynaptic muscarinic responses of adult and immature deep pyramidal piriform cortical neurones

In previous studies from our laboratory, the responses of the principal piriform cortical cell types, following mAChR activation, in adult slices (Libri *et al.*, 1994) and the first report of OXO-M-induced epileptiform bursting in the immature PC slice preparation (Postlethwaite *et al.*, 1998a) were described. In this present study, the muscarinic responsiveness of the principal PC cell types from both adult and immature animals was investigated using a larger immature sample population in an attempt to better characterize the bursting phenomenon and confirm that the results obtained were consistent with previous reports.

In recordings from 44 adult and 176 immature deep pyramidal neurones, 10 μM OXO-M (a concentration previously found to be maximally effective in evoking membrane depolarization (Libri *et al.*, 1994)) was routinely applied via the bath-superfusion medium. Interestingly, within 2 to 3 minutes, any spontaneous firing properties exhibited by the recorded cell were abolished (see (*) in Fig. 3.9B) and in 62% of adult and 42 % of immature recorded cells a small (<2 mV) transient (~20 s) hyperpolarization was observed (see (*) in Fig. 3.13A), most likely be due to the prior activation of local GABA-ergic inhibitory interneurones by OXO-M producing an increase in GABA release (McCormick & Prince, 1985), before the postsynaptic effects of OXO-M could be observed on the recorded cell. This was followed by the onset of a slow membrane depolarization (adult: 11 ± 0.8 mV; n=44; immature: 12 ± 0.7 mV; n=176) with an accompanying increase in input resistance (Table 3.3; Fig. 3.3A). This increase was significantly larger in immature deep neurones (20 ± 2%; n=176; Fig. 3.10A) than in adult deep neurones (12 ± 2%; n=44; Fig. 3.4A; Table 3.3) and was clearly demonstrated by the steeper slope of the current-voltage relationship for the immature preparation (Fig. 3.10B) compared to the adult (Fig. 3.4B). In adult deep pyramidal neurones, when the depolarization reached a threshold of around -70 mV,

repetitive firing was triggered (Fig. 3.3A). However, in a proportion (63%) of *immature* neurones, epileptiform burst firing was observed (*e.g.* Figs. 3.13, 3.14 & 3.15; Section 3.4 for details regarding bursting characteristics) or in the remaining proportion of immature neurones, repetitive firing in the same fashion as the adult was observed. In the presence of OXO-M, the sAHP elicited, following a long (2 nA; 1.6 s) depolarizing stimulus, in control conditions was reliably abolished in both adult and immature neurones and replaced by a slow afterdepolarizing potential (sADP; Fig. 3.3C) (Constanti & Bagetta, 1991). Additionally, the outward tail current underlying the sAHP (I_{AHP}) was replaced by an inward tail current (I_{ADP}; Fig. 3.3E) recorded under 'hybrid' voltage clamp. Table 3.2 shows the peak amplitudes of the elicited potentials and their underlying tail currents for all neurone types recorded from in the absence and presence of OXO-M. No other differences were found between the responses of deep pyramidal neurones from either the adult or immature preparations in OXO-M.

3.3.2 Postsynaptic muscarinic responses of adult and immature presumed piriform cortical interneurones

Five adult and 17 immature piriform cortical presumed interneurones were treated with 10 μM OXO-M and the neuronal responses to muscarinic receptor activation observed. Similarly to the response of deep pyramidal neurones, a slow depolarization (adult: 11 ± 0.4 mV; n= 5; immature: 12 ± 0.9 mV; n=17) was seen, coupled with an increased input resistance and the onset of repetitive firing (Figs. 3.5A, 3.6A & 3.11A; Table 3.3). However, no epileptiform burst firing was ever observed following the application of 10 μM OXO-M, in either adult or immature presumed interneuronal cells. As with deep pyramidal neurones, the increase in input resistance seen in immature presumed interneurones (12 ± 2%; n=17) in OXO-M was significantly larger than that seen in adults (18 ± 2%; n=5; $P<0.05$ Wilcoxon signed rank test). This was clearly illustrated by the steeper slope of the current-voltage plot for immature (Fig. 3.11B) than adult (Fig 3.6B) cells, indicating a larger change in input resistance. Application of a long depolarizing stimulus (2 nA; 1.6 s) elicited a sADP (Fig. 3.5C) and underlying inward tail current (I_{ADP}; Fig. 3.5E), as seen in deep pyramidal neurones. However, the amplitude of the I_{ADP} for both adult and immature interneurones was significantly smaller (adult: 56.5 ± 13.2%; immature: 58.8 ± 5.8%) than for adult and immature deep pyramidal neurones (Table 3.2) with a comparable change also observed in the sADP.

3.3.3 Postsynaptic muscarinic responses of adult and immature superficial pyramidal piriform cortical neurones

The responses of 7 adult and 17 immature presumed superficial pyramidal neurones to the application of 10 μM OXO-M were also examined. By contrast with the other principal cell types, OXO-M caused a small slow depolarization that did not result in repetitive firing, no obvious change in input resistance and no epileptiform burst firing in both adult and immature cells (Figs. 3.7, 3.8A & 3.12A; Table 3.3). This was also clearly illustrated in the current-voltage plots for adult and immature cells, in which there is little divergence of the plot in the presence of OXO-M from the plot in control conditions (Figs. 3.8B, 3.12B). Injection of a long depolarizing stimulus (+2 nA; 1.6 s) failed to elicit a sADP or I_{ADP} tail current (Fig 3.7C, E) of the type seen in deep pyramidal neurones and interneurones in OXO-M.

3.4 Epileptiform bursting induced by muscarinic receptor activation in immature deep pyramidal neurones

The application of 10 μM OXO-M to *immature* deep pyramidal piriform cortical neurones has been previously reported to elicit characteristic epileptiform bursting in ~40% of recorded neurones (Postlethwaite *et al.*, 1998a), a phenomenon never seen in adult neurones in these conditions. During the course of this present investigation to determine the mechanisms underlying this phenomenon, accumulated data were analysed for comparison with those presented by Postlethwaite *et al.* (1998). Additionally, a larger sample population was used in this study than in the previous investigation enabling a more detailed characterisation of the bursting phenomenon and its pharmacology to be made.

3.4.1 Characteristics of OXO-M induced epileptiform bursting in immature deep pyramidal piriform cortical neurones

In accordance with previous findings (Hoffman & Haberly, 1989a; Libri *et al.*, 1994; Postlethwaite *et al.*, 1998a), recorded adult and immature deep pyramidal piriform cortical neurones never showed spontaneous bursts of action potentials in control conditions, even following brief or prolonged depolarizing stimulus trains. However, within 3 – 15 minutes (mean=5.4 ± 2.2 mins; n=111) following the application of 10 μM OXO-M, 111/175 (63%) of recorded immature neurones displayed a sustained depolarization leading to characteristic epileptiform bursting activity; (recorded deep neurones that did not develop bursting activity behaved similarly to adult neurones,

displaying a sustained depolarization that developed into regular repetitive firing (Fig. 3.3)). The bursting phenomenon was characterized by a rapid depolarization of the neurone and an associated transient *decrease* in input resistance (Fig. 3.9A) in response to regularly applied negative current pulses. Once the regular bursting pattern became established (mean=10.4 ± 6.3 mins after exposure to OXO-M; n=111), cellular input resistance increased (Fig. 3.10; 28.5 ± 12.3% compared to peak input resistance change during bursting) during the quiescent, hyperpolarizing phase of the bursting cycle, and decreased during the burst discharge period. The burst discharges, in susceptible neurones, lasted for ~10-60 s (mean=23.2 ± 1.4 s; n=111) with the inter-burst interval varying considerably with age (10s – 2 min 30 s; Figs. 3.9, 3.13, 3.14, 3.15 & 3.16; Section 3.4.2). The periods of bursting were separated by periods of hyperpolarization (mean=24.3 s) of varying, age-dependent magnitude (Fig. 3.17B; Section 3.4.2). During these periods, the neurone was quiescent and did not discharge (Fig. 3.13A; n=84) or display spontaneous interictal depolarizing events (Fig 3.16B; 5 – 50 mV; n=27). In order to determine whether the burst frequencies and durations observed were of regular occurrence and duration, the global mean values of the percentage coefficients of variation (SD/mean} x 100%; Section 2.9.2) for interburst interval (CV_i = 33 ± 7%) and burst duration (CV_d = 38 ± 6%) were calculated for all recorded cells of any age displaying epileptiform bursting. These values were comparable with those obtained by Postlethwaite *et al.* (1998) and indicated that the bursts were of irregular occurrence and duration. However, when the possibility that both interburst interval, burst duration and other variables characterising burst behaviour, such as PDS (paroxysmal depolarizing shift that is the difference between the peak mid-burst depolarization and the peak post-burst hyperpolarization) magnitude may be age-dependent is considered, then the pooled values above (P+14 to P+30) may not provide an accurate representation of the irregularity (or regularity) of the phenomenon (*e.g.* Figs 3.13A and B). Consequently, since the number of recorded cells in the present study was much larger than in Postlethwaite *et al.* (1998), it was possible to statistically analyse burst regularity for individual ages, thereby removing any possible masking that pooling different ages would produce. The results of this analysis are presented in the following section (3.4.2).

In the proportion (27%) of recorded neurones that did not display the characteristic epileptiform bursting, many (n=17) exhibited a regular, '*wave-like*' variation in membrane potential (Fig. 3.16) following the initial mAChR-mediated membrane depolarization and increase in baseline noise in OXO-M. This phenomenon

was abolished by the application of 1 μM atropine (not shown), confirming that it was mAChR-mediated. The '*wave-like*' pattern was very similar to that seen in bursting neurones, which would suggest that although these '*non-responding*' cells were not displaying full epileptiform activity, the underlying rhythmic mechanism causing the bursting may also have been responsible for the '*wave-like*' effect indicating the continued mAChR activation of the circuitry required for bursting behaviour.

As previously reported (Postlethwaite *et al.*, 1998a), burst frequency or duration was not affected by changes in resting membrane potential produced by positive or negative current injection (Fig. 3.18; n=12) within the range -70 to -110 mV, although the magnitude of the PDS did increase as holding membrane potential increased (Fig. 3.18B). Additionally, the bursting phenomenon remained stable for as long as OXO-M was present (up to 3 hours in some neurones) and was fully reversible on washout (not shown), or fully blocked by the application of the mAChR antagonist, atropine (1 μM; Fig. 3.15B) or the addition of the M1-specific mAChR antagonists pirenzepine or telenzepine (Section 3.4.4), thereby confirming its mAChR-mediated mechanism. Apart from the higher percentage of susceptible bursting neurones encountered (63% in this study *vs.* 36 % in Postlethwaite *et al.* (1998)), no major differences from the characteristics of epileptiform busting described by Postlethwaite *et al.* (1998) were observed.

3.4.2 Age-related changes in epileptiform bursting characteristics

In the previous study of the muscarinic bursting phenomenon (Postlethwaite *et al.*, 1998a), animals within the age range of P+14 to P+22 were used. In order to further characterise any age-dependence of the phenomenon in greater detail in this investigation, attempts to elicit OXO-M induced bursting activity in a broader age range of animals, ranging from P+14 (the youngest age at which reliable intracellular recordings could be made) to P>40 were made. Recordings from slices cut from animals younger than P+14 were attempted, but the neurones were insufficiently robust to survive microelectrode impalement. This larger age-range combined with the larger population of recorded neurones (compared to the previous study) permitted a detailed analysis of any age-related changes in bursting characteristics. The overall mean percentage of recorded neurones found to burst (63%) was subdivided by age to investigate whether the number of '*bursting*' neurones varied within the age range investigated. The percentage of recorded neurones displaying bursting characteristics was significantly higher in slices taken from younger rather than older animals (*e.g.* 80

% in slices from P+14 animals (n=9) *vs.* 35% in slices from P+24 animals (n=13); Fig 3.17A). A general linear trend for burst incidence to decrease with increasing age was observed, to a point up to P>30 whereupon burst firing was never observed. The magnitude of observed PDSs (Fig. 3.13A) also showed a showed a diminishing trend with age. Thus, recorded neurones from younger animals (*e.g.* mean P+14 PDS amplitude = 35 ± 6 mV; Figs. 3.17B, 3.9A & 3.13A) showed a significantly greater PDS than older animals (mean P+24 PDS amplitude=20 ± 7 mV; Figs. 3.17B, 3.9B & 3.13B). As previously noted (Section 3.4.1), there appeared to be no correlation between the recorded values of burst frequency and duration when the results for all animal ages were grouped together. However, when the same analysis by coefficient of variation was performed on the same data *divided into age groups*, a correlation between burst duration, interburst interval and PDS *vs.* age was observed (Table 3.5). These analyses clearly showed that burst duration, interburst interval and PDS were inextricably linked with animal age, with burst duration and interburst interval increasing with age and the magnitude of PDS decreasing.

3.4.3 Location-dependence of bursting

A number of prior investigations (Biella *et al.*, 1996; Chabaud *et al.*, 1999; Haberly & Sutula, 1992; Loscher & Ebert, 1996; Mouly *et al.*, 2001; Piredda & Gale, 1985) have noted that cellular responses and epileptiform behaviour within specific neuronal populations of the piriform cortex (deep pyramidal, superficial pyramidal or interneuronal cells) vary according to the rostro-caudal location of the neurones within the piriform cortex (Fig. 3.19). With this in mind, the frequencies of burst occurrence at a given age (P+18) were assessed according to the recording electrode location rostro-caudally along the slice. Previous recordings of pyramidal neurone responses (Constanti & Bagetta, 1991; Hasselmo & Bower, 1992; Postlethwaite *et al.*, 1998a) and the majority of those made in this investigation have been made from the piriform cortical area termed the median piriform cortex (Fig. 3.19) (Haberly & Price, 1978). The muscarinic responsiveness of neurones in the anterior and posterior areas of the transverse slice preparation have not previously been examined, despite the positional evidence to suggest that differing responses might be expected. Interestingly, OXO-M-induced epileptiform bursting was observed most frequently in the posterior piriform cortex (85%; n=12), followed by the anterior piriform cortex (72%; n=11), with the median piriform cortex showing the lowest incidence of burst firing (61%; n=9), suggesting that these two areas may be more excitable (or less inhibited) than the

median area. No other obvious differences were observed in postsynaptic responses (change in input resistance, elicited slow currents *etc.*) obtained from neurones in these regions compared to those from the median area. Additionally, there were no apparent differences in the same postsynaptic muscarinic responses of adult neurones (anterior: n=5; posterior: n=5) compared to adult recordings from the median area (n=7; Tables 3.1, 3.2 & 3.3) despite evidence to the contrary obtained from *in vivo* kindling studies (Loscher *et al.*, 1995; Loscher & Ebert, 1996). Variations in response according to location for both excitatory and inhibitory synaptic responses were also investigated in an attempt to correlate the changes in the frequency of burst occurrence with differences in synaptic transmission. These results are presented and discussed in Section 4.4.

3.4.4 The effects of M1- and M2-mAChR antagonists upon the postsynaptic and epileptogenic effects of OXO-M in adult and immature deep pyramidal neurones

It was of interest to determine whether the same mAChR subtype (Section 1.6) was responsible for mediating the postsynaptic effects of OXO-M observed in adult and immature piriform cortical neurones. To this end, selective mAChR antagonists (Table 2.1) were applied after the onset of the depolarizing effect produced by 10 μM OXO-M. The M1-specific mAChR antagonists, pirenzepine (100 nM; adult n=10; immature n=18) (Brown *et al.*, 1980; Susskand & Sewing, 1979) and telenzepine (20 nM; adult n=11; immature n=21) (Londong, 1986) and the M2-specific antagonists, AFDX-116 (1 μM; adult n=13; immature n=17) (Londong, 1986) and methoctramine (300 nM; adult n=11; immature n=19) (Melchiorre *et al.*, 1987) were used. In both adult (Fig. 3.20A) and immature (Fig. 3.20B) neurones, the postsynaptic effects of OXO-M (repetitive firing, increased input resistance and epileptiform bursting in immature neurones) were consistently abolished within 15 minutes of applying M1-specific mAChR antagonists, but not after applying M2-specific mAChR antagonists (not shown) thereby confirming that these effects were mediated via mAChRs of the M1-subtype. Both pirenzepine and telenzepine also abolished the superimposed spike firing induced by OXO-M and caused a reappearance of the sAHP (Fig. 3.21A) during the first few seconds following the long depolarizing stimulus, superimposed on the sADP. In contrast, M2 antagonists had no effect upon muscarinic spike firing, the sADP or its underlying inward tail current (I_{ADP}). Comparable changes occurred, following the application of either M1-specific mAChR antagonist, in the tail currents underlying these potentials, revealing a decrease in mean peak I_{ADP} magnitude (adult: 72 ± 13.2%; n=21; immature 76 ± 15.3%; n=37; no significant difference between adult and immature changes; $P>0.05$; Students'

t-test) and the appearance of a superimposed I_{AHP}/I_{ADP} (Fig 3.21B). The appearance of both phenomena (sADP and sAHP) can be clearly seen in figure 3.21A, where the hyperpolarizing component dominated the early (~8 s) part of the post-stimulus afterpotential followed by a later depolarizing component (shown by * in Fig 3.21A). The effects of OXO-M upon all characterised neurone types were also blocked, within 5 minutes, upon application of the non-selective mAChR antagonist, atropine (n=15; 1 μM; Fig 3.15B), thereby confirming that effects seen are entirely mAChR-mediated (since OXO-M has been shown to have some nicotinic ACh receptor agonistic activity (Reitstetter *et al.*, 1994)).

3.5 Effects of a range of anticonvulsants on OXO-M induced epileptiform burst firing

A previous study (Postlethwaite *et al.*, 1998a) describing OXO-M induced epileptiform bursting in the immature rat piriform cortex only investigated the effect of a single anticonvulsant, phenobarbitone (100 μM), upon the bursting phenomenon. In order to characterize the antiepileptic profile of this epileptiform activity and to investigate whether it showed similar pharmacological characteristics to other *in vitro* models of epilepsy, a number of antiepileptic drugs (AEDs) were screened for their effectiveness against the bursting activity and also the sADP. Each AED investigated was bath-applied (at concentrations equivalent to serum concentrations measured in clinical epilepsy trials) onto recorded deep pyramidal cortical neurones exhibiting established bursting behaviour in the continued presence of 10 μM OXO-M. Results showing the effects of AEDs on synaptic transmission are described in chapter 6.

3.5.1 Gabapentin

Gabapentin (1-(aminomethyl)-cyclohexaneacetic acid; GPN; 30 μM; n=11) has been shown to bind with high affinity to the alpha(2)delta-1 subunit of voltage-dependent Ca^{2+} channels in certain subgroups of excitatory and inhibitory neurones, thereby inhibiting the release of neurotransmitter and, dependent upon the neurones type inhibited, suppressing excitatory or inhibitory synaptic transmission (van Hooft *et al.*, 2002) and is used clinically in the treatment of partial and generalised tonic-clonic seizures (Ramsay, 1993). Within ~10 minutes following bath application of gabapentin, OXO-M induced epileptiform bursting was completely abolished in all recorded neurones (11/11; Fig. 3.22A). The depolarized membrane potential and the increased input resistance induced by OXO-M both returned to control levels, whilst the mean

amplitude of the sADP elicited was reduced by 53.5 ± 4.7 %, with a corresponding decrease in the elicited I_{ADP} (Fig. 3.22B).

3.5.2 Lamotrigine

Lamotrigine (6-[2,3-dichlorophenyl]-1,2,4-triazine-3,5-diamine; LTG; 2 μM; n=5) is used clinically in the treatment of partial onset seizures, generalised tonic-clonic seizures and refractory partial seizures and is thought to act by blockade of presynaptic voltage-dependent Na^+ channels (Upton, 1994). It has more recently been shown to inhibit the slow inactivated Na^+ channel thereby acting selectively against high frequency epileptiform discharges (Schacter, 1995). Within ~8 minutes following bath-application of LTG to all bursting neurones investigated (5/5), OXO-M induced epileptiform activity was completely abolished and membrane potential and input resistance returned to control levels (Fig. 3.23A). The mean sADP magnitude was diminished by 23.2 ± 6.8 % and its time course reduced from ~40 s to ~ 5s (Fig. 3.23B). Additionally, the spiking superimposed on the sADP was abolished in the presence of LTG (Fig. 3.23B).

3.5.3 Topiramate

Topiramate (2,3:4,5-bis-O-(1-methylethylidene)-β-D-fructopyranose sulfamate; TPM; 20 μM; n=14) is a novel anticonvulsant drug used as an adjunctive therapy for patients with refractory partial and secondarily generalized seizures ((Shank *et al.*, 2000). TPM has been shown affect voltage-activated Na^+ channels in a state-dependent manner similar to the effect of carbamazepine (Section 3.5.4). Moreover, it has also been shown to affect the activity of some voltage-dependent Ca^{2+} channels (Shank *et al.*, 2000), $GABA_A$-receptors (Rogawski & Porter, 1990) and AMPA/kainate neuronal ion channels (Pina-Garza & McLean, 1996) whilst also weakly inhibiting some isozymes of carbonic anhydrase (Dodgson *et al.*, 2000). Within ~5 minutes following bath-application of TPM to nearly all bursting neurones investigated (13/14), OXO-M induced activity was abolished (Fig. 3.24A), the increased input resistance was reversed to control levels, although the cell membrane hyperpolarized to a mean 11 ± 2.1 mV more negative than the control resting membrane potential (*cf.* (Russo & Constanti, 2002). (Fig 3.24B) The sADP was also abolished and replaced by a sAHP (Fig. 3.27B) of significantly larger mean amplitude (8.8 ± 2.1 %; $P<0.05$; Students' t-test) and longer duration (16 ± 4.8 %; $P<0.05$; Students' t-test) than that elicited in control conditions prior to the application of OXO-M (not shown) (Russo & Constanti, 2002).

3.5.4 Carbamazepine

Carbamazepine (5-carbamyl-5H-dibenz-[b,f]-azepine; CBZ; 50 μM; n=11) is an antiepileptic with a long history of successful clinical use. CBZ exerts its anticonvulsant effect by means of binding to voltage-dependent Na^+ channels whilst in their inactive state (state-dependent), thereby prolonging the duration of this state (Schacter, 1995). It is used in the treatment of partial and generalised seizures and sometimes in the treatment of trigeminal neuralgia and affective disorders. Within ~8 minutes following bath application of CBZ to all bursting neurones investigated (11/11), OXO-M induced bursting was abolished and the membrane potential and increased input resistance both returned to control levels (Fig. 3.25A). Interestingly, in the presence of carbamazepine, the magnitude of the sADP was reduced by and average of 61 ± 8.6 % (Fig. 3.25B).

3.5.5 Felbamate

Felbamate (2-phenyl-1,3-propanediol dicarbamate; FBM; 300 μM; n=5) is used clinically in the treatment of partial and secondary generalised tonic-clonic seizures, Lennox-Gestaut syndrome and some absence seizures. It is currently believed to exert its effect through NMDA receptor blockade. However, other possible mechanisms of action have been proposed although it remains unclear whether they are significant to the anticonvulsant effect of FBM (Libri *et al.*, 1996). These effects include the blockade of voltage-dependent Na^+ channels, Ca^{2+} channels, potentiation of GABA-mediated inhibition, inhibition of carbonic anhydrase and adenosine uptake (Burdette & Sackellares, 1994). Within ~10 minutes following bath-application of FBM to all 5 of the bursting neurones investigated, the muscarinic bursting was abolished (Fig. 3.26A) and the membrane potential and input resistance both returned to control levels. The evoked sADP in felbamate was diminished in magnitude (53 ± 8%), although its time course was unaffected (Fig. 3.26B). These results are comparable with those previously reported by Libri *et al.* on the muscarinic sADP in adult guinea-pig piriform cortical neurones.

3.5.6 Phenobarbitone sodium

Phenobarbitone sodium (sodium 5-ethyl-5-phenylbarbiturate; PBN; 50 μM; n=6), like CBZ is one of the older established anticonvulsants that has been used to treat partial and generalised seizures. It exerts its effect by binding to GABA-gated Cl^- channels when in an '*open*' state and thereby prolonging channel lifetime (Upton, 1994). In contrast with the other AEDs tested, within ~15 minutes following bath-application of

PBN, OXO-M induced bursting was gradually abolished in only 66% (4/6) of neurones investigated, the membrane potential returned to a more hyperpolarized level (-77 ± 2.1 mV), but did not reach the original control value (Fig. 3.27A). More interestingly, the increased input resistance and the magnitude and duration of the elicited sADP were *unaffected* by PBN (Fig. 3.27B). In the neurones that did not respond to PBN (2/6), no effects upon epileptiform burst firing, membrane potential or sADP generation were observed. Although PBN was clearly the least effective of the AEDs tested, its ability to abolish burst firing in some recorded cells whilst having no effect upon sADP magnitude does raise the question of whether the sADP is linked to burst firing. However, of the other AEDs tested, all abolished burst firing *and* diminished the sADP, which would suggest some link between the phenomena may be present. Additionally, PBN was the least effective of the AEDs, abolishing burst firing only occasionally, with slower onset and never fully reversing it. It may be that the sADP and burst firing are linked, but burst firing is the first of the phenomena to disappear. Thus, the sADP may be dependent on a greater number of sensitive factors than the sADP, but the two phenomena still share many of the same generative factors. Therefore it remains plausible that the sADP is linked with burst firing despite these contrary observations following the application of PBN.

3.5.7 Summary of AED effects

This section has clearly shown that the mAChR agonist-induced epileptiform bursting is susceptible to abolition by a number of commonly used AEDs. Using the magnitude of the sADP and the time taken to abolish burst firing as measures of anticonvulsant efficacy (Table 3.4) comparisons between different AEDs could be made and a possible categorization for the mAChR agonist-induced immature piriform cortical model of epilepsy proposed (Section 3.8.7).

3.6 A possible role for intrinsic cholinergic 'tone' in epileptogenic burst generation

Since mAChR receptor activation has been clearly shown to initiate the bursting phenomenon in immature piriform cortical brain slices (Postlethwaite *et al.*, 1998a) (Section 3.4.4), an attempt was made to determine whether endogenous ACh levels in the slice preparation, arising from intrinsic cholinergic nerve terminals from the nucleus of the diagonal band (Eckenstein *et al.*, 1988; Saper, 1985), were sufficient to induce epileptiform behaviour similar to that seen following the application of OXO-M with a acetylcholinesterase inhibitor.

3.6.1 Postsynaptic effects of neostigmine incubation

The possible effects of endogenous ACh were investigated by using the acetylcholinesterase inhibitor, neostigmine (NEO; 10-30 μM) in an attempt to increase the endogenously released extracellular ACh levels within the slice preparation (n=19). Six adult and 13 immature slices were tested. OXO-M (10 μM) was also applied at the end of each experiment (following a 40 minute NEO washout period) in order to determine whether the neurone was capable of displaying OXO-M-induced spontaneous epileptiform activity. In both adult and immature recorded neurones, NEO caused a small slow depolarization (adult: 5 ± 2.1 mV; immature: 7 ± 2.6 mV; 40 minutes after application of NEO; $P>0.05$) and an increase in baseline noise (Fig. 3.28B). The rate of depolarization was slower than that seen with OXO-M, presumably due to the fact that NEO was not exerting a direct agonistic effect upon mAChRs, but preventing the breakdown of endogenously released ACh within the slice and thus raising levels of the naturally occurring neurotransmitter. An increase in spike firing frequency in response to depolarizing electrotonic stimuli, with no accommodation, was consistently seen in neurones from both adult (not shown) and immature slices (Fig. 3.28A). This was accompanied by a slight increase in input resistance that was significantly larger in the immature (31.6 ± 8.2 MΩ; n=13) than the adult (13.2 ± 4.2 MΩ; n=6; $P<0.05$ Students' t-test) preparation, as illustrated by the increase in amplitude of negative electrotonic deflections induced by negative current stimulation (Fig. 3.28B). Additionally, the mean sAHP elicited from both adult and immature neurones incubated with NEO was diminished by 31 ± 8.1 % (n=19) with a corresponding 75 ± 13.3 % (n=19) decrease in their time course (Fig 3.29). However, a transformation to a sADP or induction of spontaneous epileptiform bursting was never seen in either adult or immature cells. All the observed effects of NEO were fully reversible upon washout (minimum 40 minutes) and were blocked by atropine (1 μM; immature: n=6; adult: n=4; data not shown) confirming their muscarinic nature. These results indicate that after cholinesterase inhibition, sufficient endogenous ACh is available within the slice preparation to produce effects similar (although not of the same magnitude) to those produced by OXO-M. Although burst firing was never induced, it remains a physiological possibility that, *in vivo,* if a disorder within this brain area produced a significant increase in neuronal excitability (or local decrease in inhibition), the intrinsic cholinergic system within the PC could contribute to the initiation of epileptiform activity.

3.6.2 Long term effects of OXO-M incubation

In four of the thirteen immature neurones recorded from, the effect of OXO-M was tested *prior* to the application of neostigmine. Surprisingly, these neurones showed an enhanced response to NEO (*i.e.* a greater degree of depolarization (9 ± 2.8 mV; n=4), greater reduction in mean sAHP amplitude (48 ± 9.3 %) but similar corresponding decrease (79 ± 11.5 %) in sAHP time course to NEO applied alone. This may indicate a long-term effect of OXO-M that persists after washout of the drug that may add to or enhance the effect of NEO, that is similar to a report that has previously shown OXO-M to induce a form of long term potentiation of neuronal evoked responses in rat sensorimotor cortex (Lin & Phillis, 1991). This potentiation of the effect of NEO was never sufficient to induce epileptiform bursting.

3.7 Histological staining in the piriform cortex

3.7.1 Methylene blue staining

Transverse sections of the same orientation as used for intracellular recording, but of 30–150 μm thickness were also cut for methylene blue staining (Methods 2.8.2) in order to reveal the basic morphology of the cell layers. Slices of varying thickness were stained to determine the optimum section thickness for good visualization, whilst maintaining the structural integrity of the slice; consequently slices of 50 μm were most frequently used. Figure 3.30 shows the laminar distribution of the cell layers within the piriform cortex at different levels of magnification. The relatively cell-free layer I (Fig. 3.30; 2 and 3) containing the LOT afferents and association fibres can clearly be seen above the densely (compact) packed cell layer II (Fig 3.30; 4 and at higher magnification in Fig 3.31A), with the more sparsely-populated layer III (Fig 3.30; 5 and at higher magnification in Fig 3.31B) below and the underlying endopiriform nucleus (sometimes termed layer IV (Hoffman & Haberly, 1996a)) below that. No observable differences between sections prepared from adult or immature tissue were observed.

3.8 Discussion

The initial results presented in this section of this report essentially confirm the previously reported findings detailing the electrophysiologically recorded membrane properties of the principal neurone types present in the piriform cortex in control conditions and in the presence of OXO-M (Libri *et al.*, 1994; Protopapas & Bower, 2000; Tseng & Haberly, 1989c; Tseng & Haberly, 1989d), and also the epileptiform activity generated in immature, presumed deep pyramidal neurones by mAChR activation (Postlethwaite *et al.*, 1998a). The data clearly demonstrate significant differences exist between the electrophysiological response characteristics of different cell types in both adult and immature slices (*e.g.* lower input resistance of superficial compared to deep pyramidal cells; Table 3.1), and between the responses of individual adult and immature cell types (*e.g.* presence of a slow inward rectifier in immature *vs.* adult deep neurones). Investigation of these differences (in conjunction with differences in synaptic transmission (Chapter 4) is hoped to lead to a greater understanding of the mechanisms underlying the novel mAChR agonist-induced epileptiform bursting observed in the immature piriform cortical slice preparation, the general high susceptibility of this brain area to epileptiform activity (for a review, see (Loscher & Ebert, 1996)) and a more detailed knowledge of the neuronal circuitry that makes up the piriform cortex (Hasselmo *et al.*, 1990).

3.8.1 Comparability of control electrophysiological responses from the principal piriform cortical cell types in adult and immature slices

The control responses of recorded superficial pyramidal neurones in both adult and immature slices differed from those of corresponding interneuronal and deep pyramidal neurones (Section 3.2), in a manner consistent with a lower degree of excitability and an inability support either slow afterdepolarizations or epileptiform burst firing in OXO-M. Control responses elicited from superficial pyramidal cells, in this and previous investigations (Libri *et al.*, 1994), demonstrated a lower input resistance, strong spike accommodation, spike fractionation and no sAHP. These are all factors that suggest this cell group strongly adapts to excitatory stimuli. Contrastingly, interneuronal and deep pyramidal cells both had membrane properties consistent with being strongly responsive to excitatory stimuli (*i.e.* little spike accommodation, no fractionation, greater input resistance and the ability to elicit muscarinic sADPs) that makes them more prone to further spike discharges following a stimulus than superficial pyramidal cells. This relative unresponsiveness of piriform cortical superficial pyramidal cells has previously

been attributed to a relative lack of cellular Ca^{2+} channels, since they have been shown to be incapable of generating full Ca^{2+} spikes following intracellular Cs^{+} loading (Tseng & Haberly, 1989d). This would reduce the likelihood of the occurrence of repetitive spike firing and also suggest one reason for the absence of a prominent sADP in these cells (Constanti *et al.*, 1985). A number of pertinent differences in cellular excitability were also observed between adult and immature interneuronal and deep pyramidal cells. The absence of any fAHP, following spike firing, in deep pyramidal cells would increase the probability of further spike firing. Additionally, the slow inwardly rectifying current (I_{Slow}) (Sciancalepore & Constanti, 1998) (suggested to be similar to the h-current and linked to cAMP turnover (Dickson *et al.*, 2000, Luthi & McCormick, 1999, Luthi & McCormick, 1998) was observed in immature deep pyramidal, but not interneuronal recordings. This current is thought to be responsible for the post-stimulus rebound electrotonic depolarization elicited in response to negative current stimuli observed in deep pyramidal neurones, and the incidence of this current has subsequently been suggested to be age-dependent (Sciancalepore & Constanti, 1998). These observations were confirmed in this study and more significantly, a role proposed for this current in '*controlling the spontaneous discharge properties of young cells*' and '*counteracting excessive hyperpolarization*' (Sciancalepore & Constanti, 1998) supports the observed increased excitability observed in recordings from immature deep pyramidal cells.

The results of the present study are also consistent with similar behaviour described in immature rat neocortical (Zhou & Hablitz, 1996) and adult mouse sensory ganglion neurones (Mayer & Westbrook, 1983). It may also be significant that the observed incidence of I_{Slow} in immature deep cells (74%) was very similar to the incidence of mAChR agonist-induced epileptiform bursting (63%). Additionally, the mean magnitude of the sAHP elicited from immature interneurones was also significantly smaller than the mean amplitude measured in immature deep pyramidal cells (Table 3.2). This observation appeared to be closely linked to the different magnitude of the sADPs elicited (in the presence of OXO-M) in interneuronal and deep pyramidal cells, the proposed role of which is closely linked to burst firing (Section 3.8.2). All of these factors suggest that the immature deep pyramidal cells are more prone to persistent excitation and, may be more likely to be susceptible to the induction of epileptiform bursting.

3.8.2 Comparability of postsynaptic OXO-M responses and epileptiform burst firing with previous studies

The electrophysiological responses of the principal recorded cell types to the application of OXO-M, such as the slow depolarization (brought about by $I_{K,Leak}$ and I_M current blockade (Womble & Moises, 1992) and an increase in the Ca^{2+}-activated non-specific conductance (Andrade, 1991)), increased input resistance and repetitive (adult) or epileptiform (immature) firing were essentially the same as described in previous investigations (Libri *et al.*, 1994) (Postlethwaite *et al.*, 1998a) (Hasselmo & Bower, 1992), although a small number of distinct discrepancies were noted and consequently, additional analyses were performed on the data obtained in this study. The responsiveness of superficial pyramidal cells to mAChR activation was minimal, in keeping with the absence of any repetitive (or burst) firing or sADP generation in these cells. Similarly to the results detailed above, the differences between the responses of interneuronal and deep pyramidal cells were slight (in comparison to superficial pyramidal neurones) but nonetheless present. The magnitude of the I_{ADP} elicited from interneurones was consistently significantly smaller than that from deep pyramidal cells. It has been suggested that the mAChR agonist-induced sADP (and the underlying slow inward tail current, I_{ADP}) may be responsible for increasing the probability that a neurone will fire *if it has already fired recently*, thereby implying a potential role in memory, recall and epileptiform processes (Constanti *et al.*, 1993). The slow activation and deactivation kinetics of this phenomenon also suggest that it may be involved with the oscillatory processes underlying OXO-M-induced epileptiform burst firing in this area, since mAChR activation is a prerequisite for the generation of both phenomena. Thus, the larger sADP evoked in immature deep pyramidal neurones may make the cells prone to the creation of a self-sustaining firing environment in which the recorded cell displays epileptiform activity, whereas the smaller sADP observed in immature interneurones may not provide a sufficiant magnitude or long activation/deactivation cycle to sustain burst firing. Generation of a sADP alone is unlikely to be sufficient to produce burst firing (since the muscarinic bursting phenomenon was never seen in adult deep pyramidal neurones where the sADP is present), suggesting additional factors are involved in epileptogenesis in this area. A possible factor would be a developmental change in synaptic responsiveness (Chapters 4 and 5) coupled with other postsynaptic differences in mAChR responsiveness between adult and immature neurones, such as that illustrated by the variation in the current-voltage plots for adult and immature deep pyramidal cells. These clearly showed a greater muscarinic increase in input resistance

in the immature cells, producing increased cellular excitability and a greater probability for spike firing. This in turn could produce sufficient spike firing for sADP induction, thereby being interdependent on one another in the generation of burst firing behaviour.

3.8.3 Comparison of the proportion of recorded burst firing neurones with that reported by Postlethwaite *et al.*

The previous study of mAChR agonist-induced burst firing in the immature piriform cortical slice preparation (Postlethwaite *et al.*, 1998a) reported a lower (~40%) incidence of burst firing than the present study (63%). This disparity may be because Postlethwaite *et al.* (1998) did not separate results obtained from animals into individual ages, but instead placed data into two arbitrary groups (P+16 *to* P+22 and P>40). This approach may have obscured changes in characteristics of the epileptiform phenomenon that occurred during the period P+16 to P+22. Additionally, in the present study a larger sample population was used, thereby permitting analysis of burst incidence according to specific ages rather than age ranges (Section 3.8.5). If the previous study used a greater proportion of older animals than younger animals, then the results are likely to be skewed such that mean burst incidence appears lower than is actually the case. We have shown a clear decrease in the incidence of burst firing within the age range used by Postlethwaite *et al.* (1998). Additionally, these authors did not indicate the precise location within the slice preparation where the recording microelectrode was placed, other than *'within the olfactory cell layers II-III'*. We have demonstrated here that microelectrode position (anterior-posterior) is critical to the incidence of burst firing (Section 3.8.6).

3.8.4 M1 mAChR involvement in epileptiform burst firing and sADP generation

mAChR agonist-induced epileptiform burst firing was unaffected by the application of the M2 mAChR-specific antagonists, AFDX-116 or methoctramine, but reliably abolished by application of the M1 mAChR-specific antagonists, pirenzepine or telenzepine. This would suggest that the epileptiform burst firing is mediated (if not wholly, then in part) by the M1 mAChR subtype and is consistent with reports of the presence of M1, M2 and M4 mAChRs in the piriform cortex (Caulfield, 1993). However, the M1 mAChR antagonists were slower to abolish the postsynaptic effects of OXO-M than the general mAChR antagonist, atropine (Fig. 3.15B *vs.* Fig. 3.20B) and slower to abolish OXO-M induced immature epileptiform burst firing than adult repetitive firing. Since detailed dose-response curves for antagonist potency were not

plotted in this present study, it would not be appropriate to draw conclusions from the differences in responses obtained by the application of 1 μM atropine and nM amounts of the M1 mAChR-specific antagonists to neurones responding to to mAChR activation. However, the differences observed between the times taken for pirenzepine or telenzepine to abolish immature burst firing and adult repetitive firing would implicate M1 *and* non-M1 mAChR-mediated systems in immature epileptiform burst firing (Section 4.3.3) and warrant the investigation and identification of further pro-convulvsive mechanisms underlying this phenomenon.

3.8.5 Age-related changes in bursting

A number of reports have linked cell immaturity with increased susceptibility and/or frequency of burst incidence not only in the piriform cortex (Gruslin *et al.*, 1999; Libri *et al.*, 1998) but also in the hippocampus (Sperber *et al.*, 1998) and neocortex (Potier & Psarropoulou, 2001). The results of the present study have revealed strong correlations between animal age and a number of epileptiform bursting characteristics. Thus, slices prepared from younger (P+14 to P+17) animals demonstrated burst firing characterized by shorter interburst intervals, PDSs of larger magnitude and shorter burst durations, more frequently than those prepared from older animals (P>24). In the present study, the bursting behaviour of older animal slices was characterized by longer interburst intervals, smaller magnitude PDSs and longer burst durations. The declining trend in burst characteristics is also consistent with the development of the repetitive firing mode of response seen in adult deep pyramidal neurones in response to OXO-M application. This trend suggests that as the animal ages, PDS magnitude would eventually reach zero and the initial spate of firing would become sustained, thereby occluding any persistent mechanisms controlling burst duration (*i.e.* burst duration would be so long that no interburst interval would occur) and manifesting as repetitive firing. Since the phenomenon has been shown to be mAChR-mediated and moreover that, *'in P8 rats, the piriform cortex has attained the adult pattern with fully developed pyramidal cells in layers II and III'* (Valverde & Santacana, 1994), it is reasonable to propose that our observed changes in burst firing behaviour with age are due to changes in either the pre- or post-synaptic mAChR populations or their mechanisms; the developmental changes in mAChR populations are well known (Milburn & Prince, 1993), (Gaiarsa *et al.*, 1995), (Gaiarsa *et al.*, 1994), (Araki *et al.*, 1996), rather than due to gross anatomical differences between adult and immature slices, as was confirmed histologically.

mAChR agonist affinity has also been shown to change from neonatal to mature animals (Soreq *et al.*, 1982), with cellular localization of mAChRs concurrently altering (Rotter *et al.*, 1979). It has also been reported that the expression of mAChRs in young animals and levels of acetylcholinesterase activity are controlled by two separate mechanisms, where expression is modulated according to the development of necessary cholinergic pathways but acetylcholinesterase activity is controlled independent of this (Egozi *et al.*, 1986) It is possible that this could lead to abnormally high ACh, and low acetylcholinesterase levels, making the animal more prone to developing epileptiform seizures. Additionally, populations of rat M1 mAChRs have been shown to reach adult levels by the 28th postnatal day (Tice *et al.*, 1996)), with concurrent changes in mAChR receptor density (Lee *et al.*, 1990), increased receptor-second messenger system coupling (Tan & Costa, 1995), changes in phosphoinositol turnover (linked to mAChRs; see above) (Gonzales & Crews, 1984) and decreased cAMP levels as the animal ages, all indicating an increased tendency towards excitability in younger animals (Araki *et al.*, 1995) and consistent with the results of muscarinic burst firing incidence in the present study. Since epileptiform behaviour is understood to typically arise from an imbalance between inhibitory and excitatory mechanisms, the points above show that a number of mAChR-related developmental changes in the immature brain could give rise to such imbalances. Changes in mAChR localization, mAChR affinity for ligand, variability in mAChR expression rates in different areas and also changes in acetylcholinesterase activity all describe systems in a highly dynamic state, making them far more prone to imbalance and hence contributing to seizure incidence.

3.8.6 Location dependence of epileptiform burst firing

The present study has demonstrated a clear difference in the incidence of mAChR agonist-induced burst firing between different areas rostrocaudally situated along layer III of the piriform cortical slice preparation. The median area, routinely recorded from in the previous study of this phenomenon (Postlethwaite *et al.*, 1998a), was found to produce a lower incidence of epileptiform bursting (63%) than either the anterior (72%) or posterior (85%) areas. The deep piriform cortex (layer III and the endopiriform nucleus) has long been known to be particularly susceptible to epileptogenesis, with a number of studies having reported varied responsiveness to epileptogenesis in different areas of the piriform cortex (Goddard, 1967; Hoffman & Haberly, 1991a; Piredda & Gale, 1985). The majority of these studies took the form of *in vivo* kindling studies (for a review see (Loscher & Ebert, 1996)), with only some using *in vitro* models of epilepsy

(Demir *et al.*, 2000; Hoffman & Haberly, 1989b; Hoffman & Haberly, 1991a). However, of all of these studies, some found the posterior piriform cortex (PPC) to be most prone to bursting activity (Hoffman & Haberly, 1991a; Loscher *et al.*, 1995), whilst others have suggested that the anterior piriform cortex (APC) to be more susceptible (Doherty *et al.*, 2000; Maggio *et al.*, 1993). Despite the disparity of reported epileptogenic responsiveness by these regions of the piriform cortex, the latter reports all demonstrated that the median area shows a lower incidence of epileptiform activity. Additionally, attempts have been made to unify these observations by suggesting that a highly epileptogenic region termed the *area tempestas* (AT) (Piredda & Gale, 1985) may be the common link between the APC and PPC. Interestingly, the AT has also been demonstrated to be even more highly susceptible to epileptiform activity in the immature animal than the adult (Sperber *et al.*, 1998). However, kindling experiments that isolated specific areas of the piriform cortex using lesioning techniques have shown that, despite the extensive excitatory afferent innervation to the AT (from areas such as the entorhinal cortex, PPC, olfactory bulb, amygdaloid nuclear complex, midline thalamic nuclei, dorsal tegmental nucleus, pedunculopontine tegmental nucleus and locus coeruleus) (Browning *et al.*, 1993), the PPC remains the area most critical to the amplification and propagation of paroxysmal activity received by the PC from other brain areas (Gottfried *et al.*, 2002; Litaudon & Cattarelli, 1995; Loscher & Ebert, 1996), thereby confirming the observations seen in this present study, where the greatest incidence of mAChR agonist induced burst firing occurred in the PPC, followed by the APC.

3.8.7 The effect of AEDs on mAChR agonist-induced burst firing

In this study, the effects of a number of traditional (CBZ and PBN) and newer AEDs (GPN, TPM, FBM and LTG) were tested against mAChR agonist-induced epileptiform bursting activity (Section 3.4). Their effects were investigated to determine a possible classification for this *in vitro* epilepsy model by comparing the effects of the AEDs with existing reports of their mechanisms of action (Ramsay, 1993; Ramsay & Slater, 1993; Shank *et al.*, 1994; Upton, 1994) The two measures of effectiveness of the AEDs upon epileptiform activity used in the present study were their speed of abolition of bursting activity and their effect on sADP magnitude, the latter being considered as a possible supporting mechanism for epileptogenesis (Constanti *et al.*, 1993). As previously mentioned, PBN did not have any effect upon sADP magnitude, but did abolish burst firing in 66% of recorded neurones (consistent with the previous report (Postlethwaite *et*

al., 1998a)), thus questioning the validity of using depression of sADP amplitude as a measure of anticonvulsant efficacy. However, since PBN exerts its anticonvulsant effect through the potentiation of endogenous GABA-ergic responses rather than having a direct effect upon neuronal voltage-dependent ion channels (as is the case with the majority of the more effective AEDs screened), the relative ineffectiveness of PBN against the sADP (believed to be mediated by a novel K^+ conductance (Constanti *et al.*, 1993)) is not particularly surprising when considered in conjunction with the role postulated for the sADP in burst generation and maintenance, it seems reasonable to use suppression of sADP magnitude as a measure of anticonvulsant activity since epileptiform activity was also never observed in the absence of the sADP. Our results also showed a clear correlation between time to abolish burst firing and reduction in sADP magnitude (Table 3.4) allowing a simple order of potency to be made (in decreasing order of efficacy); topiramate> carbamazepine> felbamate= gabapentin> lamotrigine> phenobarbitone. The possible reasons for this order of activity are presented below:

3.8.7.1 Topiramate and carbamazepine

Topiramate and carbamazepine are known to act upon voltage-activated Na^+ channels in a state-dependent manner (*i.e.* binding to the channel when it is in the inactivated state) and are both used in generalised seizures (Schacter, 1995; Shank *et al.*, 1994), although topiramate has also been shown to act upon some voltage dependent calcium channels (Shank *et al.*, 2000), $GABA_A$-receptors (Rogawski & Porter, 1990) and AMPA/kainate neuronal ion channels (Pina-Garza & McLean, 1996). Given the additional, more novel anticonvulsant mechanisms of action of topiramate proposed by Russo *et al.* (2000) in the piriform cortex where it *enhanced* the sAHP (Russo & Constanti, 2002), it seems reasonable for it to be found more potent than carbamazepine.

3.8.7.2 Felbamate

Felbamate has been shown to be effective against generalised seizures by acting primarily by NMDA receptor blockade, although other mechanisms of action such as voltage-dependent Na^+ channels blockade and potentiation of GABA-mediated inhibition (Section 3.6.6) have also been proposed (Burdette & Sackellares, 1994). Felbamate has also been previously found to depress the mAChR-induced sADP in the guinea-pig piriform cortex (Libri *et al.*, 1996), by most likely blocking the activity of Ca^{2+} channels. Thus, although not acting directly on Na^+ channels like carbamazepine

or topiramate, the effects of felbamate on postsynaptic Ca^{2+} influx and excitatory and inhibitory transmission were probably sufficient to abolish the observed epileptiform bursting. Additionally, this dual effectiveness further supports the previous suggestion that the bursting is polysynaptically generated (Postlethwaite *et al.*, 1998a); *c.f.* also *in vivo* investigations reporting the effects of focal application of excitatory amino acid antagonists upon epileptiform activity in this brain area (Meldrum *et al.*, 1988; Millan *et al.*, 1986).

3.8.7.3 Gabapentin

Gabapentin is used clinically as an adjunctive therapy in the treatment of partial and generalised tonic-clonic seizures (Ramsay & Slater, 1993) by binding to the alpha2delta-1 subunit of a voltage-dependent presynaptic Ca^{2+}-channel found in brain areas containing major excitatory inputs (Luo Z.D. *et al.*, 2003) and may also limit Na^{+}-dependent action potentials (Upton, 1994). It was moderately effective in abolishing mAChR agonist induced burst firing and inhibting the sADP.

3.8.7.4 Lamotrigine

Lamotrigine is used clinically for the treatment of partial onset seizures, generalised tonic-clonic seizures and refractory partial seizures. It has been shown to act by blockade of presynaptic voltage-dependent Na^{+} channels (Upton, 1994) and by inhibition of the slow inactivated Na^{+} channel (Schacter, 1995), leading to reduced transmitter release and interference with the neuronal circuitry required for epileptiform bursting. However, its modulation of neurotransmitter release is not specific to excitatory neurotransmitters since it has also been shown to inhibit GABA release, which may limit its overall anticonvulsant effect (Leach *et al.*, 1986). Thus, despite having a similar profile to carbamazepine, its potency against specific models of epilepsy may vary depending upon the individual neurone type that it most potently affects in the tissue being tested. It would appear that in our model, lamotrigine is not as effective as the other AEDs that act primarily by Na^{+} channel blockade.

3.8.7.5 Phenobarbitone

Phenobarbitone is one of the oldest AEDs still in clinical use against partial and generalised seizures (Upton, 1994). As has been previously described in detail (this section and Section 3.5.6), phenobarbitone was the least effective of the AEDs tested against this *in vitro* model of epilepsy.

3.8.7.6 Summary of AED effects

From the results presented here, it appears that the mAChR agonist-induced model of epilepsy in the immature rat piriform cortical slice is *least* like those models of epilepsy characterized by their disruption of GABA-ergic systems (Macdonald & Kelly, 1993) and *most* like those models that manifest as generalised tonic-clonic seizures, such as the *in vivo*, kindling-induced, piriform cortical seizure model (Kalimullina *et al.*, 2000).

N.B. See chapter 6 for results and discussion of AED effects upon synaptic transmission.

3.8.8 The effects of neostigmine, on the piriform cortical slice preparation and the physiological relevance of the mAChR agonist-induced *in vitro* model of epileptiform activity

The anticholinesterase, neostigmine, was applied to the immature piriform cortical slice preparation (Section 3.6) to ascertain whether endogenous levels of ACh were sufficient to induce the epileptiform effects produced by OXO-M, a result that would be indicative of the mAChR agonist-induced model of epilepsy being physiologically relevant. The results presented here have shown that the presence of neostigmine is sufficient to raise endogenous ACh concentrations to levels capable of demonstrating mAChR-mediated excitatory effects, although these are by no means as strong as those produced by OXO-M. Neostigmine produced a slow membrane depolarization, increased firing in response to depolarizing electrotonic stimuli, a reduction in sAHP amplitude and time course (comparable to results previously reported in basolateral amygdaloid neurones, *in vitro* (Washburn & Moises, 1992)) and a small increase in input resistance; however, burst firing was never seen, despite the fact that all of the responses listed above are consistent with the effects of low (subthreshold to induce burst firing) concentrations of mAChR agonists (B.W.; unpublished observations) and all of the observed effects were fully reversed by atropine. Neostigmine has previously been shown to inhibit endogenous ACh release by a direct action upon presynaptic nicotinic acetylcholine receptors in rat cerebrocortical slices (Marchi & Raiteri, 1996), an effect that was reversed by the application of atropine, whereupon ACh release was enhanced by the same mechanism and by other means; (Nagata *et al.*, 1997) (Marchi *et al.*, 1990)). Therefore, this down-regulation of ACh release (if present in the PC) may have prevented sufficient endogenous ACh from being released in the slice preparation, thereby inhibiting the mAChR-mediated effects being sought in this investigation. Contrastingly, another anticholinesterase, eserine, has been shown to increase the

frequency of bicuculline-induced epileptiform discharges and reduce recorded evoked field potentials in immature neortical slices (Potier & Psarropoulou, 2001). This effect was again blocked by atropine, indicating a role for mAChRs (and accordingly, endogenous ACh) in burst discharges. The effects produced by neostigmine in our study clearly correlate with those described above by Potier & Psarropoulou, where an overall increase in baseline noise and excitability was seen. Additionally, incubation with eserine alone did not induce epileptiform bursting in their model, but required the presence of bicuculline, which correlates with our observations that the ACh-raising effect of neostigmine alone was insufficient to induce bursting. From the results seen in both studies, it may be reasonable to suggest that although the degree to which endogenous ACh levels were raised (and/or inhibited by the presence of the anticholinesterase) were not sufficient to induce established bursting behaviour, a disease state that raised excitability (or decreased inhibition) within these areas might reduce the threshold for the appearance of burst activity sufficiently for the excitatory effects of mAChR activation to initiate and modulate burst firing. Circumstances of this type that implicate endogenous ACh in the triggering and modulation of seizure activity have been described in monkey (Girgis, 1978; Girgis, 1981) and baboon (Meldrum *et al.*, 1970) amygdala, *in vivo* and more recently, in hybrid mouse strains, *in vivo* (Mark & Finn, 2002) and an immature and adult hippocampal *in vitro* slice preparation (Gruslin *et al.*, 1999).

N.B. See also chapter 4 for the effects of neostigmine on elicited postsynaptic potentials in this preparation.

3.9 Summary

1. Recordings were made from the three principal cell types found in a transverse piriform cortical slice preparation, prepared from a range of rats aged from P+14 (immature) to P>40 (adult), in control conditions and following the application of the mAChR agonist, oxotremorine-M, using conventional, intracellular current and '*hybrid*' voltage clamp techniques.
2. A number of differences between the responses of the principal cell types in the PC recorded from both adult and immature slices were observed. These differences were all found to be consistent with previous reports describing these responses.
3. The responses recorded from the three principal cell types (of both adult and immature animals) in OXO-M (10 μM), were generally comparable with those previously reported.
4. Application of the muscarinic agonist OXO-M (10 μM) to immature piriform cortical slices resulted in the induction of spontaneous epileptiform behaviour in 63% of recorded cells, a significantly higher proportion than previously reported (~40%) (Postlethwaite *et al.*, 1998a).
5. Paroxysmal depolarizing shift magnitude and burst firing incidence were shown to decrease with increasing postnatal age (P+14 to P+28), whilst inter-burst interval and burst duration showed a corresponding increase with postnatal development.
6. Significant variation in the incidence of epileptiform burst firing along the length (rostrocaudally) of piriform cortical layer III of the slice preparation was demonstrated. The posterior piriform cortex showed a higher incidence of burst firing than the anterior piriform cortex, which in turn showed a higher incidence than the median piriform cortex.
7. Use of mAChR subtype-specific antagonists confirmed that the postsynaptic effects of OXO-M were mostly, but not solely, M1 mAChR subtype mediated in both adult and immature deep pyramidal neurones.
8. A number of traditional and newer anti-epileptic drugs (AEDs) were screened against the observed mAChR agonist-induced epileptiform burst firing phenomenon. The relative order of potency of those AEDs tested was (in decreasing order): Topiramate> carbamazepine> felbamate= gabapentin> lamotrigine> phenobarbitone. Possible reasons for the differences in efficacy,

how it was assessed and their implications upon the mechanisms underlying burst firing are discussed.

9. The anticholinesterase, neostigmine, was bath-applied to determine the effects of raising endogenous ACh levels within the slice preparation. Neostigmine (20 μM) was found to produce a slight, but significant depolarization of the cell membrane and an increase in cellular input resistance, abolished on application of atropine (1 μM). Neostigmine incubation was never observed to induce epileptiform burst firing in adult or immature deep pyramidal neurones. These results suggest a modulatory and/or triggering role for ACh in epileptiform events, but indicate the likely requirement of additional seizure-promoting factors for established bursting to occur.
10. Slices stained with methylene blue (50 μm thick) showed no significant differences between the gross structures or morphologies of adult and immature cells in piriform cortical layers II-III.

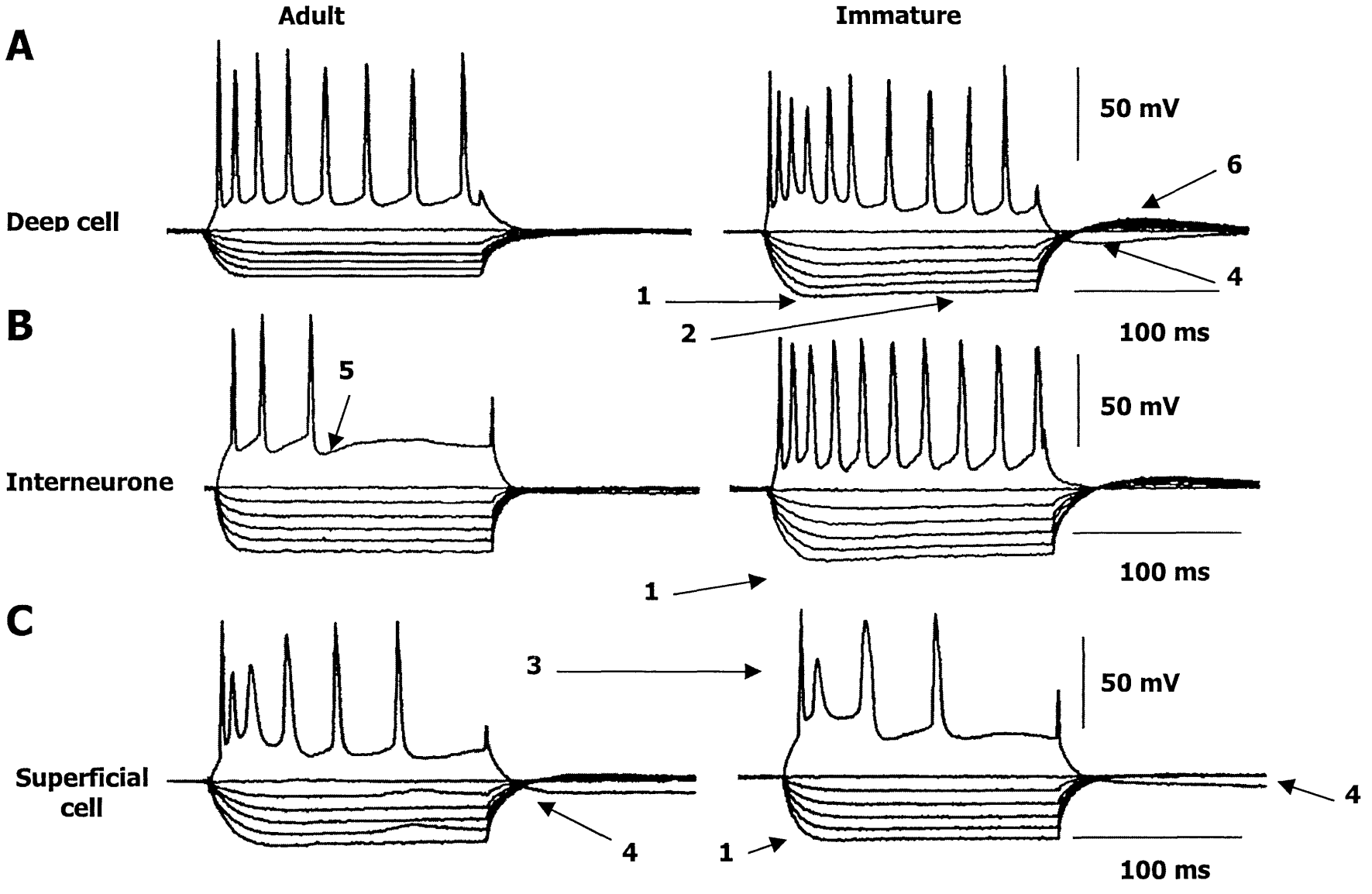
Adult
Immature
A
Deep cell
50 mV
6
4
1
2
100 ms
B
5
Interneurone
50 mV
1
100 ms
C
3
50 mV
Superficial cell
4
4
1
100 ms

Figure 3.1

Figure 3.1

Superimposed depolarizing and hyperpolarizing electrotonic potentials elicited from the three principal cell types found in immature and adult rat piriform cortex. Current pulses applied were in the range of -1.2 to +1.2 nA for a duration of 160 ms. All stimuli illustrated were applied from a holding membrane potential of -80 mV. **A.** Electrotonic responses of piriform cortical presumed 'deep' pyramidal neurones. **(Left)** Adult (P>40) neurone and **(Right)** Immature (P+17) neurone. **B.** Electrotonic responses of piriform cortical presumed interneurones. **(Left)** Adult (P>40) neurone and **(Right)** Immature (P+19) neurone. **C.** Electrotonic responses of piriform cortical presumed superficial pyramidal neurones. **(Left)** Adult (P>40) neurone and **(Right)** Immature (P+21) neurone. Note the following properties: **[1]** – fast inward rectification; **[2]** – slow inward rectification (only shown by immature deep pyramidal neurones and occasionally by immature interneurones); **[3]** – spike fractionation; **[4]** – post stimulus afterhyperpolarization (particularly characteristic of piriform cortical superficial pyramidal neurones); **[5]** – fast after-hyperpolarization (fAHP; characteristic of piriform cortical interneurones); **[6]** – rebound depolarization (characteristic of immature piriform cortical deep pyramidal neurones).

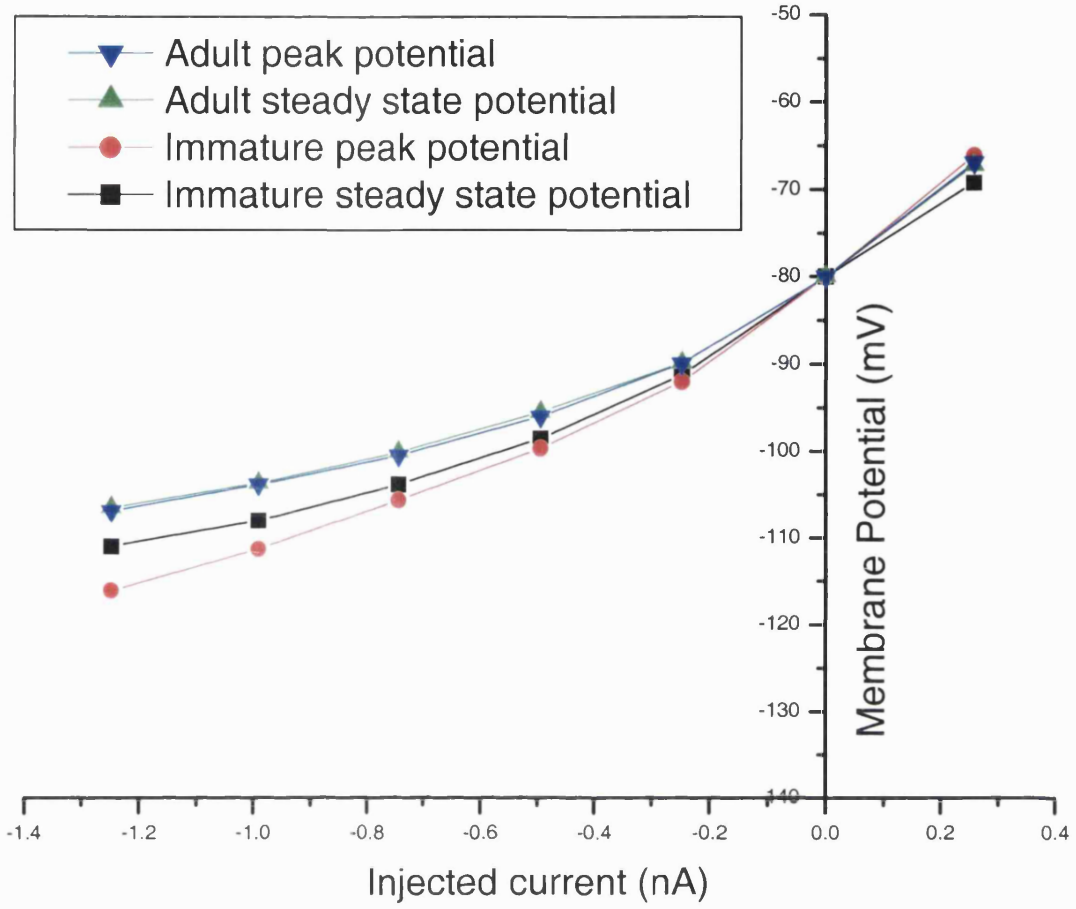
Adult peak potential
Adult steady state potential
Immature peak potential
Immature steady state potential
-50
-60
-70
-80
-90
-100
-110
-120
-130
-140
Membrane Potential (mV)
-1.4
-1.2
-1.0
-0.8
-0.6
-0.4
-0.2
0.0
0.2
0.4
Injected current (nA)

Figure 3.2

Figure 3.2

Current-voltage (I-V) relationships showing variations in membrane potential (ordinate) *vs.* injected current (abscissa) observed in adult (**blue**: peak electrotonic potential amplitude; **green**: peak steady state amplitude) and immature (**red**: peak electrotonic potential amplitude; **black**: steady state amplitude) presumed deep pyramidal neurones. Note the greater slope of the immature I-V plot indicating a typically higher cell input resistance and the significantly larger difference between peak and steady state amplitude of the hyperpolarizing electrotonic potential.

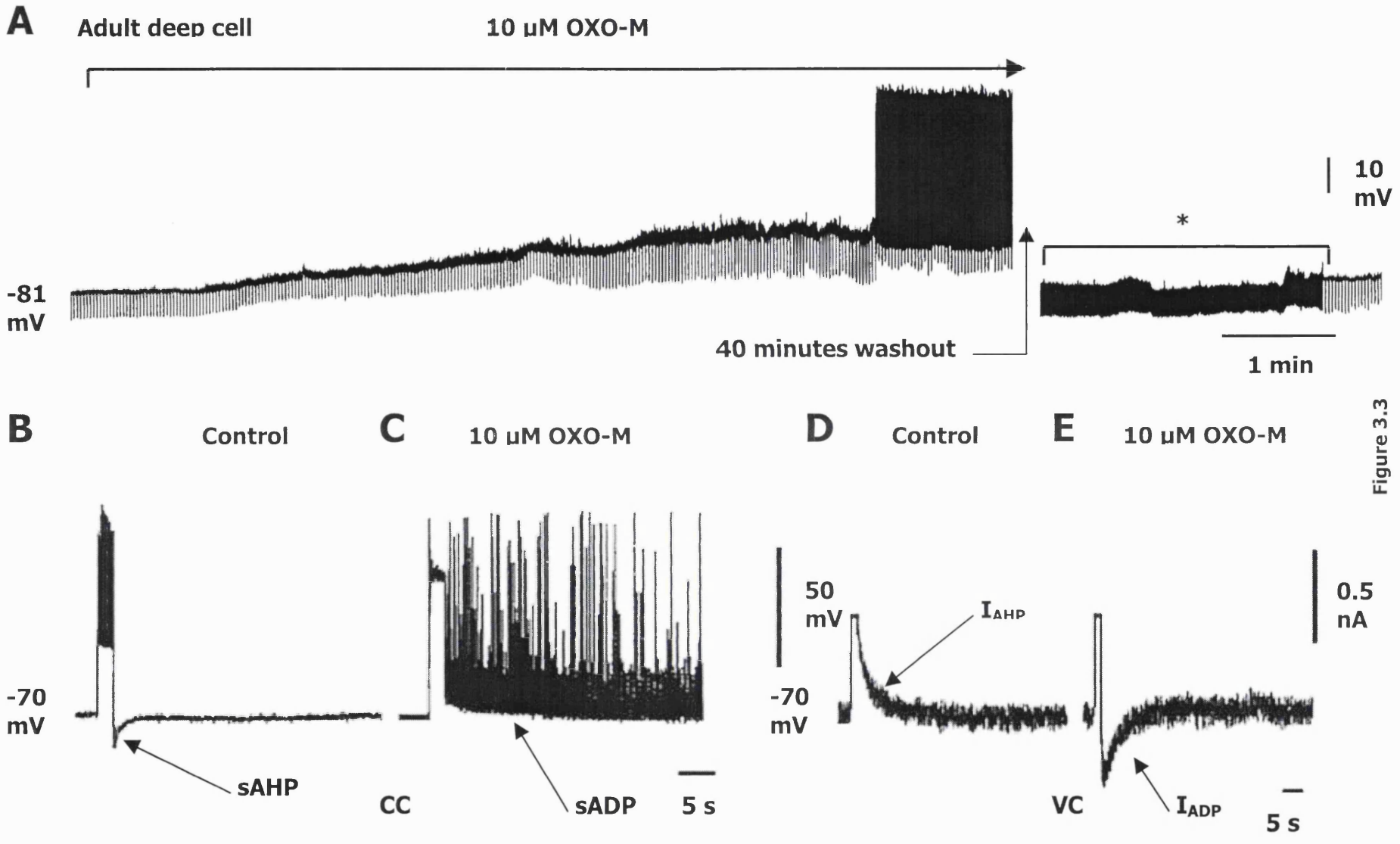
A
Adult deep cell
10 µM OXO-M
10
mV
-81
mV
*
40 minutes washout
1 min
B
Control
C
10 µM OXO-M
D
Control
E
10 µM OXO-M
-70
mV
sAHP
CC
sADP
5 s
50
mV
I_{AHP}
0.5
nA
-70
mV
VC
I_{ADP}
5 s

Figure 3.3

Figure 3.3

The postsynaptic effects of 10 μM OXO-M upon an adult (P>40) presumed deep pyramidal neurone. **A.** Chart record (0.5 mm s^{-1}) showing the effects of OXO-M upon membrane potential and input resistance. Downward deflections are electrotonic responses to 0.1 nA hyperpolarizing stimuli, applied every 2 seconds, to enable real-time observation of any input resistance changes. Approximately 1-2 minutes after application of 10 μM OXO-M, a slow depolarization began, in conjunction with an increase in baseline noise, a small increase in input resistance, followed by the onset of repetitive firing. All these observed effects were reversed after at least 40 minutes washout with OXO-M-free medium; * indicates a 5 times slower chart speed than indicated on the time trace. **B.** A control sAHP elicited following a long depolarizing stimulus train (+2 nA; 1.6 s) applied to the same neurone, maintained at –70 mV (close to threshold potential) in current clamp (CC) mode. **C.** A sADP and associated firing elicited by the same stimulus as **B**, in the presence of 10 μM OXO-M. **D.** The underlying slow outward tail current (I_{AHP}) recorded in 'hybrid' voltage clamp (VC) mode, under control conditions. The response was elicited from a cell held near to threshold (-70 mV) potential, as with the sAHP. **E.** The underlying slow inward tail current (I_{ADP}) revealed in the presence of 10 μM OXO-M, evoked using the same stimulus parameters as in **D**.

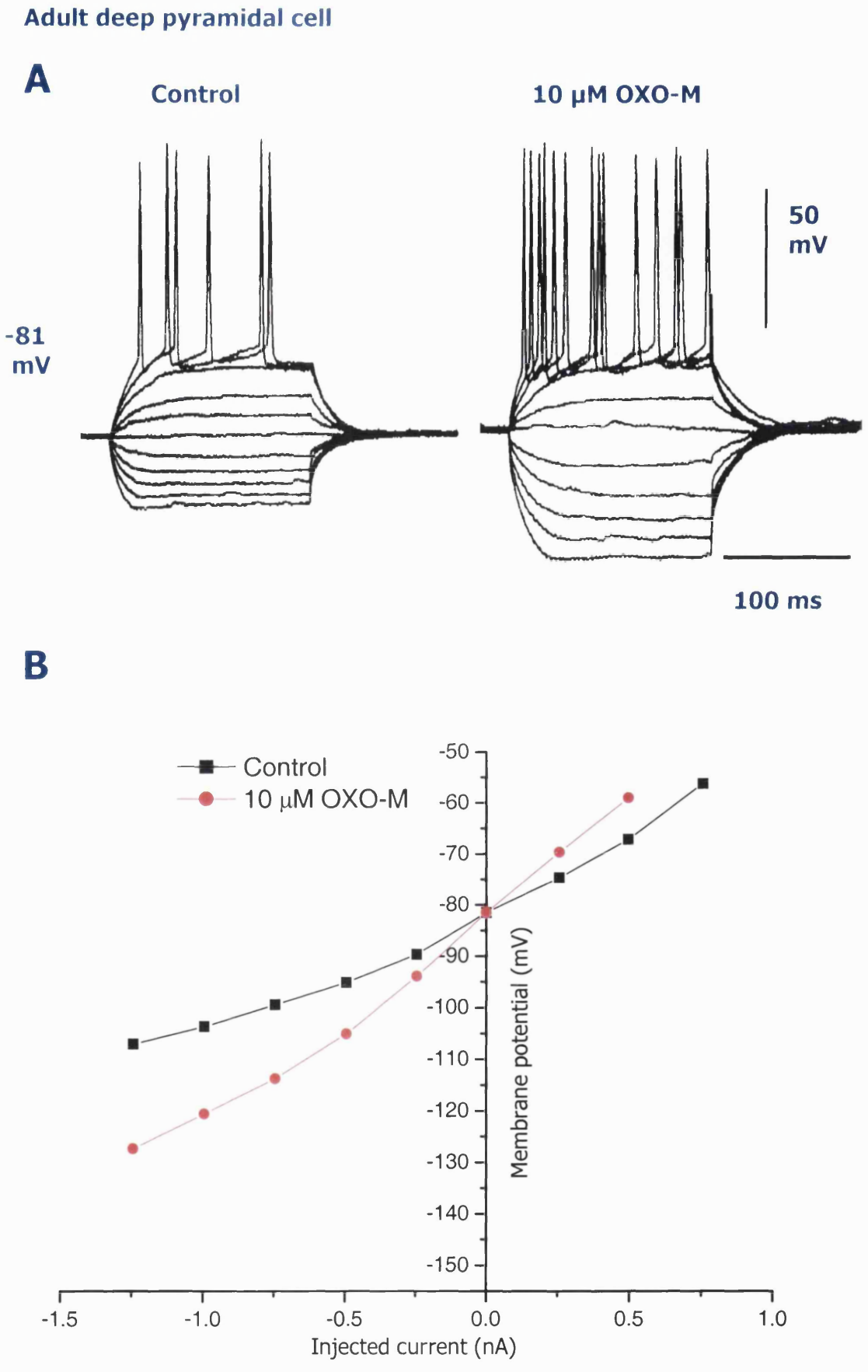
Adult deep pyramidal cell
A
Control
10 µM OXO-M
-81 mV
50 mV
100 ms
B
Control
10 µM OXO-M
-50
-60
-70
-80
-90
-100
-110
-120
-130
-140
-150
Membrane potential (mV)
-1.5
-1.0
-0.5
0.0
0.5
1.0
Injected current (nA)

Figure 3.4

Figure 3.4

Comparison of the effects of 10 μM OXO-M upon the electrotonic properties of an adult 'deep' pyramidal neurone. **A.** Superimposed electrotonic potentials evoked in response to positive and negative current pulses (-1.2 to +1.2 nA; 160 ms) applied in control (**left panel**) and after 15 mins in 10 μM OXO-M (**right panel**). The resting membrane potential in OXO-M was adjusted by application of negative holding current to offset the depolarizing effect of OXO-M prior to eliciting electrotonic responses. Note that in the presence of OXO-M there was an increase in both cell input resistance and firing rate with no observable spike fractionation. **B.** Current-voltage (I-V) relationships showing variations in membrane potential (ordinate) *vs.* injected current (abscissa) observed in the adult deep pyramidal neurone shown in **A** in control conditions (**black**) and in the presence of 10 μM OXO-M (**red**). Note the increased slope of the I-V plot in the presence of OXO-M, indicating increased input resistance in accordance with the greater deflections seen in response to hyperpolarizing stimuli in **A**. Control resting membrane potential=-81 mV.

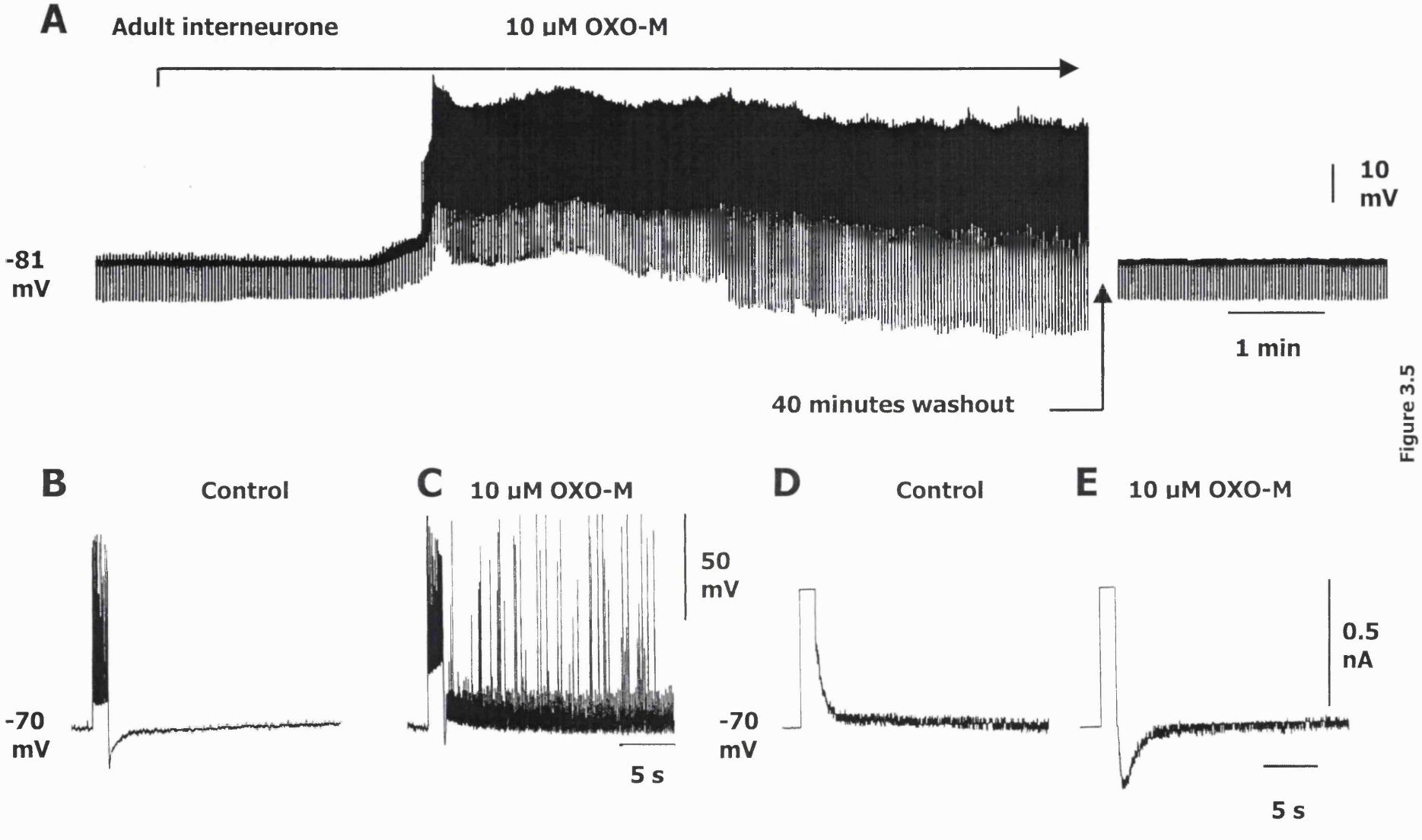
A
Adult interneurone
10 µM OXO-M
-81 mV
10 mV
1 min
40 minutes washout
B
Control
C
10 µM OXO-M
D
Control
E
10 µM OXO-M
-70 mV
50 mV
5 s
-70 mV
0.5 nA
5 s

Figure 3.5

Figure 3.5

The postsynaptic effects of 10 μM OXO-M upon an adult (P>40) piriform cortical presumed interneurone. **A.** Chart record (0.5 mm s^{-1}) showing the effects of OXO-M upon cell membrane potential and input resistance. Downward deflections are electrotonic responses to 0.1 nA hyperpolarizing stimuli, applied every 2 s. As with deep pyramidal neurones, about 1-2 minutes following application of 10 μM OXO-M, a slow depolarization was seen in conjunction with an increase in baseline noise, a small increase in input resistance and repetitive firing (*c.f.* Fig. 3.3). All these observed effects were reversed after at least 40 minutes washout. **B.** A control sAHP elicited following a long depolarizing stimulus train (+2 nA; 1.6 s) applied to the same neurone, maintained at –70 mV (close to threshold potential) in CC mode. **C.** A sADP and associated firing elicited by the same stimulus as **B**, in the presence of 10 μM OXO-M. **D.** The underlying slow outward tail current (I_{AHP}) recorded in 'hybrid' VC mode, under control conditions. The response was elicited from a cell held near to threshold (-70 mV) potential, as with the sAHP. **E.** The underlying slow inward tail current (I_{ADP}) revealed in the presence of 10 μM OXO-M, produced using the same stimulus parameters as **D**.

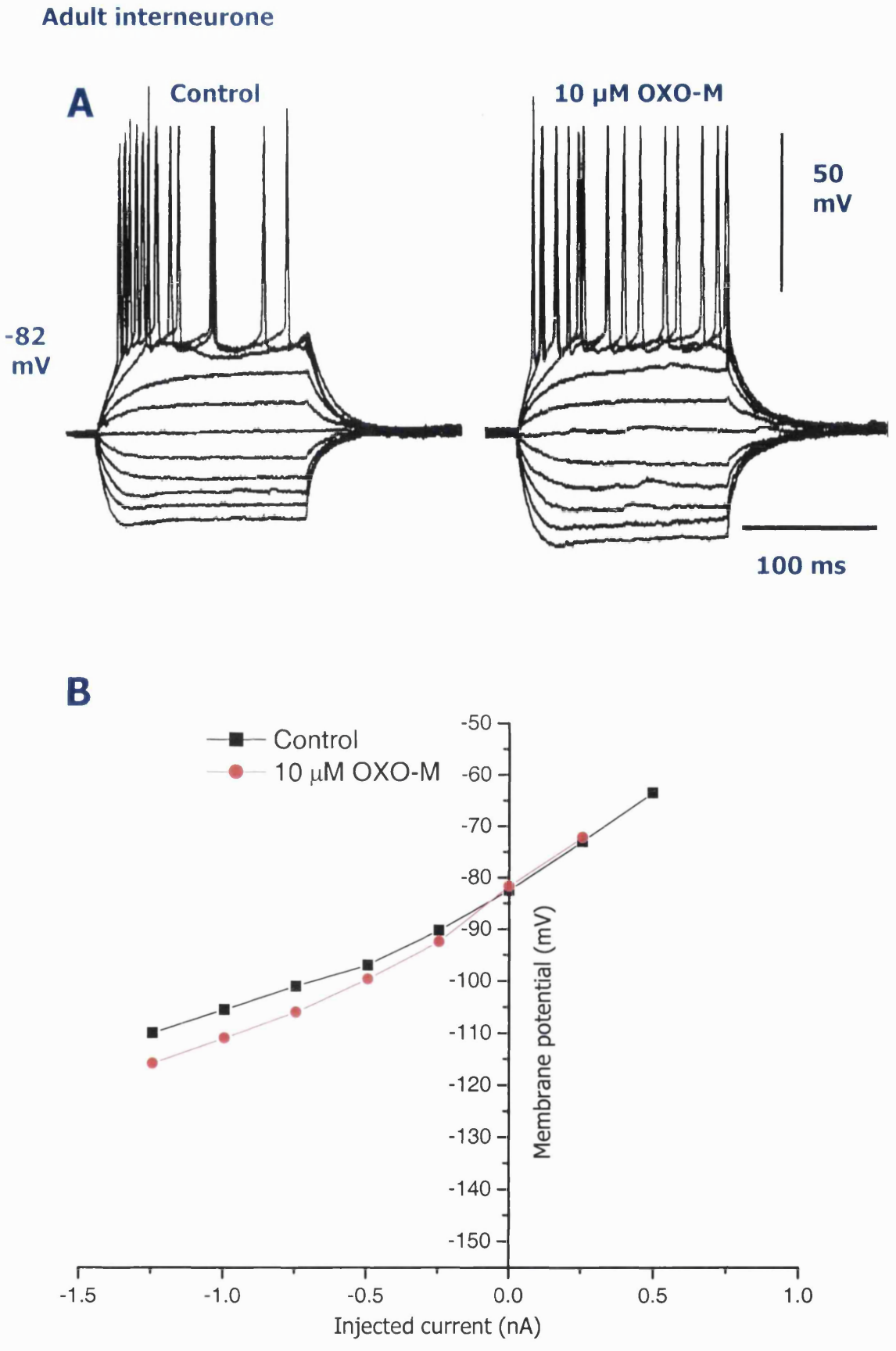
Adult interneurone
A
Control
10 µM OXO-M
50
mV
-82
mV
100 ms
B
Control
10 µM OXO-M
Membrane potential (mV)
-50
-60
-70
-80
-90
-100
-110
-120
-130
-140
-150
-1.5
-1.0
-0.5
0.0
0.5
1.0
Injected current (nA)

Figure 3.6

Figure 3.6

Comparison of the effects of 10 μM OXO-M upon the electrotonic properties of an adult interneurone. **A.** Superimposed electrotonic potentials evoked in response to positive and negative current pulses (-1.2 to +1.2 nA; 160 ms) applied in control (**left panel**) and after 15 mins in 10 μM OXO-M (**right panel**). The resting membrane potential in OXO-M was adjusted by application of negative holding current to offset the depolarizing effect of OXO-M prior to eliciting electrotonic responses. Note that in the presence of OXO-M there was an increase in both cell input resistance and firing rate with no observable spike fractionation. **B.** Current-voltage (I-V) relationships showing variations in membrane potential (ordinate) *vs.* injected current (abscissa) observed in the same adult interneurone shown in **A** in control conditions (**black**) and in the presence of 10 μM OXO-M (**red**). Note the slightly increased slope of the I-V plot in the presence of OXO-M, indicating a small increase in input resistance in accordance with the greater deflections seen in response to hyperpolarizing stimuli in **A**. Control resting membrane potential=-82 mV.

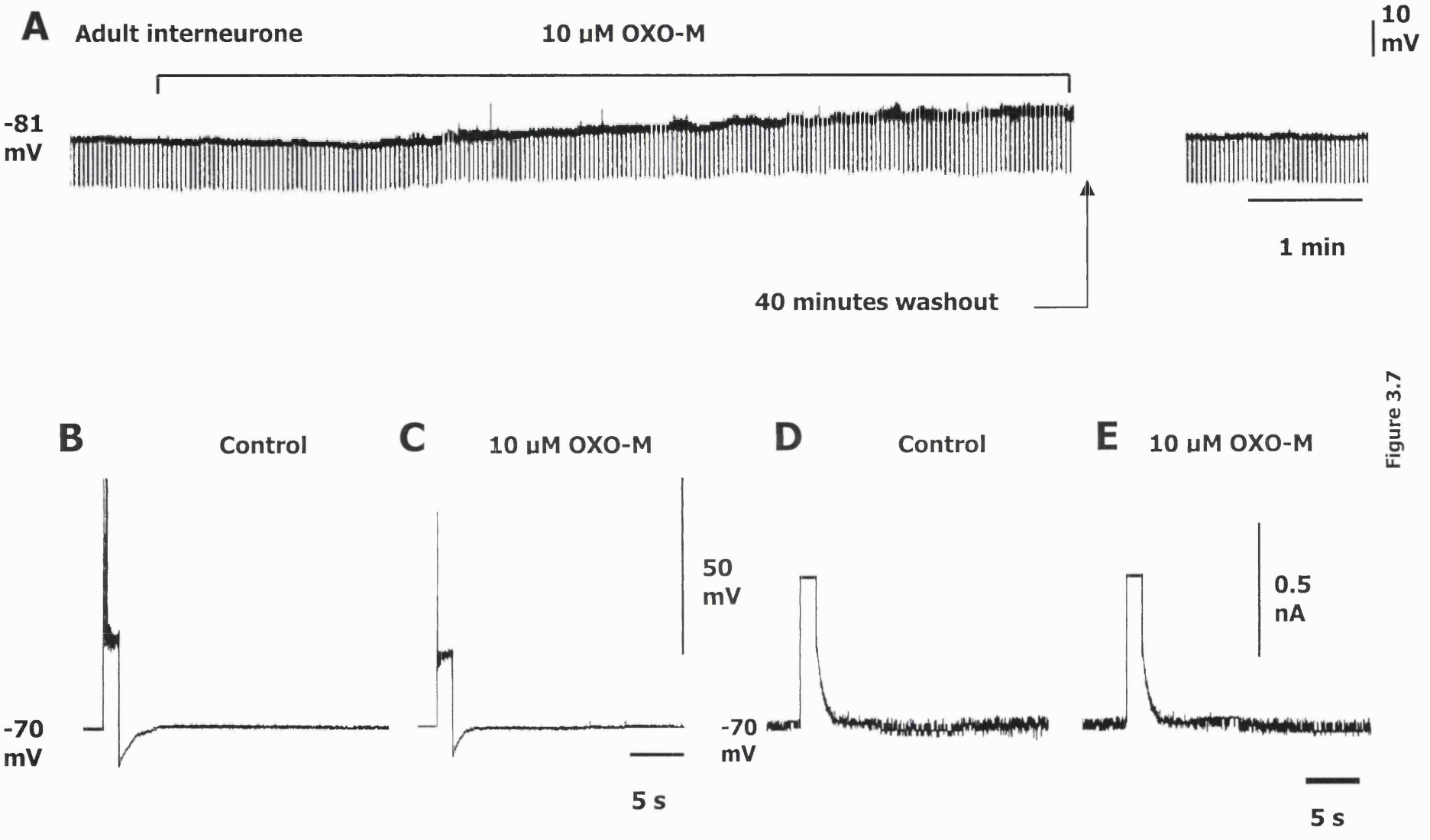
A
Adult interneurone
10 µM OXO-M
10
mV
-81
mV
1 min
40 minutes washout
B
Control
C
10 µM OXO-M
D
Control
E
10 µM OXO-M
50
mV
0.5
nA
-70
mV
-70
mV
5 s
5 s

Figure 3.7

Figure 3.7

The postsynaptic effects of 10 μM OXO-M upon an adult (P>40) piriform cortical presumed superficial pyramidal neurone. **A.** Chart record (0.5 mm s^{-1}) showing the effects of OXO-M upon cell membrane potential and input resistance. Downward deflections are electrotonic responses to 0.1 nA hyperpolarizing stimuli, applied every 2 s. Unlike deep pyramidal and interneurones only a relatively small depolarization and small increase in baseline noise are seen, with no spike firing and little change in input resistance. All the observed effects were reversed after 40 minutes washout. **B.** As with deep pyramidal and interneurones, a sAHP could be elicited following a long depolarizing stimulus (+2 nA; 1.6 s) applied to the same neurone, maintained at –70 mV (close to threshold potential) in CC mode. **C.** However, no sADP or associated firing could be elicited by the same stimulus as **B**, in the presence of 10 μM OXO-M. **D.** The underlying slow outward tail current (I_{AHP}) recorded in 'hybrid' voltage clamp (VC) mode, under control conditions. The response was elicited from a cell held near to threshold (-70 mV) potential, as with the sAHP. **E.** Unlike deep pyramidal cells and interneurones, I_{AHP} remained in the presence of OXO-M and no slow inward tail current (I_{ADP}) was revealed, using the same stimulus parameters as in **D**.

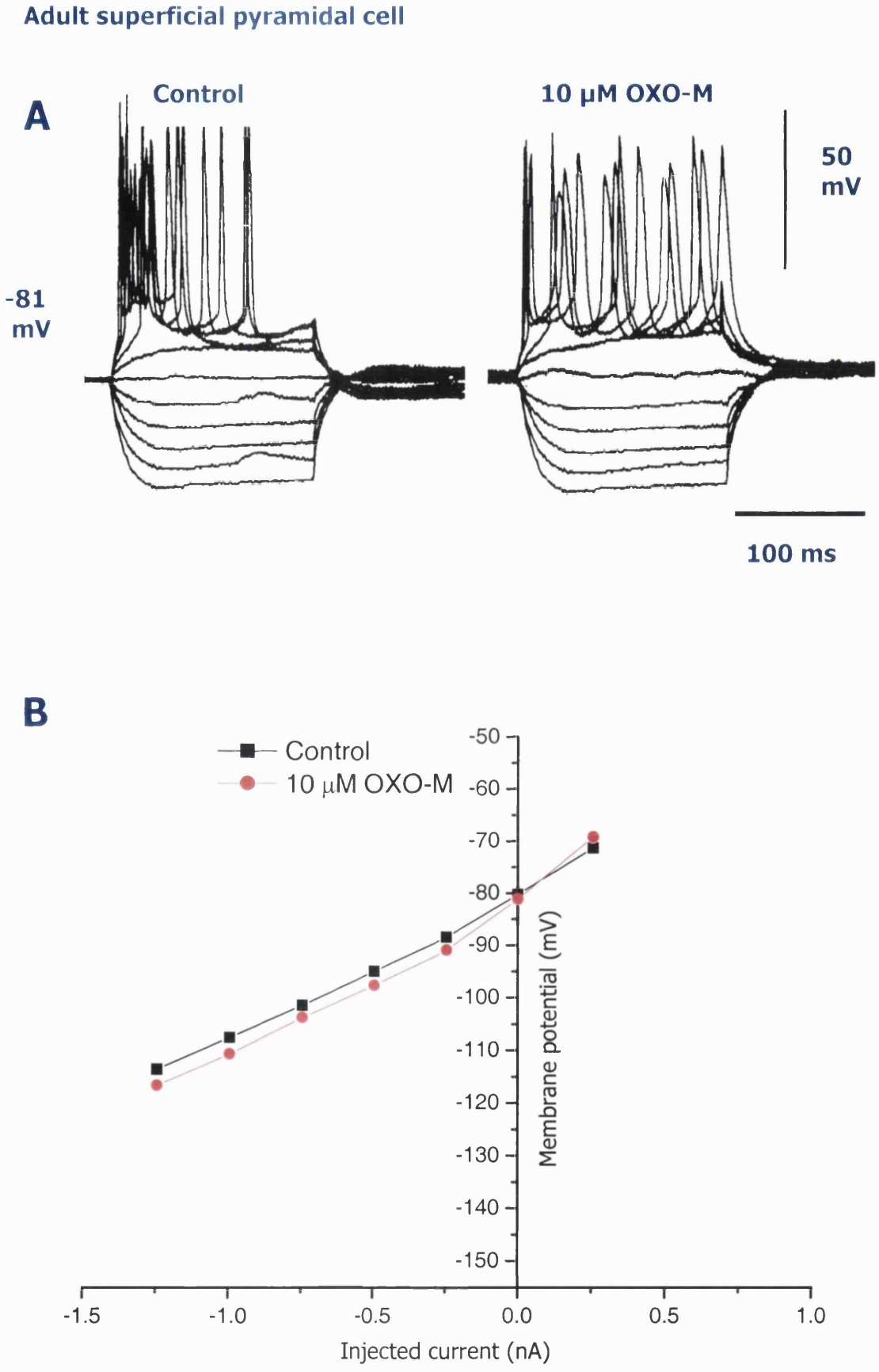
Adult superficial pyramidal cell
A
Control
10 µM OXO-M
50
mV
-81
mV
100 ms
B
Control
10 µM OXO-M
-50
-60
-70
-80
-90
-100
-110
-120
-130
-140
-150
Membrane potential (mV)
-1.5
-1.0
-0.5
0.0
0.5
1.0
Injected current (nA)

Figure 3.8

Figure 3.8

Comparison of the effects of 10 μM OXO-M upon the electrotonic properties of an adult superficial pyramidal cell. **A.** Superimposed electrotonic potentials evoked in response to positive and negative current pulses (-1.2 to +1.2 nA; 160 ms) applied in control (**left panel**) and after 15 mins in 10 μM OXO-M (**right panel**). The resting membrane potential in OXO-M was adjusted by application of negative holding current to offset the depolarizing effect of OXO-M prior to eliciting electrotonic responses. Note that in this case, the presence of OXO-M caused little increase in both cell input resistance and firing rate, but increased spike fractionation (*c.f.* Figs. 3.4 and 3.6). **B.** Current-voltage (I-V) relationships showing variations in membrane potential (ordinate) *vs.* injected current (abscissa) observed in the same adult superficial pyramidal cell shown in **A** in control conditions (**black**) and in the presence of 10 μM OXO-M (**red**). Note the slightly increased slope of the I-V plot in the presence of OXO-M, indicating a small increase in input resistance in accordance with slightly larger deflections seen in response to hyperpolarizing stimuli in **A**. Control resting membrane potential=-81 mV.

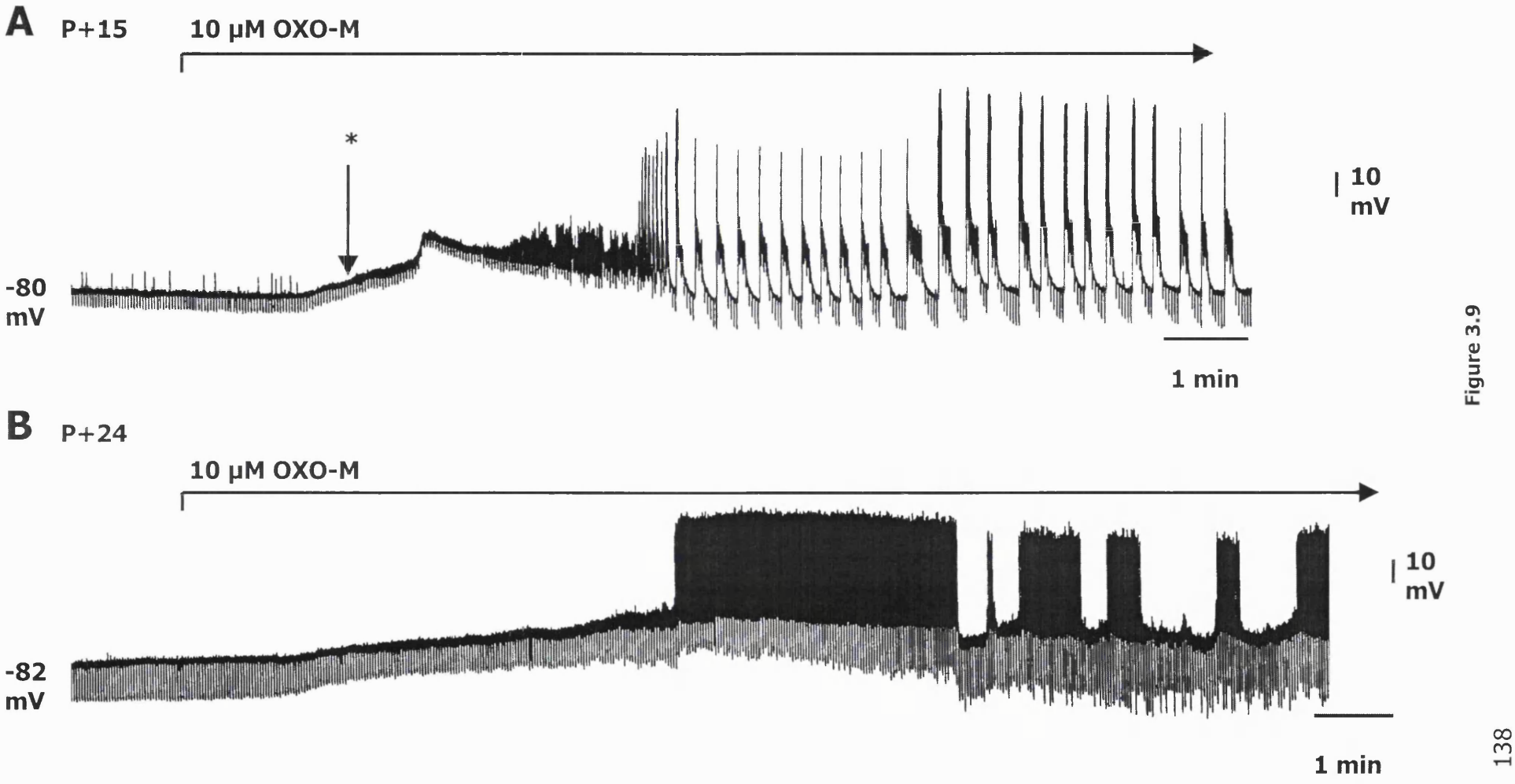
Immature deep pyramidal cells
A
P+15
10 µM OXO-M
*
10 mV
-80 mV
1 min
B
P+24
10 µM OXO-M
10 mV
-82 mV
1 min

Figure 3.9

Figure 3.9

A. Chart trace showing the effect of 10 μM OXO-M upon an immature (P+15) presumed deep pyramidal neurone of a responding cell type, with the development of typical epileptiform burst firing. Control resting membrane potential=-80 mV. **B.** Chart trace showing the effect of 10 μM OXO-M upon an older immature (P+24) presumed deep pyramidal neurone of a responding cell type, with the development of repetitive firing followed by epileptiform burst firing. Control resting membrane potential=-82 mV. Note that the difference in animal ages produces a change in the duration of the burst discharges, the accompanying input resistance change and the magnitude of post-burst hyperpolarization. * indicates the cessation of spontaneous subthreshold firing following the application of OXO-M.

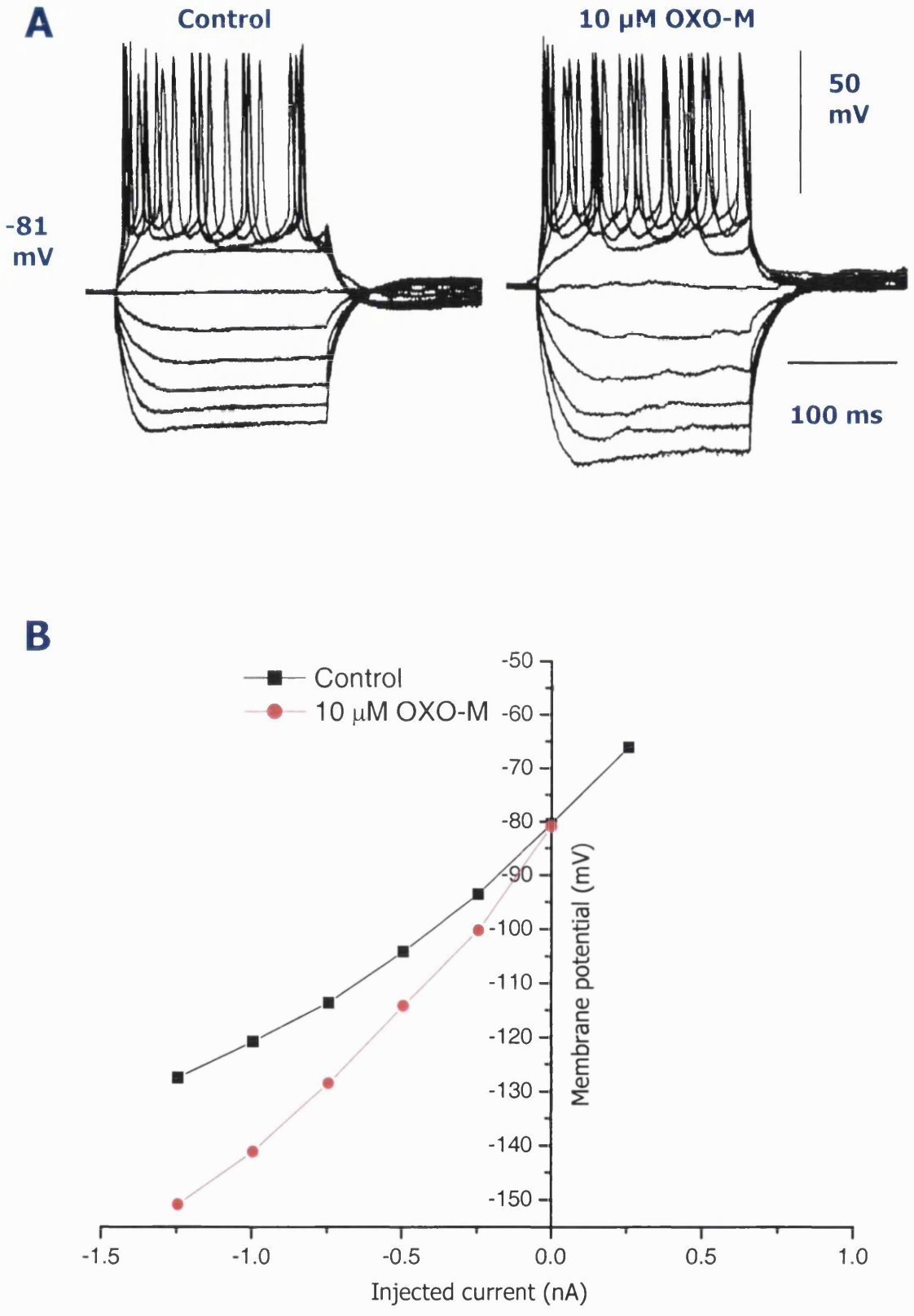
Immature (P+17) deep pyramidal cell
A
Control
10 µM OXO-M
50
mV
-81
mV
100 ms
B
Control
10 µM OXO-M
-50
-60
-70
-80
-90
-100
-110
-120
-130
-140
-150
Membrane potential (mV)
-1.5
-1.0
-0.5
0.0
0.5
1.0
Injected current (nA)

Figure 3.10

Figure 3.10

Comparison of the effects of 10 μM OXO-M upon the electrotonic properties of an immature (P+17) deep pyramidal cell. **A.** Superimposed electrotonic potentials evoked in response to positive and negative current pulses (-1.2 to +1.2 nA; 160 ms) applied in control (**left panel**) and after 15 mins in 10 μM OXO-M (**right panel**). The resting membrane potential in OXO-M was adjusted by application of negative holding current to offset the depolarizing effect of OXO-M prior to eliciting electrotonic responses. Note that in this case, the presence of OXO-M caused a large increase in both cell input resistance and firing rate, but no increase in spike fractionation. **B.** Current-voltage (I-V) relationships showing variations in membrane potential (ordinate) *vs.* injected current (abscissa) observed in the same immature deep pyramidal cell shown in **A** in control conditions (**black**) and in the presence of 10 μM OXO-M (**red**). Note the greatly increased slope of the I-V plot in the presence of OXO-M, indicating a larger increase in input resistance compared to the adult (*c.f.* Fig. 3.4). Control resting membrane potential=-81 mV.

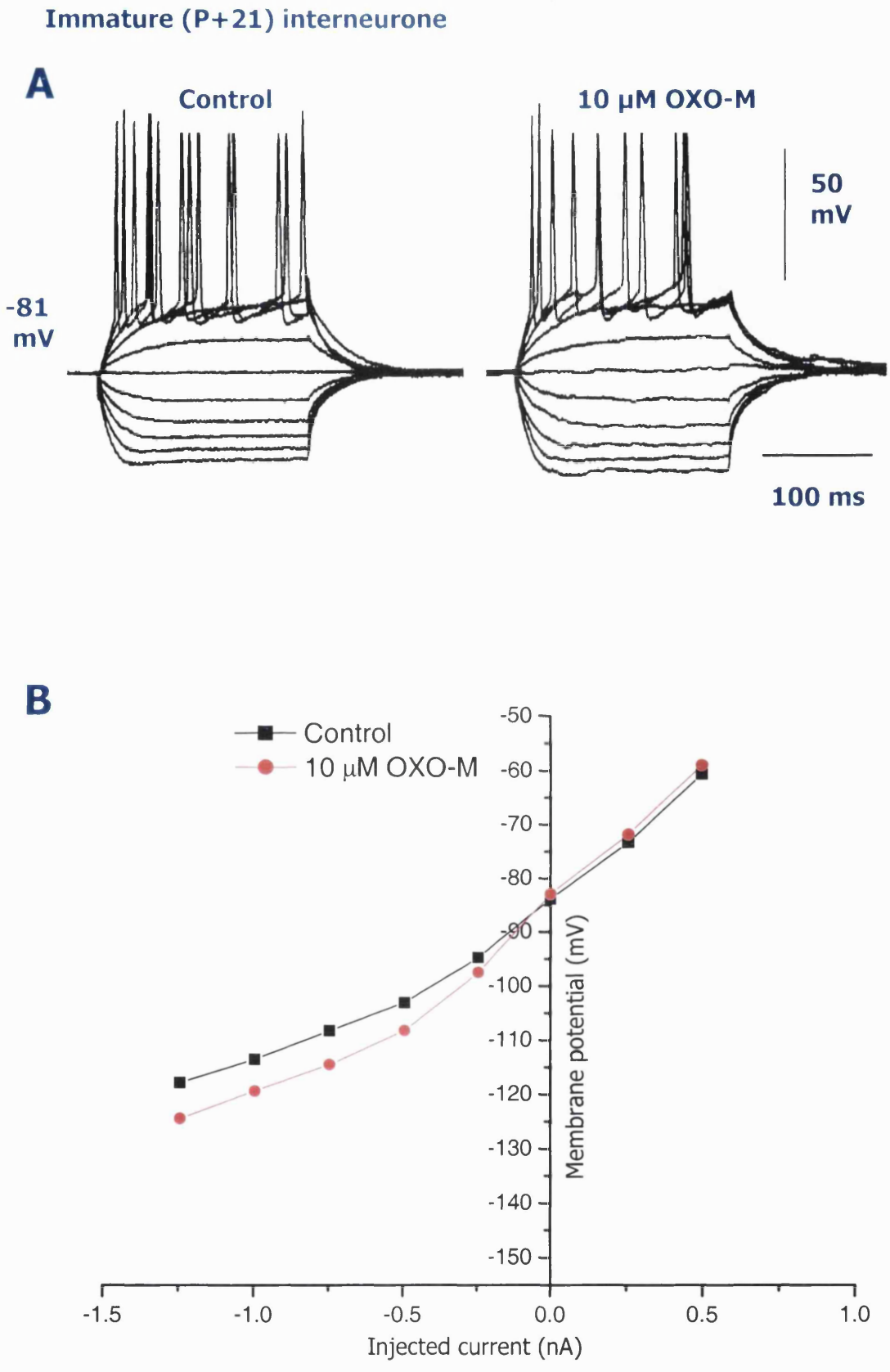
Immature (P+21) interneurone
A
Control
10 µM OXO-M
50
mV
-81
mV
100 ms
B
Control
10 µM OXO-M
-50
-60
-70
-80
-90
-100
-110
-120
-130
-140
-150
Membrane potential (mV)
-1.5
-1.0
-0.5
0.0
0.5
1.0
Injected current (nA)

Figure 3.11

Figure 3.11

Comparison of the effects of 10 μM OXO-M upon the electrotonic properties of an immature (P+21) interneurone. **A.** Superimposed electrotonic potentials evoked in response to positive and negative current pulses (-1.2 to +1.2 nA; 160 ms) applied in control (**left panel**) and after 15 mins in 10 μM OXO-M (**right panel**). The resting membrane potential in OXO-M was adjusted by application of negative holding current to offset the depolarizing effect of OXO-M prior to eliciting electrotonic responses. Note that in this case, the presence of OXO-M caused an increase in both cell input resistance and firing rate, but no increase in spike fractionation. **B.** Current-voltage (I-V) relationships showing variations in membrane potential (ordinate) *vs.* injected current (abscissa) observed in the same immature interneurone shown in **A** in control conditions (**black**) and in the presence of 10 μM OXO-M (**red**). Note the increased slope of the I-V plot in the presence of OXO-M. Control resting membrane potential=-81 mV.

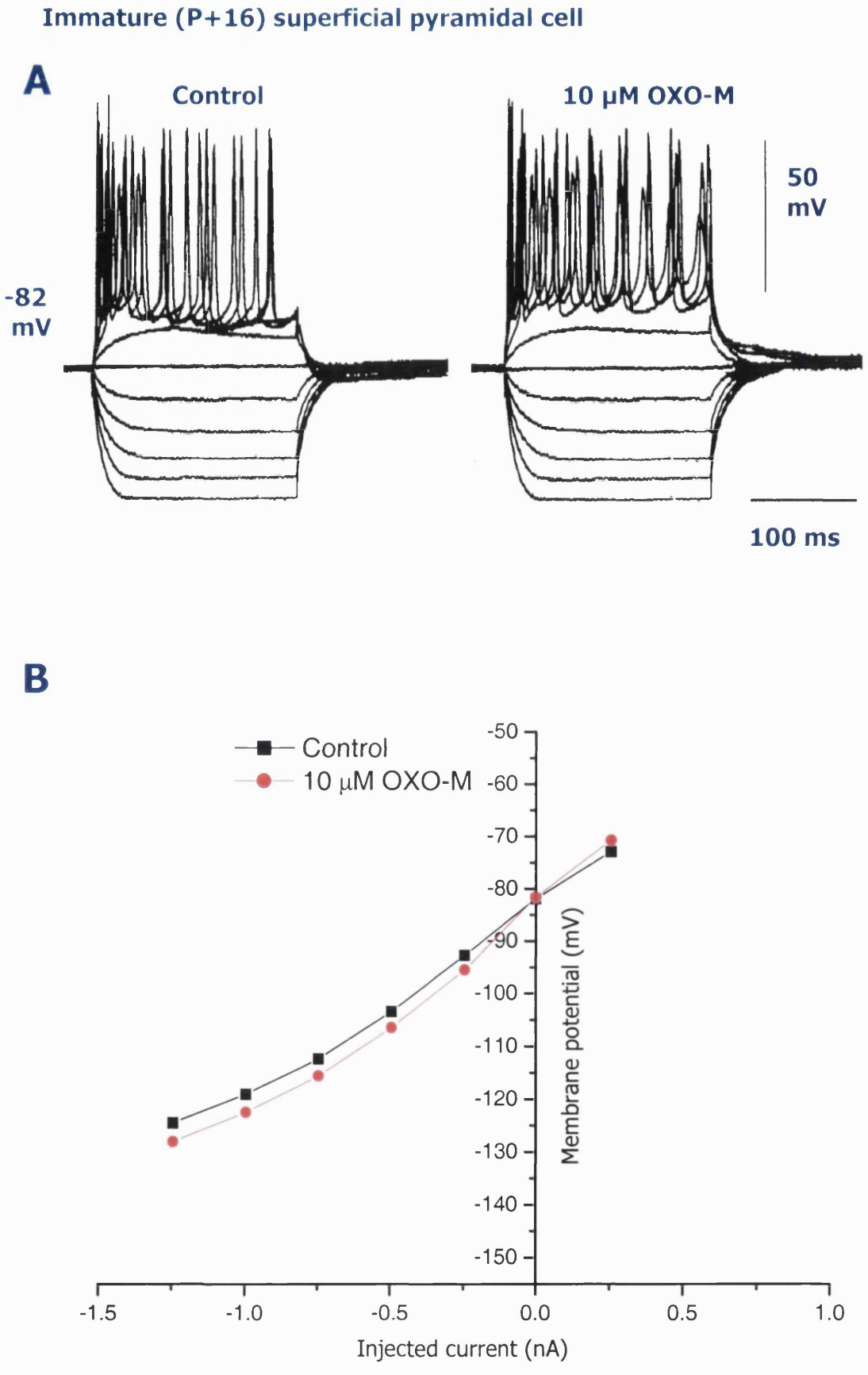
Immature (P+16) superficial pyramidal cell
A
Control
10 µM OXO-M
50 mV
-82 mV
100 ms
B
Control
10 µM OXO-M
-50
-60
-70
-80
-90
-100
-110
-120
-130
-140
-150
Membrane potential (mV)
-1.5
-1.0
-0.5
0.0
0.5
1.0
Injected current (nA)

Figure 3.12

Figure 3.12

Comparison of the effects of 10 μM OXO-M upon the electrotonic properties of an immature (P+16) superficial pyramidal cell. **A.** Superimposed electrotonic potentials evoked in response to positive and negative current pulses (-1.2 to +1.2 nA; 160 ms) applied in control (**left panel**) and after 15 mins in 10 μM OXO-M (**right panel**). The resting membrane potential in OXO-M was adjusted by application of negative holding current to offset the depolarizing effect of OXO-M prior to eliciting electrotonic responses. Note that the presence of OXO-M caused little change in both cell input resistance and firing rate, but a clear increase in spike fractionation. **B.** Current-voltage (I-V) relationships showing variations in membrane potential (ordinate) *vs.* injected current (abscissa) observed in the same immature superficial pyramidal cell shown in **A** in control conditions (**black**) and in the presence of 10 μM OXO-M (**red**). Note the slightly increased slope of the I-V plot in the presence of OXO-M. Control resting membrane potential=-82 mV.

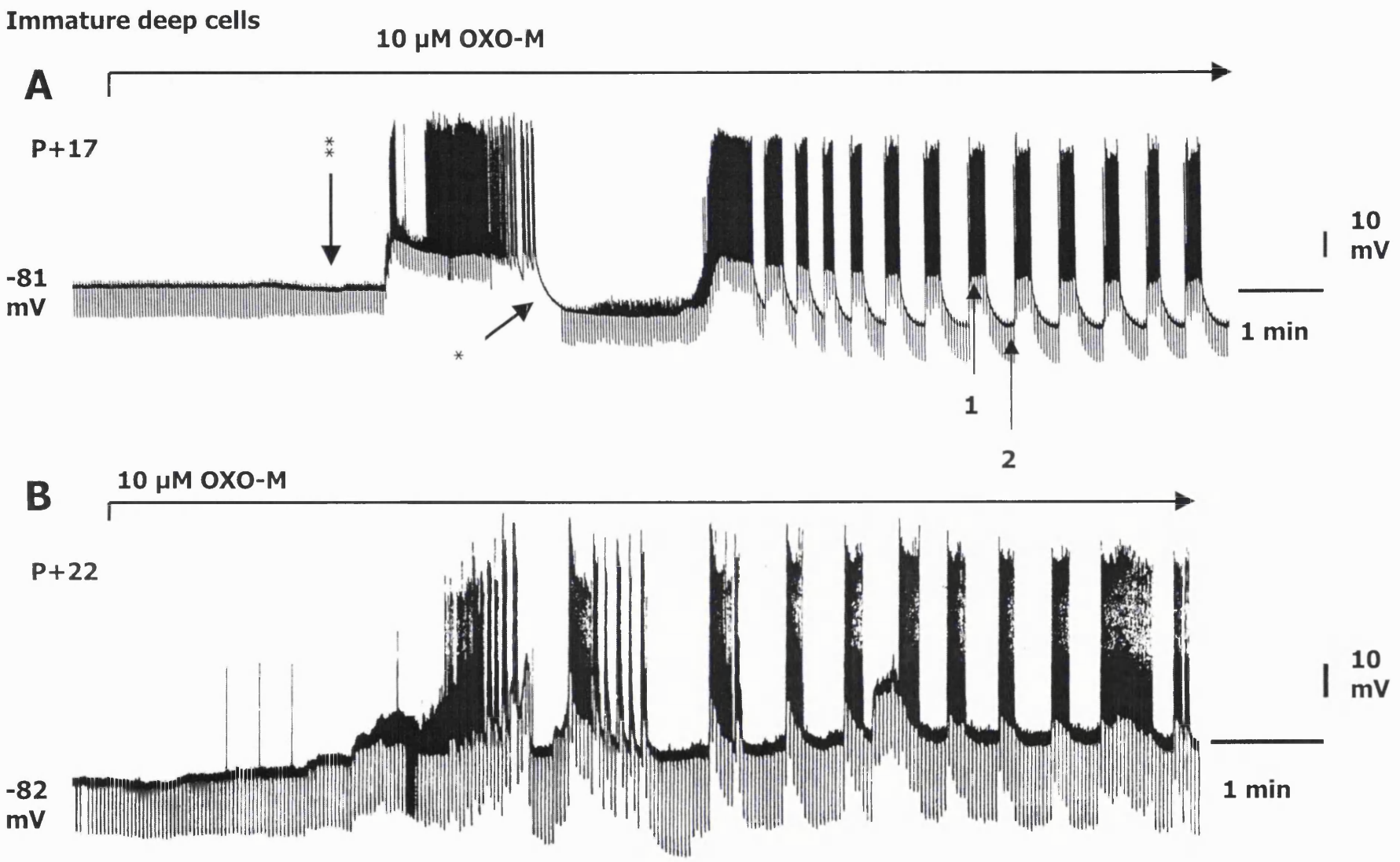
Immature deep cells
10 µM OXO-M
A
P+17
-81
mV
10
mV
1 min
1
2
10 µM OXO-M
B
P+22
-82
mV
10
mV
1 min

Figure 3.13

Figure 3.13

A. Chart trace showing the effect of 10 μM OXO-M upon an immature (P+17) presumed deep pyramidal neurone of a responding cell type, with the development of regular epileptiform burst firing. Control resting membrane potential=-81 mV. **[1]** – Peak mid-burst depolarization; **[2]** – Peak post-burst hyperpolarization; See Fig. 3.17 for details. * indicates where injections of negative current (shown by regular negative deflections) are temporarily turned off; ** indicates a slight early hyperpolarization in this cell, prior to the onset of the slow OXO-M-mediated depolarization possibly caused by mAChR-mediated activation and release of GABA from local interneurones. **B.** Chart trace showing the effect of 10 μM OXO-M upon an immature (P+22) presumed deep pyramidal neurone of a responding cell type, with the development of irregular epileptiform burst firing. Control resting membrane potential=-82 mV. Again the age related difference in post-burst hyperpolarization can be clearly seen.

Immature deep cells

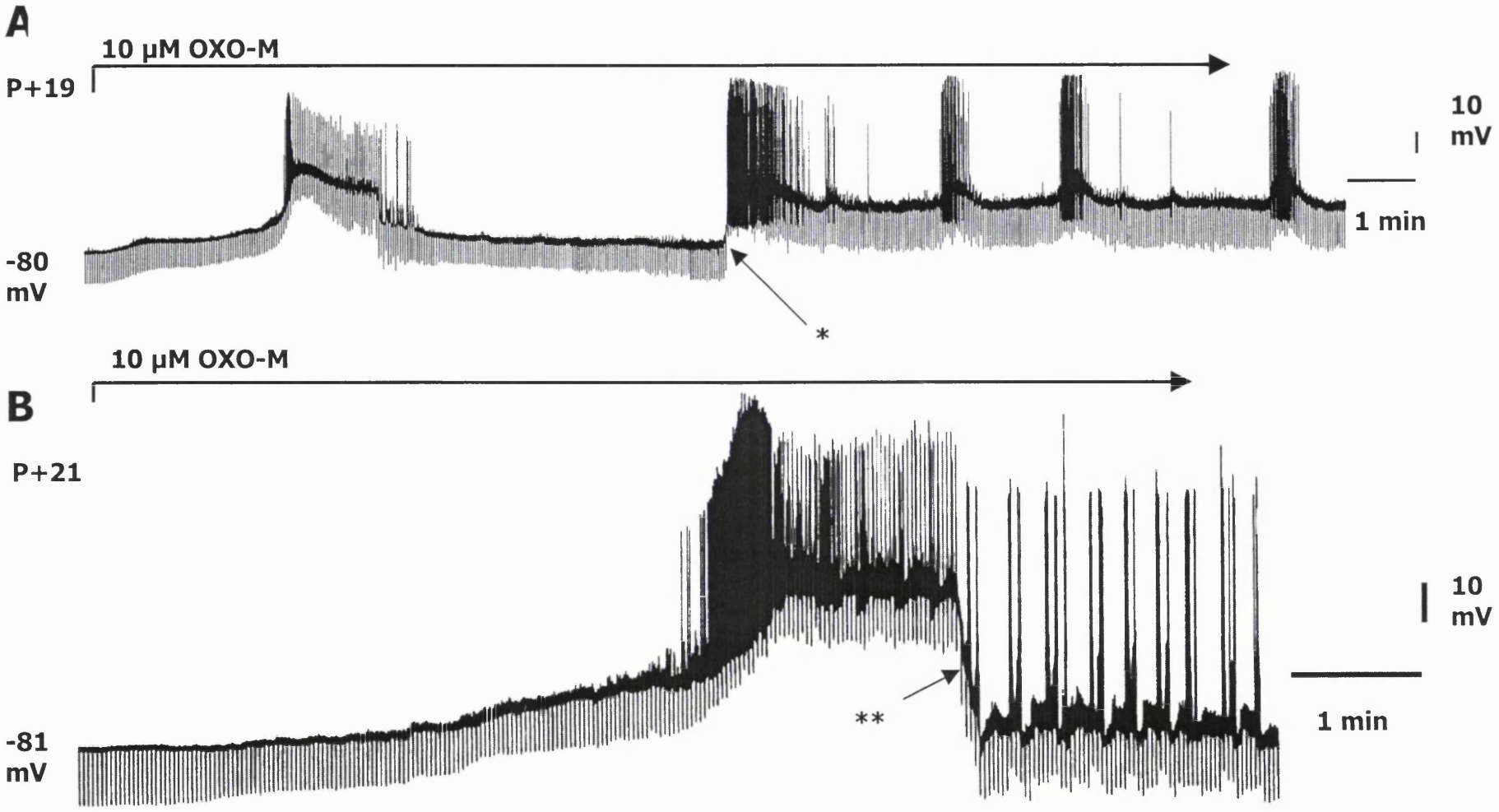

Figure 3.14

Figure 3.14

A. Chart trace showing the effect of 10 μM OXO-M upon an immature (P+19) presumed deep pyramidal neurone susceptible to OXO-M-induced epileptiform burst firing. Control resting membrane potential=-80 mV. * indicates where injections of negative current (shown by regular negative deflections) are temporarily turned off. **B.** Chart trace showing the effect of 10 μM OXO-M upon an immature (P+21) presumed deep pyramidal neurone susceptible to OXO-M-induced epileptiform burst firing. Control resting membrane potential=-81 mV. ** indicates in this cell, a rapid, large spontaneous hyperpolarization following a sustained period of repetitive firing that then developed into established epileptiform burst firing.

Immature deep cells

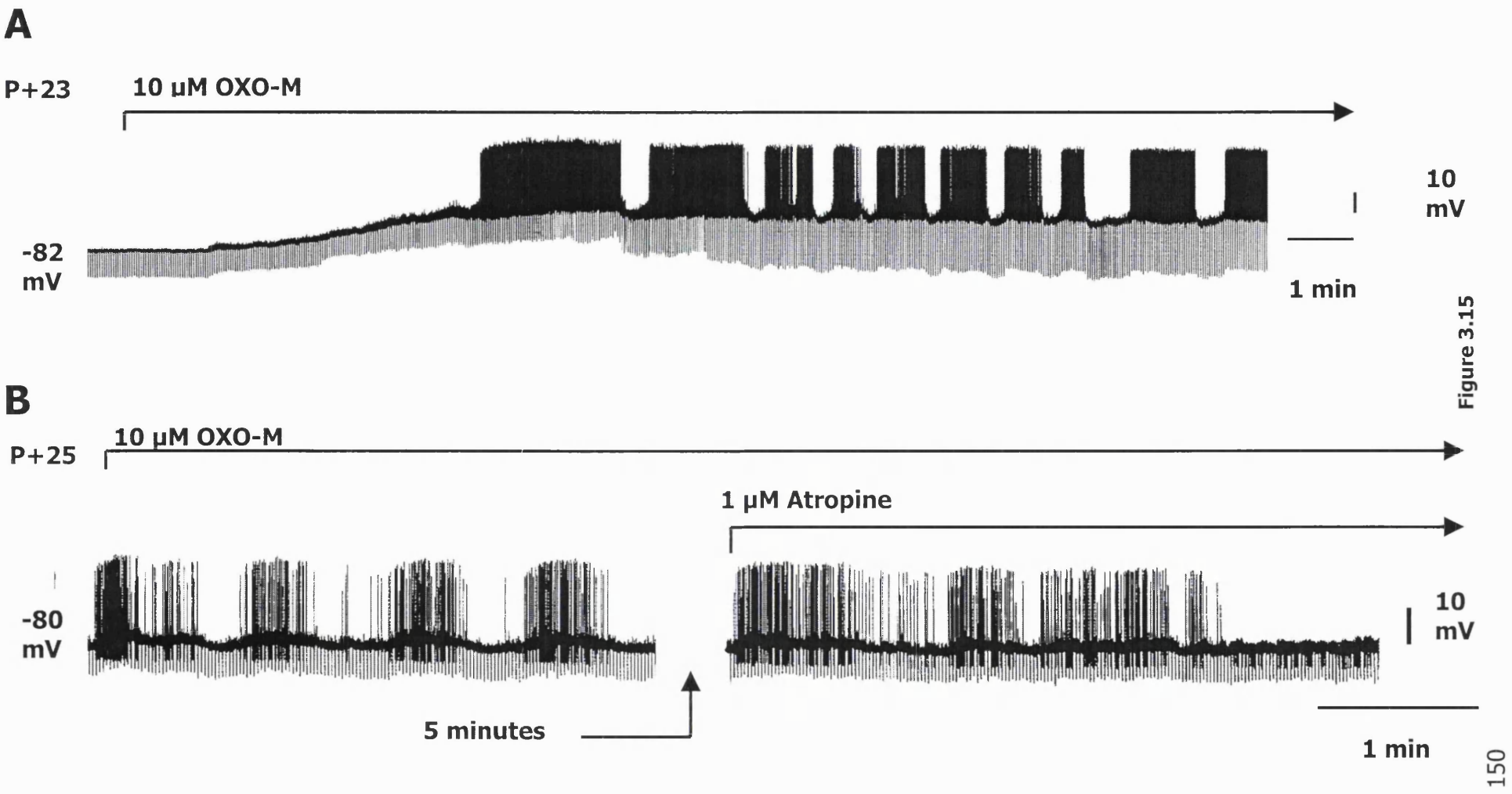

Figure 3.15

Figure 3.15

A. Chart trace showing the effect of 10 μM OXO-M upon an immature (P+23) presumed deep pyramidal neurone susceptible to OXO-M-induced epileptiform burst firing. Control resting membrane potential=-82 mV. Note the relatively small post-burst hyperpolarization in this cell, characteristic of 'older' responding neurones. **B.** Chart trace showing the blocking effect of the mAChR antagonist, atropine (1 μM) upon an immature (P+25) presumed deep pyramidal neurone showing established, OXO-M-induced epileptiform burst firing. Control resting membrane potential=-80 mV.

Immature deep pyramidal cells

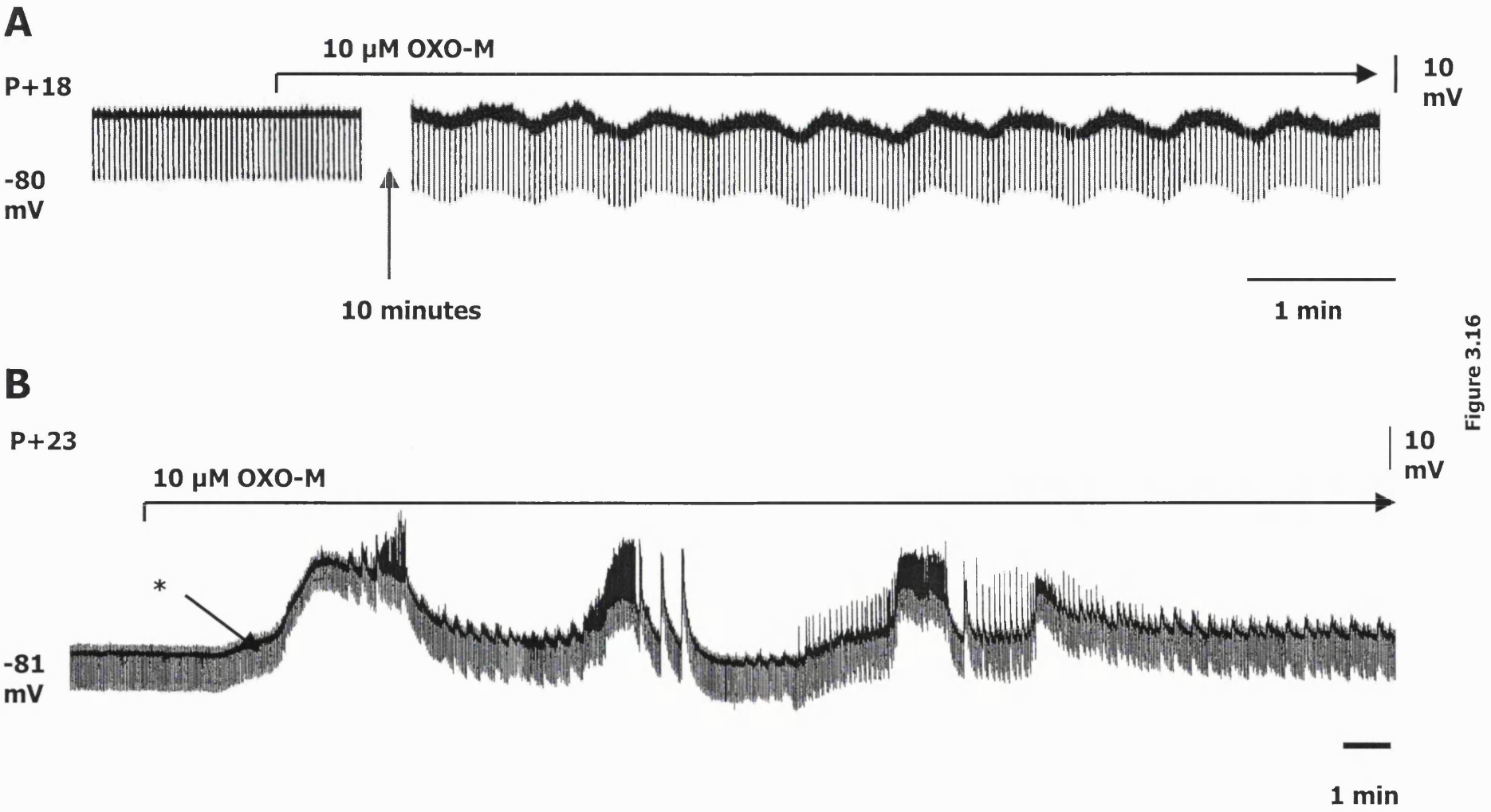

Figure 3.16

Figure 3.16

A. The effect of 10 μM OXO-M upon an immature (P+18) presumed deep pyramidal neurone, showing a '*non-responding*' cell type, with an absence of development of epileptiform burst firing or repetitive firing, but the presence of rhythmic '*wave-like*' behaviour of similar frequency as was found for the frequency of burst discharges in slices prepared from animals of this age. Control resting membrane potential=-80 mV. **B.** The effect of 10 μM OXO-M upon an immature (P+23) presumed deep pyramidal neurone, showing another '*non-responding*' cell type, with an absence of development of epileptiform burst firing or repetitive firing, but development of rhythmic interictal activity that is self-sustaining but never reaches firing threshold. Control resting membrane potential=-81 mV. * Indicates the transient decrease in input resistance during the initial depolarization following OXO-M application. Control Control resting membrane potential=-81 mV. These results would suggest that the circuitry underlying the epileptiform burst firing seen in some immature deep pyramidal PC neurones is still being activated even in those cells that do not display established bursting behaviour.

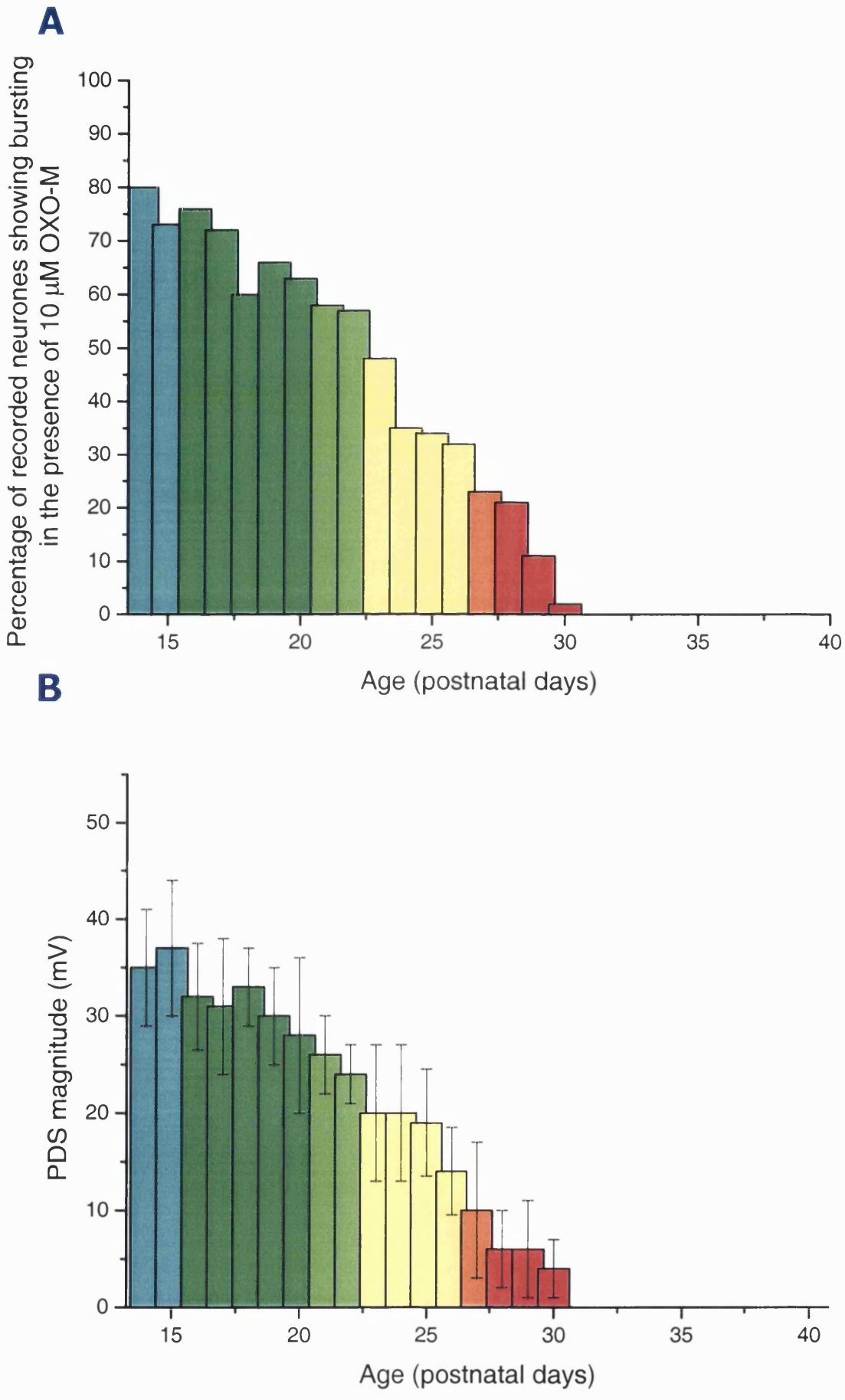
A
Percentage of recorded neurones showing bursting in the presence of 10 µM OXO-M
100
90
80
70
60
50
40
30
20
10
0
15
20
25
30
35
40
Age (postnatal days)
B
PDS magnitude (mV)
50
40
30
20
10
0
15
20
25
30
35
40
Age (postnatal days)

Figure 3.17

Figure 3.17

A. Histogram showing the variation in percentage of recorded immature deep cells exhibiting spontaneous epileptiform bursting activity following OXO-M application *vs.* postnatal age. **B.** Histogram illustrating the change in paroxysmal depolarizing shift (PDS) magnitude with postnatal age. PDSs have previously been defined as '*large amplitude and long duration ictallike discharges with multiple action potentials superimposed on a prolonged depolarizing potential*' (Postlethwaite *et al.*, 1998a). The magnitude (mV) of the PDS in these experiments was calculated from peak post-burst hyperpolarization to peak mid-burst depolarization. Histogram bars show mean ± SEM.

Numbers of experiments represented in Figure 3.20.

(P+)	n-number	(P+)	n-number	(P+)	n-number
14	9	20	7	26	11
15	11	21	11	27	10
16	7	22	12	28	12
17	10	23	13	29	13
18	9	24	13	30	11
19	8	25	10	>40	39

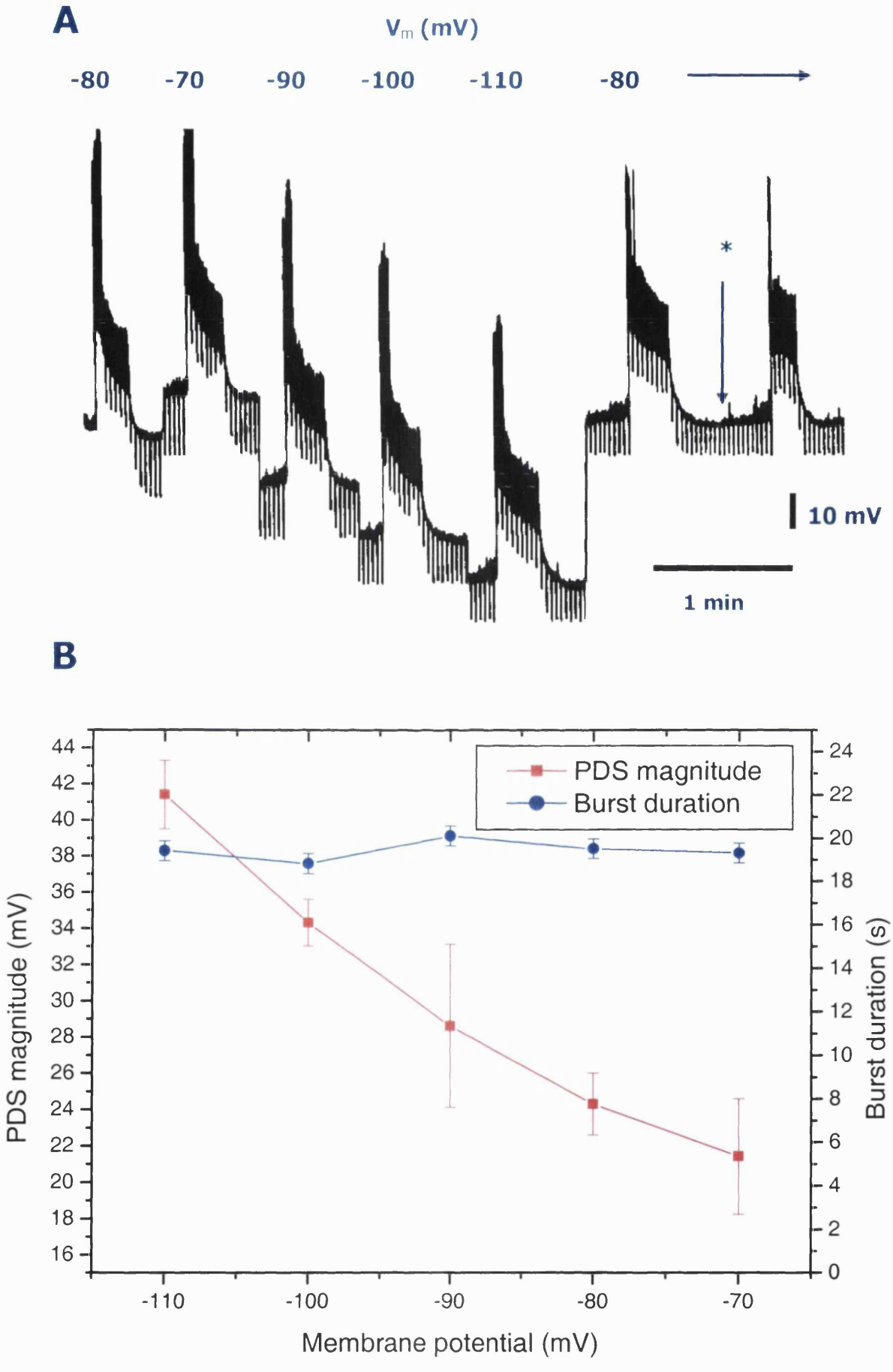
A
V_m (mV)
-80
-70
-90
-100
-110
-80
*
10 mV
1 min
B
PDS magnitude
Burst duration
PDS magnitude (mV)
Burst duration (s)
Membrane potential (mV)
44
42
40
38
36
34
32
30
28
26
24
22
20
18
16
24
22
20
18
16
14
12
10
8
6
4
2
0
-110
-100
-90
-80
-70

Figure 3.18

Figure 3.18

A. The effects of membrane potential change upon aspects of OXO-M-induced epileptiform burst firing. An immature (P+16; resting potential= -80 mV) presumed deep neurone displaying epileptiform bursting behaviour in the continued presence of 10 μM OXO-M. Injection of positive or negative current to hold the resting membrane potential at varying levels between -70 and -100 mV did not affect burst duration, but did affect the magnitude of the paroxysmal depolarizing shift (PDS; the difference between the value of the membrane potential at peak mid-burst depolarization and the same value at peak post-burst hyperpolarization; Section 3.4.2). **B.** PDS magnitude and burst duration plotted *vs.* membrane potential for a population of P+20 deep pyramidal neurones showing established OXO-M-induced epileptiform bursting (n=7). No variation in burst duration with membrane potential was observed, but there was an obvious trend for PDS magnitude to increase as membrane potential became more negative. Artificially-held membrane potentials were measured from the peak of the post burst hyperpolarization (indicated by * in trace **A**). **N.B. Fig. 3.18A** was chosen for its excellent demonstration of the invariability of burst duration with change in holding membrane potential. However, this figure does not equally well illustrate the variation in PDS magnitude shown in **Fig. 3.18B**.

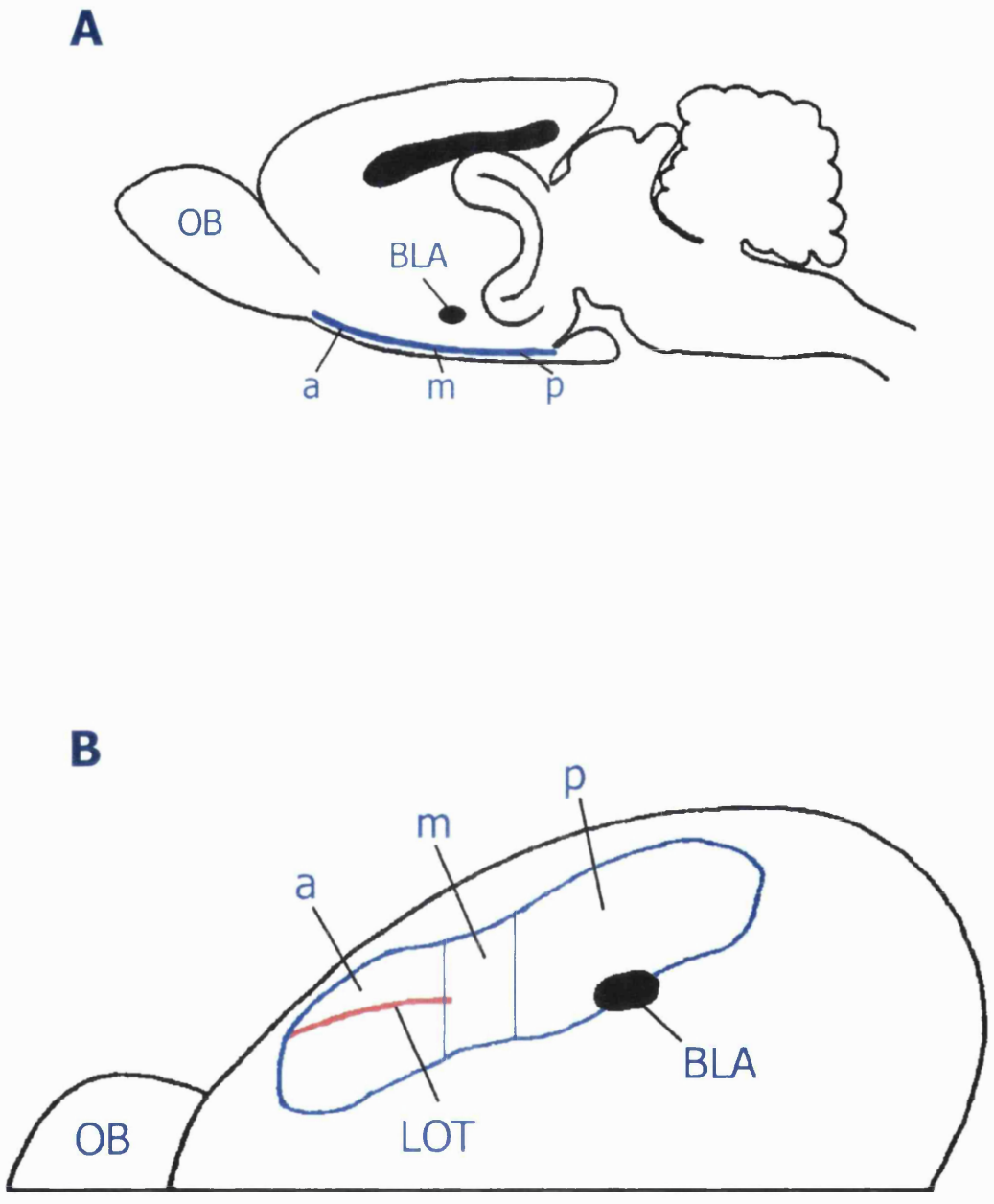

Figure 3.19

Figure 3.19

Recordings were made from different areas of the piriform cortical slice preparation to determine whether muscarinic response types differed with location. The areas investigated were arbitrarily defined as anterior, median and posterior piriform cortex. The illustrations show the locations of these areas used in this series of experiments (Section 3.4.3) **A.** Illustration of a sagittal brain section showing the anatomical areas of the piriform cortex. **B.** Illustration of a dorsal view of the brain, hemisected along the midline, showing the location of the piriform cortical areas. **Key: [OB]** – olfactory bulb; **[LOT]** – lateral olfactory tract; **[BLA]** – basolateral amygdala; **[a]** – anterior; **[m]** – median; **[p]** – posterior. These illustrations were adapted from (Loscher & Ebert, 1996) with definitions delineating anterior, median and posterior areas from those described by Haberly (Haberly & Price, 1978).

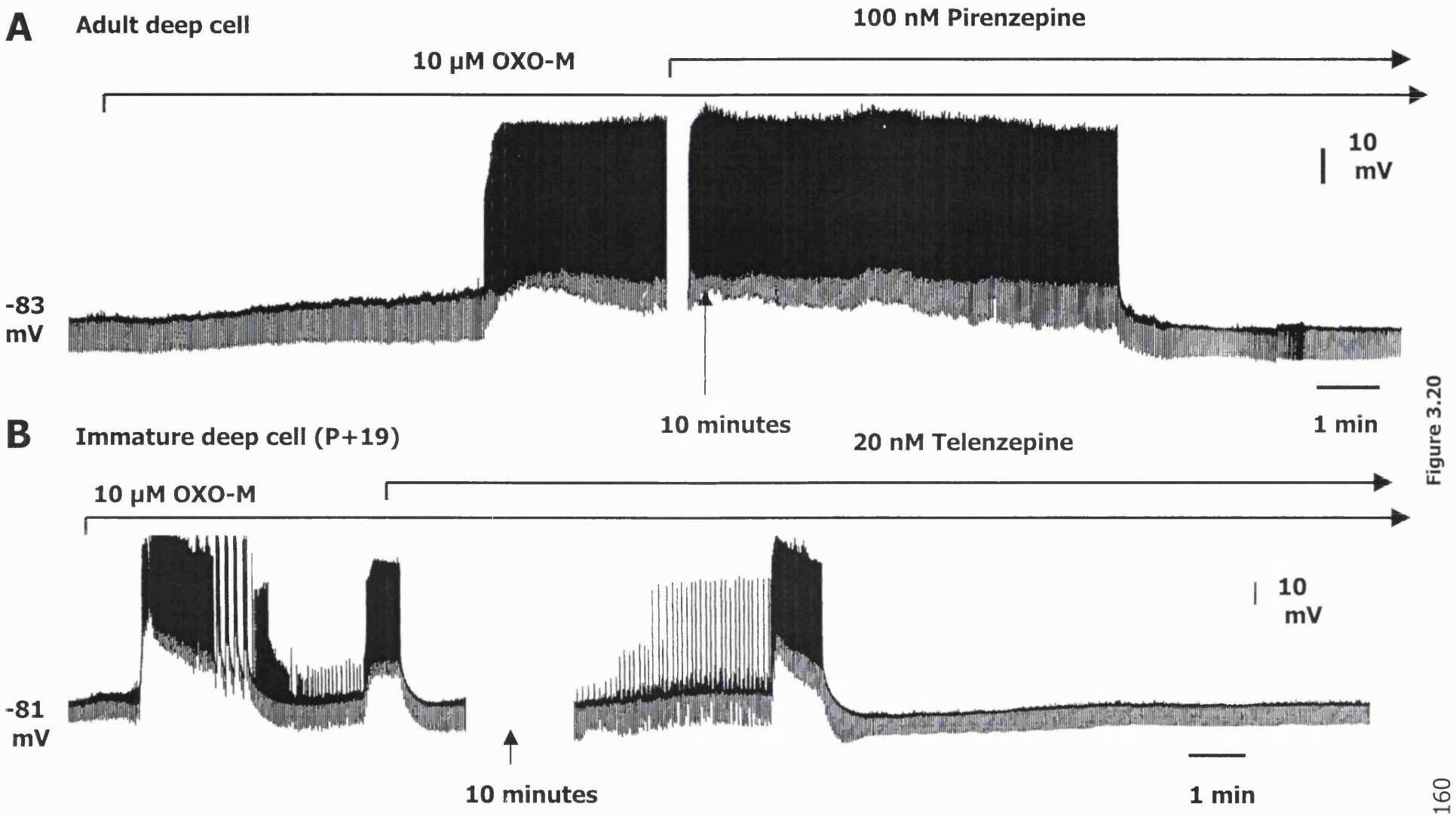
A
Adult deep cell
100 nM Pirenzepine
10 µM OXO-M
10
mV
-83
mV
10 minutes
1 min
B
Immature deep cell (P+19)
20 nM Telenzepine
10 µM OXO-M
10
mV
-81
mV
10 minutes
1 min

Figure 3.20

Figure 3.20

Block of OXO-M-induced excitatory effects by M1-specific mAChR antagonists. **A.** Induction of depolarization and repetitive firing following the application of 10 μM OXO-M to an adult presumed deep pyramidal piriform cortical neurone and its subsequent block by the M1-specific mAChR antagonist, pirenzepine (100 nM). Control resting membrane potential=-83 mV. **B.** Induction of depolarization and characteristic epileptiform burst firing following the application of 10 μM OXO-M to an immature (P+19) presumed deep pyramidal piriform cortical neurone and its subsequent block by the M1 specific mAChR antagonist, telenzepine (20 nM). Control resting membrane potential=-81 mV. Note the absence of any burst firing in the adult neurone.

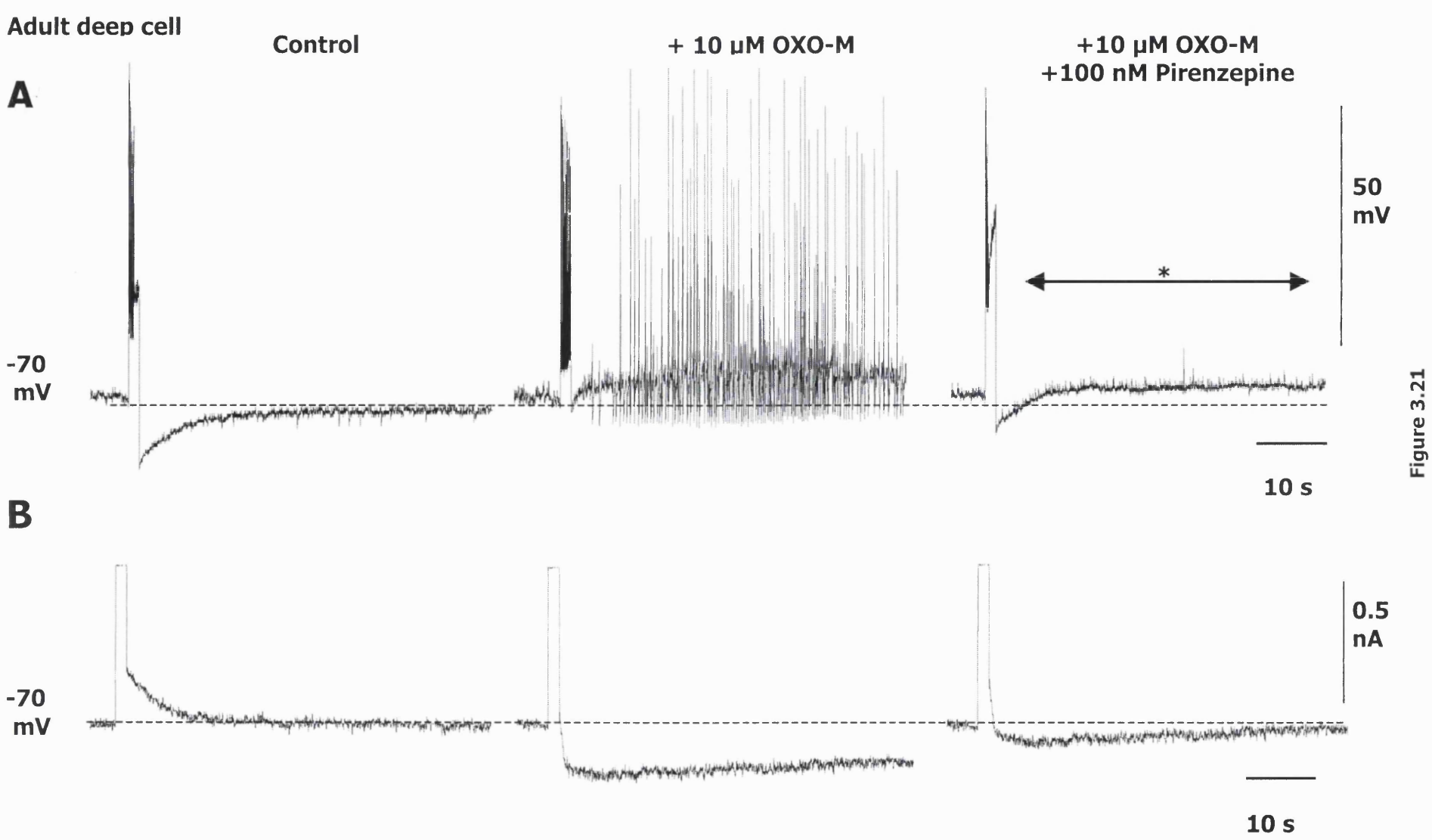
Adult deep cell
Control
+ 10 µM OXO-M
+10 µM OXO-M
+100 nM Pirenzepine
A
50
mV
*
-70
mV
10 s
B
0.5
nA
-70
mV
10 s

Figure 3.21

Figure 3.21

The effect of the M1-specific mAChR antagonist pirenzepine on the OXO-M-induced slow after-depolarization (sADP) and underlying slow inward tail current (I_{ADP}). Slow afterpotentials were elicited by application of a long depolarizing stimulus train (+2 nA; 1.6 s) in CC mode and tail currents recorded using the same stimulus train but in '*hybrid*' VC mode. **A.** The slow afterhyperpolarization (sAHP) elicited from a presumed adult deep pyramidal piriform cortical neurone in control conditions (**left panel**) was replaced by a slow after-depolarization (sADP) in the presence of 10 μM OXO-M (**middle panel**) that was, in turn, replaced by a 'combination' sAHP/sADP in the presence of 10 μM OXO-M plus 100 nM pirenzepine (**right panel**); note the later sustained depolarization without superimposed spike firing, shown by (*). **B.** Shows the corresponding slow tail currents underlying the slow afterpotentials in (**A**).

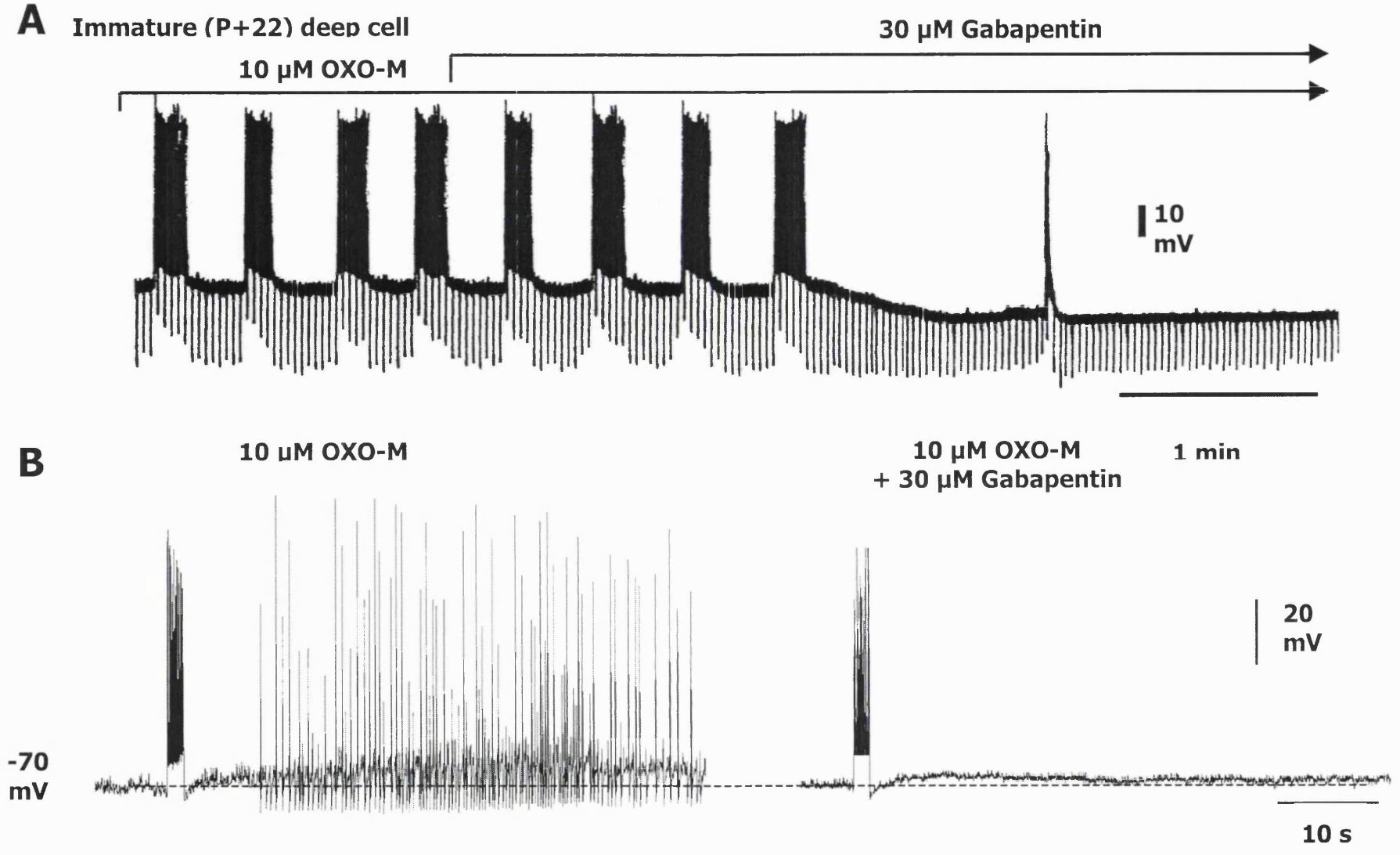
A
Immature (P+22) deep cell
10 µM OXO-M
30 µM Gabapentin
10 mV
B
10 µM OXO-M
10 µM OXO-M
+ 30 µM Gabapentin
1 min
20 mV
-70 mV
10 s

Figure 3.22

Figure 3.22

A. Chart trace showing the effect of the anticonvulsant gabapentin (GPN; 30 μM) on OXO-M induced epileptiform burst firing induced in the immature rat piriform cortical slice preparation. 30 μM GPN applied to an immature (P+22) presumed deep pyramidal neurone exhibiting established bursting behaviour in 10 μM OXO-M abolished epileptiform bursting and hyperpolarized the cell membrane back to a control resting value (-82 mV). **B.** The effect of GPN upon the OXO-M-induced slow after-depolarization (sADP) recorded from the same immature presumed deep pyramidal piriform cortical neurone as in (**A**) recorded in the presence of 10 μM OXO-M. sADPs were elicited by application of a 2 nA, 1.6 s depolarizing stimulus. **Left panel**: Control sADP in OXO-M and in 10 μM OXO-M plus 30 μM GPN (**right panel**). Note that although the sADP evoked in OXO-M (**left panel**) is not abolished and replaced by a sAHP upon addition of GPN (**right panel**) the amplitude and time course of the sADP is reduced, with an abolition of the characteristic repetitive firing.

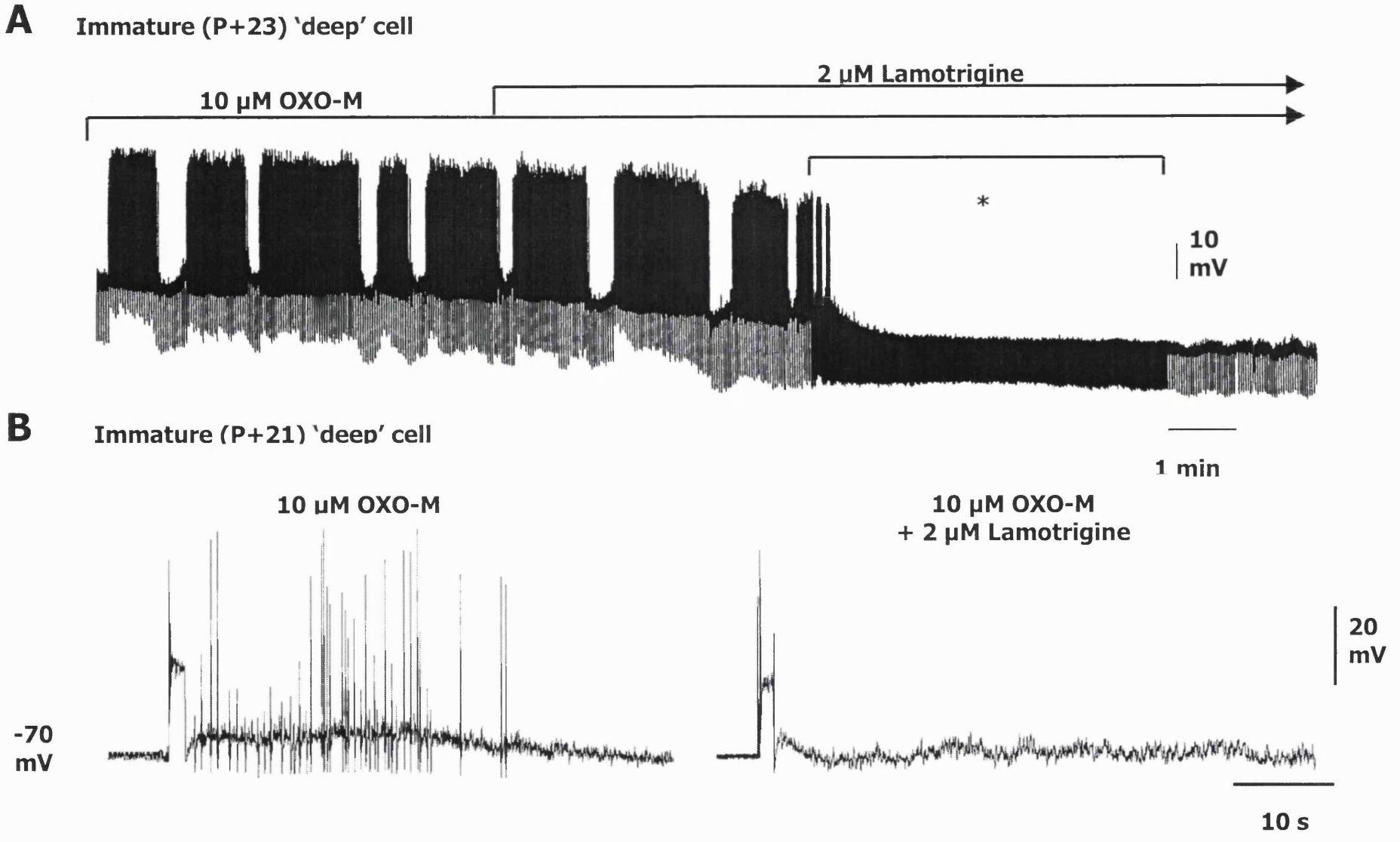
A
Immature (P+23) 'deep' cell
2 µM Lamotrigine
10 µM OXO-M
*
10
mV
1 min
B
Immature (P+21) 'deep' cell
10 µM OXO-M
10 µM OXO-M
+ 2 µM Lamotrigine
20
mV
-70
mV
10 s

Figure 3.23

Figure 3.23

A. Chart trace showing the effect of the anticonvulsant lamotrigine (LTG; 2 μM) on OXO-M induced epileptiform burst firing induced in the immature rat piriform cortical slice preparation. 2 μM LTG applied to an immature (P+23) presumed deep pyramidal neurone exhibiting established bursting behaviour in 10 μM OXO-M abolished epileptiform bursting and hyperpolarized the cell membrane back to a control resting value (-82 mV). * indicates a 3 times slower chart speed than indicated by time callibration. **B.** The effect of LTG upon the OXO-M-induced slow after-depolarization (sADP) recorded from an immature (P+21) presumed deep piriform cortical neurone recorded in the presence of 10 μM OXO-M. sADPs were elicited by application of a +2 nA, 1.6 s depolarizing stimulus. **Left panel**: Control sADP in OXO-M and in 10 μM OXO-M plus 2 μM LTG (**right panel**). Note that although the sADP evoked in OXO-M (**left panel**) is not abolished and replaced by a sAHP upon addition of LTG (**right panel**) the amplitude and time course of the sADP is reduced, with a corresponding decrease in repetitive firing.

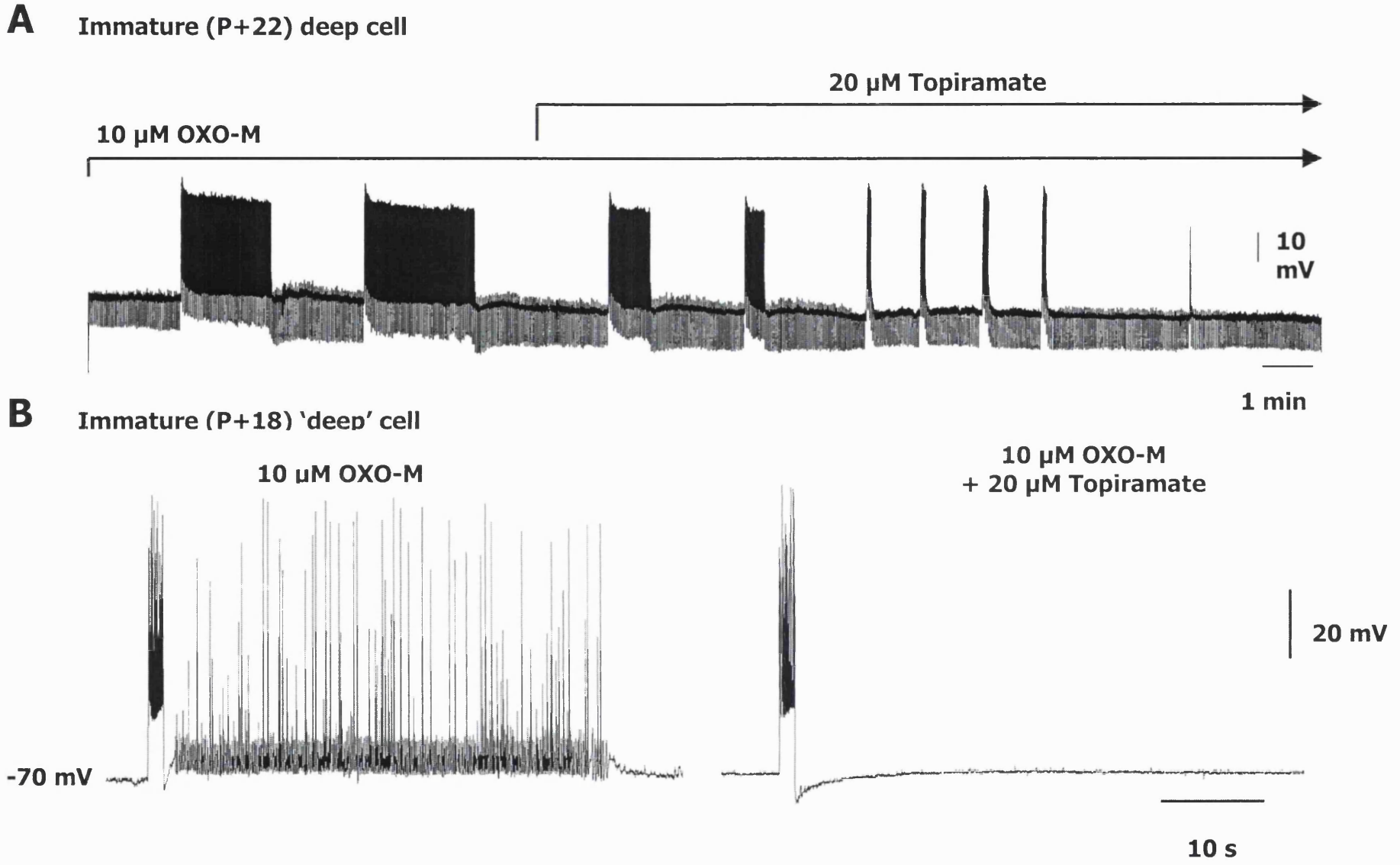
A
Immature (P+22) deep cell
20 µM Topiramate
10 µM OXO-M
10 mV
1 min
B
Immature (P+18) 'deep' cell
10 µM OXO-M
10 µM OXO-M
+ 20 µM Topiramate
20 mV
-70 mV
10 s

Figure 3.24

Figure 3.24

A. Chart trace showing the effect of the anticonvulsant topiramate (TPM; 20 μM) on OXO-M induced epileptiform burst firing induced in the immature rat piriform cortical slice preparation. 20 μM TPM applied to an immature (P+22) presumed deep pyramidal neurone exhibiting established bursting behaviour in 10 μM OXO-M abolished epileptiform bursting and hyperpolarized the cell membrane (-89 mV) past the normal control resting potential (-82 mV). **B.** The effects of TPM upon the OXO-M-induced slow after-depolarization (sADP) elicited by a +2 nA, 1.6 s stimulus in CC mode. (**Left panel**) sADP evoked from an immature (P+18) piriform cortical presumed deep pyramidal neurone in 10 μM OXO-M (**left panel**) is replaced by an enhanced slow afterhyperpolarization in 10 μM OXO-M plus 20 μM topiramate (**right panel**).

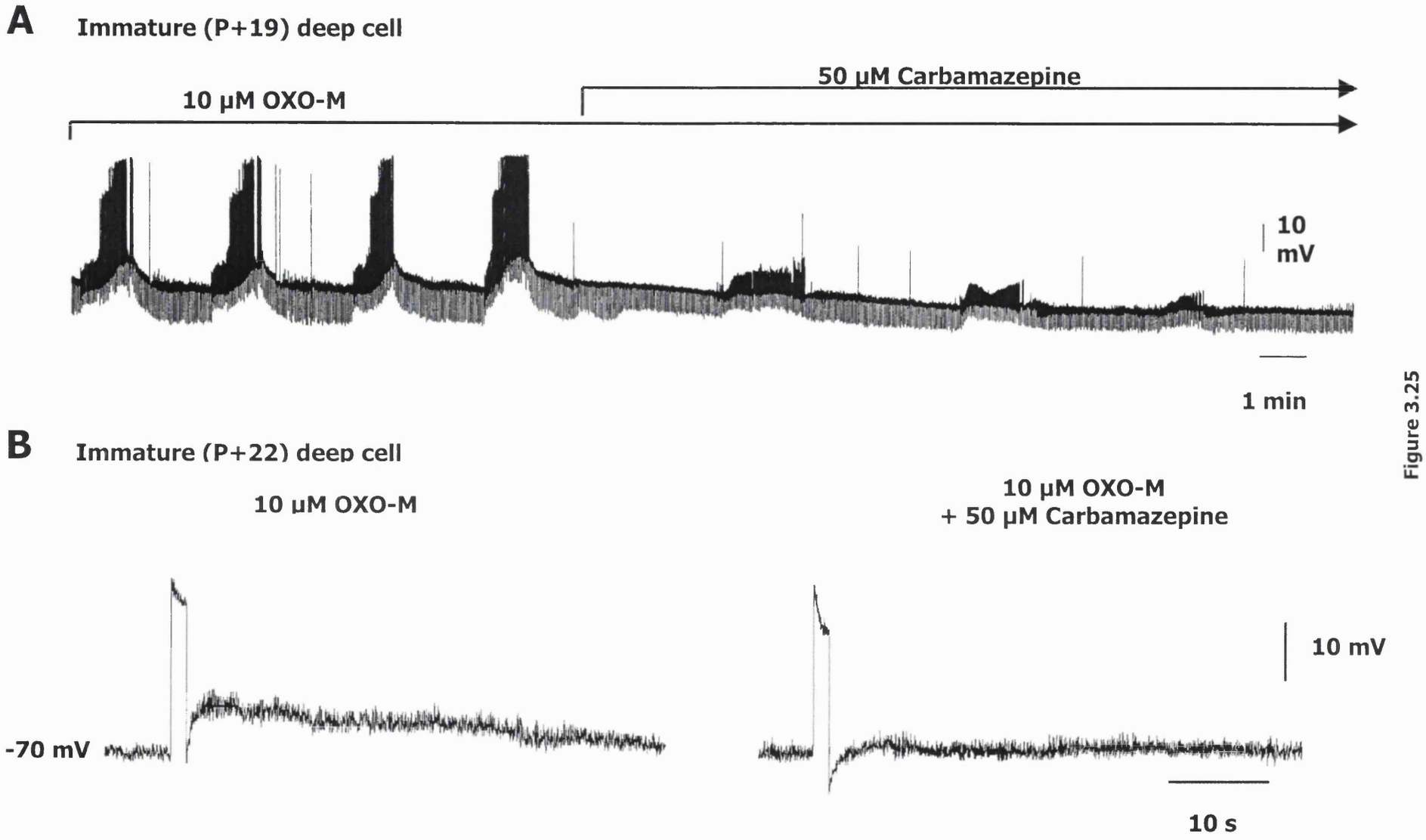
A
Immature (P+19) deep cell
10 µM OXO-M
50 µM Carbamazepine
10 mV
1 min
B
Immature (P+22) deep cell
10 µM OXO-M
10 µM OXO-M
+ 50 µM Carbamazepine
-70 mV
10 mV
10 s

Figure 3.25

Figure 3.25

Effect of the anticonvulsant carbamazepine (CBZ; 50 μM) on OXO-M induced epileptiform burst firing induced in the immature rat piriform cortical slice preparation. **A.** CBZ applied to an immature (P+19) presumed deep pyramidal neurone exhibiting bursting behaviour in 10 μM OXO-M, abolishes epileptiform activity and hyperpolarizes the cell back to control level (-83 mV). **B.** The sADP evoked from an immature (P+22) piriform cortical presumed deep pyramidal neurone in 10 μM OXO-M (**left panel**) and its replacement by a slow afterhyperpolarization in 10 μM OXO-M plus 50 μM CBZ (**right panel**).

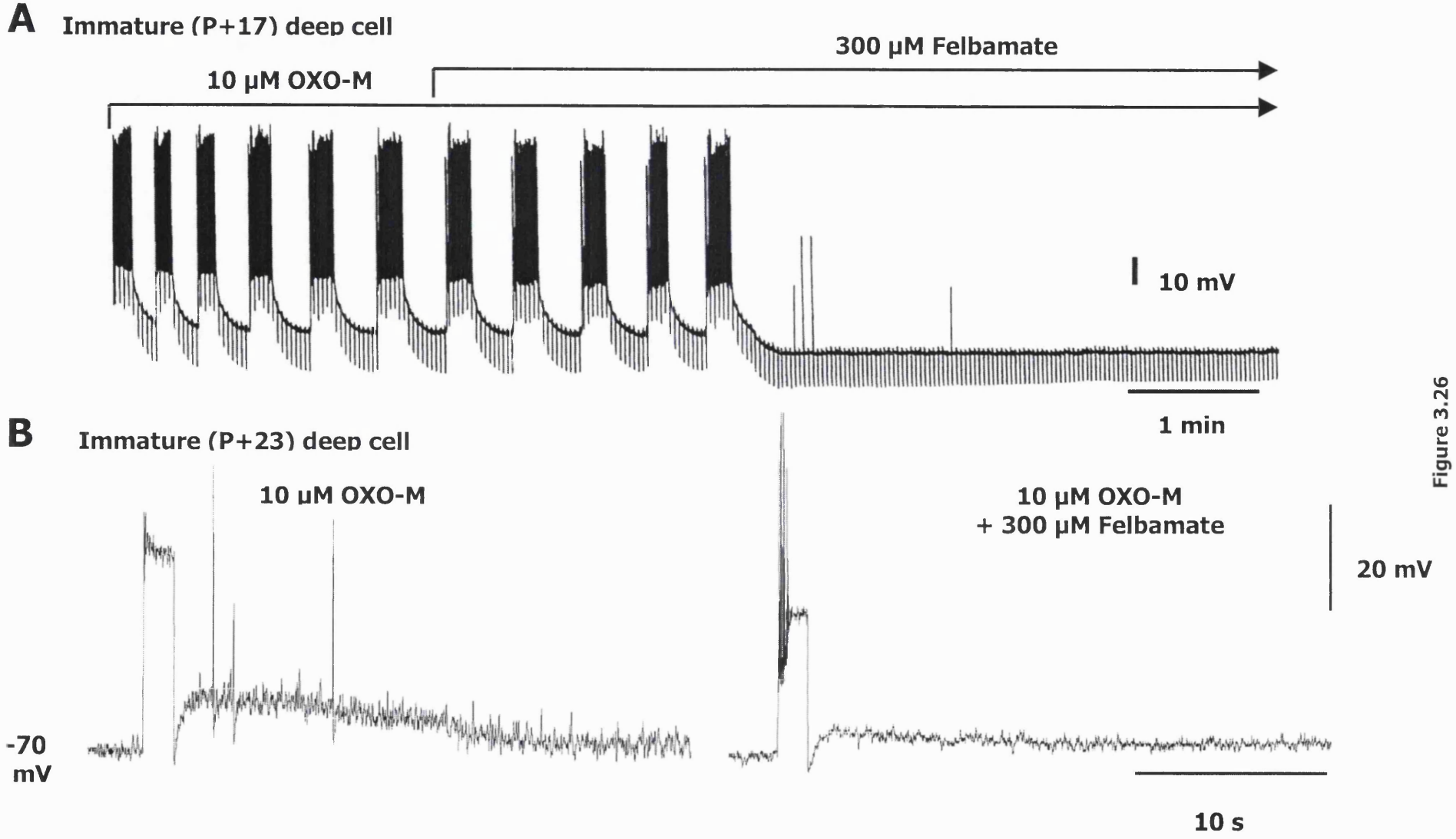
A
Immature (P+17) deep cell
300 µM Felbamate
10 µM OXO-M
10 mV
1 min
B
Immature (P+23) deep cell
10 µM OXO-M
10 µM OXO-M
+ 300 µM Felbamate
20 mV
-70
mV
10 s

Figure 3.26

Figure 3.26

A. Chart trace showing the effect of the anticonvulsant felbamate (FBM; 300 μM) on OXO-M induced epileptiform burst firing induced in the immature rat piriform cortical slice preparation. 300 μM FBM applied to an immature (P+17) presumed deep pyramidal neurone exhibiting established bursting behaviour in 10 μM OXO-M rapidly abolished epileptiform bursting and hyperpolarized the cell membrane back to a control resting value (-81 mV). **B.** Effect of FBM upon the OXO-M-induced sADP elicited by a 2 nA, 1.6 s stimulus. **Left panel**: sADP evoked from an immature (P+23) piriform cortical presumed deep pyramidal neurone in 10 μM OXO-M and its reduction in 10 μM OXO-M plus 300 μM felbamate (**right panel**).

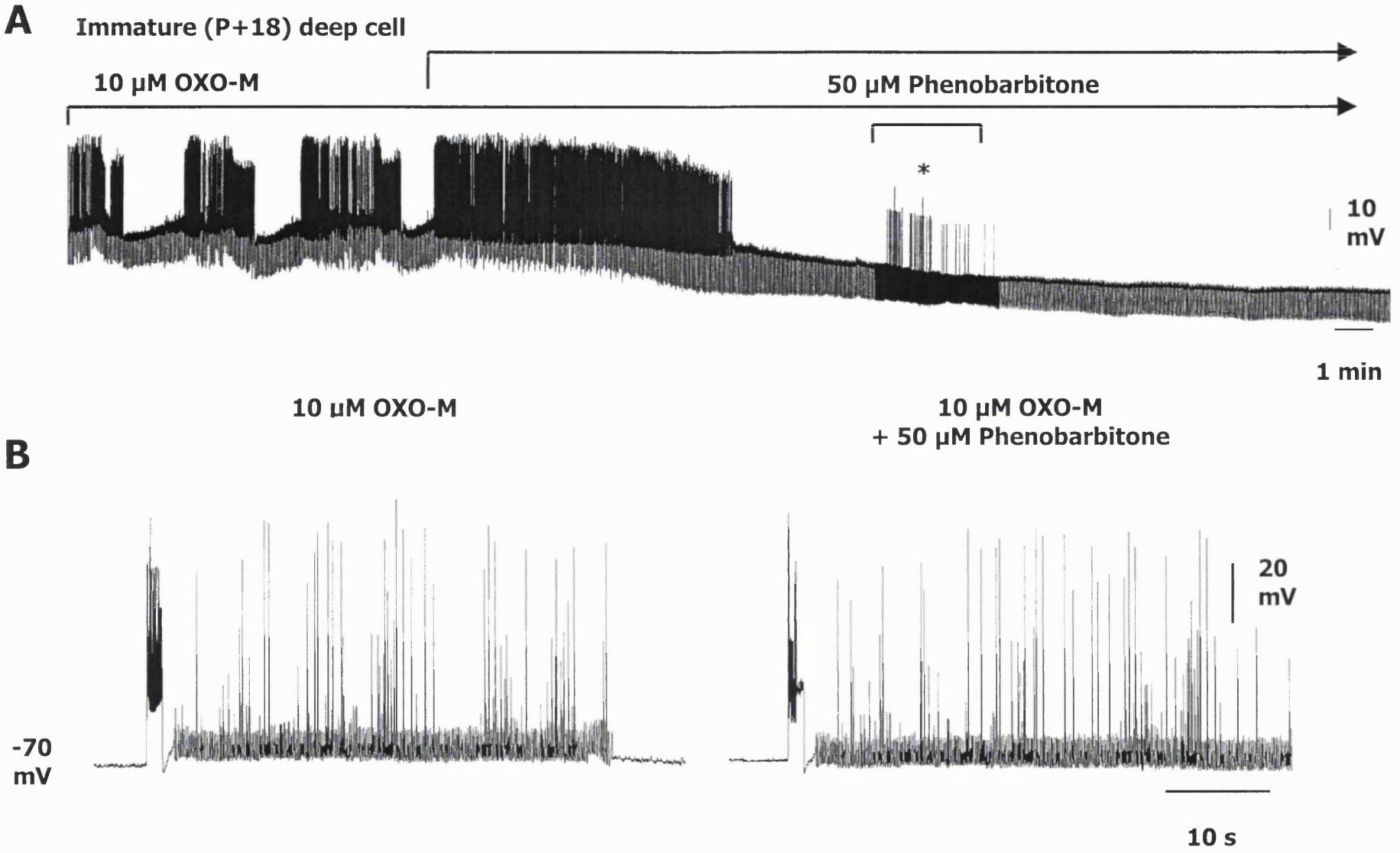
A
Immature (P+18) deep cell
10 µM OXO-M
50 µM Phenobarbitone
*
10
mV
1 min
B
10 µM OXO-M
10 µM OXO-M
+ 50 µM Phenobarbitone
20
mV
-70
mV
10 s

Figure 3.27

Figure 3.27

A. Phenobarbitone (PBN; 50 μM) applied to an immature (P+18) presumed deep pyramidal neurone exhibiting established bursting behaviour in OXO-M, slowly abolishes epileptiform activity but only hyperpolarizes the cell to ~5 mV more positive than the control resting value (-81 mV). * indicates a 5 times slower chart speed than indicated by the time callibration. **B.** The lack of effect of PBN upon the OXO-M-induced slow after-depolarization (sADP) recorded from the same immature presumed 'deep' piriform cortical neurone as in (**A**) in the presence of 10 μM OXO-M. sADPs were elicited by application of a 2 nA, 1.6 s depolarizing stimulus. **Left panel**: Control sADP in OXO-M and in 10 μM OXO-M plus 50 μM PBN (**right panel**).

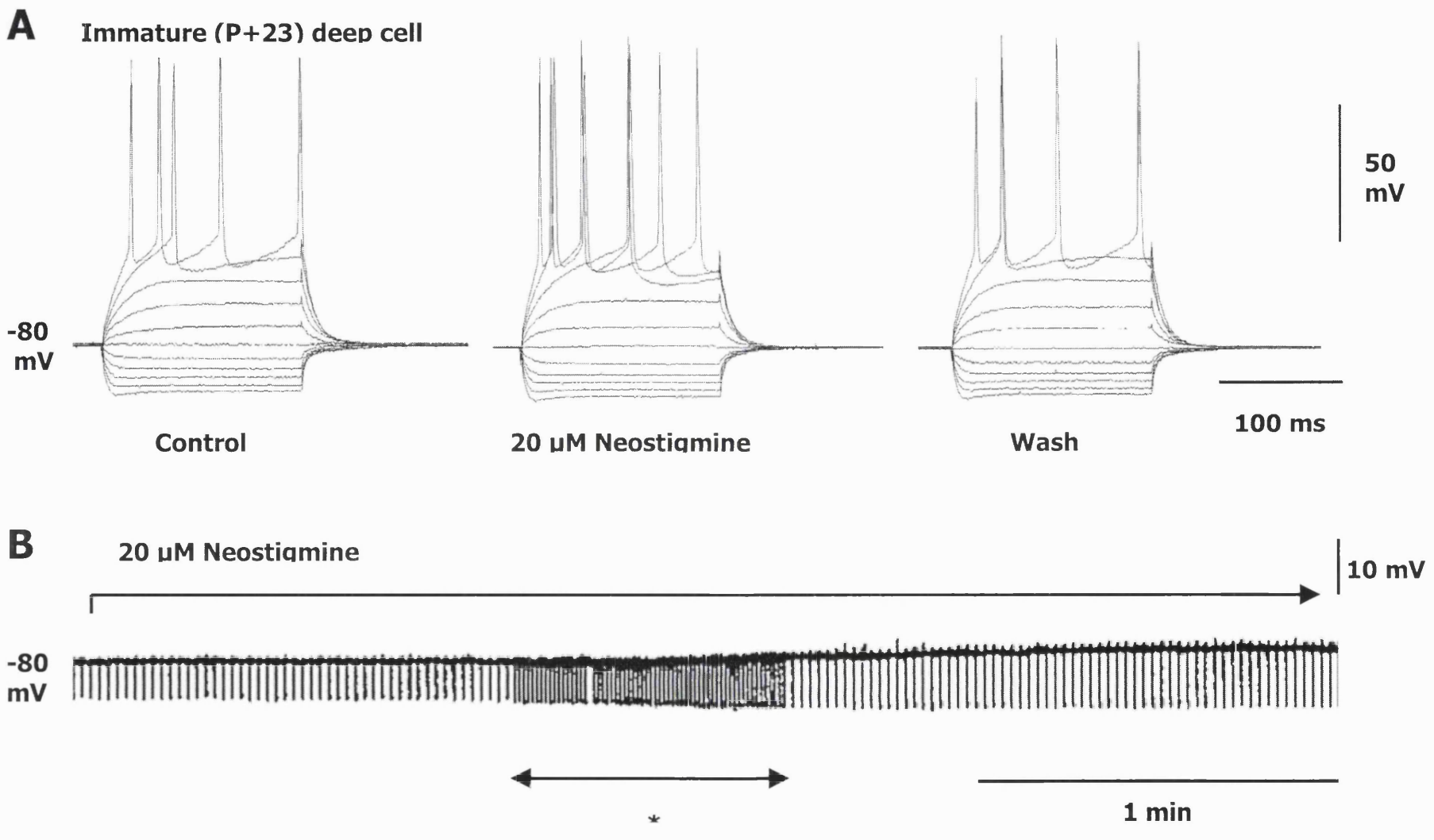
A
Immature (P+23) deep cell
-80
mV
50
mV
100 ms
Control
20 µM Neostigmine
Wash
B
20 µM Neostigmine
10 mV
-80
mV
*
1 min

Figure 3.28

Figure 3.28

Comparison of the effects of 20 μM neostigmine (NEO) on the cell membrane properties of an immature (P+23) piriform cortical presumed deep pyramidal neurone. **A.** Records show superimposed electrotonic potentials evoked in response to positive and negative current pulses (-1.2 to +1.2 nA; 160 ms) applied in control (**left panel**), after 40 mins in 20 μM NEO (**middle panel**) and after 40 mins washout (**right panel**). NEO caused a small increase in cell input resistance (**A**; **middle panel**) that was only partially reversible after washout (**A**; **right panel**). **B.** Chart recorder trace of the same neurone illustrating the slow depolarization following the application of 20 μM NEO. * shows chart recorder running at half indicated speed.

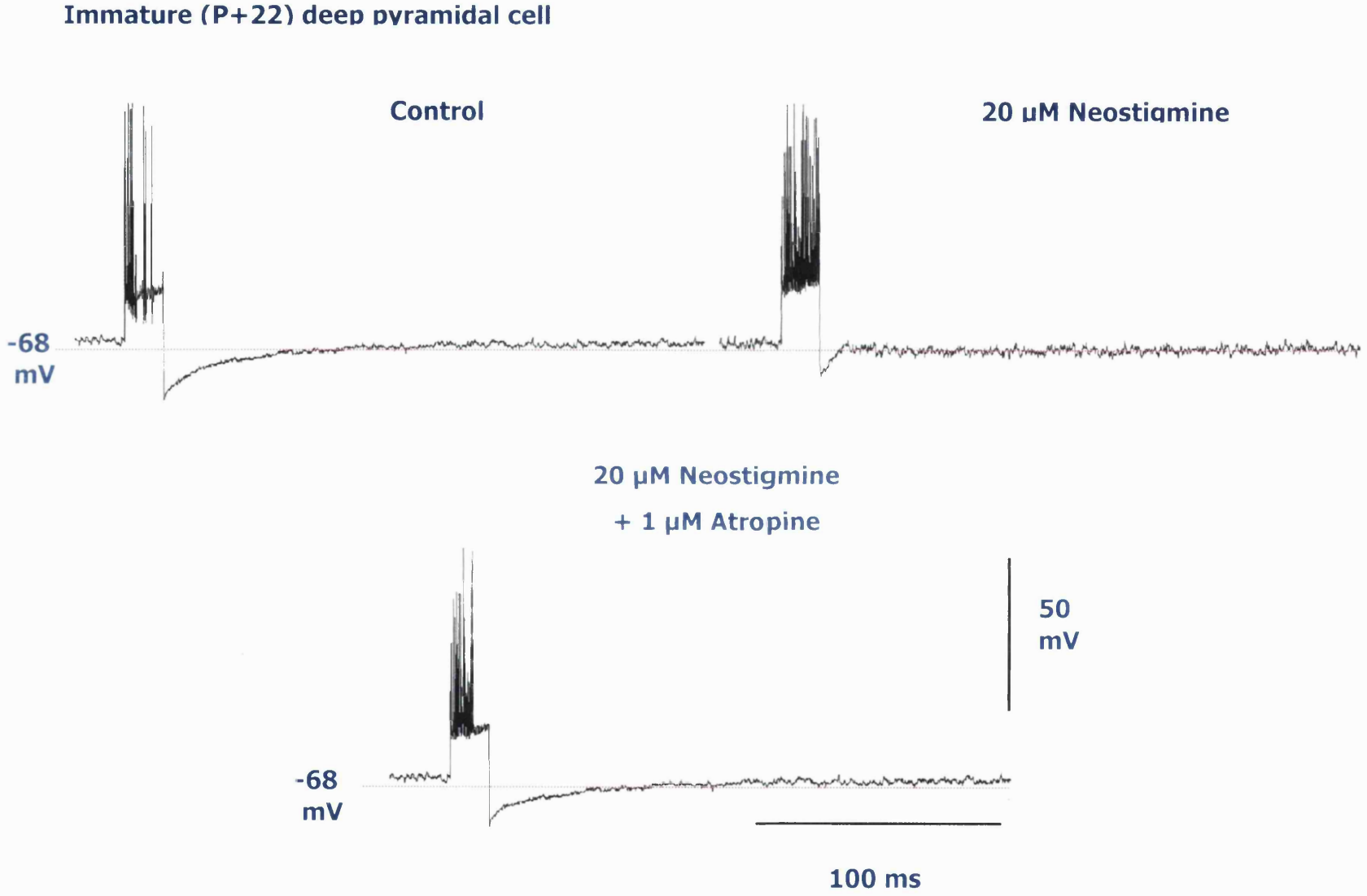
Immature (P+22) deep pyramidal cell
Control
20 µM Neostigmine
-68
mV
20 µM Neostigmine
+ 1 µM Atropine
50
mV
-68
mV
100 ms

Figure 3.29

Figure 3.29

The effect of 20 μM neostigmine (NEO) upon the slow afterhyperpolarization (sAHP). The sAHP was elicited by application of a long depolarizing stimulus train (+2 nA; 1.6 s) in CC mode. sAHPs elicited from an immature (P+22) piriform cortical neurone are shown in control conditions (**top left panel**), in 20 μM NEO (**top right panel**) and in 20 μM NEO plus 1 μM atropine (**bottom middle panel**). Note the decrease in sAHP amplitude and increase in spike firing during the depolarizing stimulus train. The mAChR-mediation of this effect is shown by its blockade by the mAChR antagonist, atropine (1 μM).

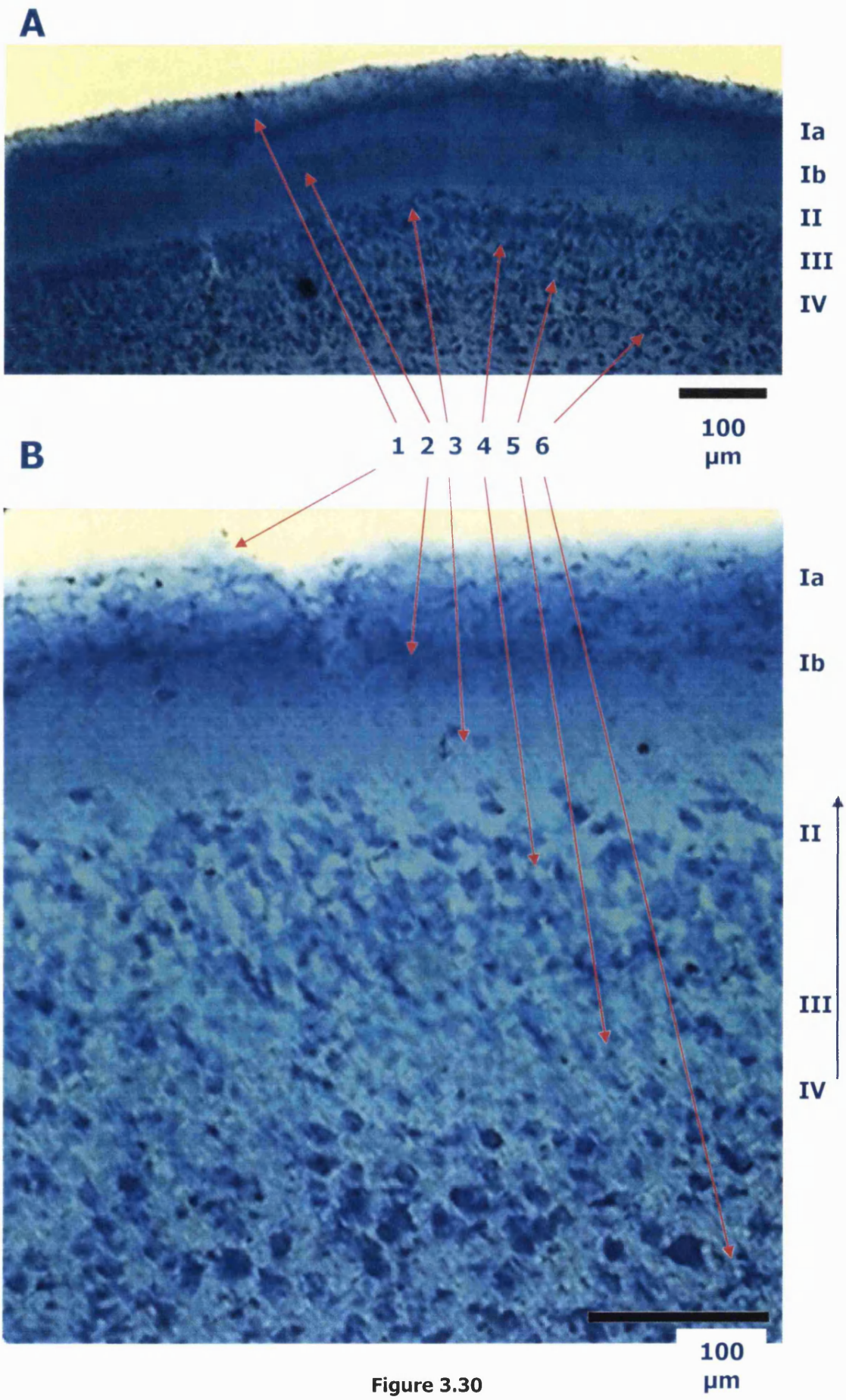

Figure 3.30

Figure 3.30

Photographs showing a methylene blue-stained 50 μm transverse section of adult rat piriform cortical tissue shown at x4 magnification (**A**) and x10 magnification (**B**). Note the characteristic laminar cortical structure. [**1**] – Pial surface; [**2**] – Layer Ia; [**3**] – Layer Ib; [**4**] – Layer II; [**5**] – Layer III; [**6**] – Underlying endopiriform nucleus (also called layer IV). Arrow indicates the direction of the pial surface of the section.

A

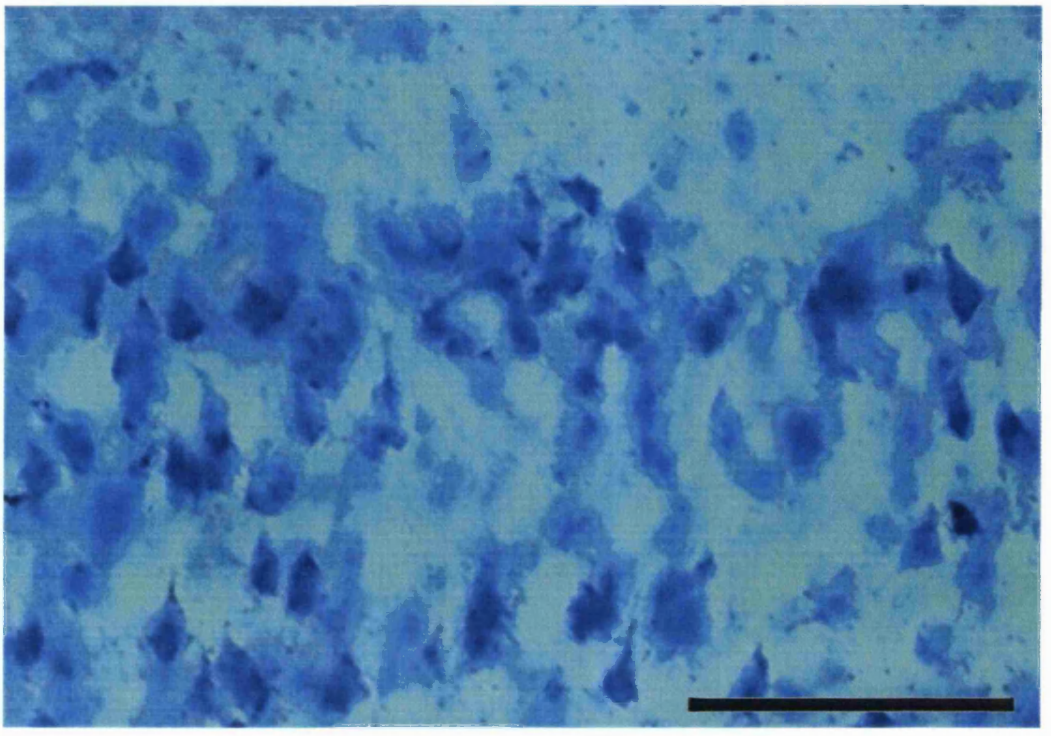

II

100
µm

B

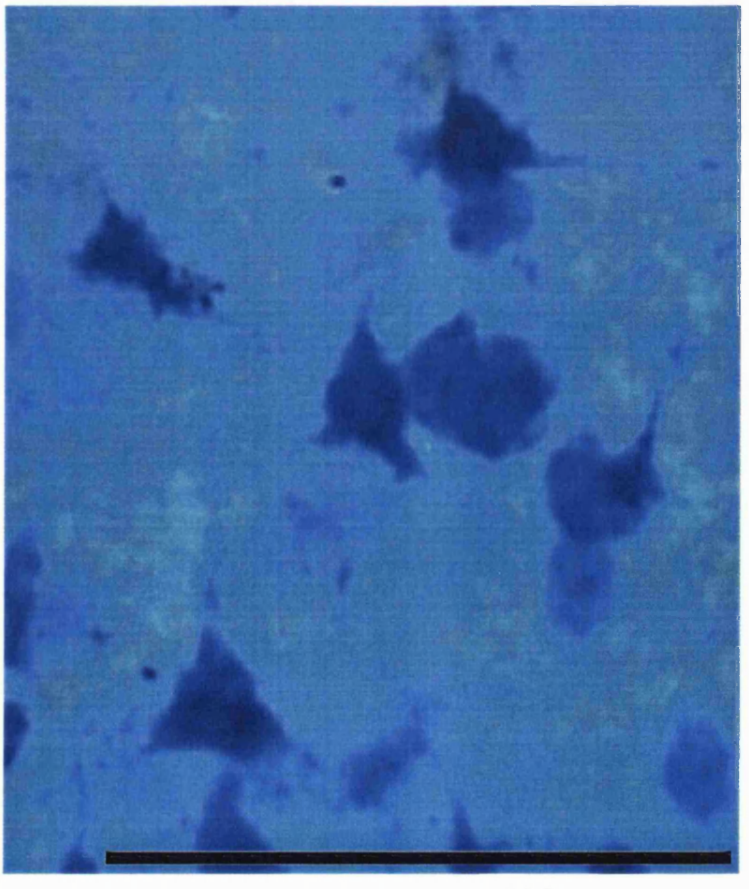

III

100
µm

Figure 3.31

Figure 3.31

Photographs showing a methylene blue-stained 50 μm transverse section of immature (P+24) rat piriform cortical tissue at x10 magnification (**A**) showing layer II with characteristic densely packed superficial pyramidal cells and at x40 magnification (**B**) showing layer III containing deep pyramidal cells with their apical dendrites pointing characteristically towards the pial surface. Arrow indicates the direction of the pial surface of the section.

Table 3.1

Basic electrical membrane properties of recorded piriform cortical cell types.

Cell Type	Resting membrane potential (V_m; mV)	Input resistance (R_{in}; MΩ)	Spike height (mV)
Adult deep pyramidal (n=86)	-84 ± 0.7	44 ± 2.1	108 ± 1.2
Immature deep pyramidal (n=266)	-83 ± 0.9	46 ± 1.8	110 ± 1.1
Adult interneurone (n=5)	-81 ± 0.6	41 ± 2.2	102 ± 1.7
Immature interneurone (n=18)	-81 ± 0.9	41 ± 2.5	104 ± 2.6
Adult superficial pyramidal (n=7)	-81 ± 1.4	25 ± 1.9*	101 ± 2.4
Immature superficial pyramidal (n=17)	-81 ± 1.7	25 ± 1.4*	102 ± 2.7

Data are means ± SEM. n=number of neurones. Spike amplitude was measured from resting potential to peak. Resting input resistance (R_{in}) was calculated from -70 mV resting membrane potential (achieved by application of positive holding current) using the steady-state electrotonic response (≤10 mV) to a -0.25 nA current pulse. Corresponding values from adult and immature neurones did not differ from one another except where indicated (*). * Significantly different from corresponding deep pyramidal and interneuronal cell type ($P<0.001$; Mann-Whitney test).

Table 3.2

Comparison of slow post-stimulus afterpotential and tail current properties.

Cell Type	Control sAHP amplitude (mV)	Control I_{AHP} amplitude (nA)	sADP amplitude in OXO-M (mV)	I_{ADP} amplitude in OXO-M (nA)
Adult deep pyramidal neurone	13 ± 1.4 (n=86)	0.81 ± 0.07 (n=83)	11 ± 1.4 (n=44)	0.53 ± 0.04 (n=44)
Immature deep pyramidal neurone	12 ± 1.2 (n=266)	0.76 ± 0.05 (n=264)	12 ± 1.2 (n=176)	0.51 ± 0.03 (n=176)
Adult interneurone	6 ± 1.6 (n=5)	0.37 ± 0.03 (n=5)	7 ± 1.4 (n=5)	0.23 ± 0.07 (n=5)
Immature interneurone	6 ± 1.3 (n=18)	0.32 ± 0.05 (n=18)	7 ± 0.9 (n=17)	0.21 ± 0.04 (n=16)

Data are means ± SEM. n=number of neurones. sADP amplitudes were measured after correcting for changes in membrane potential caused by OXO-M. Corresponding values from adult and immature neurones did not differ significantly from one another. Values from deep pyramidal neurones and interneurones significantly differed from one another ($P<0.001$; Mann-Whitney test).

Table 3.3

Comparison of OXO-M elicited effects in adult and immature piriform cortical neurones.

Cell Type	Depolarization induced by 10 μM OXO-M (mV)	Change in input resistance after application of 10 μM OXO-M (%)
Adult deep pyramidal neurone (n=44)	11 ± 0.8	12 ± 1.9
Immature deep pyramidal neurone (n=176)	12 ± 0.7	20 ± 2.1
Adult Interneurone (n=5)	12 ± 0.4	12 ± 1.6
Immature Interneurone (n=17)	11 ± 0.9	18 ± 2.3
Adult superficial pyramidal neurone (n=7)	2 ± 1.5	3 ± 1.6
Immature superficial pyramidal neurone (n=17)	3 ± 1.1	3 ± 1.4

Data are means ± SEM. n=number of neurones. OXO-M induced depolarizations were measured from -70 mV. Changes in input resistance were calculated after accounting for changes in membrane potential caused by OXO-M. Corresponding values from adult and immature deep pyramidal neurones and interneurones differed significantly from one another ($P<0.001$; Mann-Whitney test). Both values from deep pyramidal neurones/interneurones differed significantly from those for superficial pyramidal neurones ($P<0.001$; Mann-Whitney test).

Table 3.4

Comparison of the effects of some anticonvulsants upon OXO-M-induced epileptiform bursting and sADP in immature deep pyramidal piriform cortical neurones.

Anticonvulsant (Concentration)	Mean speed of burst firing abolition (minutes)	Reduction of sADP (%)
Topiramate (20 μM; n=14)	5 ± 1.1	8.8 ± 2.1*
Carbamazepine (50 μM; n=11)	8 ± 1.3	61.0 ± 8.6
Felbamate (300 μM; n=5)	9 ± 1.6	53.0 ± 8.0
Gabapentin (30 μM; n=11)	11 ± 2.1	53.5 ± 4.7
Lamotrigine (2 μM; n=5)	12 ± 1.3	23.2 ± 6.8
Phenobarbitone Sodium (50 μM; n=6)	15 ± 4.6	N/A

* Topiramate abolished the I_{ADP} completely revealing an enhanced (by the percentage shown) I_{AHP} (Fig. 3.24). Data are means ± SEM. n=number of neurones.

Table 3.5

Comparison of a number of OXO-M-induced epileptiform bursting characteristics with specific animal ages.

Age (days)	P+14 (n=9)	P+29 (n=13)	All recorded bursting neurones (n=111)
Mean burst duration (s)	15.6 ± 1	58 ± 2	23.2 ± 1.4
Mean interburst interval (s)	6 ± 1	30 ± 1.5	13 ± 2
Mean PDS (mV)	35 ± 2	6 ± 5	23.5 ± 7
CV_i (%)	72 ± 0.4	69 ± 0.5	33 ± 7
CV_d (%)	74 ± 0.5	81 ± 1	38 ± 6

Data are means ± SEM. n=number of neurones.

Chapter 4:

The excitatory synaptic responses of immature and adult deep pyramidal piriform cortical neurones; a developmental comparison

4.1 Introduction

A previous report describing OXO-M-induced epileptiform activity in the immature rat piriform cortex (Postlethwaite *et al.*, 1998a) also reported a prolonged excitatory postsynaptic potential (EPSP) with characteristic superimposed repetitive firing that could be evoked only from *immature* piriform cortical slices exhibiting established bursting behaviour in 10 μM OXO-M, following stimulation with a bipolar stimulating electrode placed in layer II/III of the slice. This result and the long-established knowledge that epileptiform phenomena typically require neuronal circuitry that is not only conducive to burst generation but also to burst maintenance and propagation (Loscher & Ebert, 1996) suggested a significant synaptic component to the mAChR agonist-induced epileptiform phenomenon being investigated. Consequently, EPSPs were evoked, as previously described with an external bipolar stimulating electrode placed gently onto the surface of the slice preparation (see Methods, Section 2.5.3). During early experiments, a single stimulating electrode was routinely placed in layer II/III of the slice preparation, as previously reported (Postlethwaite *et al.*, 1998a), however, in later experiments, an additional stimulating electrode was placed in layer I. This was done to allow stimulation of *either* intrinsic cortico-cortical (layer II/III) *or* afferent axonal fibres, arising from the LOT in layer I (L1) as previously described (Hasselmo & Bower, 1992) and *c.f.* also (Carmichael *et al.*, 1994; Datiche *et al.*, 1996; Demir *et al.*, 2001; Hori *et al.*, 1988), and avoided the possibility of stimulating both fibre systems simultaneously (*cf.* (Postlethwaite *et al.*, 1998a)). Additionally, finer stimulating electrode tips (~45 μm total diameter) were used in the present study, compared to those used in previous studies (*cf.* (Hasselmo & Bower, 1990; Postlethwaite *et al.*, 1998a)), which reduced the degree of physical damage done to the slice on contact, thereby maintaining the neuronal circuitry of the preparation to a greater degree.

Sub- and suprathreshold EPSPs, elicited following layer I (L1) or layer II/III (intrinsic fibre) stimulation, were compared in control conditions and in the presence of 10 μM OXO-M, using slices from both adult and immature animals. This protocol permitted the investigation and elucidation of any layer-specific synaptic differences that might be implicated in the generation and maintenance of the observed mAChR agonist-induced epileptiform bursting phenomenon seen in the immature preparation. The pharmacology of presynaptic receptors modulating elicited EPSPs (Williams & Constanti, 1988b) was also tested using mAChR subtype-specific antagonists, to determine whether any differences in the mAChR subtype responsible for the mAChR-

mediated effects could be observed. Additionally, the effects of varying the location of the recording microelectrode within the slice (rostro-caudally along layer III) upon the characteristics of elicited EPSPs and their muscarinic pharmacology (Section 3.4.4) were also investigated.

All figures of synaptic potentials presented here comprise averages of at least 3 traces, unless otherwise indicated.

All EPSPs were routinely elicited from a membrane potential of -90 mV, held by the injection of steady negative current into the recorded cell through the recording microelectrode.

All recorded cells were electrophysiologically characterized as presumed deep pyramidal neurones (Section 3.2.1), unless otherwise stated. All significant differences between data sets in this chapter were calculated using non-parametric Wilcoxon signed rank tests unless explicitly stated otherwise.

4.2 EPSPs elicited from adult deep pyramidal neurones

Sub-threshold (Fig. 4.1A) and supra-threshold (Fig. 4.1B) EPSPs elicited from adult and immature neurones comprised an initial, fast, excitatory (EPSP), (spike) and subsequent, fast and slow inhibitory (IPSP) components. The excitatory fast component has been shown to be primarily mediated by the excitatory neurotransmitter, glutamate (Fig. 4.1B;1) (Lester *et al.*, 1988). The inhibitory components comprised an initially, fast depolarizing phase, mediated by the inhibitory neurotransmitter, GABA, acting upon $GABA_A$ receptors ($GABA_ARs$; Fig. 4.1B;2) and a slower, later stage mediated by the same neurotransmitter acting upon $GABA_B$ receptors ($GABA_BRs$; Fig. 4.1B;3)(Tseng & Haberly, 1988).

4.2.1 EPSPs elicited from adult deep pyramidal cortical neurones are input specific

Conventional current clamp recordings were made from a total of 65 adult deep pyramidal piriform cortical neurones, following L1 or intrinsic fibre stimulation. Even in control conditions, noticeable differences were seen between EPSPs elicited following L1 (Fig. 4.1) or intrinsic (Fig. 4.2) fibre stimulation. The mean time course (measured from stimulus application to return to baseline) for suprathreshold EPSPs evoked following L1 fibre stimulation was significantly longer (21 ± 6.6 %; $P<0.01$) than that calculated for EPSPs elicited following intrinsic fibre stimulation. Also, in a number of experiments (64%), EPSPs elicited following L1 fibre stimulation showed a characteristic prolonged phase in the later stages of the EPSP (Fig. 4.1B). Additionally,

in 15% of EPSPs elicited following L1 fibre stimulation only an *'all or nothing'* response could be obtained, whereby no subthreshold EPSP could be evoked and no gradual increase in EPSP magnitude to a maximum and an action potential firing was seen. This phenomenon has been suggested to be closely linked to the integration of new information into memory and may have a role in generation of epileptiform burst firing (Tseng & Haberly, 1989d).

4.2.2 Muscarinic AChR activation selectively inhibits intrinsic but not afferent transmission

Individual subthreshold EPSPs recorded from adult deep pyramidal neurones and elicited following L1 fibre stimulation appeared unchanged in the presence of 10 μM OXO-M (20 mins after application; Fig. 4.1A; *c.f.* (Hasselmo & Bower, 1992)). However, suprathreshold EPSPs, elicited in the same manner, exhibited a prolongation of the EPSP (shown by (*) in Fig. 4.1B) with a corresponding significant (51 ± 11.1%; $P<0.01$) increase in EPSP time course compared with control. Additionally, an occasional (32% of recordings) superimposed action potential (following the initial action potential) was observed (Fig. 4.1B; middle panel). A previous study has shown the prolongation (with superimposed firing) of EPSPs elicited following generalised stimulation of layer II and III, in the presence of 10 μM OXO-M and recorded from the *immature* deep pyramidal piriform cortical neurones (Postlethwaite *et al.*, 1998b), but this is the first report of synaptic prolongation of any type in the *adult* slice preparation induced by mAChR activation. Conversely, EPSPs elicited following subthreshold intrinsic fibre stimulation were significantly inhibited in OXO-M (Fig. 4.2; 77 ± 6.2%; $P<0.01$ *vs.* control) compared to control. This observed inhibition was consistent with results published in other studies performed on superficial piriform cortical pyramidal cells (See Section 4.1) (Hasselmo *et al.*, 1992).

When a log dose-response curve was plotted the degree of OXO-M-induced suppression of adult subthreshold intrinsic fibre-elicited EPSPs *vs.* OXO-M concentration, a typically sigmoidal curve was produced and an ED_{50} of 2.6 μM OXO-M was calculated (Fig. 4.3). All reported effects of OXO-M application (presumed presyaptic) were fully reversed following the application of the mAChR antagonist, atropine (1 μM; not shown). The proportion of *'all or nothing'* EPSPs elicited following L1 fibre stimulation was unchanged from controls following the application of 10 μM OXO-M. The postsynaptic effects of OXO-M that caused a sustained depolarization (Chapter 3) were routinely corrected for by the injection of negative current through the

recording microelectrode to return the membrane potential to -90 mV when evoking EPSPs.

4.2.3 OXO-M induced inhibition of intrinsic transmission is M1 AChR mediated in adult rats

The mAChR subtype mediating the presynaptic effects of OXO-M on excitatory synaptic transmission in the adult slice preparation was investigated by using subtype specific mAChR antagonists (see Section 3.4.4 for a description of the postsynaptic effects of these antagonists *vs.* OXO-M-induced depolarization). Application of the M1-specific mAChR antagonists, pirenzepine (100 nM: 7/7 cells; Fig. 4.4) or telenzepine (20 nM: 7/7 cells; Fig. 4.4) to adult slices caused a full reversal of the observed inhibition of intrinsic fibre evoked excitatory synaptic transmission, induced by 10 μM OXO-M. In contrast, application of the M2-specific mAChR antagonists, methoctramine (300 nM: 7/7 cells; Fig. 4.4) or AFDX-116 (1 μM: 7/7 cells; Fig. 4.4) to adult slices did not affect the OXO-M-induced synaptic inhibition of intrinsic synaptic transmission, indicating that the modulation observed is M1 mAChR-mediated in the adult rat piriform cortical slice preparation. These results contrasted results reporting a small inhibition of excitatory synaptic transmission by M3 mAChR antagonists (Bagetta & Constanti, 1991) and inhibition of postsynaptic mAChR-mediated effects by M1 mAChR specific antagonists in the adult guinea pig (Williams & Constanti, 1988).

4.3 EPSPs elicited from immature deep pyramidal neurones

EPSPs were also elicited from recorded immature presumed deep pyramidal neurones using the same protocols as described above (Section 4.2).

4.3.1 Characteristics of EPSPs elicited from immature deep pyramidal cortical neurones are also input specific

Recordings made in current clamp mode were obtained from 136 immature neurones and their responses, following either L1 or intrinsic fibre stimulation, observed. In control conditions, noticeable differences were again observed between EPSPs elicited following L1 (Fig. 4.5) and intrinsic (Fig. 4.6) fibre stimulation. In a manner similar to that seen in the adult preparation, there was a significant prolongation of suprathreshold EPSPs elicited following L1 fibre stimulation that manifested as a sustained depolarization following initial recovery from the action potential. Consequently, the mean time course of suprathreshold EPSPs elicited following L1 fibre stimulation was

found to be 32 ± 12.1 % (P<0.01 *vs.* intrinsic) longer than that for EPSPs elicited following intrinsic fibre stimulation. This difference was also significantly larger than the mean time course difference between L1 and intrinsic fibre elicited EPSPs observed in the adult preparation (21 ± 6.6 %; P<0.05; n=65; Section 4.2.1). Additionally, a larger proportion (32%) of EPSPs elicited following L1 fibre stimulation were seen to be of the '*all or nothing*' type (Section 4.2.1) when recorded from immature cells rather than adult cells.

4.3.2 Muscarinic AChR activation also selectively inhibits intrinsic but not afferent transmission in immature rat piriform cortex

Evoked subthreshold EPSPs recorded from cells in immature piriform cortical brain slices following L1 fibre stimulation were visibly prolonged and multiphasic in the presence of 10 μM OXO-M, either demonstrating prolongation of the depolarized period of the PSP (83%; not shown) or EPSPs and repetitive superimposed spike firing of the type described by Postlethwaite *et al.* (16%; Fig. 4.5A; 1) (Postlethwaite *et al.*, 1998a). Elicited L1 suprathreshold EPSPs that exhibited a prolongation of the EPSP in OXO-M were indistinguishable from adult EPSPs evoked in the same manner (Fig. 4.1B), aside from having a slightly, but significantly longer time course relative to their respective controls (immature: 68 ± 8%; n=136; adult: 51 ± 11.1%; n=65; P<0.05). The remaining 16% of evoked EPSPs that showed a large prolongation of the EPSP with the appearance of multiphasic components and repetitive superimposed action potentials in OXO-M (4.1B; 2) were *never* recorded from immature non-responding (non-epileptiform bursting) neurones. A previous report described EPSPs of this type as being regularly observed in immature cells with layer II/III stimulation in OXO-M (Postlethwaite *et al.*, 1998a), consequently, the disparity in frequency of occurrence of the phenomenon between that report and the results presented here is discussed in Section 4.4.

Changes in the L1 suprathreshold EPSP time course of neurones that showed repetitive superimposed spike firing of this type could not be accurately measured since the stimulus was typically sufficient to send the cell into its next epileptiform bursting period. Conversely, EPSPs evoked following subthreshold intrinsic fibre stimulation, in the presence of 10 μM OXO-M and recorded from immature neurones, were consistently *inhibited.* Interestingly, this inhibition was significantly smaller (25 ± 5.4%; P<0.01; n=136; Figs. 4.6 & 4.7B) than was observed in the adult preparation (77 ± 6.2%; n=65; Section 4.2.2). Additionally, the proportion of '*all or nothing*' EPSPs

elicited following L1 fibre stimulation was, like the adult preparation, unchanged from controls in OXO-M. In order to further compare the effects of OXO-M upon intrinsic fibre excitatory synaptic transmission in the immature preparation, a log-dose response curve was constructed showing the degree of suppression of subthreshold intrinsic fibre transmission *vs.* OXO-M concentration using pooled data from *all recorded immature neurones* (Fig. 4.7; P+14 to P+28). This plot clearly shows that OXO-M is less effective in suppressing intrinsic fibre synaptic transmission in the immature (OXO-M ED_{50}=3.6 μM) preparation than in the adult (OXO-M ED_{50}=2.6 μM). However, since it has already been demonstrated that the postsynaptic effects of OXO-M not only vary between the immature and the adult preparations, but also between the ages P+14 and P+28 (Section 3.5.2), log dose-response curves were also constructed for the ages P+28 and P+14 and plotted alongside the curve describing the mean immature response previously plotted (Fig. 4.7A). These plots clearly show that the same kind of developmental variation in response to OXO-M, observed postsynaptically in Section 3.5.2, is also seen presynaptically. Thus, the sensitivity of the preparation to OXO-M increased between P+14 (ED_{50}=4.5 μM) and P+28 (ED_{50}=2.5 μM) as indicated by the changing ED_{50} values obtained. This demonstrated that not only does OXO-M inhibit intrinsic fibre excitatory synaptic transmission, *at maximal concentrations* (16 μM), to a lesser degree in the immature preparation than in the adult, but was also less potent (independent of the final degree of inhibition achieved) in the immature preparation than the adult. It can be clearly seen from these results that OXO-M caused a greater prolongation of afferent (L1) synaptic transmission but a smaller inhibition of intrinsic synaptic transmission in the *immature* preparation than the *adult*. This developmentally-based difference in synaptic responsiveness to mAChR activation, would appear to produce a '*shift*' in synaptic transmission dynamics in this immature preparation toward a state of greater excitability and hence a state more prone to epileptiform burst firing.

4.3.3 OXO-M induced inhibition of intrinsic transmission is M2 AChR mediated in immature rat piriform cortex

The same protocol used to determine the mAChR subtype responsible for inhibiting intrinsic excitatory synaptic transmission in the adult slice preparation (Section 4.2.3) was also used on the immature preparation. In contrast with the adult, application of the M1-specific mAChR antagonists, pirenzepine (100 nM: 9/9 cells; Fig. 4.8) or telenzepine (20 nM: 9/9 cells; Fig. 4.8) to immature slices did *not* reverse the inhibition of intrinsic fibre excitatory synaptic transmission induced by OXO-M. However,

application of the M2-specific mAChR antagonists, methoctramine (300 nM: 10/10 cells; Fig. 4.8) or AFDX-116 (1 μM: 9/9 cells; Fig. 4.8) to immature slices fully reversed the OXO-M-induced inhibition of intrinsic fibre excitatory synaptic transmission, suggesting that unlike the adult preparation (where the inhibition was shown to be M1 mAChR-mediated), the modification of immature intrinsic fibre excitatory synaptic transmission was M2 mAChR-mediated. These results indicate a clear developmental switch between presynaptic mAChR subtypes from M2 to M1 as the animal grows to maturity, with the M2 subtype apparently being less efficacious in inhibiting intrinsic excitatory synaptic transmission.

4.4 Elicited EPSPs vary according to positioning of recording microelectrode and stimulating electrodes in piriform cortex

Results presented in Chapter 3 demonstrated that there was a considerable variation in the frequency with which mAChR agonist-induced epileptiform bursting occurred (independently of other factors affecting burst incidence frequency *e.g.* age) with variation of the rostro-caudal position of the recorded cell within the immature slice preparation (Section 3.4.3). Thus, mAChR agonist-induced burst firing was recorded more frequently in cells at the anterior (APC) and posterior (PPC) ends of the slice preparation than the median (MPC; middle) area (Fig. 4.9). Therefore, it was of interest to investigate whether any corresponding variation in excitatory synaptic responsiveness with location within the slice preparation could be found.

Evoked EPSPs from a total of 27 immature cells (APC: 8 cells; MPC: 10 cells; PPC: 9 cells) were elicited following stimulation of either L1 or intrinsic fibres in control conditions and in the presence of 10 μM OXO-M, as previously described. In control conditions, no significant differences were observed between the (sub- and suprathreshold) results recorded following intrinsic fibre stimulation from the different areas within the slice preparation (not shown). Additionally, no observable differences were noted between the *subthreshold* EPSPs elicited following L1 fibre stimulation from the different areas (not shown). However, when *suprathreshold* EPSPs were elicited following L1 fibre stimulation, a number of notable differences were observed: in control conditions, EPSPs elicited from the APC consistently (8/8 cells) featured one or two superimposed action potentials that appeared directly after the first action potential (Fig 4.9A; 1). This phenomenon was never observed in EPSPs recorded from either the MPC (0/10 cells) or the PPC (0/9 cells) in control conditions. Evoked EPSPs recorded from both the APC (8/8 cells) and PPC (9/9 cells) also routinely showed a late

depolarizing phase to the elicited EPSP (Fig 4.9A; 2) that was not observed in EPSPs recorded from cells in the MPC (0/10 cells). Additionally, a higher number of '*all or nothing*' responses were seen in APC (62%) and PPC (54%) recorded cells compared with those recorded from the MPC (32%), and, as previously reported, these proportions were unaffected by the addition of 10 μM OXO-M. Following the application of 10 μM OXO-M, no significant differences between the degree of OXO-M-induced suppression of intrinsic fibre excitatory transmission was found between the APC (23 ± 6.2%; $P>0.05$) or the PPC (28 ± 4.3%; $P>0.05$) compared with those obtained from the MPC (25 ± 5.4%). Sub- and suprathreshold EPSPs elicited following L1 fibre stimulation and recorded from immature cells within the APC or the PPC reliably produced repetitive spike firing following the initial stimulus (APC: 8/8 cells; PPC: 9/9 cells), of the type shown in Figure 4.5 (middle panels). As previously stated, this behaviour was only observed in 16% of previously recorded neurones (Section 4.3.2) and in only 2/10 recorded neurones from the MPC in this section of the study.

Responses were also recorded under the same conditions as described above, from adult deep pyramidal neurones following L1 or intrinsic fibre stimulation, in the same three areas of the piriform cortical slice preparation. Similarly to the immature preparation, no change in the observed OXO-M-induced inhibition of intrinsic fibre excitatory transmission was seen between the APC (72 ± 5.8%; 8 cells), MPC (77 ± 6.2%; 65 cells) and PPC (74 ± 8.3%; 7 cells). However, in control conditions, suprathreshold EPSPs evoked following L1 fibre stimulation and recorded from the APC and PPC consistently showed a superimposed second action potential after the initial, short latency action potential, indistinguishable from the response recorded from immature APC neurones following L1 fibre stimulation (Fig 4.9; left panel) that were unaffected by the addition of 10 μM OXO-M. Additionally, as seen in the immature preparation, a higher proportion of '*all or nothing*' responses were recorded from neurones in the APC (35%) and the PPC (30%) compared with those recorded from the MPC (15%). These frequencies were, like the adult preparation, also unchanged by the addition of 10 μM OXO-M.

In summary, the above results demonstrated that there exist clear, location dependent differences in the responses of presumed deep pyramidal piriform cortical neurones following afferent (L1), but not intrinsic fibre stimulation. The median area is clearly less excitable than either the anterior or posterior regions of the piriform cortex, a result that is in keeping with data presented elsewhere in this study showing a higher incidence of epileptiform bursting behaviour in these regions (Sections 3.4.3 & 3.8.6).

Additionally, a previous study (Postlethwaite *et al.*, 1998a) regularly observed prolonged, multiphasic layer II/III EPSPs with superimposed spike firing (see also Section 4.3.2) in the immature slice preparation following the application of 10 μM OXO-M, a phenomenon that was less frequently observed in this present study. It seems possible that recordings in their study were made more frequently in the PPC, explaining the higher incidence of this phenomenon than seen in the present study.

4.5 A comparison of input specific EPSPs by paired pulse analysis

Since the results above have made it clear that a number of differences exist in the excitatory synaptic responsiveness of deep pyramidal neuronal responses according to synaptic input type, a further investigation of these effects was undertaken using a paired-pulse analysis in an attempt to confirm that they were truly presynaptic in origin. Paired-pulse ratio (PPR) analysis is standard method used to assess whether neuromodulators are able to influence transmission by affecting presynaptic release probability. Thus, a mAChR agonist acting presynaptically to inhibit transmission, would be expected to significantly *increase* early paired-pulse facilitation of synaptically evoked EPSPs or IPSPs. This protocol therefore allows confirmation of whether the mAChR-mediated inhibition of intrinsic transmission and prolongation of L1 synaptic transmission were indeed being mediated via presynaptic mechanisms (Stuart & Redman, 1991). The paired-pulse protocol used comprised two small (eliciting <10 mV magnitude subthreshold PSPs) stimuli separated by a variable (but known) inter-stimulus interval (ISI; 0 – 500 ms; See Methods, Section 2.5.3.4). The cellular response to the second stimulus was primarily dependent upon the length of the ISI, whereupon a short (0-200 ms) ISI typically produced a facilitation of the second pulse (paired-pulse facilitation; PPF; Fig. 4.10; 1), whilst a longer (200-500 ms) ISI produced an inhibition of the magnitude of the second pulse (paired-pulse inhibition; PPI; Fig. 4.10; 3; in this preparation) (Papatheodoropoulos & Kostopoulos, 1996; Stuart & Redman, 1991). Consequently, protocols of this type have been termed '*use-dependent models*' of paired-pulse ratio (Zucker & Regehr, 2002). These early (facilitatory) effects are considered to be the products of presynaptic mechanisms, specifically, facilitation being considered to be due to the first, *'conditioning'* pulse causing a dynamic increase in presynaptic intracellular Ca^{2+} levels, raising the probability of neurotransmitter release upon application of the second pulse. Since this increase in intracellular Ca^{2+} is transitory, the facilitation drops thereafter as Ca^{2+} is expelled (or taken up into intracellular stores) and presynaptic inhibitory mechanisms switch on in response to the

conditioning pulse. Eventually (~250 ms after the conditioning pulse, in this preparation and under control conditions), the increasing inhibitory mechanisms (such as Ca^{2+} reuptake and increased pre- (Deisz, 1999) and postsynaptic $GABA_BR$-mediated inhibition (Stanford *et al.*, 1995)) attain a point of balance with the declining facilitatory mechanisms and no facilitatory or inhibitory effects are observed (Fig. 4.10; 2). Thereafter, the inhibitory effects begin to dominate and an overall inhibition of synaptic transmission is observed (Fig. 4.10; 3), eventually disappearing at an ISI of ~450 ms (in control conditions in this preparation). From these data, the ratio of the second pulse to the first pulse (P2/P1) for various values of ISI may be plotted (*e.g.* Fig. 4.11) and comparisons made between the various levels of facilitation and inhibition under different experimental circumstances. All significant differences between data sets in this section were calculated at the point of maximal facilitation/inhibition.

Unless otherwise stated, all synaptic potentials were elicited from a membrane potential of -90 mV, maintained by negative current injection.

4.5.1 Paired-pulse responses elicited following L1 or intrinsic fibre stimulation in the adult and immature slice preparations, in control conditions

Since earlier experiments presented in this report indicated significant differences in the responses of deep pyramidal neurones to either L1 or intrinsic fibre stimulation in control conditions and following mAChR activation, it was necessary to confirm the results obtained earlier in this chapter that indicated mAChR-mediated presynaptic inhibition/facilitation of excitatory synaptic transmission to show developmental variation. Confirmation of a presynaptic mechanism for these phenomena was sought using paired-pulse techniques and, if possible, further quantification of these developmental differences. With this in mind, paired-pulse data were obtained using the standard methodology (Stanford *et al.*, 1995; Stuart & Redman, 1991) and plotted as paired-pulse ratio *vs.* ISI. In the first instance, differences between the results obtained following L1 and intrinsic fibre stimulation of both adult (Fig. 4.11A) and immature (Fig. 4.11B) preparations, in control conditions, were examined. In control conditions, a clear difference in the degree of paired-pulse inhibition recorded following intrinsic fibre stimulation compared to that seen following L1 fibre stimulation was observed. In the adult preparation, the difference between peak L1 fibre PPI and peak intrinsic fibre PPI (35 ± 3.6%; n = 51; Fig. 4.11A) was found to be significantly greater than the equivalent difference recorded form the immature preparation (11 ± 2.1%; $P<0.01$; n = 61; Fig. 4.11B). The results obtained showed relatively little PPI following L1 fibre

stimulation in either the adult or immature preparations and also very little difference between the peak adult and immature L1 fibre stimulation inhibitory ratios (adult: 0.85 ± 0.07; n=19; immature: 0.83 ± 0.05; n=21; Fig. 4.12A), suggesting less presynaptic inhibitory control and few differences in either presynaptic excitatory or inhibitory mechanisms on the L1 fibres of the adult or immature preparations.

The results above clearly contrast with the differences observed between the adult (0.57 ± 0.07; n=19) and immature (0.72 ± 0.08; n=21) peak intrinsic fibre inhibitory ratios obtained (Fig. 4.12B), where, overall, more PPI was seen, but there was significantly less peak inhibition in the immature preparation compared to the adult ($P<0.05$). This was consistent with earlier observations in this present study demonstrating a reduced degree of inhibitory activity in the intrinsic fibres of the immature animal and the epileptogenic characteristics exhibited by L1-evoked suprathreshold EPSPs (Sections 4.2 and 4.3). Consequently, the paired-pulse analysis would suggest that the reduced inhibition seen in immature slices and the prolonged L1-evoked EPSPs seen in immature (and to a lesser degree in adult) slices to be at least partly due to reduced levels of postsynaptic $GABA_BR$-mediated inhibition (Dutar & Nicoll, 1988b; McCarren & Alger, 1985).

4.5.2 Paired-pulse responses elicited following L1 or intrinsic fibre stimulation in the adult and immature slice preparations following the application of OXO-M

The effects of the mAChR agonist, OXO-M (10 μM) upon PPF and PPI following L1 or intrinsic stimulation in both the adult (n=19) and immature (n=21) preparations were also investigated. Responses elicited following L1 fibre stimulation in control conditions and in 10 μM OXO-M for either adult (Fig. 4.13A) or immature (Fig. 4.14A) cells revealed a slight increase in PPF at ISI=50-100 ms in both adult and immature responses in the presence of OXO-M when compared to control. This difference was not found to be statistically significant in the adult preparation ($P>0.05$), however, it was found to be slightly, but significantly different from control in the immature preparation (6 ± 3.2%; $P<0.05$). This slight increase in facilitation was likely to be caused by the activation of presynaptic inhibitory mAChRs by OXO-M, causing a reduction in the amount of neurotransmitter released by the first, conditioning pulse. Thus, the presynaptic bouton is left in a state where an increased number of neurotransmitter-containing vesicles are membrane-bound and ready for release at the presynaptic terminal. When the second pulse was applied, there was a higher probability of neurotransmitter release that was manifested as a relatively larger second pulse

(Stuart & Redman, 1991). No changes in peak PPI, following L1 fibre stimulation, were observed in either the adult or immature preparation, suggesting no mAChR modulation of $GABA_BR$ function or, alternatively few, if any, postsynaptic $GABA_BRs$. Contrastingly, responses elicited following intrinsic fibre stimulation showed significant increases in early facilitation *and* late inhibition in both the adult (Fig. 4.13B) and immature (Fig. 4.14B) preparations. The peak increase in PPF compared to controls observed in the adult preparation (14 ± 1.3%) was found to be slightly, but significantly different from that observed in the immature preparation (10 ± 2.2%; $P<0.05$). As detailed above, this increase in observed facilitation was likely due to the action of presynaptic inhibitory mAChRs and consequently, from these results, it may be postulated that either a larger functional population of inhibitory mAChRs exist upon the presynaptic terminals of intrinsic fibres than L1 fibres or that the receptors present on intrinsic fibre terminals were, in some way, more effective at inhibiting excitatory synaptic transmission compared with those on L1 fibres. Additionally, the differences observed between the responses from adult and immature cells suggested a larger or more effective inhibitory mAChR population on adult presynaptic intrinsic terminals.

The PPI was also found to increase (in both recordings from adult and immature neurones) in the presence of 10 μM OXO-M compared to controls. The peak increase was found to be significantly greater in the adult (35 ± 3%; Fig. 4.13B) than the immature preparation (21 ± 1.3%; $P<0.05$; Fig. 4.14B), whilst the duration of the observed PPI was also found to be greater in the adult (~900 ms to return to a paired-pulse ratio of 1; not shown) than the immature (~600 ms; not shown) preparation. In figures 4.13B and 4.14B, a point at which the paired-pulse plots under control conditions and in the presence of OXO-M cross can be seen. It is notable that this crossover point for recordings made from immature cells occurred at a mean ISI of 223 ± 12 ms (n=21), whilst in recordings made from adult cells it occurred significantly earlier, at a mean ISI of 186 ± 16 ms (n=19; $P<0.05$; Students t-test). This demonstrated that stronger $GABA_BR$-mediated inhibitory factors are present in the adult than immature brain slice, since the facilitatory and inhibitory synaptic effects clearly equilibrate earlier in the adult. The increased PPI observed was most likely due to a combination of increased postsynaptic $GABA_BR$-mediated inhibition (as a consequence of the OXO-M-induced increase in overall excitability of the system) and the prolonged action of OXO-M upon inhibitory mAChRs on the intrinsic terminal boutons, exerting a greater inhibitory effect upon excitatory synaptic transmission in the adult than immature preparations.

4.5.3 Abolition of OXO-M induced changes in L1 and intrinsic fibre elicited paired-pulse responses by atropine in adult and immature deep pyramidal neurones

In order to confirm that the observed effects of OXO-M upon the paired-pulse results were indeed mAChR-mediated, recordings were made from adult (n=11) and immature (n=12) slices in the presence of 10 μM OXO-M plus the muscarinic antagonist, atropine (1 μM) and compared with those obtained in control conditions. No significant differences were found between the peak PPF or PPI obtained following L1 fibre stimulation in the adult preparation in control conditions and 10 μM OXO-M plus 1 μM atropine (not shown). The results plotted from responses obtained following stimulation of adult (Fig. 4.15A) and immature (Fig. 4.15B) intrinsic fibres showed the abolition of the increased PPF produced by the application of 10 μM OXO-M (*cf.* Figs. 4.13B and 4.14B) and a significant *upward shift* (adult: 17 ± 3.4%; immature: 8% ± 1.2%; $P<0.05$ for both results compared to respective controls) in the PPI section of each plot. This unexpected change could possibly be explained if atropine were blocking inhibitory presynaptic mAChRs thereby abolishing the effects (facilitatory and inhibitory) of applied OXO-M *and* also of endogenous ACh present tonically in the preparation, thereby shifting the plot upwards, beyond the values obtained under control conditions where the effects of endogenous ACh were present. The upward shift observed during the inhibitory section of the immature plot was not as great as that seen in the adult plot, which would suggest that the intrinsic inhibitory cholinergic mechanisms present in the adult preparation are more pronounced than in the immature preparation, thereby confirming our earlier results with neostigmine (Section 3.6).

4.5.4 The demonstration of endogenous cholinergic tone within the piriform cortical slice preparation using the muscarinic antagonist, atropine

The implication that a significant endogenous cholinergic '*tone*' exists within the piriform cortical slice preparation (in the absence of neostigmine) suggested by the results presented in Section 4.5.3 and the previous chapter was further investigated by comparing the paired-pulse results obtained following L1 and intrinsic fibre stimulation of adult (n=12) and immature (n=13) neurones in control conditions with equivalent results obtained in the presence of 1 μM atropine. It was hoped that this would demonstrate that the results obtained in Section 4.5.3 were truly due to an abolition of endogenous cholinergic tone and not an undocumented (nicotinic?) effect of OXO-M (Reitstetter *et al.*, 1994). In accordance with the results seen in Section 4.5.3, the

application of 1 μM atropine alone had no significant effect upon the results obtained following L1 fibre stimulation in either adult or immature recorded neurones (not shown), that would confirm that there were few, if any, presynaptic inhibitory mAChRs present on the terminals of the L1 LOT fibres, or that sufficient endogenous ACh was not released in this area of the slice to activate any presynaptic mAChRs that may have been present (Macrides *et al.*, 1981; Wenk *et al.*, 1977). However, the initial observations made above, suggesting endogenous cholinergic tone at intrinsic fibre terminals (Section 4.5.3), were confirmed. Thus, a significant reduction in peak PPI in both adult (19% ± 4.1%; Fig. 4.16A) and immature (10 ± 2.7%; Fig. 4.16B) recorded neurones was observed, a result clearly comparable with those obtained in the previous section. The greater reduction in peak PPI in the adult preparation with atropine, suggested either greater levels of tonic ACh compared to the immature preparation, a larger population of presynaptic mAChRs or more effectively-coupled mAChRs in the adult, an observation that correlates with earlier results presented showing reduced cholinergic inhibition of excitatory intrinsic fibre transmission in the immature preparation.

4.5.5 The effect of the $GABA_B$ receptor-specific antagonist upon paired-pulse responses elicited following L1 and intrinsic fibre stimulation from recorded adult and immature presumed deep pyramidal neurones

Having confirmed the novel presence of significant endogenous cholinergic tone within the piriform cortical slice preparation, the consequences of blocking another principle mediator of synaptic transmission, GABA, acting on presynaptic $GABA_BRs$, were also investigated, and any differences between the responses of the adult and immature preparations noted. $GABA_BRs$ are considered to be the primary mediators of presynaptic inhibition during the PPI phase (ISI ≥250 ms) of the paired-pulse response (Stuart & Redman, 1991) and consequently any differences in the contribution of $GABA_BRs$ to the observed L1 and intrinsic fibre-elicited responses in the adult and immature preparations might have implications upon the incidence of epileptiform bursting seen within this brain area.

Paired-pulse responses were elicited following L1 and intrinsic fibre stimulation and recorded from adult (n=13) and immature (n=15) neurones in control conditions and in the presence of the specific $GABA_BR$ antagonist CGP-52432 (1 μM) (Libri *et al.*, 1998), using the same paired-pulse protocols detailed above. Comparison of these results would hopefully provide an indication of the relative levels of endogenous

$GABA_BR$-mediated GABA-ergic tone (following the conditioning stimulus) and relative proportions of functional $GABA_BRs$ present in these areas. Paired pulse results obtained following L1 fibre stimulation to both adult and immature neurones showed no significant differences from control (not shown), indicating there are few, if any, presynaptic $GABA_BRs$ present on presynaptic excitatory L1 fibre terminals (Tang & Hasselmo, 1994). This result supports the observations made earlier (Sections 4.2.1 and 4.3.1), where a sustained depolarizing PSP following the firing of a single fast EPSP/action potential was seen. This depolarization may now be postulated to be due to a deficit of presynaptic $GABA_BR$ inhibition on these terminals. In contrast, results obtained following the stimulation of intrinsic fibres showed a significant upward shift of the peak PPI sections of both the adult ($36 \pm 5.2\%$; n=13; Fig. 4.17A) and immature ($17 \pm 2.3\%$; n=15; Fig. 4.17B) paired-pulse plots, with no change in PPF. The shift seen in recorded adult neurones was significantly larger ($P<0.01$) than that observed in recordings from immature neurones, suggesting that $GABA_BR$-mediated presynaptic inhibition is stronger in adult cells than immature cells. Also notable is the extended duration of the inhibitory period of the paired-pulse plot for the adult preparation in CGP-52432 (Fig. 4.17A) compared with the equivalent plot for the immature (Fig. 4.17B) preparation. This would suggest that adult intrinsic fibre terminals, once inhibited by GABA activation of $GABA_BRs$, remain more inhibited for longer than equivalent immature neurones (*c.f.* longer presynaptic muscarinic response in adult intrinsic fibres). Interestingly, it was also noted that suprathreshold EPSPs recorded from adult or immature neurones, elicited following intrinsic fibre stimulation in 1μM CGP-52432, displayed a sustained depolarization-phase indistinguishable from that seen in EPSPs elicited following L1 fibre stimulation in control conditions (*cf.* Fig. 4.1; 2). Additionally, the time courses of adult and immature EPSPs elicited following intrinsic fibre stimulation in the presence of 1μM CGP-52432 were not significantly different ($P>0.05$ for both adult (n=13) and immature (n=15) preparations) from the time courses of EPSPs elicited following L1 fibre stimulation in *control conditions.* The slower section of the IPSP (Fig. 4.1; 3) is known to be mediated by postsynaptic $GABA_BRs$ (Tseng & Haberly, 1988), that, in control conditions, may have contributed to the rapid repolarization of the intrinsic fibre EPSP (Fig. 4.2B), which again suggests that the sustained depolarization observed following L1 fibre stimulation in control conditions is due to a relative (*cf.* intrinsic fibres) lack of pre- and/or postsynaptic $GABA_BR$-mediated inhibition, $GABA_BR$ effectiveness or GABA-ergic interneurones in this area.

4.5.6 The kinetics of evoked EPSPs and their implications upon paired-pulse results

Rate of rise and half-width

Subthreshold EPSP kinetic variables, such as rate of rise and half-width, calculated from individual EPSPs elicited (following either L1 or intrinsic fibre stimulation in adult and immature recorded neurones) were not found to be significantly different ($P>0.05$) from one another, regardless of the conditions under which they were recorded (Table 4.1; *ie.* in control conditions, in the presence of drug *etc.*) and therefore it may be proposed that modifications made to the paired-pulse dynamics (increases or decreases in PPF or PPI) by the presence of drug were not the result of changes in postsynaptic neuronal properties (Stuart & Redman, 1991).

Variation in standard deviation of PPF values

Additionally, no significant differences were found between the standard deviations from the means of the PPF results, calculated for results obtained following L1 or intrinsic fibre stimulation and recorded from the adult or immature preparations in control conditions or in drug. This demonstrated that any observed change in PPF occurred in most neurones synapsing with the recorded cell rather than a specific subgroup (*e.g.* solely interneurones or solely superficial pyramidal neurones) of those neurones (Saar *et al.*, 1999).

Variation in decay rate between pulses

Individually-elicited PSP complexes evoked in the piriform cortical slice preparation commonly show a fast, $GABA_AR$-mediated IPSP which is in turn followed by a late, $GABA_BR$-mediated IPSP mediated by an increase in cellular K^+ conductance (Tseng & Haberly, 1988). This phenomenon was illustrated by the observation that the decay rate of the second paired-pulse EPSP (Fig. 4.18; left panel) was apparently faster than that of the conditioning pulse (or a single isolated pulse) EPSP (Fig. 4.18; right panel), indicating an increase in membrane conductance in the recorded cell during the second pulse produced by postsynaptic $GABA_BR$ activation. However, this change in conductance was not consistent, therefore unlikely to be involved with the observed changes in PPF/PPI. Thus, the mean variations in decay rate between the first and second pulses were not found to significantly differ when averaged for all experiments (*ie.* in control conditions and in drug; $P>0.05$ for all groups). These results correlate with the observations of (Barkai & Saar, 2001) whose investigation of superficial (layer 1b/II) pyramidal neurones elicited similar results. These data did not however apply to

those experiments where CGP-52432 was tested, since its $GABA_B$-antagonistic effect clearly affected this faster EPSP decay phenomenon.

4.6 Synaptic effects of neostigmine incubation

Finally, having demonstrated the presence of endogenous cholinergic tone within the piriform cortical slice preparation and that incubation with the anticholinesterase, neostigmine (20 μM) produced significant postsynaptic effects (Section 3.6.1), its effects upon excitatory postsynaptic potentials, elicited following L1 or intrinsic fibre stimulation, were also investigated to further examine the effects of endogenous ACh within the piriform cortical slice preparation. Suprathreshold EPSPs, elicited following L1 stimulation of immature (3/8 cells; Fig. 4.19A), but not adult (0/6 cells; not shown) neurones treated with 20 μM neostigmine showed a progressively increasing potentiation and prolongation, with superimposed spike firing, as neostigmine incubation time increased (to a maximum reached after ~40 minutes), although this prolongation was not to the same degree as that seen following the application of 10 μM OXO-M (Fig. 4.5B) to some immature slices and no changes in subthreshold EPSPs elicited following L1 fibre stimulation were ever seen. Subthreshold EPSPs, elicited following intrinsic fibre stimulation in the immature (not shown) and adult (Fig. 4.19B) preparations, however, were both significantly ($P<0.01$ for both groups) and progressively inhibited compared with controls, with increasing neostigmine incubation time. Adult neurones showed a mean 25 ± 4.6 % (n=6) maximal inhibition of intrinsic fibre transmission, whilst immature neurones showed a maximal inhibition of 12 ± 5.1 % (n=8). These results clearly correlate with those above (Section 4.5.4) in demonstrating the existence of significant endogenous cholinergic tone within this transverse piriform cortical slice preparation and furthermore, show that increasing endogenous cholinergic tone, with an anticholinesterase, in the immature preparation, has a greater excitatory effect than that seen in the adult preparation due to reduced intrinsic fibre inhibition and increased L1 fibre potentiation. Although established epileptiform bursting was never seen following neostigmine incubation, it is clear that the differences in mAChR synaptic sensitivity demonstrated here are integral to this phenomenon.

4.7 Discussion

This discussion deals solely with the developmental and pharmacological differences observed in evoked *excitatory postsynaptic potentials* (EPSPs); differences observed (under similar experimental conditions) in *inhibitory postsynaptic potentials* (IPSPs) are reported in Chapter 5.

Excitatory inputs to deep and superficial pyramidal cells of the piriform cortex have been shown to have three distinct origins; afferent fibres arising from the lateral olfactory tract (carrying new, odour responses from the olfactory bulb), intrinsic connections via the local axon collaterals of other pyramidal cells and association connections between pyramidal cells (via long association axons synapsing primarily with the apical dendrites of pyramidal cells) (Haberly & Bower, 1984). By contrast, inhibitory functions within the piriform cortex are considered to be primarily controlled by interneurones (Tseng & Haberly, 1988) that are activated through the axon collaterals of pyramidal cells in response to excitatory stimuli (Satou *et al.*, 1982; Satou *et al.*, 1983a; Satou *et al.*, 1983b). Control of relative synaptic strengths of the various input types have been considered for some time to be important to epileptogenesis (Ketchum & Haberly, 1993a) and the functions of learning and memory in this brain area (Barkai *et al.*, 1994; Barkai & Hasselmo, 1994; Haberly & Bower, 1989). In this present study it has been clearly demonstrated that the input type innervating recorded deep pyramidal cells has critical bearing upon the cellular response. The possible physiological significance of these results, the observed developmental variations and their possible role in the mechanisms underlying mAChR agonist-induced epileptiform burst firing are discussed below.

4.7.1 Significance of the observed variations in EPSPs evoked following L1 or intrinsic fibre stimulation

The results obtained have revealed a number of clear differences between EPSPs evoked following the stimulation of L1 fibres and those evoked by intrinsic fibre stimulation. The stimulating electrode placed in L1 primarily stimulated afferent fibres arising from the lateral olfactory tract, thereby simulating the cellular response to the receipt of new, encoded odour information. The stimulating electrode placed in layers II/III primarily stimulated intrinsic fibre connections, simulating the excitatory, associational connections between pyramidal cells of the piriform cortex (Fig. 1.3) and the inhibitory interneurones located in these layers. The PSP complexes evoked in the present study are comparable with those previously described in this brain area and have

been shown to be composed of a fast, excitatory (EPSP; glutamate receptor-mediated) with a superimposed spike and subsequent, fast ($GABA_A$ receptor-mediated Cl^- conductance) and slow ($GABA_B$ receptor-mediated K^+ conductance) inhibitory (IPSP) components (Lester *et al.*, 1988; Scholfield, 1978c; Scholfield, 1978b). The PSPs elicited following L1 fibre stimulation in control conditions also shared a number of common characteristics with PSPs elicited in a similar previous investigation of the piriform cortex, including a proportion of *'all or nothing'* synaptic responses and a prolonged depolarizing phase (Tseng & Haberly, 1989b). It has been proposed that these characteristics are necessary to produce the long latency EPSPs that are a prerequisite for effective interpretation of new olfactory information (Macrides, 1977) and also may be necessary for the maintenance of epileptiform bursting in the piriform cortex (Hoffman & Haberly, 1989b). It is also interesting to note the increased frequency with which these *'all or nothing'* responses were found to occur in the immature preparation and in the APC and PPC compared to the adult preparation and the MPC respectively that would suggest a higher probability of seizure initiation in the immature animal. These areas (Loscher *et al.*, 1995) and the immature preparation (Postlethwaite *et al.*, 1998a) have all been shown to demonstrate a greater susceptibility to epileptiform burst generation. This correlation demonstrates not only a clear link between excitatory synaptic responsiveness and epileptogenesis but also a potential link between the manner in which new odour information is received by the piriform cortex (Illig & Haberly, 2003) and epileptiform activity. EPSPs elicited following intrinsic fibre stimulation may be considered as simulating the activation of excitatory association fibres (Fig. 1.3) connecting superficial and deep pyramidal neurones within the piriform cortex (Haberly & Behan, 1983). Additionally, inhibitory interneurones may also be activated following intrinsic fibre stimulation. It is the combination of the association fibre system and inhibitory internerones that are considered primarily responsible for the integration of new odour information into memory and memory retrieval (Barkai & Hasselmo, 1997). Thus, the continuity of response characteristics of EPSPs elicited from these fibres, in control conditions, rostro-caudally along the slice preparation is indicative of similar intrinsic synaptic processes operating along the length of the piriform cortex (Ketchum & Haberly, 1993b), in direct contrast to the results found in response to L1 fibre stimulation.

4.7.2 Possible significance of the developmental variation of L1 fibre evoked responses

The results presented here have demonstrated clear differences between the kinetics of EPSPs evoked following L1 fibre stimulation in the immature preparation compared with the adult preparation. The longer time course seen in EPSPs elicited in control conditions and the higher proportion of *'all or nothing'* EPSPs recorded from immature neurones compared with adult neurones both indicate the immature preparation to be in a state of greater excitability than the adult preparation. Additionally, the greater degree of excitability, compared with the adult preparation, seen in the areas of the piriform cortex known to be more excitable (the APC and the PPC) further support the observation that the immature preparation exists in a heightened state of excitability. It has been known for some time that immature animals generally exhibit higher levels of synaptic excitability, and a number of reasons have been proposed for its existence. It is primarily considered to be required to drive synaptic growth in the young animal (Barkai *et al.*, 1994) and associated increases in synaptic plasticity (Holliday & Spitzer, 1990). Additionally, a number of studies have indicated the increased excitability to be implicated in epileptogenesis, *in vitro*, in the hippocampus (Milburn & Prince, 1993), piriform cortex (Sperber *et al.*, 1998) and also *in vivo* (Velisek *et al.*, 1995). Additionally, this increased excitability has been linked to the long term potentiation (LTP) of synaptic responsiveness. This phenomenon has previously been demonstrated, in response to mAChR activation, in the piriform cortex (Hasselmo & Barkai, 1995) and has been shown to be further enhanced by simultaneous stimulation of the afferent and intrinsic fibres (Patil *et al.*, 1998)in this brain area.

4.7.3 The consequences of mAChR activation upon synaptic transmission to deep pyramidal cells in the piriform cortex

Analysis of the results obtained from both isolated EPSPs and paired-pulse analyses have shown that synaptic transmission conducted by both afferent (L1) and intrinsic fibre systems are differentially affected following mAChR activation by OXO-M. Cholinergic effects upon L1 excitatory transmission (prolongation of PSP) were most pronounced in the immature preparation (Section 4.3; Fig. 4.5), with a considerably reduced effect seen in the adult preparation (Fig. 4.1). However, the mAChR-mediated inhibition of excitatory intrinsic fibre transmission was considerable in both preparations. Cholinergic agonists have previously been shown to selectively suppress excitatory postsynaptic potentials elicited from intrinsic (association) but not afferent

(LOT) fibres (Hasselmo & Bower, 1992) when recorded from *superficial* pyramidal neurones. This effect was postulated to allow the preferential input of new data, arising from the LOT, over existing '*memory*' type inputs controlled via the association fibre system. However, this study only examined the responses of *superficial* pyramidal neurones, that have been demonstrated to show less postsynaptic cholinergic sensitivity, both in this present study and elsewhere (Libri *et al.*, 1994), than *deep* pyramidal neurones. Thus, although comparable differences in the cholinergic modulation of synaptic transmission to superficial neurones have been observed, it is likely that the consequences of this modulation would be less pronounced in superficial cells, since the postsynaptic excitability of deep pyramidal neurones is significantly raised by mAChR activation, thereby producing a much greater potential amplification of the consequences of cholinergic synaptic modulation. The broadly diffuse cholinergic innervation of the piriform cortex, showing little point-to-point topography (Luskin & Price, 1983) is considered to arise from the horizontal limb of the diagonal band of Broca (HDB) (Eckenstein *et al.*, 1988; Macrides *et al.*, 1981; Wenk *et al.*, 1977) and although no laminar specificity of this innervation has been reported, figures showing cholineacetyltransferase and acetylcholinesterase staining (Eckenstein *et al.*, 1988; Kiss & Patel, 1992) do appear weaker in the superficial piriform cortical layers compared to the deeper layers. These gross physiological observations therefore correlate with the results obtained in this present study showing intrinsic (layer II/II) fibres to respond more strongly to cholinergic modulation than those in the more distant layer I.

A similar effect has also been described in the barrel cortex (Gil *et al.*, 1997), in which the two excitatory pathways of the neocortex were examined. Here, thalamocortical synapses mediate afferent inputs, whilst intracortical inputs mediate the recombination of existing cortical information. It was demonstrated that the intracortical synapses were suppressed by the activation of $GABA_BRs$, thalamocortical inputs by nAChR activation and both inputs were equally inhibited following mAChR activation. The visual cortex has also been shown to display comparable behaviour (Kimura *et al.*, 1999) where ACh again selectively suppressed intracortical inputs over thalamocortical inputs. Contrastingly, the glutamic acid analogue, 2-amino-4-phosphonobutyric acid, has been shown to inhibit afferent (L1) fibre transmission, but not intrinsic fibre transmission (Hasselmo & Bower, 1991). Therefore, this observed cholinergic modulation of intrinsic excitatory transmission is clearly vital in the process of interpreting and integrating new sensory stimuli into existing associative memory (Barkai & Hasselmo, 1997) in a number of systems in the CNS.

4.7.4 Developmental significance of the observed mAChR subtype '*switch*'.

In this present study, it has been demonstrated for the first time that there exists a developmental variation in intrinsic excitatory fibre sensitivity to mAChR activation. The reduced degree of mAChR-mediated suppression of intrinsic excitatory transmission seen in the immature compared to the adult preparation has a number of implications upon learning, memory and epileptogenesis in the immature animal. As stated above, in the adult preparation, the preferential inhibition of intrinsic fibre transmission following mAChR activation has been proposed to enhance associative memory performance (Hasselmo *et al.*, 1992) by shifting input dominance from intrinsic to afferent input. This permits deep and superficial pyramidal cells to preferentially accept information from the LOT rather than intrinsic, modulatory inputs. This enhances the response to new stimuli rather than to existing, entrenched pathways. Thus, new sensory stimuli are given a greater probability of affecting the neuronal circuitry than modulatory stimuli arising from existing pathways, a factor considered vital in the modification of associative memory(Barkai & Saar, 2001; Hasselmo & Bower, 1993; Loscher & Ebert, 1996; Patil & Hasselmo, 1999). However, in the case of the immature animal, three critical factors differentiate it from the '*normal*' adult state following mAChR activation. Firstly, afferent (L1) excitatory transmission, already more prolonged in control, is further prolonged, thus increasing the strength of afferent input to the target neurone. Secondly, intrinsic fibre excitatory transmission is less inhibited than in the adult, further raising the excitatory drive to pyramidal neurones. Finally, as was demonstrated in Chapter 3, deep pyramidal neurones show a far greater response to postsynaptic mAChR activation than superficial pyramidal neurones, with immature deep pyramidal neurones showing a greater response than their adult counterparts. Thus, the immature deep pyramidal neurone, following mAChR activation receives enhanced afferent excitatory inputs (a larger proportion of which are *'all or nothing'*, thereby further raising the excitatory drive), and has not had transmission arising from intrinsic fibres appropriately down-regulated, therefore is in a highly excitable postsynaptic state that will grossly amplify incoming excitatory signals. It is likely that, as stated previously, this state of heightened excitability is used to drive synaptic growth and improve the efficiency of associative memory in the immature animal. However, as has been demonstrated in this study, this also places the immature piriform cortex in a state where spontaneous epileptiform burst behaviour occurs. It has also been demonstrated that the reason for the observed variation in cholinergic responsiveness between the immature and adult animals is a change in the presynaptic

mAChR subtype present on excitatory intrinsic fibre terminals from M2 in the immature animal to M1 in the adult, with an associated *increase* in inhibitory efficacy. Since the postsynaptic response to OXO-M varies little with increasing age and is mediated by the M1 mAChR subtype (Chapter 3) and the incidence of OXO-M-induced bursting activity gradually decreases with age, it is likely that there is a gradual move from M2 to M1 between P+14 and P+30 rather than a rapid '*switch*' at a certain age, thereby implicating this distinct piriform cortical synaptic circuitry in the observed seizure phenomenon. Other studies (Araki *et al.*, 1996; Milburn & Prince, 1993) have demonstrated comparable time courses of increasing cholinergic activity within other areas of the rat brain, although this is the first time a clear change in mAChR subtype has been demonstrated pharmacologically, with corresponding functional changes and implications for generating an epileptic disease state.

4.7.5 Significance of EPSP variations with location within the piriform cortical slice preparation

Although no obvious variations in EPSPs elicited following intrinsic fibre stimulation (in control conditions or in the presence of 10 μM OXO-M) were observed with rostro-caudal variation of the recording electrode position, the clear variations seen in this present study, following L1 fibre stimulation, have a number of functional implications. As previously discussed (Section 3.4.3), the location of the recorded cell within the piriform cortical slice preparation has a considerable effect upon its postsynaptic responsiveness and susceptibility to OXO-M-induced epileptiform bursting. A previous study using simultaneous paired-cell recording (Hoffman & Haberly, 1991a) has showed that deep pyramidal neurones were responsible for the initiation and maintenance of bursting behaviour in a Mg^{2+}-free *in vitro* model of epileptiform behaviour in the piriform cortex, whilst a number of other *in vitro* studies have demonstrated potentiated extracellular field potentials in the APC and PPC that clearly correlate with the potentiated EPSPs seen following L1 fibre stimulation in the present study (Biella *et al.*, 1996; de Curtis *et al.*, 1996). It has been suggested that both the APC and PPC are more closely involved with associative memory function than the MPC, that has been proposed to retain greater responsibility for the integration of new odour information (Zinyuk *et al.*, 2001). This associative memory function requires greater synaptic plasticity than integrative function, which correlates well with the current observations showing increased L1 *'all or nothing'* EPSPs and increased EPSP prolongation, factors strongly linked to associative memory function (Macrides, 1977)

and epileptiform activity (Hoffman & Haberly, 1989a). Once again, it is clear that the observed variation in developmental sensitivity to mAChR activation seen in the present study produced amplified responses in the APC and the PPC due to the inherent structure of their synaptic circuitry, being more prone to developing epileptiform characteristics following an increase in excitability. Given this understanding of the synaptic circuitry of the piriform cortex, this may further explain the discrepancy observed between the incidence of muscarinic burst firing seen in this present study and a previous study that used essentially the same experimental conditions (Postlethwaite *et al.*, 1998a).

4.7.6 Observed variation in endogenous cholinergic tone between adult and immature piriform cortical brain slices

Results presented in Chapter 3 demonstrated for the first time the presence of endogenous cholinergic tone within the piriform cortical slice preparation used in these experiments, when incubation with the anticholinesterase, neostigmine (20 μM) produced a clear increase in postsynaptic excitability. In this chapter, application of the muscarinic antagonist, atropine (1 μM) produced significant shifts in the paired-pulse ratios recorded from adult and immature neurones away from control values, indicating an endogenous cholinergic tone without the need to artificially raise ACh levels with neostigmine. Additionally, incubation with 20 μM neostigmine produced effects upon synaptic transmission that were consistent with increased ACh levels and weakly imitating the effects of applied OXO-M.

4.7.7 Functional implications of the observed developmental variation in $GABA_BR$-mediated responses

Application of the $GABA_BR$-specific antagonist, CGP-52432 (1 μM) produced a significant decrease in PPI in the adult and, to a lesser degree, in the immature preparations. One of the principle mechanisms controlling the degree of PPI is the GABA-mediated activation of presynaptic $GABA_BRs$, resulting in decreased Ca^+ conductance and, therefore, inhibition of transmission. The results of this present study clearly showed that there exists a reduced level of presynaptic $GABA_BR$-mediated inhibition in the immature preparation, compared to the adult that produced an overall increase in excitability. It was also shown that EPSPs recorded from adult and immature neurones evoked following L1 fibre stimulation produced little $GABA_BR$-mediated inhibition. This result would explain the sustained depolarization that characterized suprathreshold EPSPs evoked following L1 fibre stimulation in this preparation. These

results are consistent with previously reported surface field potential recordings from piriform cortical brain slices (Collins *et al.*, 1982; Collins & Howlett, 1988) where the $GABA_BR$ agonist, baclofen was shown to have no effect upon early N-waves, whilst suppressing the late N-wave and the inverted P-wave. The early N-wave was tentatively proposed to represent the depolarization of the apical dendrites of pyramidal neurones following afferent fibre activation and the late-N and P-waves, activation following association (intrinsic) fibre stimulation, clearly correlating with the effects reported in the present study and confirming the hypothesis of Collins *et al.* (1992). Additionally, another extracellular field potential study demonstrated that baclofen selectively suppressed intrinsic, but not afferent excitatory synaptic transmission in the piriform cortex (Tang & Hasselmo, 1994), in support of the present data. Our results therefore not only correlate with existing reports on $GABA_BR$-mediated differences in excitatory synaptic transmission in the piriform cortex, but once again, a clear difference in developmental sensitivity has been demonstrated that, by virtue of its reduction of local GABA-ergic presynaptic inhibition, is like to promote convulsive activity in this brain area.

4.8 Summary

1. Suprathreshold EPSPs elicited in control conditions, by afferent fibre stimulation from adult and immature slices were found to have significantly longer time courses than those elicited following intrinsic fibre stimulation.
2. The time course of suprathreshold afferent-evoked EPSPs in immature slices were significantly longer than those evoked in adult slices in control conditions.
3. A proportion of afferent-evoked suprathreshold EPSPs in both adult and immature slices provided *'all or nothing'* responses. The incidence of this response type was significantly greater in the immature preparation than the adult.
4. In OXO-M, adult afferent-evoked suprathreshold EPSPs were further prolonged and displayed occasional afterpotential spikes, whilst adult intrinsic-evoked suprathreshold EPSPs were consistently inhibited.
5. In OXO-M, the majority of immature afferent-evoked suprathreshold EPSPs exhibited significant prolongation of the depolarised phase of the PSP (greater than that seen in the adult) with superimposed repetitive spike firing. The remaining proportion of afferent-evoked EPSPs were indistinguishable from those evoked from adult slices. Both sub- and suprathreshold immature intrinsic-evoked EPSPs were inhibited by OXO-M, by a significantly smaller degree than seen in the adult preparation.
6. OXO-M-induced inhibition of intrinsic excitatory synaptic transmission was mediated by the M1 presynaptic mAChR subtype in the adult preparation and by the M2 presynaptic mAChR subtype in the immature preparation.
7. A significantly larger number of both adult and immature EPSPs evoked, following afferent fibre stimulation, from the anterior and posterior piriform cortex exhibited epileptogenic characteristics (superimposed spike firing, prolonged depolarising phase *etc.*) compared with those evoked in the median piriform cortex.
8. The presynaptic action of OXO-M to produce inhibition of intrinsic excitatory synaptic transmission was confirmed using paired-pulse analysis.
9. Paired-pulse analysis was also used to reveal the presence of native endogenous cholinergic tone within the slice preparation.
10. Paired-pulse analysis revealed reduced postsynaptic $GABA_BR$-mediated inhibition following afferent fibre stimulation that may have given rise to the observed prolongation of the depolarized phase of the PSP.

11. $GABA_BR$-mediated inhibition following intrinsic fibre stimulation was relatively diminished in the immature preparation compared with the adult.
12. Incubation of immature slices with the anticholinesterase, neostigmine, revealed a number of epileptogenic synaptic characteristics in afferent-evoked EPSPs (superimposed spike firing, prolonged depolarised phase *etc.*), whilst intrinsic-evoked EPSPs were consistently inhibited, although not to the same degree as seen in OXO-M.

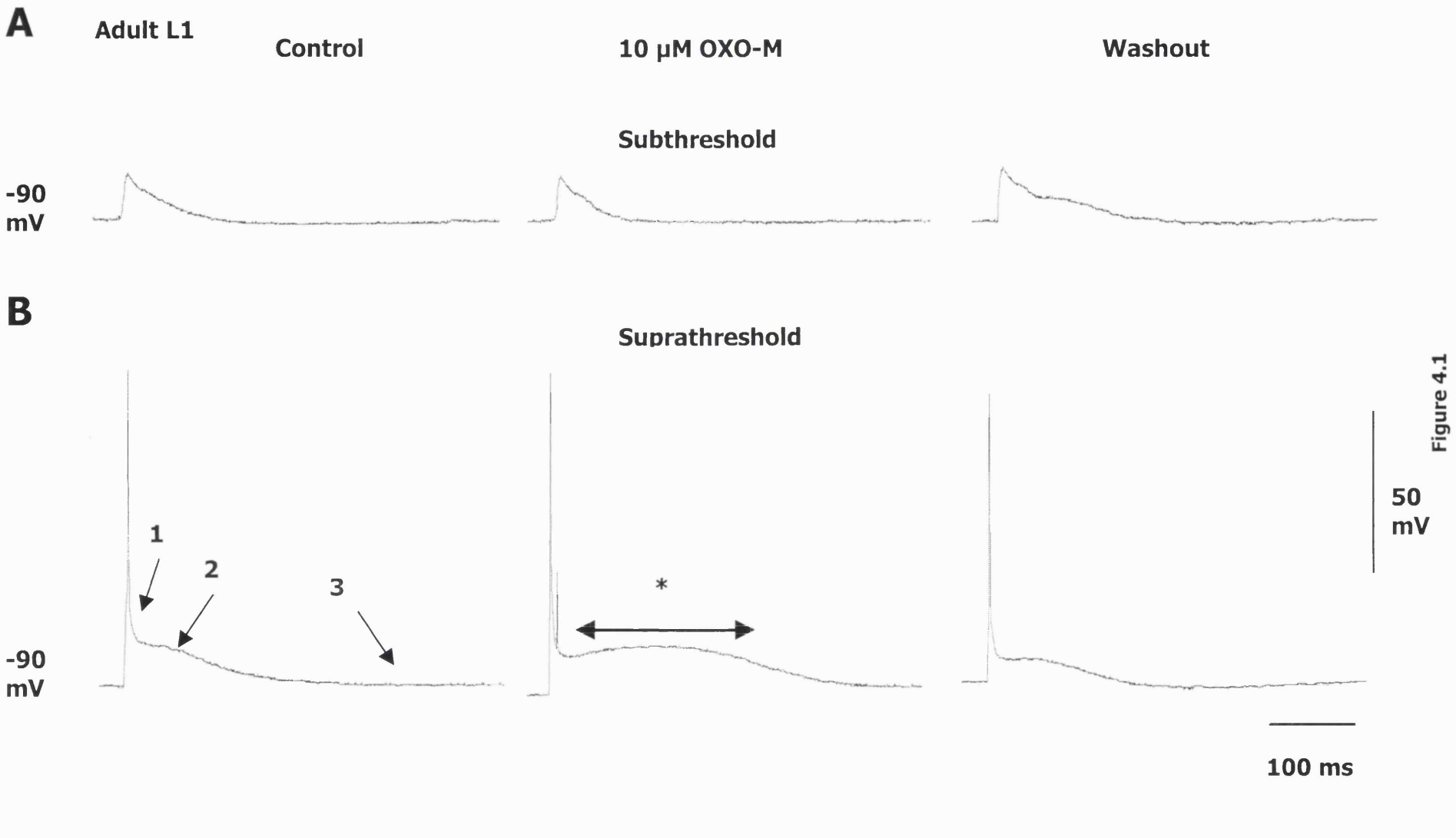
A
Adult L1
Control
10 µM OXO-M
Washout
Subthreshold
-90
mV
B
Suprathreshold
1
2
3
*
-90
mV
50
mV
100 ms

Figure 4.1

Figure 4.1

Sub- and suprathreshold EPSPs elicited by a fine stimulating electrode situated in layer I (L1) of an adult piriform cortical slice and recorded from a presumed deep pyramidal neurone in control conditions (**left panels**), 30 mins following the application of 10 μM OXO-M (**middle panels**) and after 40 mins washout (**right panels**). **Top panel** shows subthreshold (no elicited action potential) EPSPs following a single 7 V, 0.2 ms stimulus. **Bottom panel** shows suprathreshold (eliciting an action potential) EPSPs elicited from the same neurone following a 9 V, 0.2 ms stimulus. These traces represent individual EPSPs **not** averages of three traces. Cell resting membrane potential = -82 mV, held at -90 mV by the injection of steady negative current during EPSP recording. (**1**), (**2**) and (**3**) indicate the excitatory, fast inhibitory and slow inhibitory components of the PSP respectively (Section 4.2). OXO-M had little or no effect on subthreshold EPSPs (**top panel**), but prolonged suprathreshold EPSPs (*; **bottom panel**) in this cell. This effect was not seen in subthreshold potentials, suggesting that action potential firing may be a prerequisite for this phenomenon.

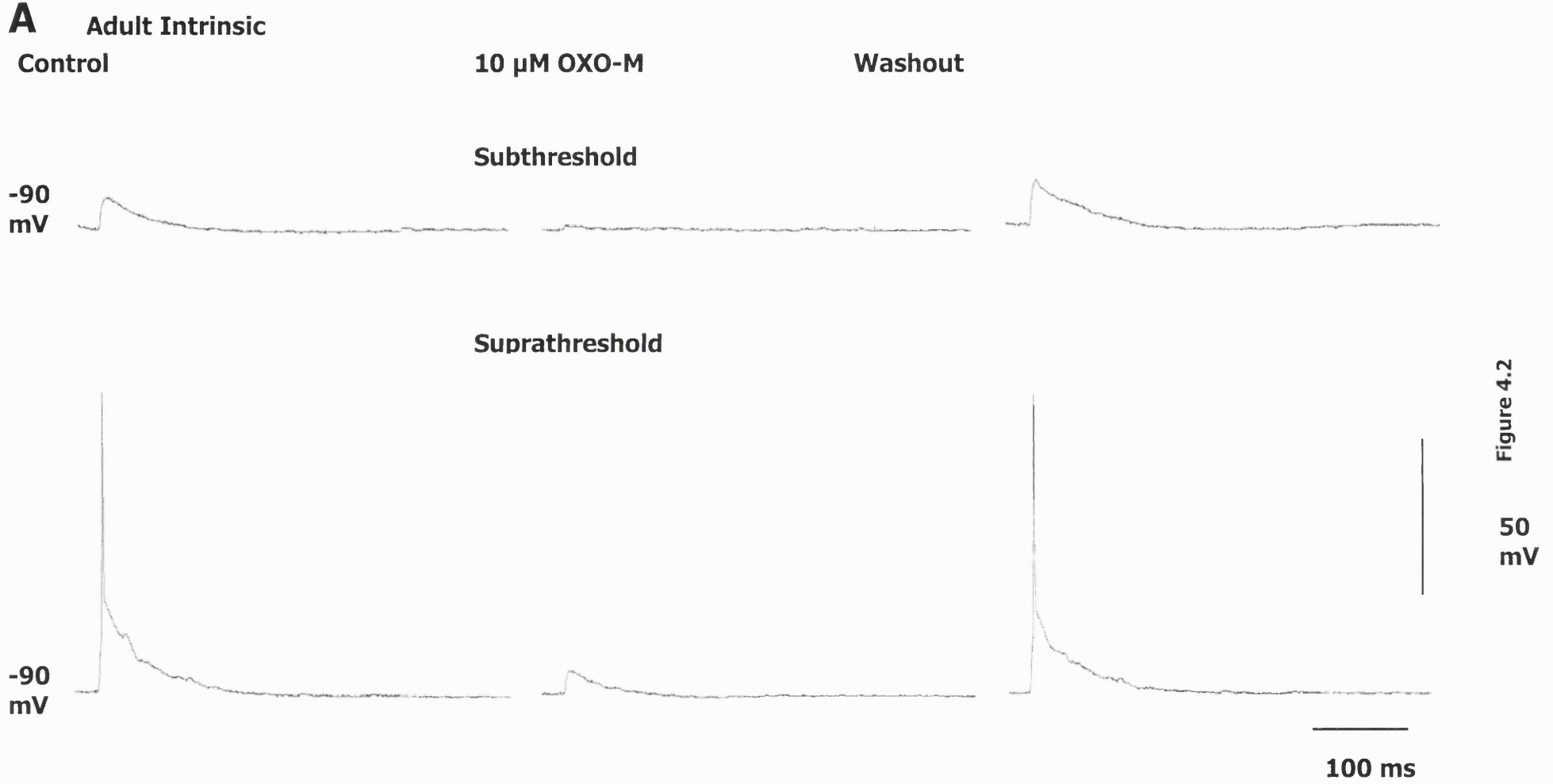
A
Adult Intrinsic
Control
10 µM OXO-M
Washout
Subthreshold
-90
mV
Suprathreshold
-90
mV
50
mV
100 ms

Figure 4.2

Figure 4.2

Sub- and suprathreshold EPSPs elicited by a fine stimulating electrode situated in layer II/III (intrinsic) of an adult piriform cortical slice and recorded from the same presumed deep pyramidal neurone as Figure 4.1, in control conditions (**left panels**), 30 mins following the application of 10 μM OXO-M (**middle panels**) and after 40 mins washout (**right panels**). **Top panel** shows subthreshold (no elicited action potential) EPSPs following a single 12 V, 0.2 ms stimulus. **Bottom panel** shows suprathreshold (eliciting an action potential) EPSPs elicited from the same neurone following an 18 V, 0.2 ms stimulus. Cell resting membrane potential = -82 mV, held at -90 mV by the injection of steady negative current during EPSP recording. OXO-M clearly inhibited both sub- and suprathreshold EPSPs. This effect appears to be the opposite of that seen on suprathreshold EPSPs following L1 stimulation in OXO-M (Fig 4.1).

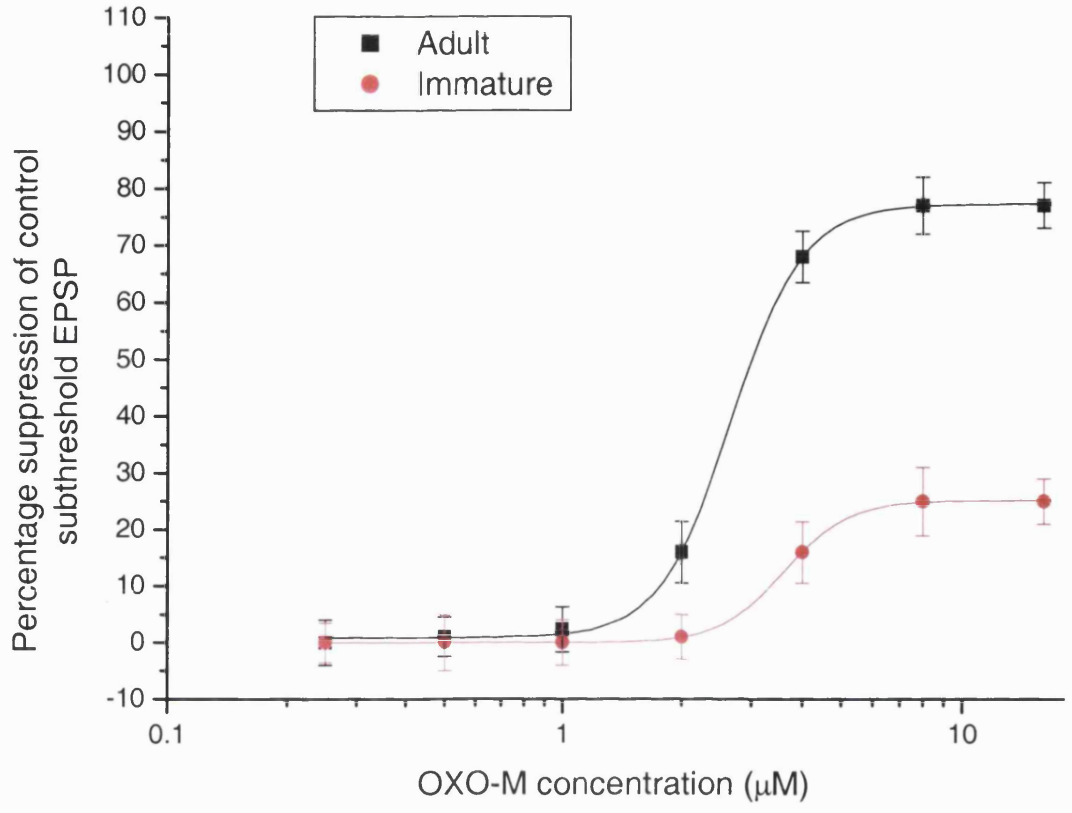
Adult
Immature
Percentage suppression of control subthreshold EPSP
110
100
90
80
70
60
50
40
30
20
10
0
-10
0.1
1
10
OXO-M concentration (μM)

Figure 4.3

Figure 4.3

A log dose-response plot showing the effect of varied concentrations of OXO-M (0.5 - 16 μM) upon EPSP magnitude elicited following subthreshold intrinsic fibre stimulation in adult (**black**; n=65) and immature (**red**; n=136) neurones. Data are means ± SEM. Response is shown as the percentage by which the subthreshold EPSP is suppressed compared to control EPSP amplitude for each concentration of OXO-M used. Calculated ED_{50}s were: adult=2.6 μM; immature=3.6 μM. Curves were fitted using a least squares fit equation and calculated mean confidence intervals for each data set (adult=96%; immature=94%). One-way ANOVA significance tests showed a significant difference ($P<0.05$) between the adult and immature ED_{50} values. Curve fitting, confidence intervals and significance test were performed by Origin plotting and analysis software (Microcal Inc, MA, USA).

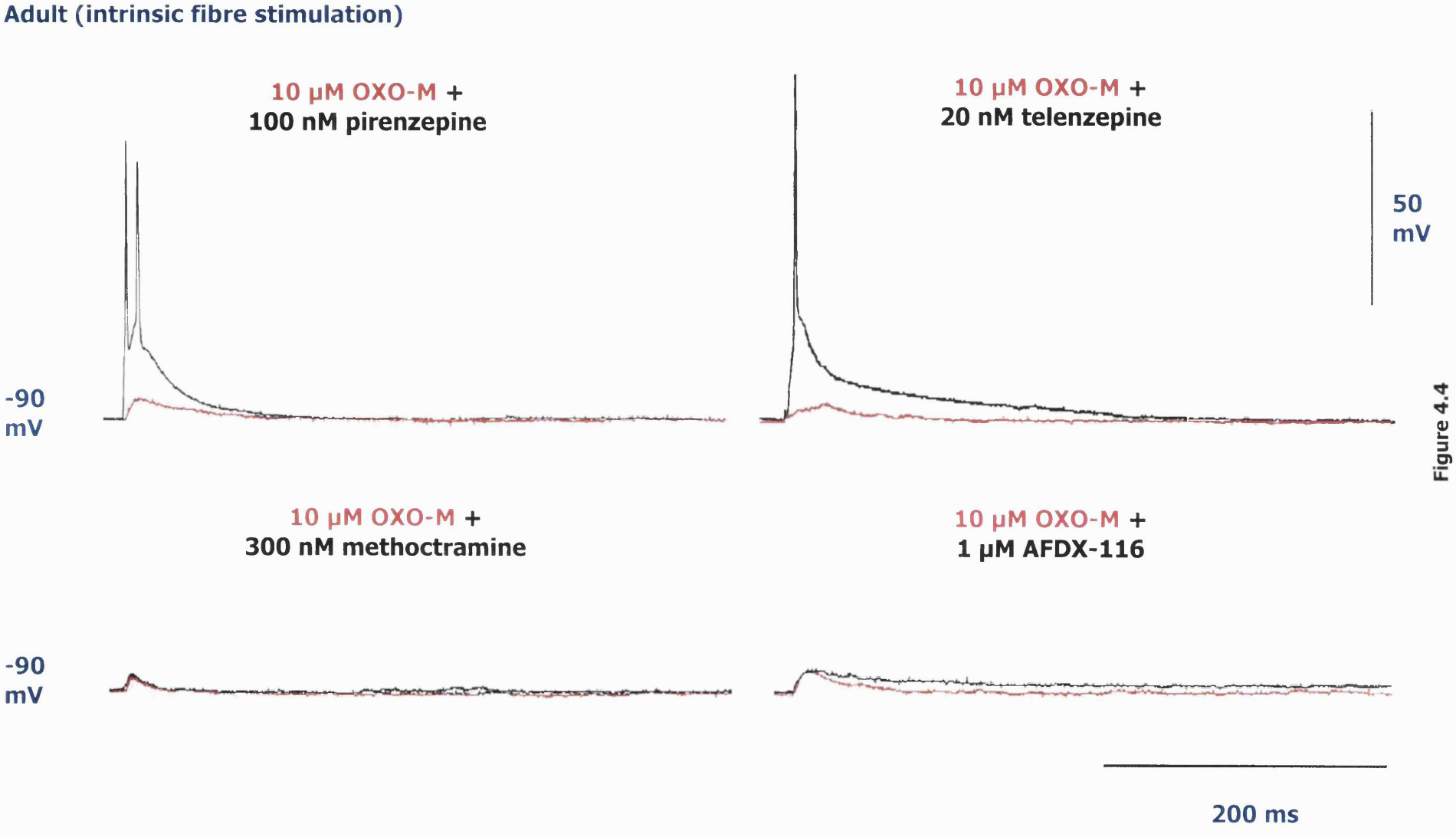
Adult (intrinsic fibre stimulation)
10 µM OXO-M +
100 nM pirenzepine
10 µM OXO-M +
20 nM telenzepine
50
mV
-90
mV
10 µM OXO-M +
300 nM methoctramine
10 µM OXO-M +
1 µM AFDX-116
-90
mV
200 ms

Figure 4.4

Figure 4.4

EPSPs elicited by a stimulating electrode situated in layer II/III (intrinsic) of ***adult*** piriform cortical slices recorded from presumed deep pyramidal neurones, illustrating the effect of subtype-specific mAChR antagonists upon OXO-M-induced inhibition of intrinsic synaptic transmission. Responses in the presence of 10 μM OXO-M are shown in **red**, whilst responses in the presence of OXO-M *plus* a selective antagonist are shown in **black**. (**Top left panel**) 10 μM OXO-M alone and OXO-M plus 100 nM pirenzepine (M1-specific mAChR antagonist; 3 V, 0.2 ms; cell resting membrane potential= -83 mV). (**Top right panel**) 10 μM OXO-M and OXO-M plus 20 nM telenzepine (M1-specific mAChR antagonist; 2 V, 0.2 ms; cell resting membrane potential= -83 mV). (**Bottom left panel**) 10 μM OXO-M and OXO-M plus 300 nM methoctramine (M2-specific mAChR antagonist; 3 V, 0.2 ms; cell resting membrane potential= -83 mV). (**Bottom right panel**) 10 μM OXO-M and OXO-M plus 1 μM AFDX-116 (M2-specific mAChR antagonist; 2 V, 0.2 ms; cell resting membrane potential=-83 mV). All cells were held at -90 mV by the injection of steady negative current during EPSP recording. mAChR agonist-induced inhibition of intrinsic synaptic transmission was clearly demonstrated to be mediated by the M1 mAChR subtype in the adult slice preparation (*cf.* Fig. 4.8).

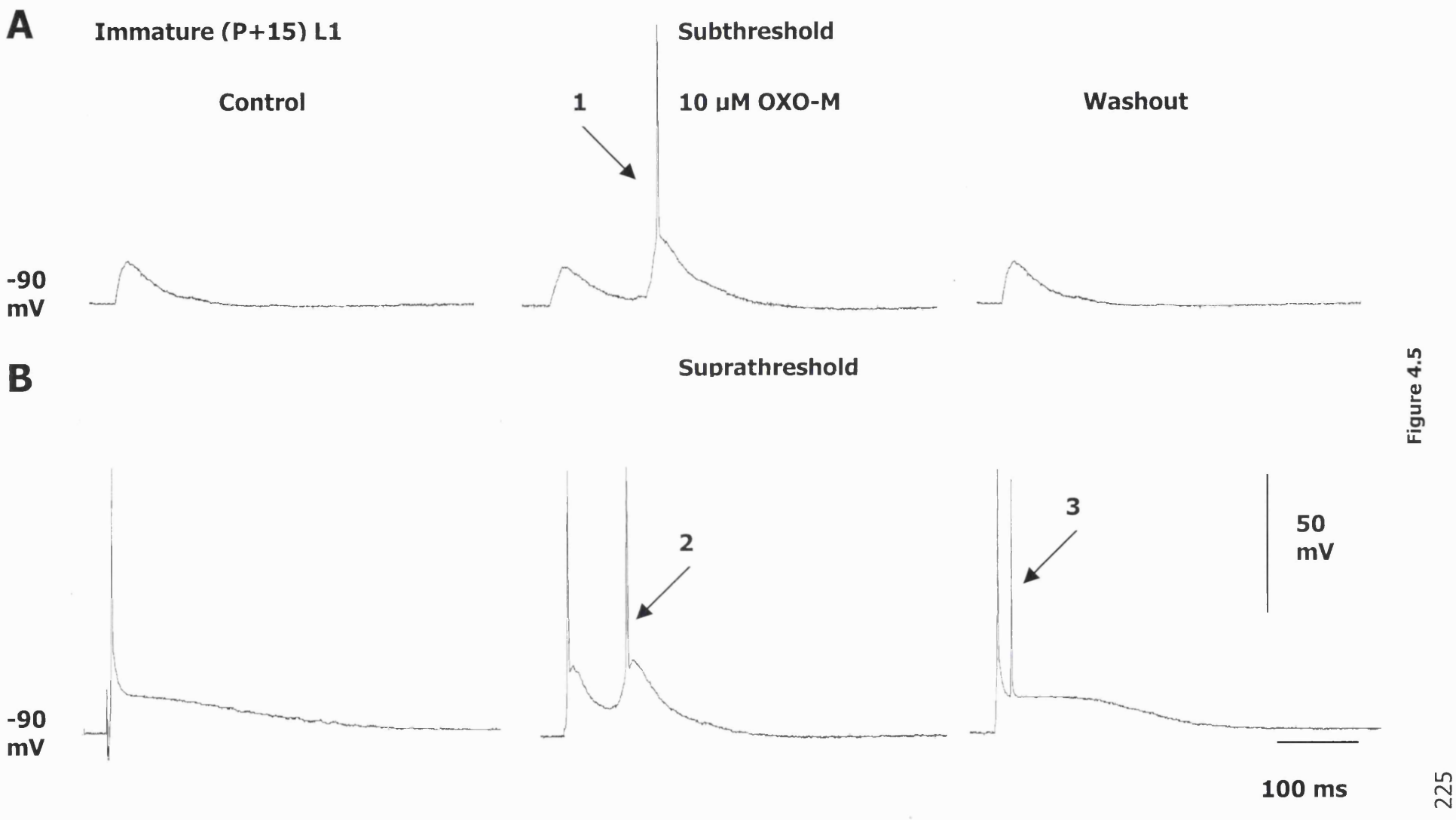
A
Immature (P+15) L1
Subthreshold
Control
1
10 µM OXO-M
Washout
-90
mV
B
Suprathreshold
2
3
50
mV
-90
mV
100 ms

Figure 4.5

Figure 4.5

Sub- and suprathreshold EPSPs elicited by a stimulating electrode situated in layer I (L1) of an immature (P+15) piriform cortical slice and recorded from a presumed deep pyramidal neurone in control conditions (**left panels**), 30 mins following the application of 10 μM OXO-M (**middle panels**) and after 40 mins washout (**right panels**). **Top panel** shows subthreshold (no action potential in control conditions) EPSP following a single 4 V, 0.2 ms stimulus. **Bottom panel** shows suprathreshold (eliciting an action potential in control) EPSP elicited from the same neurone following a 6 V, 0.2 ms stimulus. Cell resting membrane potential=-82 mV. The cell was held at -90 mV by negative current injection. Note the multiphasic EPSP and superimposed action potential following a subthreshold stimulus in OXO-M (**1**) and the same phenomenon following a suprathreshold stimulus (**2**). This clearly suggested a facilitation of afferent (L1) synaptic transmission by OXO-M that (seen to a lesser extent in the adult; Fig. 4.1), that is sufficient to induce repetitive spike firing in the immature preparation. (**3**) shows a small superimposed spike following an initial action potential that was frequently observed in immature cells following washout of OXO-M. The traces in this figure represent individual EPSPs, not averages of three traces.

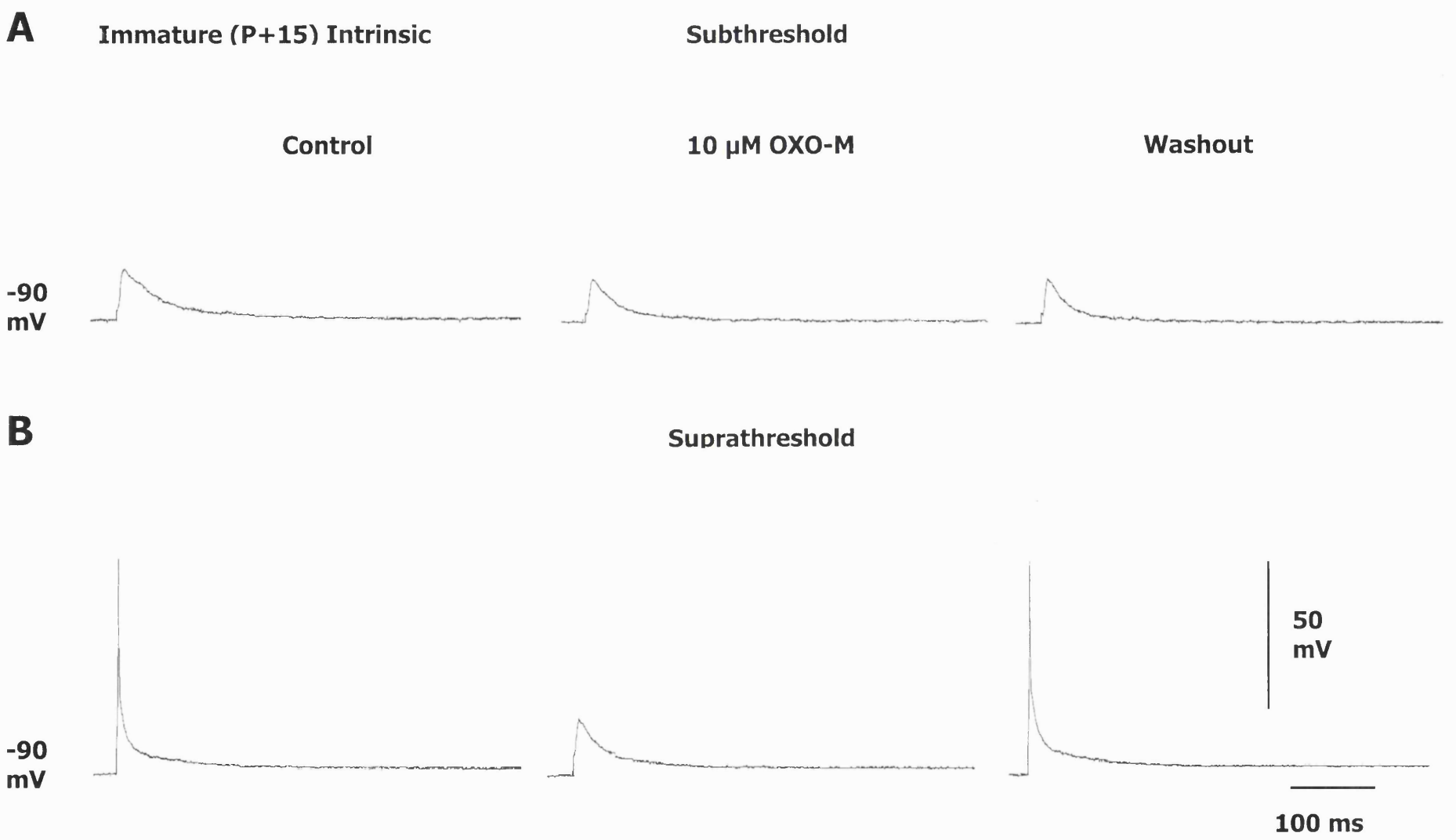
A
Immature (P+15) Intrinsic
Subthreshold
Control
10 µM OXO-M
Washout
-90
mV
B
Suprathreshold
50
mV
-90
mV
100 ms

Figure 4.6

Figure 4.6

Sub- and suprathreshold EPSPs elicited by a stimulating electrode situated in layer II/III (intrinsic) of an immature (P+15) piriform cortical slice and recorded from the same presumed deep pyramidal neurone as Figure 4.5, in control conditions (**left panels**), following the application of 10 μM OXO-M (**middle panels**) and after 40 mins washout (**right panels**). **Top panel** shows subthreshold (no action potential in control conditions) EPSPs following a single 4 V, 0.2 ms stimulus. **Bottom panel** shows suprathreshold (eliciting an action potential in control) EPSPs elicited from the same neurone following a 6 V, 0.2 ms stimulus. Resting potential=-82 mV, held at -90 mV by steady negative current injection. OXO-M slightly inhibited both sub- and suprathreshold EPSPs, but not to the same degree as that seen in the adult preparation (Fig 4.2).

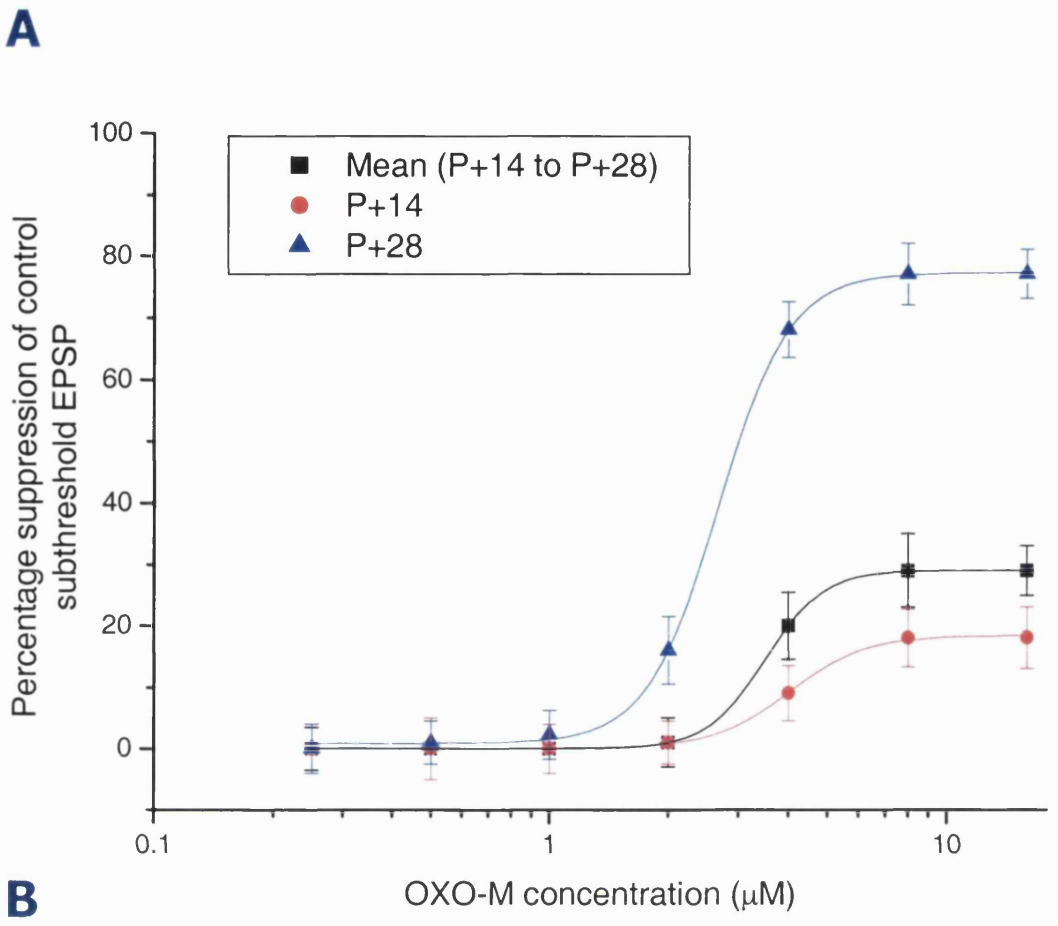
A
100
80
60
40
20
0
Percentage suppression of control subthreshold EPSP
Mean (P+14 to P+28)
P+14
P+28
0.1
1
10
OXO-M concentration (μM)
B
Intrinsic stimulation
Adult
Immature (P+16)
-90 mV
10 mV
200 ms

Figure 4.7

Figure 4.7

A. Log dose-response plots showing the effect of varied concentrations of OXO-M (0.5-16 μM) upon EPSP magnitude elicited following subthreshold intrinsic fibre stimulation in P+14 (**red**; n=7; ED_{50}=4.1 μM) and P+28 (**blue**; n=8; ED_{50}=2.6 μM) neurones. The mean response of all immature (P+14 to P+28; n=136; even distribution of ages; ED_{50}=3.6 μM) neurones is shown in **black**. Response is shown as a percentage of the maximal suppression of intrinsic fibre excitatory transmission induced by OXO-M to produce equivalent curves despite OXO-M producing a smaller maximal inhibitory effect in the P+14 slice preparation than the P+28 preparation. Curves were again fitted using a least squares fit equation and calculated mean confidence intervals for each data set (P+14=97%; P+28e=91%; mean (P+14 to P+28)=97%). One-way ANOVA significance tests showed significant differences ($P<0.05$) between all three ED_{50} values. Curve fitting, confidence intervals and significance test were performed by Origin plotting and analysis software (Microcal Inc, MA, USA). **B.** Subthreshold EPSPs elicited by a stimulating electrode situated in layer II/III (intrinsic) of adult (**left panel**) and immature (P+16; **right panel**) piriform cortical slices recorded from typical presumed deep pyramidal neurones. Responses in control conditions are indicated in **black**, whilst responses in the presence of 10 μM OXO-M are shown in **red**. Note the greater suppression of intrinsic synaptic transmission shown in the adult preparation compared to the immature. Curves were fitted using an arbitrary logistical equation provided by Origin plotting software (Microcal Inc, MA, USA).

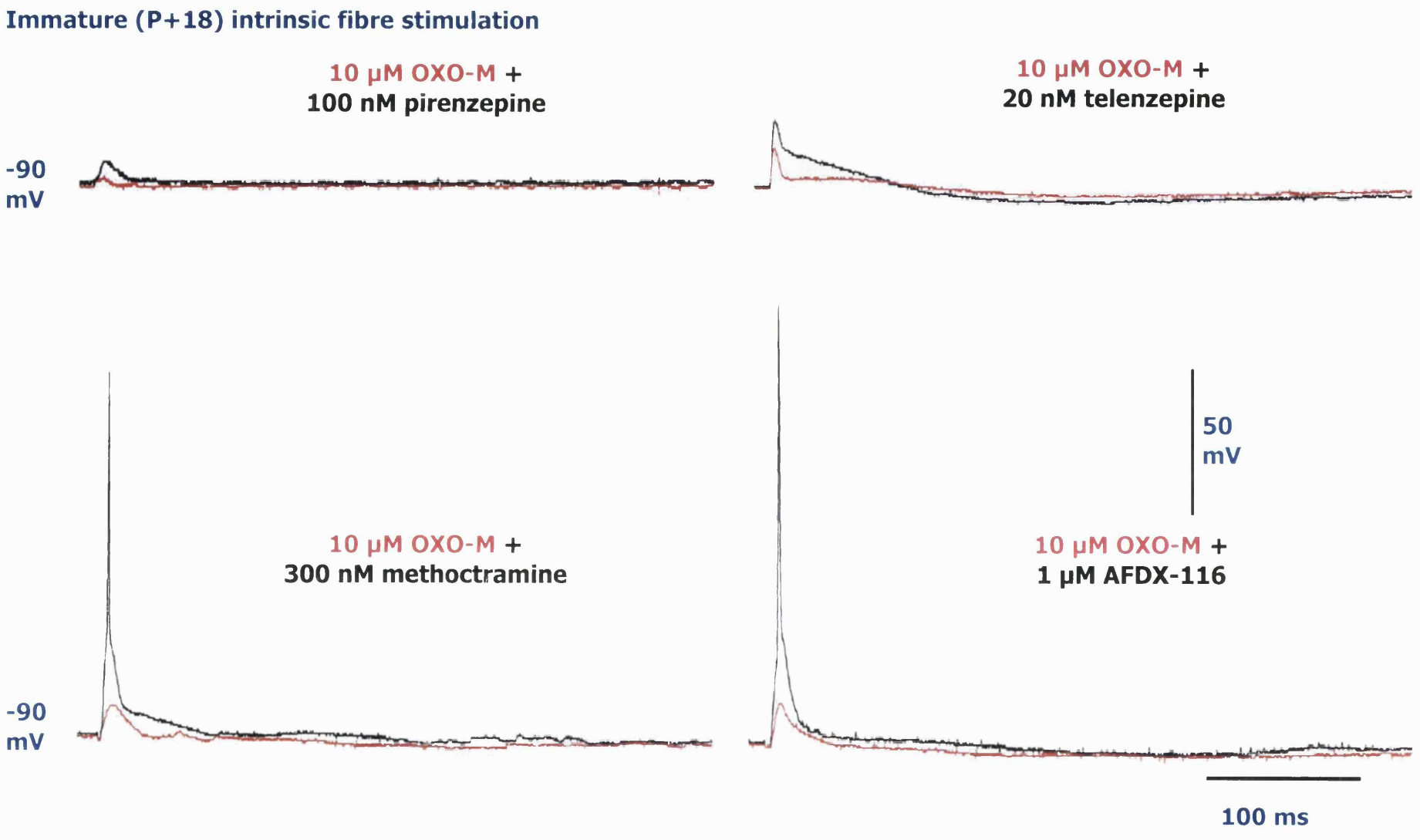
Immature (P+18) intrinsic fibre stimulation
10 µM OXO-M +
100 nM pirenzepine
10 µM OXO-M +
20 nM telenzepine
-90
mV
50
mV
10 µM OXO-M +
300 nM methoctramine
10 µM OXO-M +
1 µM AFDX-116
-90
mV
100 ms

Figure 4.8

Figure 4.8

EPSPs elicited by a stimulating electrode situated in layer II/III (intrinsic) of ***immature*** piriform cortical slices and recorded from presumed deep pyramidal neurones, showing the effect of subtype-specific mAChR antagonists upon OXO-M-induced inhibition of intrinsic synaptic transmission. Responses in the presence of 10 μM OXO-M alone are indicated in **red**, whilst responses in the presence of OXO-M *plus* a selective antagonist are shown in **black**. (**Top left panel**) OXO-M and OXO-M plus 100 nM pirenzepine (M1-specific mAChR antagonist; 3 V, 0.2 ms stimulus; Resting potential=-81 mV; P+17). (**Top right panel**) OXO-M and OXO-M plus 20 nM telenzepine (M1-specific mAChR antagonist; 2 V, 0.2 ms stimulus; Resting potential=-82 mV; P+19). (**Bottom left panel**) OXO-M and OXO-M plus 300 nM methoctramine (M2-specific mAChR antagonist; 3 V, 0.2 ms stimulus; Resting potential=-82 mV; P+17). (**Bottom right panel**) OXO-M and OXO-M plus 1 μM AFDX-116 (M2-specific mAChR antagonist; 2 V, 0.2 ms stimulus; Resting potential=-82 mV; P+19). Cells were held at -90 mV by steady negative current injection. mAChR agonist-induced inhibition of intrinsic synaptic transmission was clearly observed to be mediated by the M2 mAChR subtype in the immature slice preparation, unlike the adult preparation, in which the M1 subtype was found to be responsible (*cf.* Fig. 4.4)

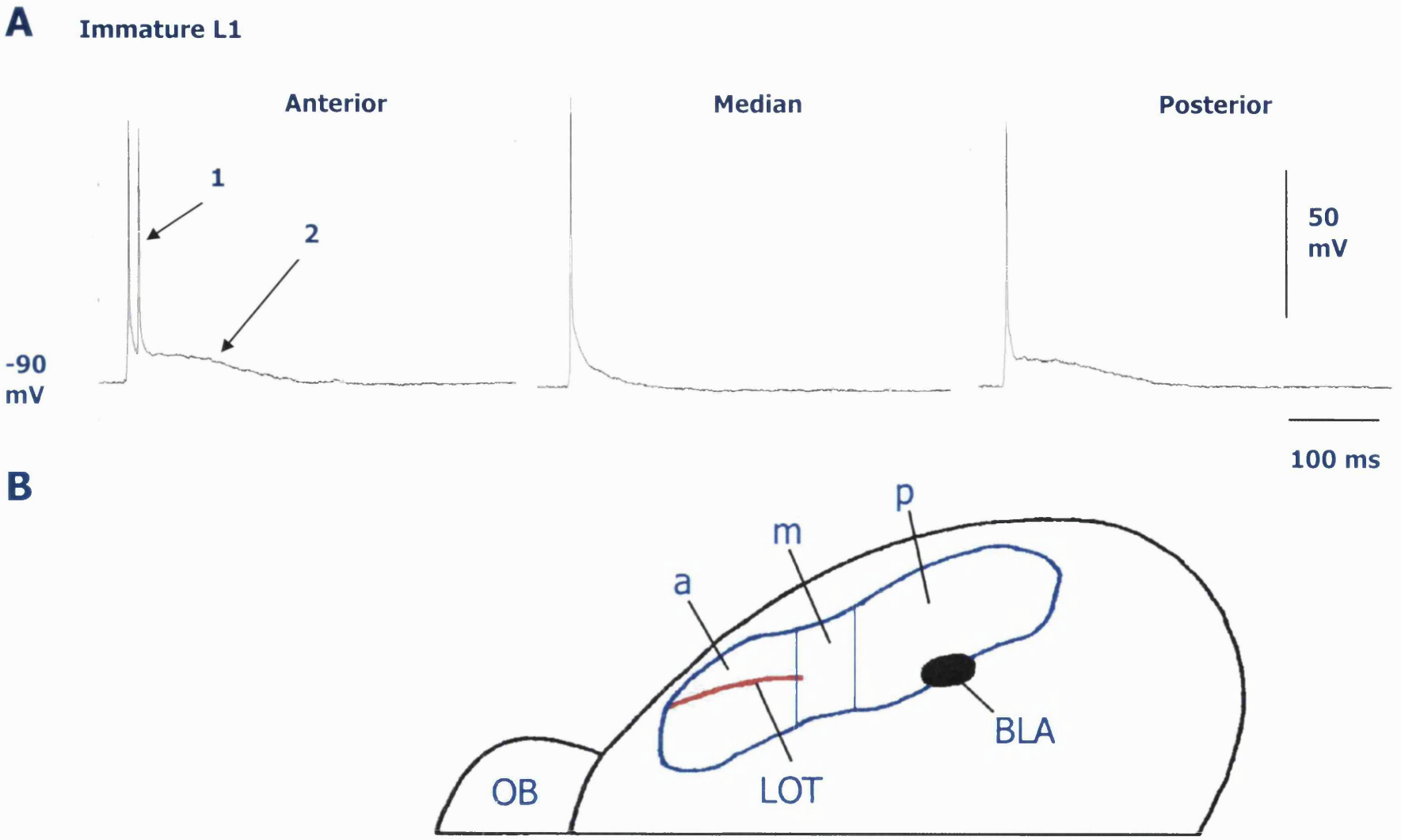
A
Immature L1
Anterior
Median
Posterior
1
2
-90
mV
50
mV
100 ms
B
p
m
a
BLA
OB
LOT

Figure 4.9

Figure 4.9

A. Suprathreshold EPSPs elicited by a stimulating electrode situated in layer I (L1) of immature piriform cortical slices from three recorded presumed deep pyramidal neurones. The **left panel** shows the response of a typical recorded cell located in layer III of the anterior piriform cortex (APC; Resting potential=-83 mV), the **middle panel**, a recorded cell in layer III of the median piriform cortex (MPC; Resting potential=-82 mV) and the **right panel**, a recorded cell in layer III of the posterior piriform cortex (PPC; Resting potential=-83 mV). Cells were held at -90 mV by injection of steady negative current. Traces shown were recorded from different neurones. Note the superimposed spike firing seen in the EPSP recorded from the anterior cell (**1**) and the sustained depolarization (**2**; also seen in the posterior cell). Note the absence of these phenomena from the median cell. **B.** Illustration of a dorsal view of the brain, hemisected along the midline, showing the location of the piriform cortical areas. **Key:** **[OB]** – olfactory bulb; **[LOT]** – lateral olfactory tract; **[BLA]** – basolateral amygdala; **[a]** – anterior; **[m]** – median; **[p]** – posterior. These illustrations were adapted from (Loscher & Ebert, 1996) with definitions delineating anterior, median and posterior areas from those described by Haberly (Haberly & Price, 1978).

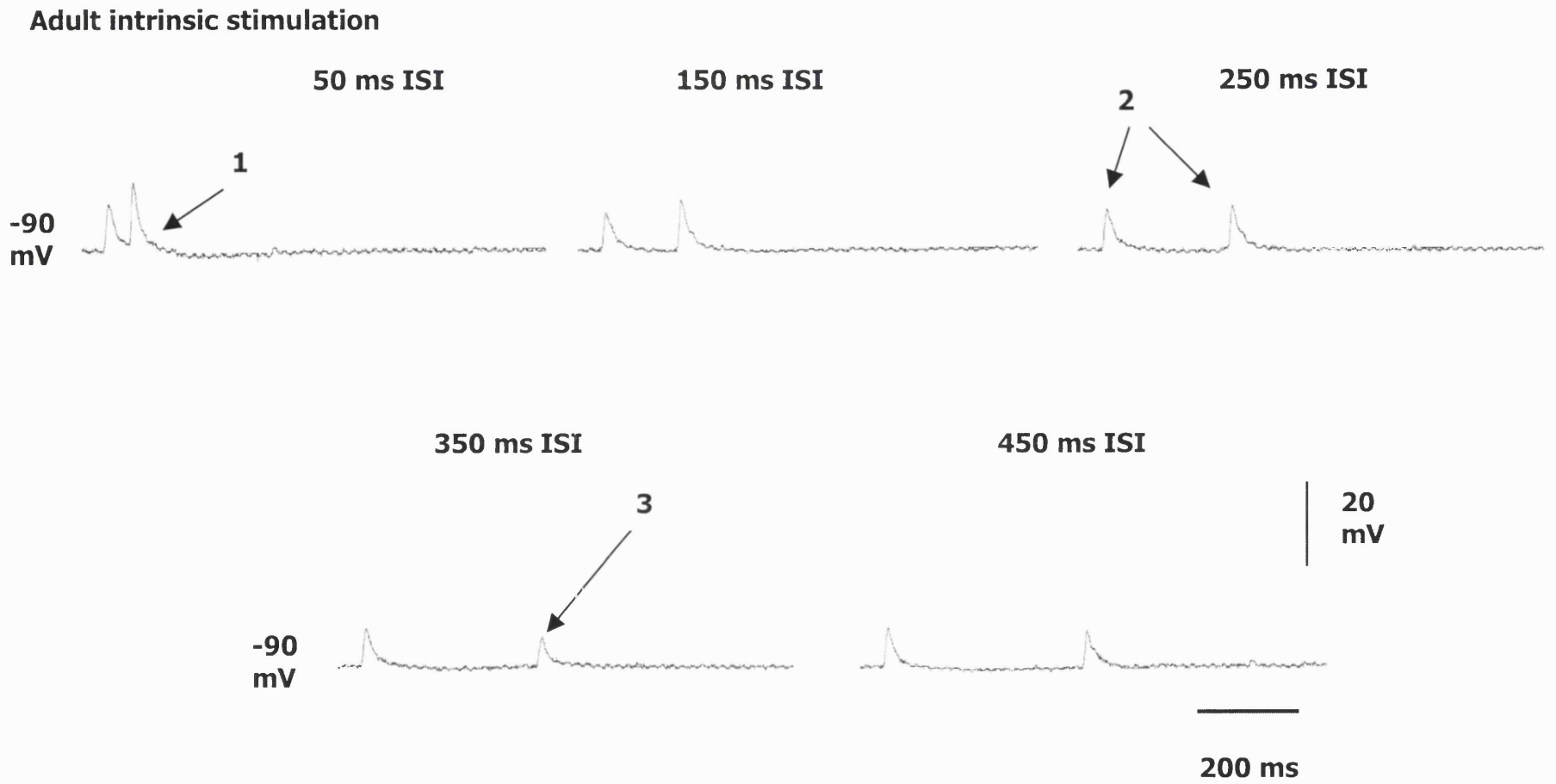
Adult intrinsic stimulation
50 ms ISI
150 ms ISI
250 ms ISI
1
2
-90
mV
350 ms ISI
450 ms ISI
3
20
mV
-90
mV
200 ms

Figure 4.10

Figure 4.10

Paired-pulse responses elicited from an immature (P+17) presumed deep pyramidal piriform cortical neurone following intrinsic fibre stimulation (2 V, 0.2 ms) at varying inter-stimulus intervals (ISI=50-450 ms). Control resting membrane potential=-82 mV. All responses were elicited from a membrane potential of -90 mV, maintained by negative current injection. (**1**) – Paired-pulse facilitation, whereby the second pulse is potentiated by the first, conditioning pulse. This effect is seen most clearly at smaller ISI intervals, diminishing as ISI is increased (*cf.* second pulse magnitude at 50 ms ISI and at 150 ms ISI.). (**2**) – The '*crossover*' point for this preparation was at an ISI of 250 ms, at which point no facilitation or inhibition was observed as one effect presumably balanced the effect of the other. (**3**) – Paired-pulse inhibition, whereby the second pulse is inhibited by the conditioning pulse. Under control conditions and in this preparation, this effect appeared at ISIs >250 ms.

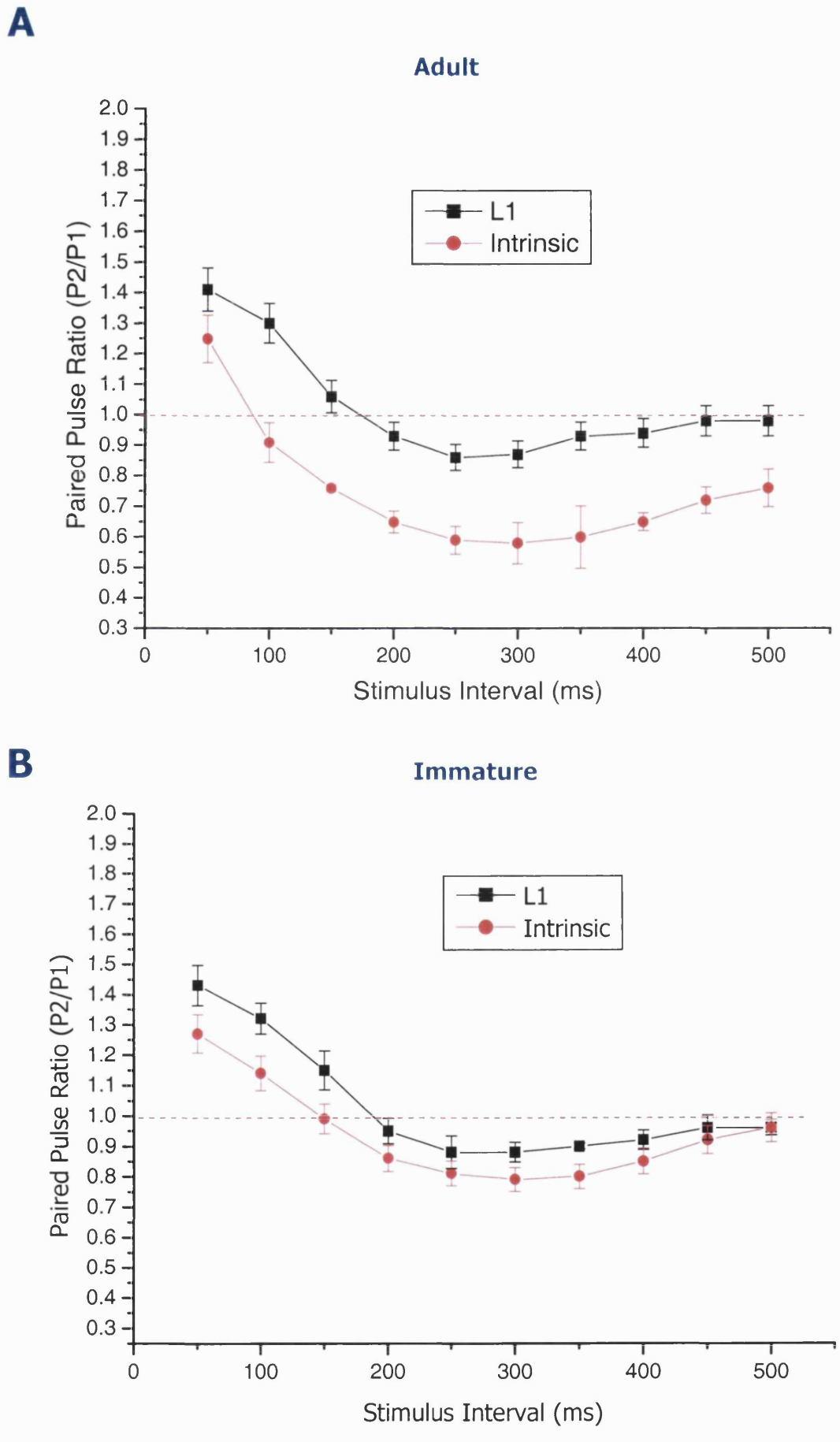
A
Adult
Paired Pulse Ratio (P2/P1)
Stimulus Interval (ms)
L1
Intrinsic
B
Immature
Paired Pulse Ratio (P2/P1)
Stimulus Interval (ms)
L1
Intrinsic

Figure 4.11

Figure 4.11

Paired-pulse ratios (second pulse magnitude/first pulse magnitude), calculated from stimuli applied to presumed deep pyramidal neurones and plotted *vs.* inter-stimulus interval (ISI; ms) for: **A.** Adult (n=51) recorded presumed deep pyramidal neurones following L1 fibre stimulation (**black**) or intrinsic fibre stimulation (**red**) and **B.** immature (n=61) recorded presumed deep pyramidal neurones following L1 fibre stimulation (**black**) or intrinsic fibre stimulation (**red**). Note that although PPF (at ISI-50 ms) for adult and immature intrinsic fibres did not vary greatly, a large difference was observed between their respective peaks of PPI; the immature intrinsic plot is shifted upwards, demonstrating a reduced degree of inhibition (Sections 4.5.1 and 4.5.2).

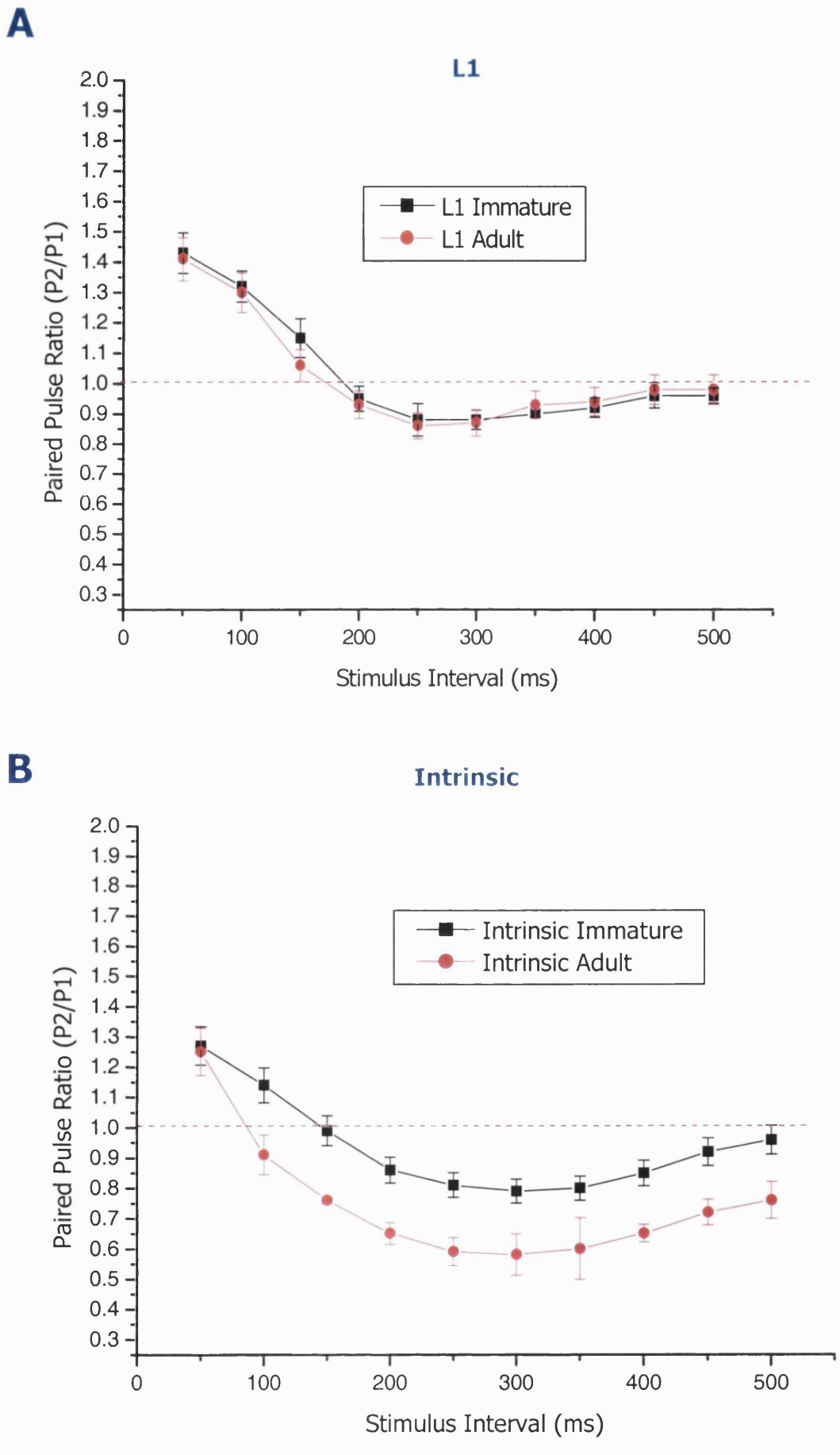
A
L1
L1 Immature
L1 Adult
Paired Pulse Ratio (P2/P1)
Stimulus Interval (ms)
B
Intrinsic
Intrinsic Immature
Intrinsic Adult
Paired Pulse Ratio (P2/P1)
Stimulus Interval (ms)

Figure 4.12

Figure 4.12

Paired-pulse ratios (second pulse magnitude/first pulse magnitude), calculated from stimuli applied to recorded presumed deep pyramidal neurones and plotted *vs.* inter-stimulus interval (ISI; ms) for: **A.** L1 fibre stimulation of adult (**red**; n=51) and immature (**black**; n=61) neurones and **B.** intrinsic fibre stimulation of adult (**red**; n=51) and immature (**black**; n=61) neurones. Note that there was very little observable difference between the L1 fibre stimulation plots for adult and immature recorded cells (**A**), but a clear difference in the intrinsic fibre stimulation plots (**B**), showing a relative reduction in peak PPI in the immature animal.

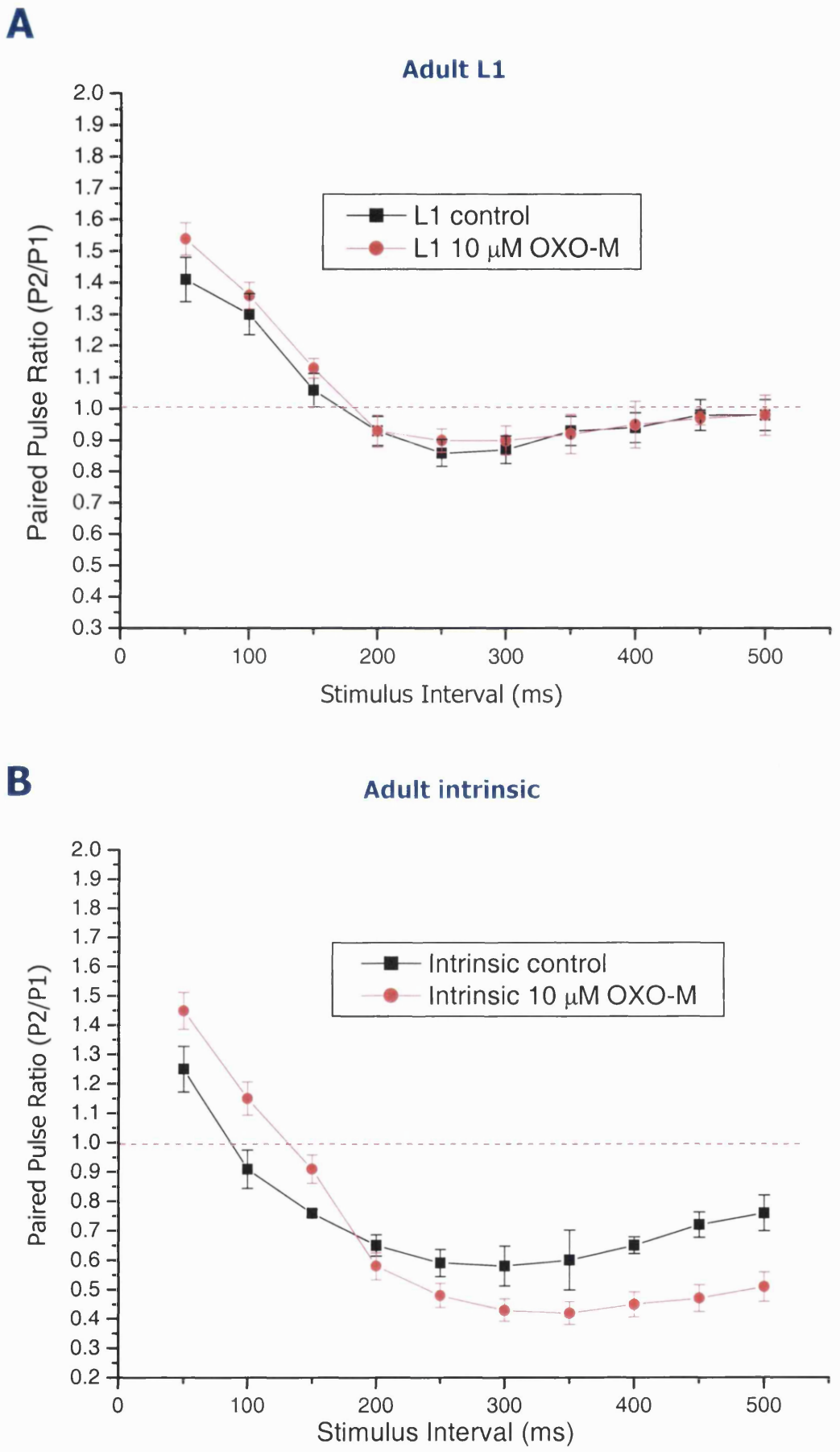
A
Adult L1
L1 control
L1 10 μM OXO-M
Paired Pulse Ratio (P2/P1)
Stimulus Interval (ms)
B
Adult intrinsic
Intrinsic control
Intrinsic 10 μM OXO-M
Paired Pulse Ratio (P2/P1)
Stimulus Interval (ms)

Figure 4.13

Figure 4.13

Paired-pulse ratios (second pulse magnitude/first pulse magnitude), calculated from stimuli applied to recorded adult (n=19) presumed deep pyramidal neurones and plotted *vs.* inter-stimulus interval (ISI; ms) for **A.** L1 fibre stimulation in control conditions (**black**) and in the presence of 10 μM OXO-M (**red**) and **B.** intrinsic fibre stimulation in control conditions (**black**) and in the presence of 10 μM OXO-M (**red**). Note that, similar to the recorded immature responses (Fig. 4.14), there was a slight increase in facilitation of L1 responses, with no change in inhibition. Contrastingly, intrinsic fibre responses showed a large increase in facilitation and inhibition suggesting the presence of a significant population of presynaptic mAChRs (Section 4.5.2).

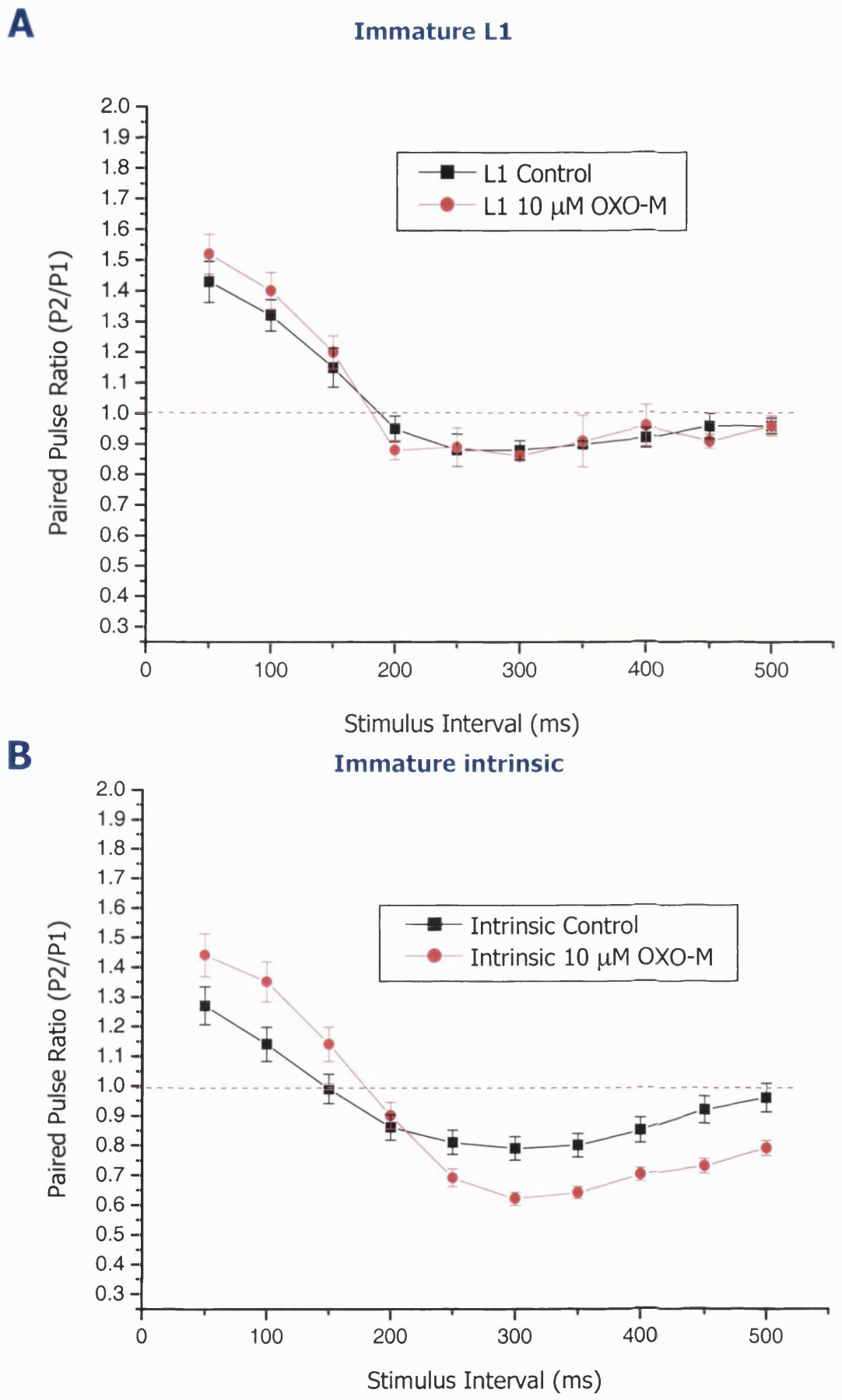
A
Immature L1
L1 Control
L1 10 µM OXO-M
Paired Pulse Ratio (P2/P1)
Stimulus Interval (ms)
B
Immature intrinsic
Intrinsic Control
Intrinsic 10 µM OXO-M
Paired Pulse Ratio (P2/P1)
Stimulus Interval (ms)

Figure 4.14

Figure 4.14

Paired-pulse ratios (second pulse magnitude/first pulse magnitude), calculated from stimuli applied to recorded immature (n=21) presumed deep pyramidal neurones and plotted *vs.* inter-stimulus interval (ISI; ms) for **A.** L1 fibre stimulation in control conditions (**black**) and in the presence of 10 μM OXO-M (**red**) and **B.** intrinsic fibre stimulation in control conditions (**black**) and in the presence of 10 μM OXO-M (**red**). Note that slight increases in facilitation following L1 stimulation at shorter ISIs were observed, with no change in the degree of inhibition at longer ISIs. Contrastingly, intrinsic fibre responses showed a large increase in both PPF and PPI suggesting the presence of a significant population of presynaptic mAChRs (Section 4.5.2). However, the PPI was not found to be as pronounced or as prolonged as that observed in the adult preparation (Fig. 4.13).

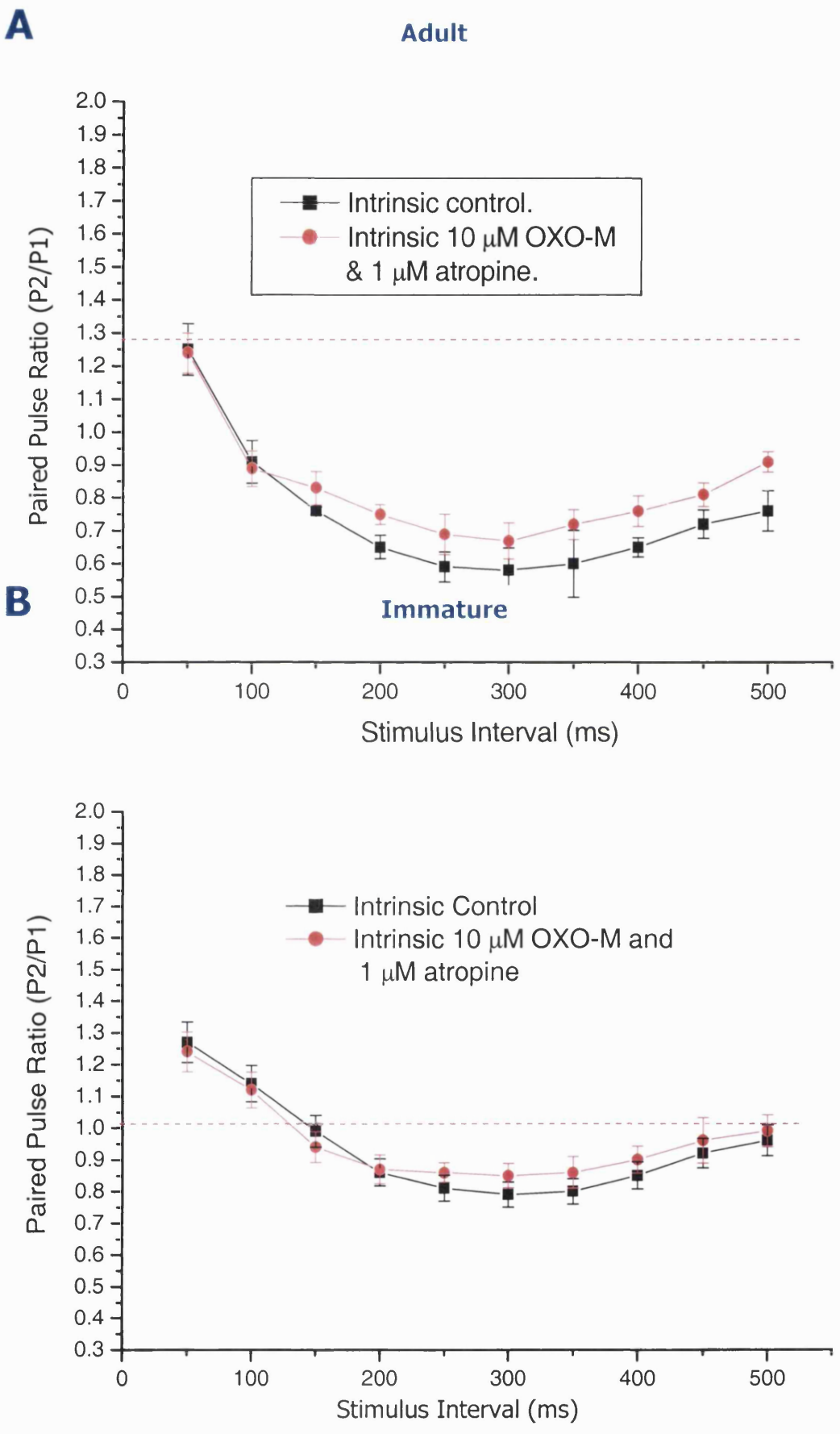
A
Adult
Intrinsic control.
Intrinsic 10 μM OXO-M
& 1 μM atropine.
Paired Pulse Ratio (P2/P1)
Stimulus Interval (ms)
B
Immature
Intrinsic Control
Intrinsic 10 μM OXO-M and
1 μM atropine
Paired Pulse Ratio (P2/P1)
Stimulus Interval (ms)

Figure 4.15

Figure 4.15

Paired-pulse ratios (second pulse magnitude/first pulse magnitude), calculated from stimuli applied to intrinsic fibres in control conditions (**black**) and in the presence of 10 μM OXO-M plus 1 μM atropine (**red**), recorded from presumed deep pyramidal neurones and plotted *vs.* inter-stimulus interval (ISI; ms) for **A.** adult (n=11) and **B.** immature (n=12) neurones. Note that although there are no apparent differences in the facilitatory sections of each plot, the inhibitory sections of both (**A**) and (**B**) show PPI to be siightly, but significantly reduced in the presence of OXO-M plus atropine compared to control conditions. This would suggest the presence of significant endogenous cholinergic tone within the piriform cortical slice preparation (particularly in the adult).

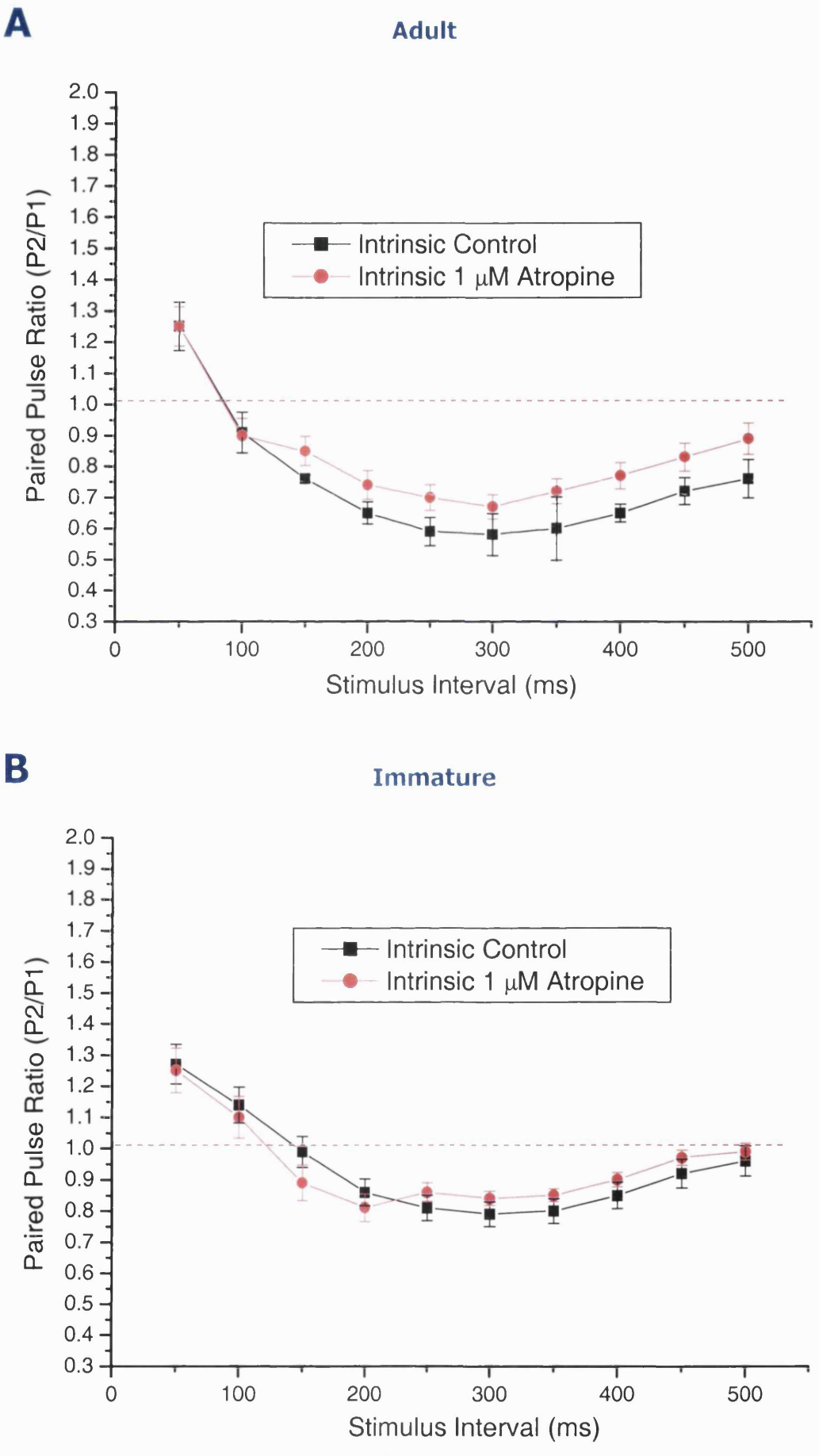
A
Adult
Paired Pulse Ratio (P2/P1)
Intrinsic Control
Intrinsic 1 μM Atropine
Stimulus Interval (ms)
B
Immature
Paired Pulse Ratio (P2/P1)
Intrinsic Control
Intrinsic 1 μM Atropine
Stimulus Interval (ms)

Figure 4.16

Figure 4.16

Paired-pulse ratios (second pulse magnitude/first pulse magnitude), calculated from stimuli applied to intrinsic fibres in control conditions (**black**) and in the presence of 1 μM atropine (**red**), recorded from presumed deep pyramidal neurones and plotted *vs.* inter-stimulus interval (ISI; ms) for **A.** adult (n=12) and **B.** immature (n=13) neurones. Note that the PPI sections of both (**A**) and (**B**) show inhibition to be slightly, but significantly reduced in the presence of atropine compared to control conditions, again suggesting the presence of significant endogenous cholinergic tone within the piriform cortical slice preparation (See Fig. 4.13). Additionally, the adult results showed a greater upward shift of the plot, suggesting either greater intrinsic cholinergic tone or perhaps more effective inhibitory receptor mechanisms responding to that tone in such preparations.

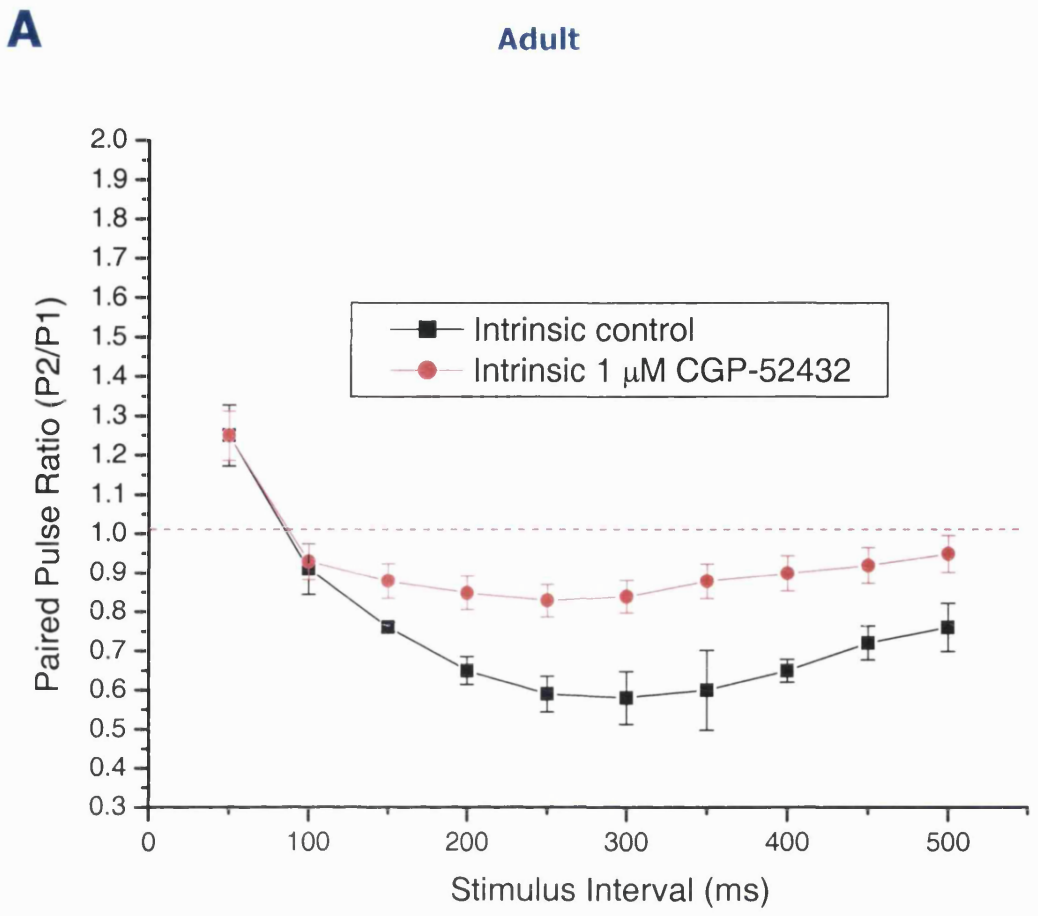
A
Adult
Intrinsic control
Intrinsic 1 μM CGP-52432
Paired Pulse Ratio (P2/P1)
Stimulus Interval (ms)
2.0
1.9
1.8
1.7
1.6
1.5
1.4
1.3
1.2
1.1
1.0
0.9
0.8
0.7
0.6
0.5
0.4
0.3
0
100
200
300
400
500

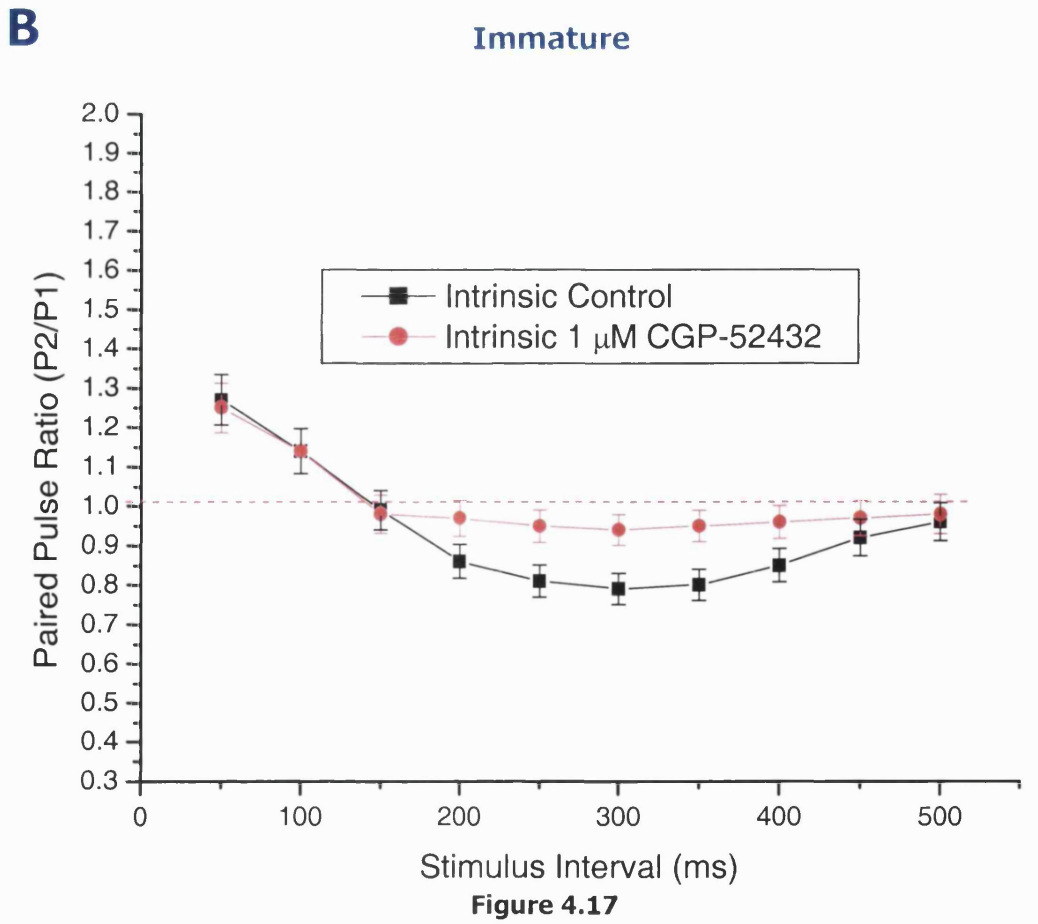
B
Immature
Intrinsic Control
Intrinsic 1 μM CGP-52432
Paired Pulse Ratio (P2/P1)
Stimulus Interval (ms)
2.0
1.9
1.8
1.7
1.6
1.5
1.4
1.3
1.2
1.1
1.0
0.9
0.8
0.7
0.6
0.5
0.4
0.3
0
100
200
300
400
500

Figure 4.17

Figure 4.17

Paired-pulse ratios (second pulse magnitude/first pulse magnitude), calculated from stimuli applied to intrinsic fibres in control conditions (**black**) and in the presence of the $GABA_B$ receptor-specific antagonist, CGP-52432 (**red**; 1 μM), recorded from presumed deep pyramidal neurones and plotted *vs.* inter-stimulus interval (ISI; ms) for **A.** adult (n=13) and **B.** immature (n=15) recorded neurones. Note that the inhibitory sections of both (**A**) and (**B**) show reduced PPI in the presence of CGP-52432 compared to control conditions, suggesting the presence of significant endogenous $GABA_B$-ergic tone within the preparation following the conditioning stimuus. Additionally, greater and more persistent endogenous $GABA_B$-ergic tone is indicated in the adult preparation since a greater shift of the plot from control can be seen, together with a slower return to baseline.

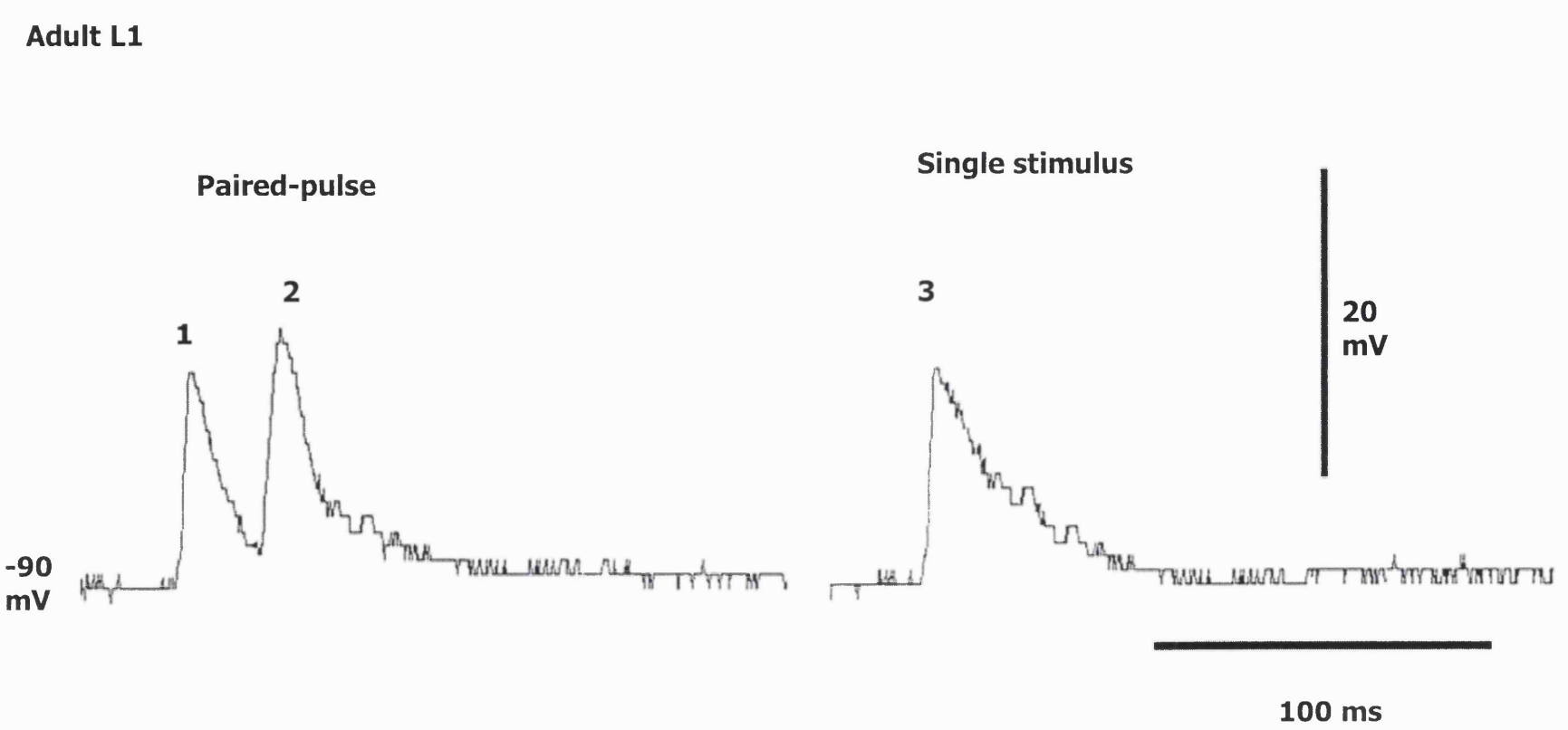

Figure 4.18

Figure 4.18

Subthreshold EPSPs elicited following L1 fibre stimulation using two different protocols (4V; 0.2 ms; single stimulus and paired-pulse stimuli), in control conditions and recorded from the same adult presumed deep pyramidal neurone held at -90 mV by the application negative holding current. **Left panel** shows a routinely elicited paired pulse response (ISI=50 ms) comprising a conditioning pulse (**1**) and a facilitated pulse (**2**). **Right panel** shows a single EPSP elicited from the same neurones in the same conditions. Resting potential=-83 mV, held at -90 mV by steady negative current injection. Note the faster decay rate of the facilitated pulse (**2**) compared to that of the isolated, single pulse (**3**). This is considered to be due to increased cellular K^+ conductance produced by postsynaptic $GABA_BR$ activation (Section 4.5.6).

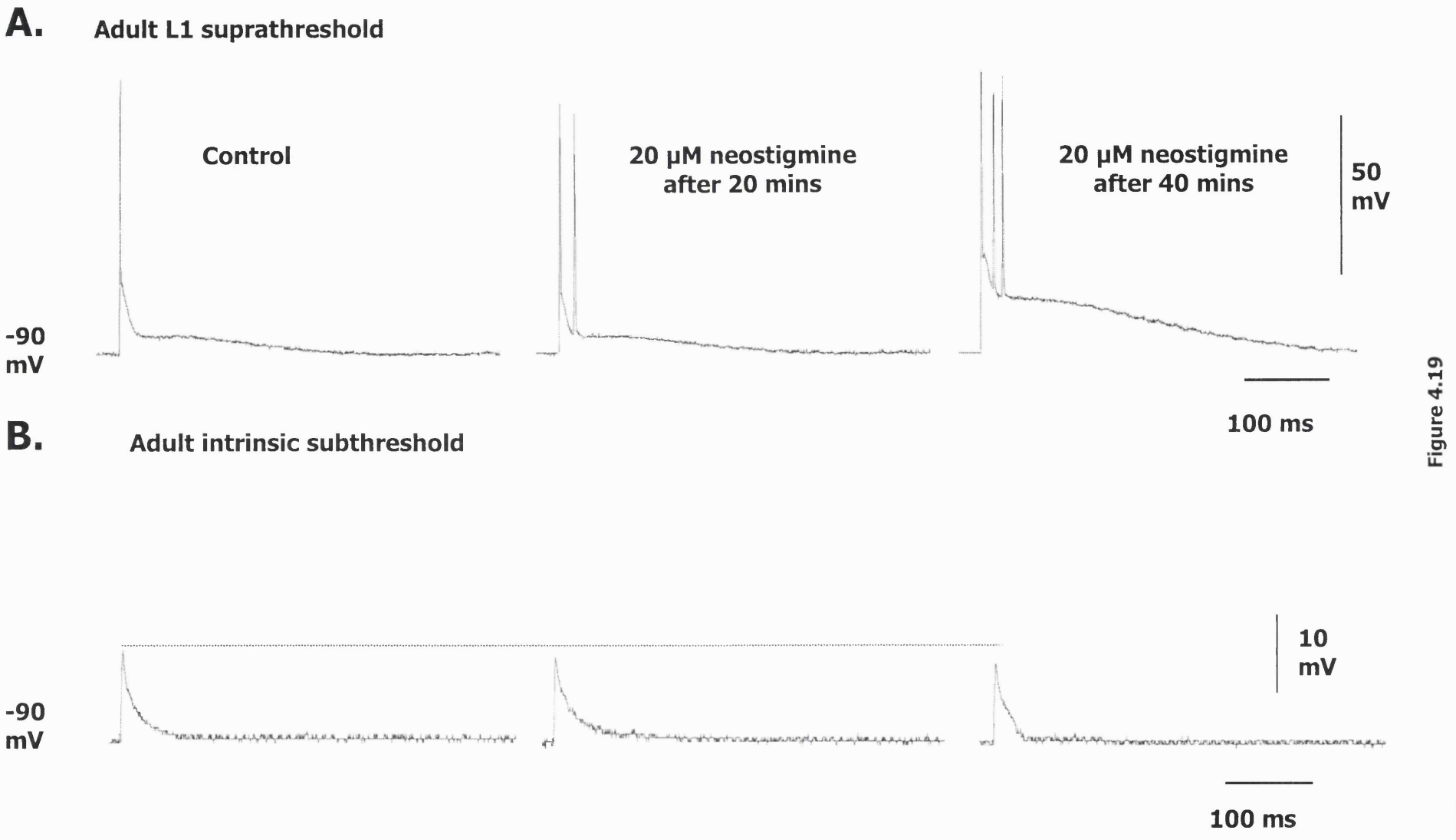
A.
Adult L1 suprathreshold
Control
20 µM neostigmine
after 20 mins
20 µM neostigmine
after 40 mins
50
mV
-90
mV
100 ms
B.
Adult intrinsic subthreshold
10
mV
-90
mV
100 ms

Figure 4.19

Figure 4.19

EPSPs elicited following L1 or intrinsic fibre stimulation to presumed deep pyramidal neurones in control conditions (**left panels**), 20 minutes after application of 20 μM neostigmine (**middle panels**) and 40 minutes after neostigmine (**right panels**). **Top panels** show suprathreshold EPSPs (8 V, 0.2 ms) elicited following L1 fibre stimulation recorded from an immature (P+16; resting potential = -81 mV, held at -90 mV by steady negative current injection) deep pyramidal neurone. **Bottom panels** show subthreshold EPSPs (6 V, 0.2 ms) elicited following intrinsic fibre stimulation recorded from an adult presumed deep pyramidal neurones. Resting potential = -83 mV, held at -90 mV by steady negative current injection. Broken red line highlights the slight but significant inhibition of intrinsic fibre-elicited EPSPs. Note the superimposed spikes seen on L1 fibre-elicited EPSPs that increased in occurrence as the neostigmine incubation period increased, whereas the amplitude of subthreshold EPSPs elicited by intrinsic fibre stimulation progressively decreased with increasing neostigmine incubation time. Results shown for 40 minutes neostigmine incubation represent maximal effects.

Table 4.1

Group	Adult L1		Adult Intrinsic		Immature L1		Immature Intrinsic	
Drug	Rate of Rise (mV/ms)	Half width (ms)	Rate of Rise (mV/ms)	Half width (ms)	Rate of Rise (mV/ms)	Half width (ms)	Rate of Rise (mV/ms)	Half Width (ms)
Control	0.7 ± 0.35 (n=19)	50 ± 12.6 (n=19)	0.6 ± 0.32 (n=19)	62 ± 14.2 (n=19)	0.6 ± 0.32 (n=21)	59 ± 11.6 (n=21)	0.7 ± 0.41 (n=21)	56 ± 18.3 (n=21)
10μM OXO-M	0.5 ± 0.27 (n=19)	44 ± 13.2 (n=19)	0.8 ± 0.23 (n=19)	65 ± 11.2 (n=19)	0.5 ± 0.27 (n=21)	64 ± 17.3 (n=21)	0.6 ± 0.35 (n=21)	58 ± 19.2 (n=21)
10μM OXO-M and 1μM Atropine	0.7 ± 0.45 (n=11)	48 ± 10 (n=11)	0.6 ± 0.37 (n=11)	59 ± 13.6 (n=11)	0.6 ± 0.41 (n=12)	71 ± 13.2 (n=12)	0.7 ± 0.51 (n=12)	61 ± 23.6 (n=12)
1μM Atropine	0.7 ± 0.55 (n=12)	53 ± 12.1 (n=12)	0.7 ± 0.43 (n=12)	69 ± 17.1 (n=12)	0.5 ± 0.28 (n=13)	65 ± 15.9 (n=13)	0.5 ± 0.29 (n=13)	71 ± 32.1 (n=13)
1μM CGP-52432	0.7 ± 0.44 (n=13)	46 ± 15.6 (n=13)	0.8 ± 0.28 (n=13)	74 ± 14.5 (n=13)	0.7 ± 0.45 (n=15)	60 ± 17.6 (n=15)	0.6 ± 0.45 (n=15)	63 ± 36.4 (n=15)

Table 4.1

Effects of drugs on kinetics of EPSPs evoked by L1 or intrinsic fibre stimulation in adult or immature slices. During paired pulse experiments, individual stimuli were applied to produce standardised ~10mV amplitude subthreshold EPSPs recorded at a membrane potential held (by negative current injection) at –90 mV. The rate of rise was calculated from stimulus application to EPSP peak, whilst the half-width was calculated as the time interval between the two points at which the trace was at 50% of the maximal EPSP amplitude. Each value represents the mean ± SEM. n=number of neurones.

Chapter 5:

Fast inhibitory synaptic responses of adult and immature deep pyramidal piriform cortical neurones

5.1 Introduction

Continuing from the detailed investigation of presynaptic mAChR-mediated modulation of excitatory synaptic transmission presented in chapter 4, the possible effects of presynaptic mAChR activation upon fast, $GABA_AR$-mediated synaptic transmission and any likely developmental differences in its efficiency and pharmacology investigated in the present section. A number of previous studies have pharmacologically investigated the mechanisms that underlie the fast inhibitory processes of PSP complexes evoked from piriform cortical slices, and a generally accepted model of the piriform cortical synaptic circuitry has been proposed (Figs. 1.2 and 1.3) which includes these fast inhibitory elements (Satou *et al.*, 1983b; Satou *et al.*, 1983c; Tseng & Haberly, 1988). Briefly, excitatory synapses arising from the LOT (within layer Ia) and intrinsic fibres (predominantly in layers Ib/II, but permeating all layers and arising from axon collaterals of deep and superficial pyramidal neurones) activate inhibitory, GABA-ergic interneurones located in layer Ib and in layers II/III. The interneurones consequently exert their inhibitory effect upon the same pyramidal neurones that LOT and association fibres also excite, thus giving rise to a feed-forward inhibitory pathway. It has also been suggested that the association fibre system modulates feed-back inhibition (Barkai *et al.*, 1994) in the piriform cortex. In this case, association fibres arising from pyramidal neurone axon collaterals stimulate interneurones that, in turn inhibit the pyramidal neurones from which the axons arose.

In the present study, the fast $GABA_AR$-mediated component of the IPSP was pharmacologically isolated by blockade of excitatory and $GABA_BR$-mediated synaptic transmission and inhibitory interneurones in either layers Ib or II/III activated by direct focal electrical stimulation. Any developmental variation in evoked fast IPSP responses and mAChR sensitivity were then investigated. Recordings were routinely made in the presence of 10 μM DL-APV and 20 μM CNQX to block glutamatergic (NMDA and AMPA receptor mediated) transmission and 1 μM CGP-52432 to block $GABA_BR$-mediated transmission respectively. The recorded neurone was then depolarized by the application of positive current through the recording microelectrode; this caused the recorded neurone to repetitively fire until adaptation occurred. Firing then ceased and a steady membrane potential of ~-40 mV was achieved. This protocol was designed to maximise the amplitude of the fast IPSPs recorded (*c.f.* (Patil & Hasselmo, 1999)). At this point recordings of the fast IPSP component, following stimuli applied through bipolar stimulating electrodes (located in either layer I or layer II/III), were made. The strength of the stimulus pulses applied was determined by eliciting subthreshold EPSPs

in control conditions of the same magnitude (~10 mV) from both electrodes. The same stimulus strengths were then used following the pharmacological blockade of excitatory synaptic transmission and membrane depolarization to -40 mV as described above (Methods 2.5.3.3). All recorded cells were electrophysiologically characterized as presumed deep pyramidal neurones in control conditions (Section 3.3.1). Significant differences between data sets in this chapter were calculated using Students t-tests unless explicitly stated otherwise.

5.2 Fast $GABA_AR$-mediated IPSPs elicited from adult presumed deep pyramidal neurones

Isolated fast, $GABA_AR$-mediated IPSPs were elicited following stimulation in either layer I or layers II/III from a total of 18 adult presumed deep pyramidal neurones, recorded in current clamp mode from transverse piriform cortical brain slice preparations, as previously described. The $GABA_AR$-mediated nature of the fast IPSPs evoked was confirmed by their abolition by the $GABA_AR$ antagonist, bicuculline (10 μM; not shown) (Galvan *et al.*, 1985) to the bath medium. Initially, fast IPSPs elicited following stimulation in either layer I or layer II/III were observed in control conditions. The mean peak amplitude for fast IPSPs elicited following layer I stimulation (18 ± 0.7 mV) was found to be significantly larger than the mean peak amplitude of fast IPSPs elicited following stimulation in layer II/III (13 ± 0.8 mV; $P<0.05$ *vs.* layer I; Fig 5.1; left panels). Following the application of 10 μM OXO-M, fast IPSPs elicited following layer I stimulation were significantly suppressed compared to controls (mean reduction in amplitude=35 ± 5.5%; $P<0.05$ *vs.* controls; Wilcoxon signed rank test; Fig. 5.1A; middle panel). However, those elicited following stimulation in layer II/III were consistently unaffected by OXO-M (Fig 5.1B; middle). No significant differences were found between the mean time courses (measured from application of the focal stimulus to the time at which the membrane potential returned to -40 mV) of the evoked fast IPSPs in control conditions (71 ± 13.4 ms) or in 10 μM OXO-M (61 ± 18.6 ms; $P>0.05$ *vs.* controls) The membrane depolarizing effects of OXO-M were compensated for by varying current injection through the recording microelectrode. This OXO-M-mediated suppression of fast inhibitory synaptic transmission was found to be fully reversible on washout (not shown) or following the addition of the mAChR antagonist, atropine (1 μM; not shown) or the M1 subtype-specific mAChR antagonist, pirenzepine (100 nM; Fig. 5.1A) to the bathing medium (not shown). These results show an interesting correlation with those presented describing excitatory synaptic transmission in the

previous chapter. Thus, a similar, but apparently *opposite* manifestation of synaptic layer input sensitivity to OXO-M has now been shown here for fast $GABA_AR$-mediated inhibitory responses in the piriform cortical brain slice.

5.3 Fast $GABA_AR$-mediated IPSPs elicited from immature deep pyramidal neurones

Since EPSPs elicited from the immature slice preparation were found, in this present study, to show a number of differences from those elicited from the adult preparation (Chapter 4), the possibility that similar differences in fast inhibitory synaptic transmission might also be present within the slice preparation was investigated. Consequently, the same protocol as described above was used to elicit fast IPSPs from immature piriform cortical brain slices. A total of 20 immature presumed deep pyramidal neurones were recorded from and, similarly to the adult preparation, the mean peak amplitude of fast IPSPs elicited following layer I stimulation (9 ± 0.3 mV; Fig. 5.2A; left panel) was found to be significantly larger than those obtained following layer II/III stimulation (5 ± 0.4 mV; $P<0.05$ *vs.* layer I; Fig. 5.2B; left panel). Moreover, the magnitude of both layer I- and layer II/III-elicited fast IPSPs from immature slices were both found to be significantly smaller than the equivalent responses elicited from the adult preparation (layer I: 18 ± 0.7 mV; layer II/III: 13 ± 0.8 mV; $P<0.05$ for both layers I and II/III respectively *vs.* adult equivalents). Additionally, the difference between layer I- and layer II/III-elicited peak IPSP magnitudes was found to be slightly, but significantly greater (45 ± 4.8%) in the immature preparation than in the adult (35 ± 5.6%; $P<0.05$; Wilcoxon signed rank test). Interestingly, the peak magnitude of fast IPSPs elicited following layer I stimulation was found to be significantly inhibited (72 ± 5.2%; $P<0.05$ *vs.* controls; Wilcoxon signed rank test; Fig. 5.2A; middle panel) following the application of 10 μM OXO-M when compared to controls whilst, like the adult preparation, fast IPSPs elicited following stimulation in layer II/III were unaffected by OXO-M (Fig. 5.2B; middle panel). The degree of OXO-M-induced inhibition of layer I-evoked fast IPSPs was found to be significantly greater in the immature slice preparation than the adult ($P<0.01$), indicating that following mAChR activation, already lower levels of inhibitory control in the immature animal are further reduced to a greater degree than in the adult (where inhibitory control was shown to be greater; Chapter 4). The mean time courses of IPSPs elicited following either layer I or layer II/III stimulation did not vary significantly from one another in control conditions (layer I: 112 ± 12.9 ms; layer II/III: 63 ± 19.1 ms) or in the presence of 10 μM OXO-M

(layer I: 115 ± 14.7 ms; layer II/III: 69 ± 17.2 ms; P>0.05 control *vs.* OXO-M for either layer I or II/III). However, the time course of fast IPSPs elicited following layer I stimulation was found to be significantly greater (112 ± 12.9 ms) than the equivalent measurement following layer II/III stimulation (63 ± 19.1 ms; P<0.05 *vs.* layer I). OXO-M-mediated suppression of layer I-evoked fast IPSPs was found to be fully reversible on washout (not shown) or following the addition of the mAChR antagonist, atropine (1 μM; not shown) or the M2 subtype-specific mAChR antagonist, AFDX-116 (1 μM; Fig. 5.2A) to the bathing medium.

To further characterize the differences in the responses elicited from adult and immature neurones, log dose-response curves to demonstrate any differential potency of OXO-M in suppressing fast inhibitory synaptic transmission were constructed (Fig. 5.3). ED_{50} values for OXO-M, estimated from the plots by best curve fits, were found to be lower in the immature preparation (2.5 μM; n=6) than the adult (4.0 μM; n=5), indicating a relatively greater muscarinic sensitivity to suppression of layer I inhibitory synaptic terminals in the immature piriform cortical slice preparation.

5.4 Elucidation of the mAChR subtype responsible for mediation of OXO-M-induced suppression of layer I-evoked fast IPSPs

The mAChR subtypes responsible for mediating the suppression of intrinsic, but not afferent excitatory synaptic transmission in the adult and immature piriform cortical slice preparations were shown, in the previous chapter (Sections 4.2.3 and 4.3.3), to be the M1 and M2 mAChR subtypers respectively. A similar protocol was now used to determine the mAChR subtype responsible for the suppression of layer I-evoked fast IPSPs described above.

Application of the M1 mAChR-specific antagonists, pirenzepine (100 nM; 9/9 cells; Fig. 5.1A; right panel) or telenzepine (20 nM; 8/9 cells; not shown) to presumed deep pyramidal neurones recorded from adult piriform cortical brain slices fully reversed the muscarinic suppression of layer I-evoked suppression of fast inhibitory synaptic transmission by OXO-M. Conversely, the M2 mAChR-specific antagonists, methoctramine (300 nM; 9/9 cells; not shown) or AFDX-116 (1 μM; 9/9 cells; not shown) had no effect upon the observed suppression of layer I fast inhibitory transmission in the adult preparation. These results clearly correlate with the results obtained from the adult preparation in the previous chapter where mAChR-mediated suppression of excitatory synaptic transmission in the *intrinsic* fibre layer II/III was also mediated by the M1 mAChR-subtype. Conversely, when the same protocol was applied

to the immature preparation, neither 100 nM pirenzepine (10/10 cells; not shown) nor 20 nM telenzepine (10/10 cells; not shown) had any effect upon OXO-M-induced suppression of layer I-evoked fast inhibitory transmission. However, application of 1 μM AFDX-116 (10/10 cells; Fig. 5.2A; right panel) or 300 nM methoctramine (10/10 cells; not shown) to the immature preparation fully reversed the OXO-M-induced inhibition of fast inhibitory transmission. This also correlates with previous results (Chapter 4), where the M2 mAChR subtype was found to mediate cholinergic inhibition of *intrinsic* fibre excitatory synaptic transmission in the immature preparation. When the results presented here are considered in conjunction with the comparable developmental change in mAChR subtypes mediating *intrinsic* EPSP suppression in the PC (Whalley & Constanti, 2003), these differences in the mAChR-mediated modulation of *excitatory and inhibitory* synaptic transmission maintains the immature PC in a heightened excitatory state following presynaptic mAChR activation and therefore may be important for the generation of the mAChR agonist-induced epileptiform bursting previously described. In the whole animal, this property may play a role in driving synaptic growth, learning and memory (Barkai & Hasselmo, 1997; Hasselmo & Bower, 1993).

5.5 Variations in fast IPSP amplitude with different recording microelectrode positions, in the adult or immature piriform cortical slice preparation

In the previous chapter (Section 4.4), significant variations in afferent and intrinsic excitatory synaptic responsiveness were observed in different areas of the piriform cortical slice preparation. The possibility that corresponding variations in $GABA_AR$-mediated inhibitory synaptic responsiveness might also exist was therefore investigated. Fast, $GABA_AR$-mediated IPSPs were evoked as previously described and recorded from neurones located in the APC (adult: n=4; immature: n=4), the MPC (adult: n=14; immature: n=16) or the PPC (adult: n=5; immature: n=4). Fast IPSPs recorded from either adult or immature slices evoked following stimulation of layer I in the APC (adult: 17 ± 0.9 mV; immature: 9 ± 0.6 mV), the MPC (adult: 18 ± 0.7 mV; immature: 9 ± 0.3 mV) or the PPC (adult: 19 ± 1.0 mV; immature: 10 ± 0.8 mV), were not found to be significantly different from one another ($P>0.05$; Table 5.1) in control conditions and were unaffected (as previously described) in the presence of 10 μM OXO-M. In contrast, fast IPSPs recorded from the APC (8 ± 1.1 mV) and PPC (7 ± 0.9 mV) of *adult* piriform cortical slices, following stimulation in layers II/III were found to be significantly smaller than fast IPSPs elicited under the same conditions, but recorded

from the MPC (13 ± 0.8 mV; P<0.05 *vs.* IPSPs in either the APC or PPC; Table 5.1). The same responses elicited from the APC and PPC of the immature preparation also appeared to be slightly smaller than the same response recorded in the MPC, however the difference was not found to be significant (P>0.05; MPC *vs.* both APC and PPC; Table 5.1). The absence of a measurable difference may have been due to the the small amplitude of fast IPSPs elicited following layer II/III stimulation of the immature preparation (~4 mV) and consequently, measurement of significant changes in values of this size approaches the practical limits of the recording system. The degree of muscarinic inhibition of the fast IPSPs elicited following stimulation in layer I did not vary with recording microelectrode position in both the adult and immature preparations (Table 5.1). The present study has already shown the incidence of OXO-M-induced epileptiform bursting in the immature preparation to be raised in the APC and PPC; consequently the results presented here would indicate that aspects of this increased susceptibility to bursting behaviour may be due to differences in fast inhibitory synaptic transmission in these areas.

5.6 A comparison of IPSP input specificity by paired-pulse analysis

In the same way that paired-pulse analysis was used to confirm the presynaptic nature of muscarinic modulation of excitatory synaptic transmission (Section 4.5), a similar paired-pulse protocol was utilised to corroborate the apparent presynaptic mechanism of OXO-M-induced inhibition of layer I-evoked fast inhibitory synaptic transmission. Since the isolation of fast, $GABA_AR$-mediated IPSPs required the blockade of $GABA_BR$-mediated, results were not obtained at inter-stimulus intervals (ISIs) greater than 250 ms as the usual, principally $GABA_BR$-mediated PPI would not be present. Consequently, the results presented here deal solely with variations in paired-pulse facilitation. Fast IPSPs were evoked over a range of ISIs (25-250 ms; in 25 ms increments) following either layer I or layer II/III stimulation of adult (n=18) and immature (n=20) piriform cortical slice preparations, in control conditions, 10 μM OXO-M and OXO-M plus 1 μM atropine.

5.6.1 Paired-pulse responses elicited following layer I or II/III stimulation of adult and immature piriform cortical slice preparations in control conditions

The results presented earlier in this chapter demonstrated clear differences between the magnitudes of the fast IPSPs evoked following layer I and layer II/III stimulation. When the paired-pulse protocol described above was applied to the adult slice preparation in

control conditions, a clear difference was also found between the degrees of paired-pulse facilitation (PPF) observed following layer I or layer II/III stimulation. At an ISI=25 ms, the peak facilitation following layer I stimulation was significantly greater (15 ± 2.3%; P<0.05; Wilcoxon signed rank test) than the peak facilitation following layer II/III stimulation (Fig. 5.4A). When the same comparison was made using results obtained from the immature slice preparation, a similar variation between layer I- and layer II/III-evoked responses was seen (Fig. 5.4B). In the immature preparation, peak facilitation following layer I stimulation was significantly greater (9 ± 1.9%; P< 0.05; Wilcoxon signed rank test) than the facilitation seen following layer II/III stimulation. Interestingly, there was a slight, but significant (6 ± 3.1%) difference in peak facilitation following layer I stimulation between the immature and adult preparations. These results have demonstrated for the first time that significant differences exist between the terminals of inhibitory interneurones located in layer I and layer II/III of the rat piriform cortex. Additionally, the difference in degrees of facilitation, following layer I stimulation, between the adult and immature preparations may be one of the reasons why smaller IPSP magnitudes were observed in the immature preparation (Section 5.3). Since degree of facilitation is closely linked to raised Ca^{2+} levels in the presynaptic bouton (Stuart & Redman, 1991), the higher degree of facilitation seen in the adult preparation would suggest higher Ca^{2+} concentrations and thus potentially greater release of inhibitory neurotransmitter.

5.6.2 Paired-pulse responses elicited following layer I or layer II/III stimulation of adult and immature piriform cortical slice preparations following application of M OXO-M

Since significant differences were previously observed in paired-pulse responses elicited following stimulation of excitatory afferent (LOT) or intrinsic fibres in the presence of 10 μM OXO-M (Section 4.5), the effect of OXO-M upon paired-pulse inhibitory responses was also investigated. Control paired-pulse responses were elicited, as described above, from adult and immature slice preparations and compared with responses elicited in the presence of 10 μM OXO-M or OXO-M plus 1 μM atropine. In both the adult and immature preparations, PPF following layer I stimulation was significantly increased in the presence of 10 μM OXO-M, with the increase seen in the immature preparation (26 ± 2.2%; Fig. 5.5B) being significantly greater than that observed in the adult (18 ± 2.1%; P<0.05; Wilcoxon signed rank text; Fig. 5.5A). On adding 1 μM atropine, the increased facilitation described above was abolished (Fig.

5.5). Interestingly, in atropine there was a very slight upward shift in the plot relative to control (Fig. 5.5; blue lines); however, this shift was not significant at any ISI ($P>0.05$; Wilcoxon signed rank text) and consequently, there was no indication of significant endogenous cholinergic '*tone*' being exerted on inhibitory transmission, as seen with excitatory synaptic transmission (*cf.* Section 4.5.3 and 4.5.4), under these experimental conditions. Contrastingly, the PPF observed following layer II/III stimulation in both the adult and immature piriform cortical slice preparations, was unaffected (compared with controls) in the presence of 10 μM OXO-M (Fig. 5.6), in accordance with the results obtained in Sections 5.2 and 5.3 that little or no presynaptic muscarinic modulation of inhibitory neurotransmitter release from layer II/III interneurone terminals.

5.6.3 Effects of OXO-M on kinetics of evoked fast IPSPs and consequent influence upon paired-pulse analysis

Rate of rise and half-width

The rate of rise and half width of evoked IPSPs were calculated in the same manner as previously described for EPSPs (Section 4.5.6) in the presence of OXO-M and OXO-M plus atropine and were not found to be significantly different ($P>0.05$; Wilcoxon signed rank test) from control, regardless of the conditions under which they were recorded (Table 5.2). Therefore it may be proposed that possible modifications made to the paired pulse dynamics (increases or decreases in PPF or PPI) by the presence of drug were unlikely to be the result of changes to post-synaptic neuronal membrane properties (Stuart & Redman, 1991). See section 4.5.6 for additional theoretical detail on this analytical approach.

Variation in standard deviation of PPF values

No significant differences were also found between the standard deviations calculated from PPF means obtained in any of the experimental conditions used ($P>0.05$; Students t-test), following either layer I or II/III stimulation and recorded from either the adult or immature preparations. This demonstrated that any observed change in facilitation occurred in most neurones synapsing with the recorded cell rather than a specific subgroup of those neurones (Saar *et al.*, 1999). However, given that the experimental conditions used in this section restricted transmission solely to fast inhibitory synaptic transmission, no neurones, other than the inhibitory GABA-ergic interneurones being stimulated, were likely to be firing under the present experimental conditions, hence the lack of any significant differences between the calculated standard deviations.

5.7 Discussion

The results presented herein have demonstrated a number of clear laminar and developmental differences in the fast inhibitory responses of presumed deep pyramidal neurones recorded from adult and immature piriform cortical slices. A number of previous studies have investigated fast (and slow) inhibitory responses in this brain area (Patil & Hasselmo, 1999; Rosin *et al.*, 1999; Satou *et al.*, 1983b; Satou *et al.*, 1983a; Tseng & Haberly, 1988), although only one study investigated isolated fast inhibitory processes (Kapur *et al.*, 1997a); the remainder interpreted variation in inhibitory effects from changes in the EPSP/IPSP complex. These previous studies have provided the evidence for the current model of inhibitory synaptic transmission in the piriform cortex that is now generally accepted (Section 5.1 and Figs. 1.2 & 1.3).

5.7.1 Fast, $GABA_AR$-mediated IPSPs

This present study showed for the first time that fast IPSPs elicited from adult and immature slices, following layer I stimulation, were of a consistently greater magnitude than those elicited following layer II/III stimulation. This clearly indicated that a greater degree of $GABA_AR$-mediated inhibition (either from a greater number of GABA-ergic neurones, greater release of GABA or greater postsynaptic responsiveness to $GABA_AR$ activation) existed in the more superficial layer I than in the deeper layers II/III. This correlates well with a previous report (Kapur *et al.*, 1997a) that found $GABA_AR$-mediated inhibition to be mainly generated in the apical dendrites of pyramidal cells rather than in somatic regions and that the circuits responsible for fast $GABA_AR$-mediated inhibition in the apical dendritic and somatic regions were independent of one another. This finding has now been confirmed by a study that visualised selectively stained inhibitory interneurones within the piriform cortex, identified distinct subpopulations of these neurones and showed that the hypothesis of separate somatic and apical dendritic inhibitory subsystems proposed by Kapur *et al.* (1997) did physically exist (Ekstrand *et al.*, 2001a). Kapur *et al.* (1997) proposed that if feed forward inhibition were selectively decreased in layer I, then integrative dendritic processes would be enhanced whilst feedback inhibition in the somatic region would restrain system excitability. This could allow changes '*in the functional state of the* (piriform) *cortex by altering the excitability of interneurones that mediate dendritic inhibition without increasing the propensity for regenerative bursting*'. However, their study did not investigate which systems might be responsible for the selective modulation of fast inhibitory transmission they saw. The present experiments have

shown that fast inhibitory transmission in layer I (dendritic) was selectively modulated by mAChR activation whilst the same process in layers II/III (somatic and/or distal dendritic) was unaffected by mAChR activation. This clearly satisfies the requirements suggested by Kapur *et al.*, making the mAChR system a strong candidate as a selective modulator of fast inhibitory synaptic transmission, and therefore dendritic integration in this brain region.

Distinct subgroups of neurones affected by different modulators and mediating fast inhibitory transmission of the type described above, have also been described in rat auditory cortex (Aramakis *et al.*, 1997) (where mAChR activation was also found to be the modulator), cat visual cortex (Tamas *et al.*, 1997), rat neocortex (Thomson *et al.*, 1996) and hippocampus (Traub *et al.*, 1987; Vu & Krasne, 1992). The hippocampal studies have shown that and equivalent division of apical dendritic and somatic inhibitory systems exists, with the dendritic component regulating NMDAR-mediated excitation. Therefore, the ability to selectively modulate NMDAR-mediated excitatory transmission with the dendritic inhibitory system without affecting the separate somatic inhibitory system improves associative memory function (by increased NMDAR-mediated excitatory transmission) without increasing the propensity of the system to suffer epileptiform bursting activity.

This present report has also demonstrated that fast IPSPs elicited (following the stimulation of either layer I or II/III) in the adult preparation were consistently larger than the equivalent responses elicited from the immature preparation. This indicated that fast inhibitory transmission was significantly reduced in the immature preparation, a situation that would lead to increased excitability and therefore a greater likelihood of epileptiform activity. Interestingly, mAChR activation was found to inhibit layer I-elicited fast IPSPs, but not layer II/III-elicited fast IPSPs in both the adult and immature preparations. Moreover, mAChR activation was found to inhibit layer I-elicited fast IPSPs to a greater degree in the immature preparation than in the adult. Consequently, both the selective laminar sensitivity of fast inhibitory transmission and the observed developmental variation in mAChR-mediated modulation of fast inhibitory transmission clearly predispose the immature preparation to a greater degree to over-excitability and epileptiform behaviour, independent of the developmental variation in excitatory responses previously described (Chapter 4). Interestingly, this variation in mAChR responsiveness was found to be due to the same mAChR subtype '*switch*' as previously described (Chapter 4), whereby the M2 mAChR subtype had a modulatory effect upon

fast inhibitory transmission in the immature animal, whilst the same function is performed by the M1 mAChR subtype in the adult.

Of considerable significance to the present study is the fact that whilst the M2 mAChR-mediated suppression of immature intrinsic *excitatory* synaptic transmission was *less effective* than the M1 mAChR-mediation of the same process in the adult, the M2 mAChR-mediated inhibition of fast *inhibitory* synaptic transmission was *more effective* than the M1 mAChR-mediation of that process in the adult. Although the underlying mechanistics to these mAChR-mediated effects are beyond the remit of this investigation, it appears reasonable to suggest that differences in magnitudes of transmission inhibition are not due to one subtype being individually less effective than the other, but most likely due to varying subtype presynaptic population numbers.

This present report also found that the time course of layer I-elicited fast IPSPs was greater in the immature preparation than the adult. Interestingly, Kapur *et al.* (1997) showed that $GABA_AR$-mediated IPSPs elicited following electrical stimulation in layer I/II of the immature piriform cortex, *in vitro*, were composed of fast and slow components, with dendritic IPSPs having a significantly larger slow component (compared to their somatic counterparts), an observation supported by the results obtained from the immature preparation in this present report. The absence of a more significant slow component in layer I-elicited IPSPs from the adult preparation was interesting, in that the previous report (Kapur *et al.*, 1997a) examined immature neurones using a patch clamp technique, so any reduction in the slow component with increasing age was not observed. It has been proposed that the slower time course of the distal dendritic IPSP is critical to the regulation of the NMDAR-mediated component of EPSPs generated in this brain area (Kapur *et al.*, 1997b) and is regulated by presynaptic $GABA_BR$ inhibition whereas the fast component is not. This type of $GABA_BR$-mediated control has been closely linked to the expression of long-term potentiation, with the corresponding lack of $GABA_BR$-mediated sensitivity of the fast component linked to the prevention of epileptiform bursting. Therefore, a reduced fast component, as seen in the immature preparation, would be likely to increase the risk of seizure activity, corresponding to the observed OXO-M-induced epileptiform bursting phenomenon seen in the young animal. Interestingly, Libri *et al.* showed that reduced pre- and postsynaptic $GABA_BR$-mediated inhibition facilitated OXO-M-induced epileptiform bursting in the immature piriform cortical slice preparation (Libri *et al.*, 1998). It may now be proposed that this facilitation may not be solely due to reduced presynaptic $GABA_BR$-mediated inhibition of excitatory terminals (previously

demonstrated in the immature preparation), but also by a corresponding lack of $GABA_BR$-mediated regulation of the slow component of the $GABA_AR$-mediated IPSP.

Contrastingly, another report (Patil & Hasselmo, 1999) showed that, greater mAChR-mediated suppression of fast ($GABA_AR$-mediated) and slow ($GABA_BR$-mediated) postsynaptic inhibitory transmission in the piriform cortex would be required in layer Ib/II (association fibres) than layer I (LOT afferents) for effective associative memory function. Since other reports have shown that the axon collaterals of intrinsic fibres tend to concentrate within layer Ib (Figs. 1.2 & 1.3), before passing back into the deeper layers to synapse with their target neurone(s) (Carmichael *et al.*, 1994; Haberly & Price, 1978), it is reasonable to suggest that the inhibitory responses recorded following '*association fibre*' stimulation in layer Ib by Patil & Hasselmo (1999) were in fact the responses of *intrinsic* fibre activation of inhibitory interneurones in layer II/III of the piriform cortex. This would obviously contradict the results presented here, where mAChR-mediated suppression of fast inhibitory transmission was only seen following stimulation in layer I. A number of reasons for this apparent disparity present themselves: firstly, Patil & Hasselmo (1999) examined the effect of mAChR activation upon both fast ($GABA_AR$-mediated) and slow ($GABA_BR$-mediated) inhibitory processes by interpreting changes observed in the EPSP/IPSP complex rather than isolating fast or slow IPSPs. This approach has the advantage of being closer to physiological reality, in that the transmitter systems normally present in the preparation (other than those being investigated) are still functional. Contrastingly, the approach used in this present study isolated the fast IPSPs by blocking excitatory and slow ($GABA_BR$-mediated) inhibitory transmission, an approach that, compared with that of Patil & Hasselmo (1999), is less physiologically realistic. However, this approach prevented other transmitter systems from affecting the recorded responses and consequently, the effects of mAChR activation upon fast IPSPs were known to be a *direct* mAChR-mediated effect upon the inhibitory terminals rather than being mediated indirectly by release of agents from other systems being affected by mAChR activation. Secondly, the present report has shown that there is difference in the laminar (and developmental) effectiveness of presynaptic $GABA_BR$-mediated inhibition (Section 4.5.5) of the type described by Patil & Hasselmo (1999) that clearly corroborates with these previous results. Finally, the disparity between the results obtained here, describing suppression of layer I-elicited fast IPSPs, not seen by Patil & Hasselmo (1999), may be explained by the fact that Patil & Hasselmo (1999) used adult rats for their study where the fast IPSPs have been shown here to be less inhibited following

mAChR activation than in immature animals and the amplitude of their evoked IPSPs was typically <3 mV at -60 mV resting potential. Thus, any mAChR-mediated inhibition of their fast IPSP amplitude (typically ~35% in the present work) would be <1 mV, a value that would be particularly difficult to measure accurately, if at all, within the constraints of the experimental methods used.

5.7.2 Paired-pulse analysis of fast IPSPs and the effects of OXO-M

As previously explained (Section 4.5), a greater degree of PPF is an indication of larger amounts of Ca^{2+} entering the presynaptic terminal with the conditioning pulse (P1) and/or consequently more neurotransmitter being made available for release. Therefore the greater degree of facilitation observed in control conditions following layer I stimulation in the adult or immature preparations indicated that there was greater transmitter release from layer I terminals than layer II/III terminals. This correlated with the observation that individual fast IPSPs elicited following layer II/III stimulation were of a smaller amplitude than equivalent fast IPSPs elicited following stimulation in layer I and suggested that the smaller amplitude was most probably due to reduced transmitter release rather than a reduced postsynaptic sensitivity to released transmitter. The same reasoning may be applied to the reduced fast IPSP amplitude seen in the immature preparation compared with the adult, again corroborating the results obtained following single pulse responses.

Application of OXO-M had no effect upon the paired-pulse responses obtained following layer II/III stimulation, confirming earlier results (Sections 5.2 and 5.3) and indicating a relative absence of presynaptic mAChRs on these terminals. In contrast, the results showing mAChR-modulation of layer I-evoked fast IPSPs were confirmed by the paired-pulse data showing increased PPF in the presence of OXO-M. This supported the idea that OXO-M was activating presynaptic inhibitory mAChRs that were reducing the amount of neurotransmitter released by the first conditioning pulse and consequently proportionally increasing the probability of neurotransmitter release by the second pulse. This reduced neurotransmitter release presumably left more neurotransmitter containing vesicles bound to the terminal membrane ready for release following the second pulse (Stuart & Redman, 1991). The relatively greater increase in PPF following the application of OXO-M seen in the immature preparation suggests the presence of greater numbers and/or more effective inhibitory presynaptic mAChRs than in the adult and corroborates the observation that, following a single pulse, fast inhibitory

neurotransmission was more inhibited following mAChR activation in the immature than the adult preparation.

This investigation into laminar and developmental differences of fast inhibitory synaptic responses in control conditions and following mAChR activation has provided further details critical to our understanding of the mAChR agonist-induced epileptiform burst firing phenomenon seen in the immature slice preparation. A number of previous studies have shown that reduced levels of GABA-ergic inhibition in the piriform cortex have considerable effects upon epileptogenesis in this brain region (Bloms-Funke *et al.*, 1999; Gernert *et al.*, 2000; Kanter & Haberly, 1993). Additionally, in a different study, GABA-producing mouse cortical neurones were transplanted into the median piriform cortex and the effect of this procedure upon kindling thresholds investigated (Gernert *et al.*, 2002). It was found that the transplanted GABA-producing cells had increased both seizure threshold and latency to first seizure, results that clearly implicate changes in GABA-ergic transmission in epileptogenesis. Interestingly, a similar effect has been shown to occur naturally, following kindling in rat forebrain (including piriform cortex), where the number of gamma-aminobutyric acid transporter-1 (GAT-1) immunoreactive neurones was significantly increased in number following corticotrophin-releasing hormone-induced seizures (Orozco-Suarez *et al.*, 2000).

The present study has therefore confirmed previous reports (Forti *et al.*, 1997) and contributed further to the general understanding of the role played by $GABA_AR$-mediated synaptic transmission in seizures. The reduced levels of fast $GABA_AR$-mediated synaptic transmission and the greater mAChR-mediated suppression of that transmission in dendritic regions, in the immature piriform cortical brain slice preparation, was integral to the generation and maintenance of the circuitry required for epileptiform activity and the results presented herein not only further our understanding of this novel model of epileptiform bursting (Postlethwaite *et al.*, 1998a) but also provide additional context in which to consider other reports describing mAChR agonist-mediated effects reported in the piriform cortex (Gruslin *et al.*, 1999) and other cortical areas (Kimura & Baughman, 1997).

5.7.3 Rostro-caudal variations in GABA-ergic responsiveness in the piriform cortical slice preparation: possible implications

A limited number of studies have investigated the distribution of GABA-ergic neurones within the piriform cortex using immunocytochemical staining techniques (Haberly *et al.*, 1987; Loscher *et al.*, 1998). These studies agree that the majority of GABA-ergic

neurones are located within layer I (~50%), with ~5% and ~15% in layers II and III respectively. These values clearly correlate with the results obtained in this present study where fast IPSPs elicited following stimulation in layer I were found to be considerably larger than those elicited following stimulation in layers II/III. More pertinently, the study performed by Löscher *et al.* (1998) demonstrated that the area defined as the MPC in this study contains a significantly greater number of GABA-ergic neurones in layers II/III than the APC or PPC. This result also correlates well with the present observations, since reduced $GABA_AR$-mediated responses were observed following stimulation in layers II/III of the APC and PPC compared with equivalent results elicited from the MPC. These results also support another report that demonstrated an absence of GABA-ergic cartridge endings, few cholecystokinin-positive basket cells and very little GAT-1 immunoreactivity in the ventro-rostral anterior piriform cortex (Ekstrand *et al.*, 2001b) (also referred to as the *area tempestas* (Piredda & Gale, 1985)). Unfortunately, their investigation only examined areas of the APC and consequently data from the MPC and PPC are not available. Within layers II/III the numbers of afferent and association fibre terminals have been found to be at their highest levels (Haberly *et al.*, 1987; Haberly & Presto, 1986; Satou *et al.*, 1983d) and in light of the results of this present study and those of Löscher *et al.* (1998), it would be reasonable to postulate that the increased density of GABAergic neurones in the MPC form an inhibitory '*barrier*' that acts to disrupt feed-forward (anterior to posterior) and feed-back (posterior to anterior) excitatory circuits that meet in the MPC and thereby prevent the occurrence of epileptiform bursting activity, a hypothesis certainly supported by kindling studies within the MPC demonstrating this phenomenon (Loscher & Ebert, 1996).

5.8 Summary

1. Fast, $GABA_AR$-mediated IPSPs elicited following stimulation in layer Ia of the transverse piriform cortical preparation were found to be significantly larger in amplitude than equivalent IPSPs elicited following stimulation in layers II/II in both the adult and immature preparations.

2. Fast, $GABA_AR$-mediated IPSPs elicited following stimulation in either layer I or layers II/III were found to be significantly larger in the adult than the immature piriform cortical brain slice preparation.

3. mAChR activation by 10 μM OXO-M significantly depressed fast IPSPs elicited following stimulation in layer I, but not layer II/III in both the adult and immature piriform cortical slice preparations. This depression was significantly less in the adult than in immature slices.

4. OXO-M-induced inhibition of fast inhibitory synaptic transmission, elicited following stimulation in layer I was found to be mediated by M1-type mAChRs in adult preparations and by M2-type mAChRs in immature slices.

5. Increased paired-pulse facilitation in the presence of 10 μM OXO-M confirmed the presynaptic mechanism of action of the observed mAChR-mediated suppression of fast inhibitory synaptic transmission in layer I and accorded with the differences in degrees of suppression seen between the adult and immature preparations.

6. No variation in the magnitude of fast IPSPs, elicited following stimulation in layer I was found when the location of the recording microelectrode was varied, rostro-caudally along the slice preparation. The degree of mAChR–mediated inhibition of fast IPSPs elicited following stimulation in layer I was also unaffected by changes in recording position.

7. The magnitudes of fast IPSPs elicited from the APC and PPC following stimulation in layers II/III were found to be significantly smaller than those elicited from the MPC in the adult, but not the immature preparation.

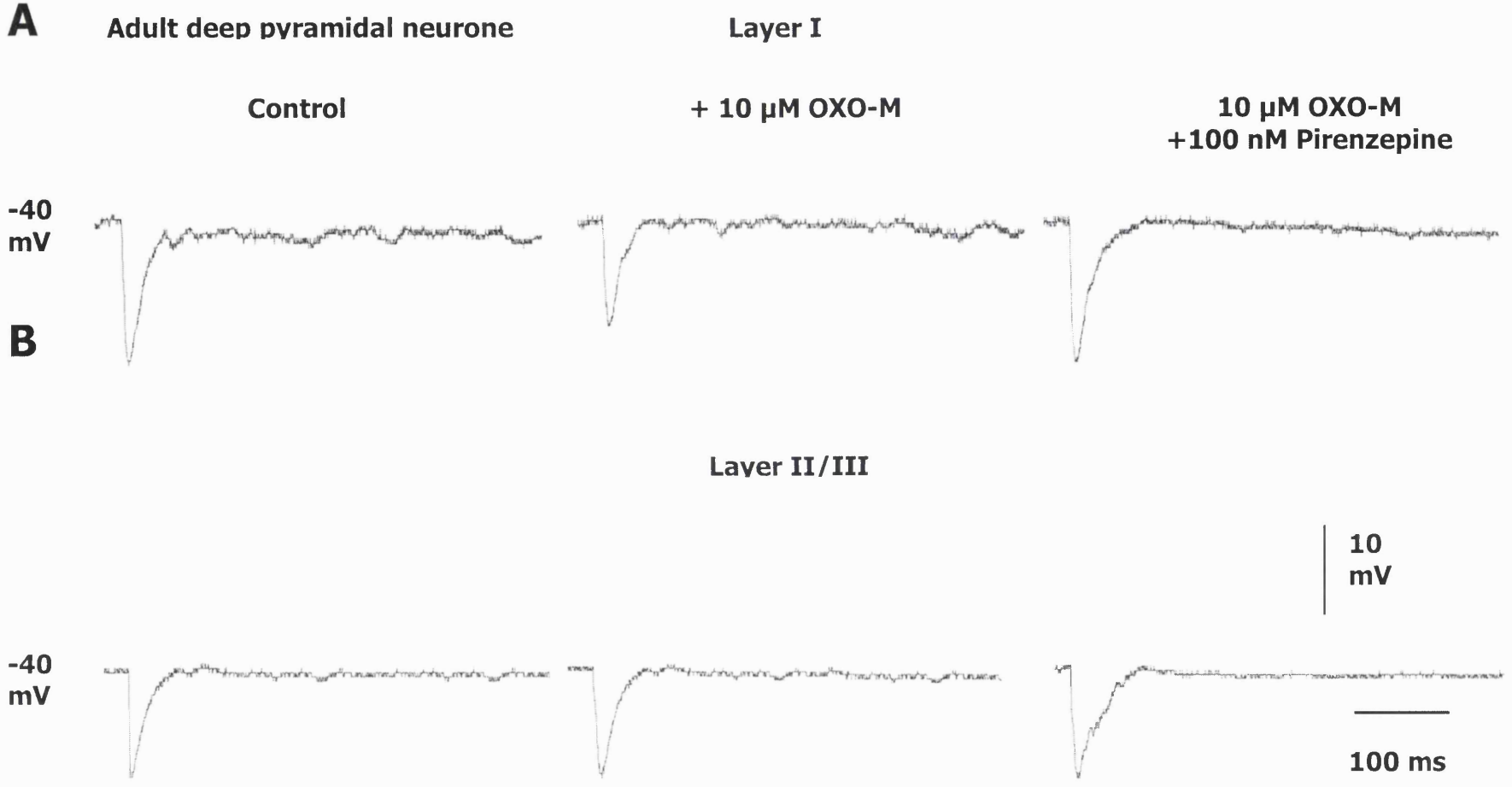
A
Adult deep pyramidal neurone
Layer I
Control
+ 10 μM OXO-M
10 μM OXO-M
+100 nM Pirenzepine
-40
mV
B
Layer II/III
10
mV
-40
mV
100 ms

Figure 5.1

Figure 5.1

Isolated fast, $GABA_AR$-mediated IPSPs elicited by stimulating electrodes situated in layer I (**top**; 6 V; 0.2 ms stimulus) and in layer II/III (**bottom**; 4 V; 0.2 ms stimulus) of an adult piriform cortical slice and recorded from a presumed deep pyramidal neurone in control conditions (**left panels**), following the application of 10 μM OXO-M (**middle panels**) and in 10 μM OXO-M plus 100 nM pirenzepine (**right panels**). 10 μM DL-APV, 20 μM CNQX and 1 μM CGP-52432 were also present in the bathing medium to block glutamatergic and $GABA_BR$-mediated transmission respectively, thereby isolating the fast, $GABA_AR$-mediated IPSP. Resting potential=-83 mV in control conditions. The cell was held at -40 mV by the injection of steady positive current through the recording microelectrode during IPSP recording. Note the inhibition of the layer I-evoked fast IPSP by OXO-M (**top middle**) and its reversal by the M1 mAChR-specific antagonist, pirenzepine (**top right**). In contrast, the fast IPSP evoked following layer II/III stimulation was unaffected by OXO-M (**bottom middle**). Note, the fast IPSP evoked in control solution following layer I stimulation was significantly larger than that elicited following layer II/III stimulation. Membrane potential changes caused by OXO-M were compensated for by the injection of current through the recording electrode.

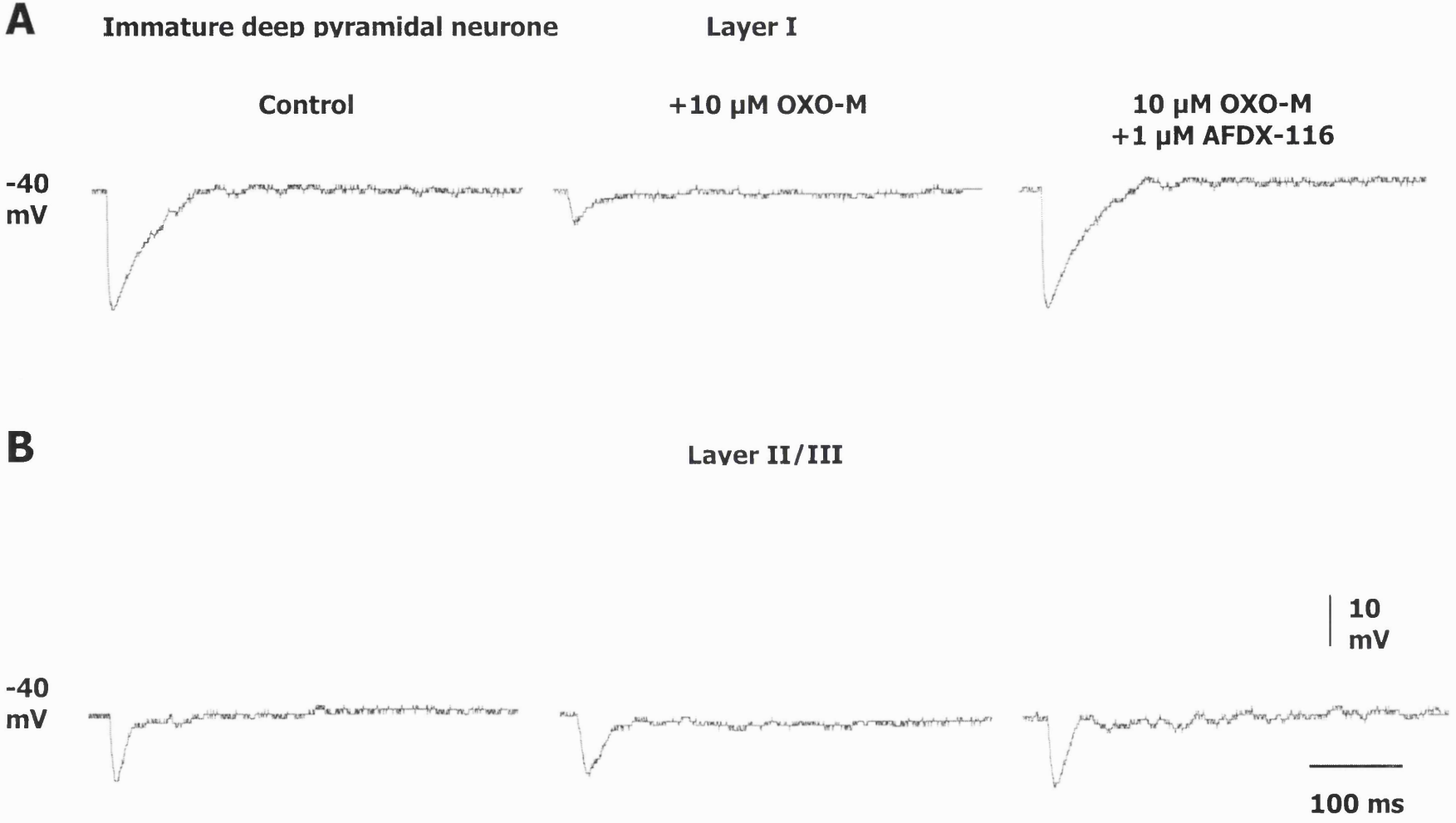
A
Immature deep pyramidal neurone
Layer I
Control
+10 µM OXO-M
10 µM OXO-M
+1 µM AFDX-116
-40
mV
B
Layer II/III
10
mV
-40
mV
100 ms

Figure 5.2

Figure 5.2

Isolated fast, $GABA_AR$-mediated IPSPs elicited by stimulating electrodes situated in layer I (**top**; 6 V; 0.2 ms stimulus) and in layer II/III (**bottom**; 4 V; 0.2 ms stimulus) of an immature (P+15) piriform cortical slice and recorded from a presumed deep pyramidal neurone in control conditions (**left panels**), following the application of 10 μM OXO-M (**middle panels**) and in 10 μM OXO-M plus 1 μM AFDX-116 (**right panels**). 10 μM DL-APV, 20 μM CNQX and 1 μM CGP-52432 were also present in the bathing medium to block glutamatergic and $GABA_BR$-mediated transmission. Resting potential=-81 mV in control conditions. The cell was held at -40 mV by positive current injection during IPSP recording. Note the strong inhibition of the layer I-evoked IPSP by OXO-M (**top middle**) and its reversal by the M2 mAChR-specific antagonist, AFDX-116 (**top right**). In contrast, the fast IPSP evoked following layer II/III stimulation was unaffected by OXO-M (**bottom middle**). Note the IPSP evoked following layer I stimulation was larger than that elicited following layer II/III stimulation. The proportional degree of suppression of layer I-evoked fast IPSPs by OXO-M in the immature preparation was also greater than that observed in the adult (Fig. 5.1). Membrane potential changes caused by OXO-M were compensated for by the injection of current through the recording electrode.

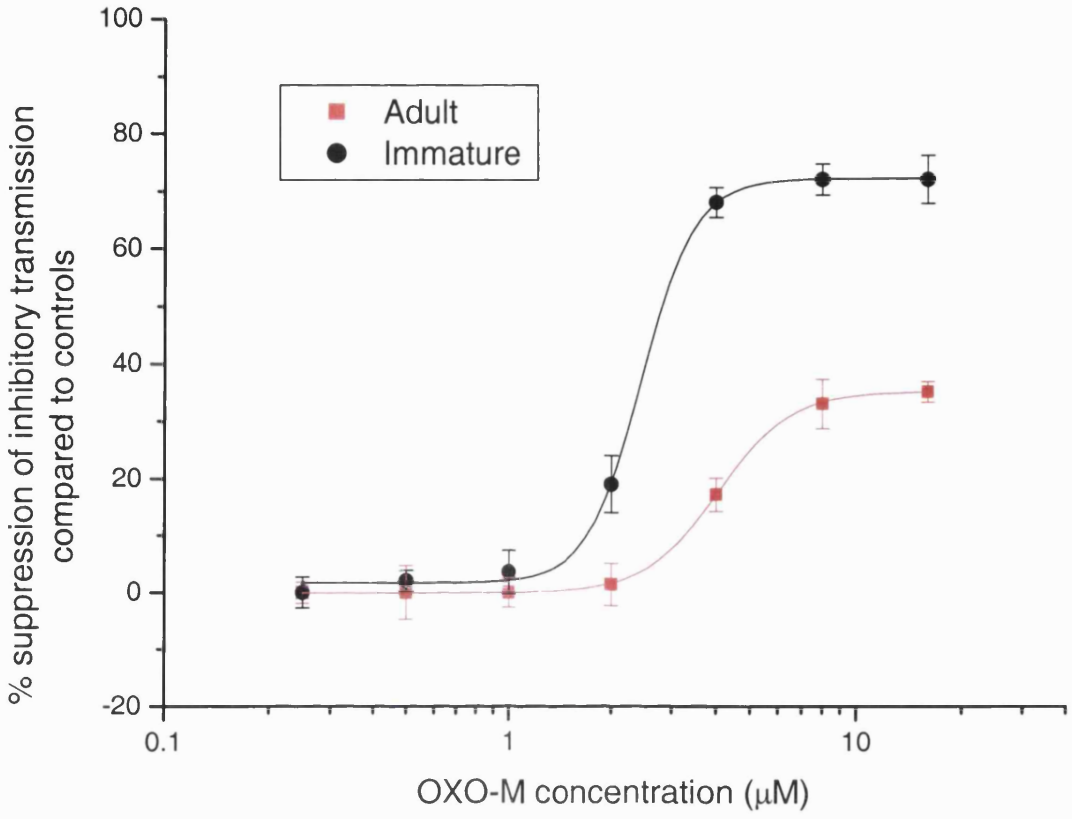
100
80
60
40
20
0
-20
0.1
1
10
% suppression of inhibitory transmission compared to controls
OXO-M concentration (μM)
Adult
Immature

Figure 5.3

Figure 5.3

Log dose-response curves showing the effect of varied concentrations of OXO-M (0.5 - 16 μM) upon mean peak IPSP amplitude elicited following layer I stimulation, of adult (**red**; n=5) or immature (**black**; n=6) presumed deep pyramidal neurones. Ordinate shows percentage suppression of layer I-evoked inhibitory transmission induced by OXO-M compared to controls. ED_{50} values for OXO-M, estimated from these plots were 2.5 μM in the immature preparation and 4.0 μM in the adult, indicating a greater muscarinic sensitivity of layer I inhibitory synaptic terminals in the immature slice preparation. Curves were fitted using a least squares fit equation and calculated mean confidence intervals for each data set (adult=93%; immature=97.5%). One-way ANOVA significance tests showed a significant difference ($P<0.05$) between the adult and immature ED_{50} values. Curve fitting, (using an arbitrary logistical equation provided by Origin plotting software) confidence intervals and significance test were performed by Origin plotting and analysis software (Microcal Inc, MA, USA).

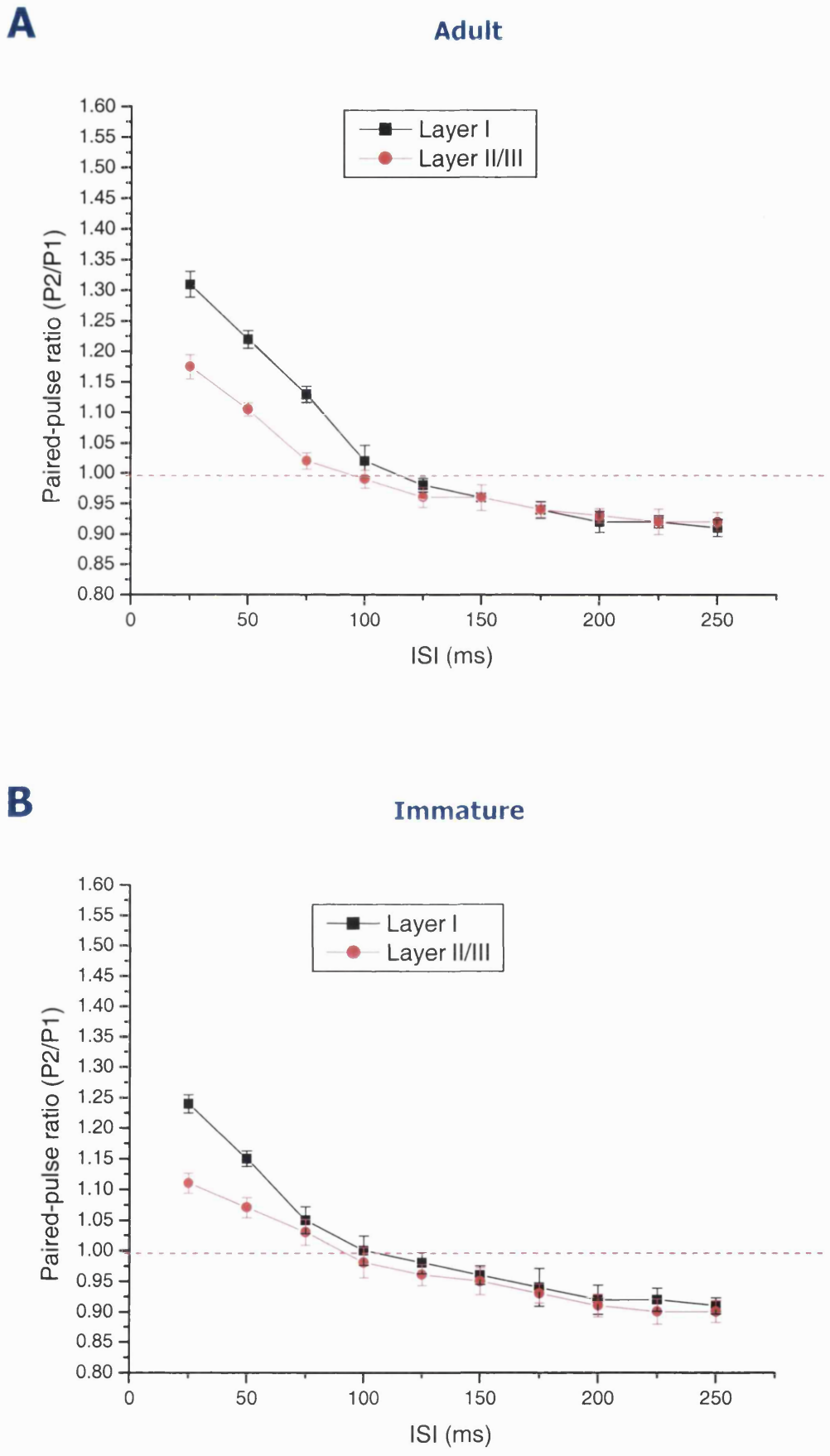
A
Adult
Layer I
Layer II/III
Paired-pulse ratio (P2/P1)
ISI (ms)
B
Immature
Layer I
Layer II/III
Paired-pulse ratio (P2/P1)
ISI (ms)

Figure 5.4

Figure 5.4

Paired-pulse ratios (second pulse magnitude/first pulse magnitude; P2/P1), calculated from recordings made from presumed deep pyramidal neurones and plotted *vs.* inter-stimulus interval (ISI; ms) following layer I (**black**) or layer II/III (**red**) stimulation in **A.** adult (n=14) and **B.** immature (n=16) piriform cortical slices. All paired-pulse stimuli were elicited from a set membrane potential of -40 mV, maintained by injection of positive holding current through the recording microelectrode. Note the reduced degree of paired-pulse facilitation following layer II/III fibre stimulation compared with layer I stimulation in both adult and immature slices. Additionally, the degree of facilitation following layer I stimulation was found to be greater in the adult than the immature preparation.

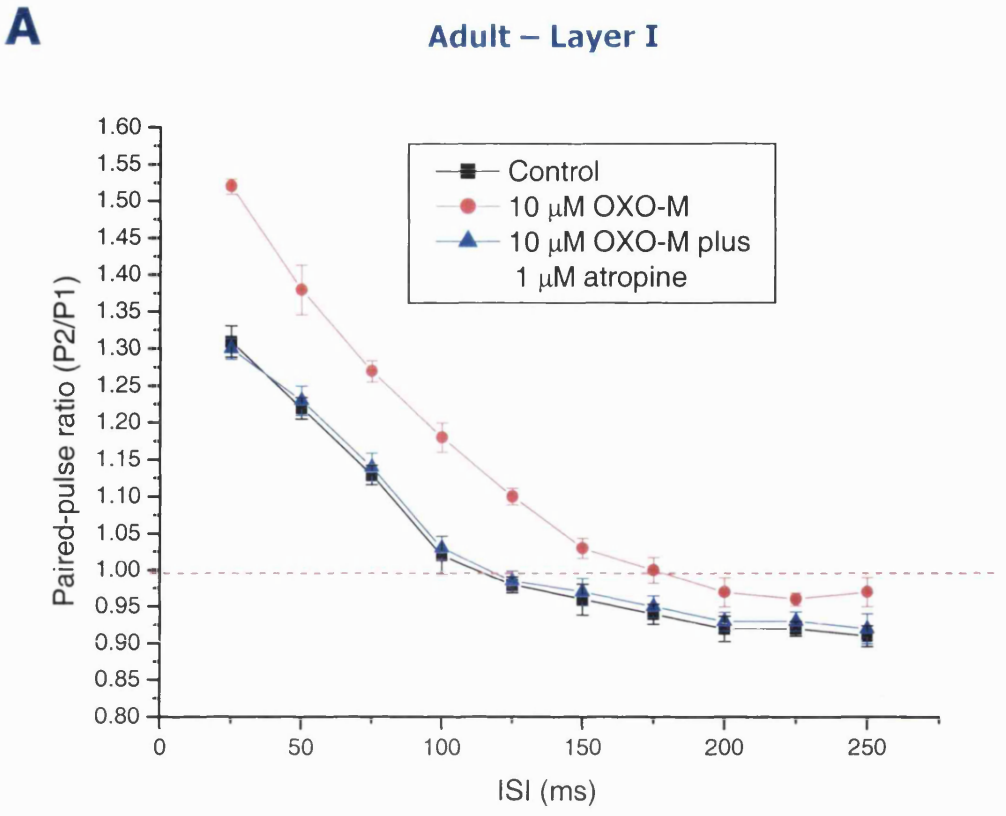
A
Adult – Layer I
Control
10 μM OXO-M
10 μM OXO-M plus
1 μM atropine
Paired-pulse ratio (P2/P1)
1.60
1.55
1.50
1.45
1.40
1.35
1.30
1.25
1.20
1.15
1.10
1.05
1.00
0.95
0.90
0.85
0.80
0
50
100
150
200
250
ISI (ms)

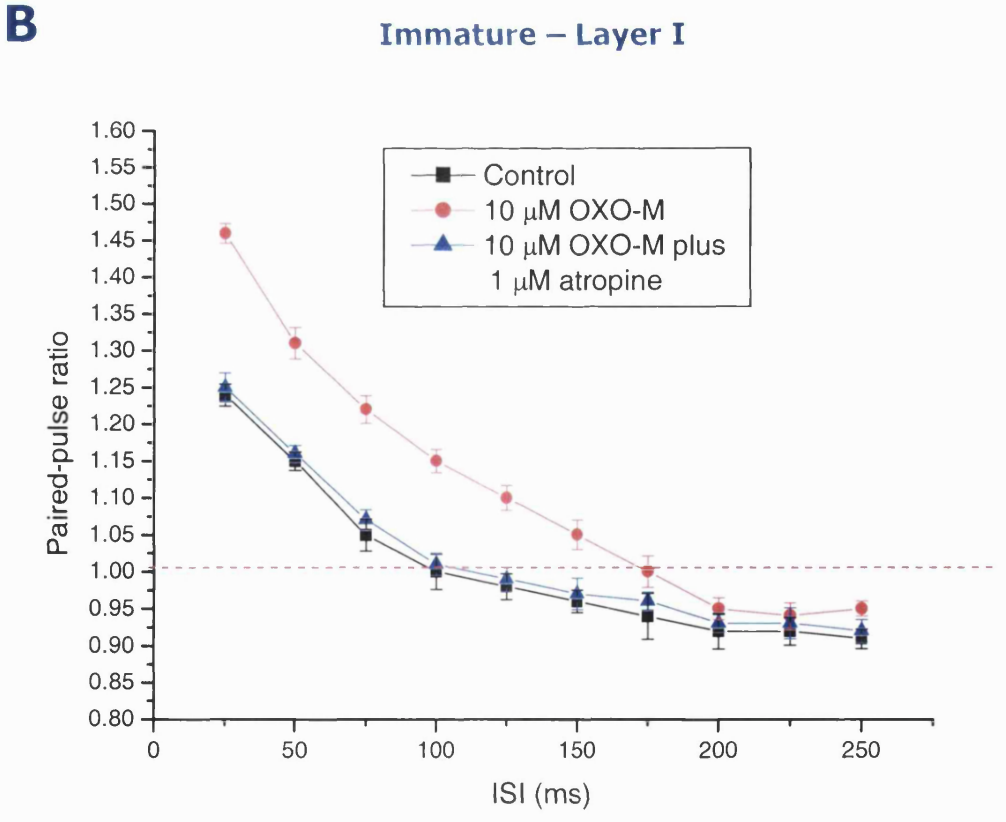
B
Immature – Layer I
Control
10 μM OXO-M
10 μM OXO-M plus
1 μM atropine
Paired-pulse ratio
1.60
1.55
1.50
1.45
1.40
1.35
1.30
1.25
1.20
1.15
1.10
1.05
1.00
0.95
0.90
0.85
0.80
0
50
100
150
200
250
ISI (ms)

Figure 5.5

Figure 5.5

Paired-pulse ratios (second pulse magnitude/first pulse magnitude; P2/P1) calculated from recordings made from presumed deep pyramidal neurones and plotted *vs.* inter-stimulus interval (ISI; ms) following layer I stimulation in control conditions (**black**), in 10 μM OXO-M (**red**) and in OXO-M *plus* 1 μM atropine (**blue**) in **A.** adult (n=14) and **B.** immature (n=16) piriform cortical slices. All paired-pulse stimuli were elicited from a set membrane potential of -40 mV. Note that OXO-M increased the degree of paired-pulse facilitation observed in both the adult and immature preparations, a change that was fully reversed by 1 μM atropine (or 40 minutes washout; not shown).

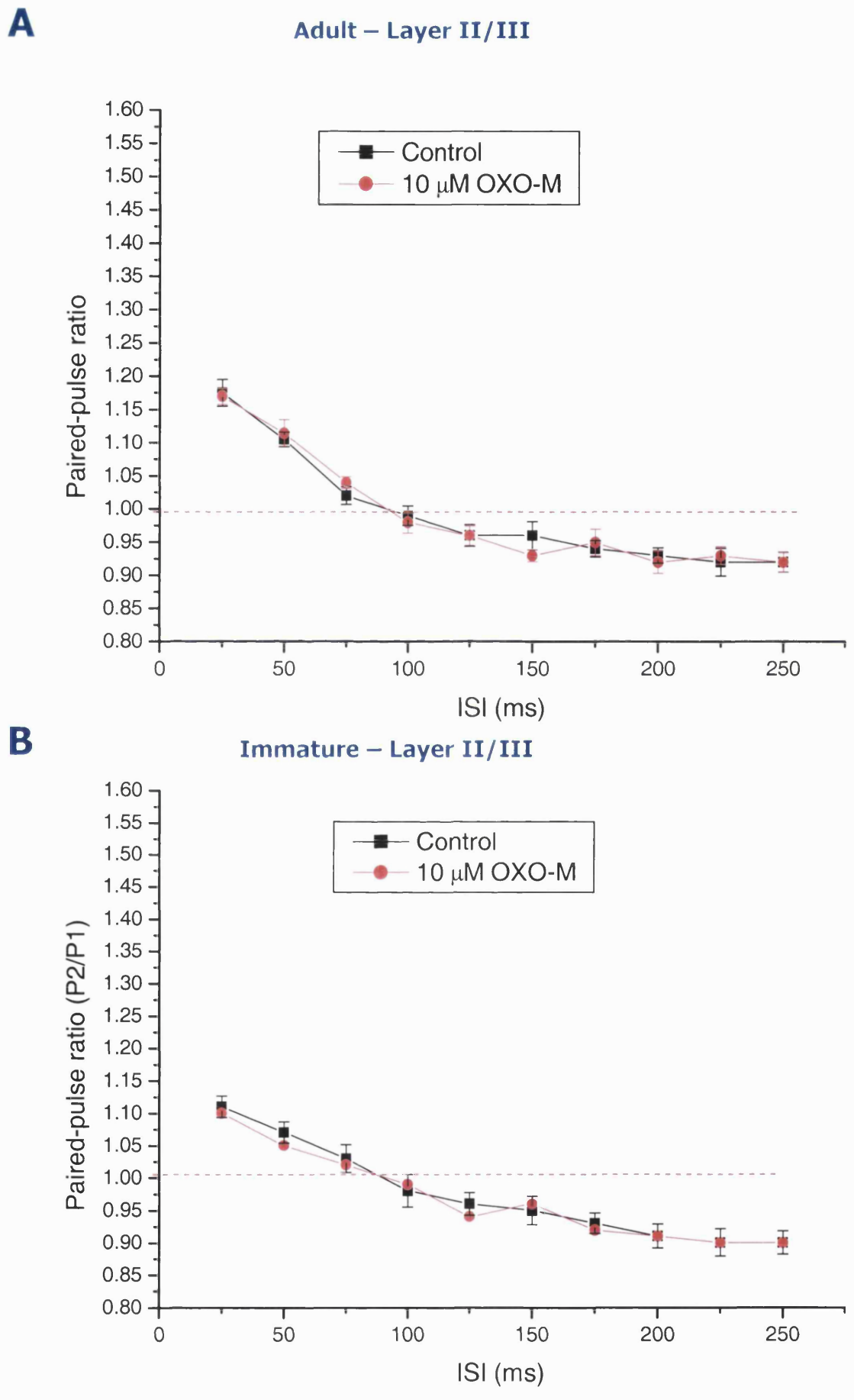
A
Adult – Layer II/III
Control
10 μM OXO-M
Paired-pulse ratio
ISI (ms)
B
Immature – Layer II/III
Control
10 μM OXO-M
Paired-pulse ratio (P2/P1)
ISI (ms)

Figure 5.6

Figure 5.6

Paired-pulse ratios (second pulse magnitude/first pulse magnitude; P2/P1) calculated from recordings made from presumed deep pyramidal neurones and plotted *vs.* inter-stimulus interval (ISI; ms) following layer II/III stimulation in control conditions (**black**) and in 10 μM OXO-M (**red**) from **A.** adult (n=14) and **B.** immature (n=16) piriform cortical slices. All paired-pulse stimuli were elicited from a set membrane potential of -40 mV. Note the absence of a significant increase in PPF in OXO-M in either adult or immature preparations.

Table 5.1

Region	APC	MPC	PPC
Mean IPSP amplitude (mV) Layer I; adult	17 ± 0.9 (n=4)	18 ± 0.7 (n=14)	19 ± 1.0 (n=5)
Mean IPSP amplitude (mV) Layer I; immature	9 ± 0.6 (n=4)	9 ± 0.3 (n=16)	10 ± 0.8 (n=4)
Mean IPSP amplitude (mV) Layer II/III; adult	8 ± 1.0 (n=4)	13 ± 0.8 (n=14)	7 ± 0.9 (n=5)
Mean IPSP amplitude (mV) Layer II/III; immature	4 ± 1.1 (n=4)	5 ± 0.4 (n=16)	4 ± 1.3 (n=4)
% suppression of IPSP by OXO-M Layer I; adult	41 ± 6.2 (n=4)	35 ± 5.5 (n=14)	39 ± 5.8 (n=5)
% suppression of IPSP by OXO-M Layer I; immature	68 ± 7.3 (n=4)	72 ± 5.2 (n=16)	73 ± 6.4 (n=4)

Table 5.1

Differences in mean IPSP amplitudes (±SEM) in layer I and layer II/III of adult and immature piriform cortical brain slices, and their dependence on rostro-caudal recording position. Variation in recording position changed the magnitude of IPSPs evoked following stimulation in layer II/III but not layer I. Fast IPSPs elicited from the APC or PPC, in control conditions, following stimulation in layers II/III were found to be significantly smaller than those elicited from the MPC ($P<0.05$; Students t-tests). The magnitude of fast IPSPs recorded following stimulation in layer II/III in the presence of 10 μM OXO-M were unchanged from control values. Variation in recording location had no effect upon layer I-evoked IPSPs in control or in 10 μM OXO-M, from adult or immature slice preparations. **APC**: anterior piriform cortex; **MPC**: median piriform cortex; **PPC**: posterior piriform cortex. n=number of neurones.

Table 5.2

	Adult Layer I		Adult Layer II/III		Immature Layer I		Immature Layer II/III	
Measurement	Rate of Rise (mV/ms)	Half width (ms)	Rate of Rise (mV/ms)	Half width (ms)	Rate of Rise (mV/ms)	Half width (ms)	Rate of Rise (mV/ms)	Half Width (ms)
Control	0.5 ± 0.3	60 ± 12	0.7 ± 0.2	81 ± 14	0.6 ± 0.2	56 ± 13	0.7 ± 0.3	54 ± 15
10μM OXO-M	0.7 ± 0.2	71 ± 12	0.8 ± 0.45	56 ± 11	0.4 ± 0.3	71 ± 15	0.9 ± 0.1	66 ± 13
10μM OXO-M plus 1μM Atropine	0.6 ± 0.34	58 ± 13	0.7 ± 0.3	67 ± 18	0.8 ± 0.3	69 ± 11	0.9 ± 0.4	55 ± 16

Table 5.2

Kinetics of IPSPs in layer I or layer II/III in adult and immature piriform cortex slices in control, OXO-M or OXO-M plus atropine. The results shown were obtained from the first (conditioning) pulse of a paired-pulse protocol or a single, isolated pulse. During paired pulse experiments, individual stimuli were applied to produce IPSPs recorded at a membrane potential held (by positive current injection) at –40 mV. The rate of rise of the conditioning pulse was calculated from stimulus application to IPSP peak, whilst the half-width was calculated as the time interval between the two points at which the trace was at 50% of the maximal IPSP amplitude. Each value represents the mean ± SEM. For the adult preparation, n=18, for the immature preparation, n=20.

Chapter 6:

The effects of a range of anticonvulsants upon excitatory synaptic transmission in immature and adult deep pyramidal piriform cortical neurones

6.1 Introduction

Following earlier results presented in this report describing the postsynaptic effects of a number of anticonvulsants upon OXO-M-induced epileptiform bursting phenomenon in immature slices (Section 3.5), the possible effects of the same anticonvulsants upon evoked EPSPs were also investigated. It was hoped that a comparison of the effects of these anticonvulsants against their known mechanisms of action might provide a greater understanding of the mechanisms that underlie this epileptiform bursting phenomenon. The effects of the anticonvulsants upon EPSPs, elicited following L1 or intrinsic fibre stimulation (see Chapter 4 for details), were investigated in control conditions and in the presence of 10 μM OXO-M in immature presumed deep pyramidal neurones displaying epileptiform bursting characteristics. All figures of synaptic potentials shown comprise the averages of at least 3 traces, unless otherwise indicated. All EPSPs were elicited from a membrane potential of -90 mV, maintained by steady negative current injection. Recorded cells were electrophysiologically characterized as presumed deep pyramidal neurones by the criteria described in Section 3.2.1. Significant differences between data sets in this chapter were calculated using non-parametric Wilcoxon signed rank tests unless explicitly stated otherwise.

6.2 Gabapentin

Gabapentin (GPN; 30 μM; n=10; Section 3.5.1) was designed as an analogue of the inhibitory neurotransmitter, GABA, that would mimic the actions of the endogenous transmitter (Upton, 1994). However, it has been shown not to affect ligand binding to $GABA_ARs$, $GABA_BRs$ or the benzodiazepine binding site (Ramsay, 1993), but to act upon an binding site specific to GPN on the alpha2delta-1 subunit of a voltage-dependent Ca^{2+}-channel (Luo Z.D. *et al.*, 2003)) found in brain areas containing major excitatory inputs.

GPN (30 μM) inhibited subthreshold EPSPs (elicited following intrinsic fibre stimulation) by 22 ± 5.7% when applied alone and by 36 ± 8.4% ($P<0.05$ *vs.* GPN alone; Fig. 6.1A) when applied to bathing medium already containing 10 μM OXO-M. Conversely, sub- and suprathreshold EPSPs, elicited following the stimulation of L1 fibres, were unaffected by GPN in either control conditions or the presence of 10 μM OXO-M (not shown), although the superimposed repetitive spike firing frequently seen (5/10 cells) following L1 fibre stimulation in the presence of 10 μM OXO-M was sometimes abolished (3/5 cells). It is unlikely that this was due to synaptic effects, since

the L1 fibre elicited EPSPs were unaffected by GPN in control conditions. The observed effects of GPN were fully reversed following 40 minutes washout.

6.3 Lamotrigine

It has been proposed, (Section 3.5.2) that the anticonvulsant action of lamotrigine (LTG; 2 μM; n=5) is due to its ability to block voltage gated Na^+-channels at presynaptic sites, thus stabilizing the presynapse and consequently reducing the release of synaptic transmitters (Cunningham & Jones, 2000; Upton, 1994). It has also been shown to inhibit the slow inactivated Na^+ channel thereby acting selectively against high frequency epileptiform discharges (Schacter, 1995) and to increase GABA release in rat entorhinal cortex, *in vitro* (Cunningham & Jones, 2000). Subthreshold EPSPs elicited following L1 (48 ± 4.2%; not shown) or intrinsic (51 ± 5.7%; Fig. 6.1B) fibre stimulation in the presence of 2 μM LTG were significantly inhibited ($P<0.01$ for both L1 and intrinsic fibre elicited EPSPs) compared to controls. There was no significant difference ($P>0.05$; L1 *vs.* intrinsic in 2μM LTG) between the suppression of excitatory transmission observed following either L1 or intrinsic fibre stimulation. After addition of 2 μM LTG cells displaying established epileptiform bursting (in OXO-M), subthreshold EPSPs evoked following L1 fibre stimulation were inhibited by 24 ± 8.2%, significantly less ($P<0.05$) than the degree of LTG-induced L1 fibre suppression observed in the absence of OXO-M. Additionally, the superimposed repetitive firing (4/5 cells) seen in L1 fibre elicited EPSPs (Section 4.3.2) was consistently abolished (4/4 cells). Subthreshold EPSPs evoked following intrinsic fibre stimulation in the presence of OXO-M plus LTG were inhibited by 71 ± 8.7%, a significantly greater ($P<0.05$; Fig. 6.1B) degree of suppression than that observed following the application of LTG alone. The observed effects of LTG were fully reversed following 40 minutes washout.

6.4 Topiramate

Topiramate (TPM; 20 μM; n=14; Section 3.5.3) has been shown affect voltage-activated sodium channels (in a state dependent manner similar to that of carbamazepine), some voltage-dependent Ca^{2+} channels (Shank *et al.*, 2000), $GABA_A$-receptors (Rogawski & Porter, 1990) and AMPA/kainate neuronal ion channels (Pina-Garza & McLean, 1996) whilst also weakly inhibiting some isozymes of carbonic anhydrase (Dodgson *et al.*, 2000). Subthreshold EPSPs elicited following L1 fibre stimulation in the presence of 20 μM TPM were significantly inhibited (21 ± 7.2%; $P<0.05$; not shown) compared with controls. In the presence of 20 μM TPM plus 10 μM OXO-M subthreshold EPSPs

elicited following L1 fibre stimulation were significantly less inhibited (9 ± 6.1%; P<0.05; not shown) than those elicited in the presence of 20 μM TPM alone. Interestingly, subthreshold EPSPs elicited following stimulation of intrinsic fibres were also inhibited (26 ± 5.3%; Fig. 6.2A) in the presence of 20 μM TPM alone, but significantly further inhibited (44 ± 8.9%; Fig 5.8A; P<0.05 compared with 20 μM TPM alone) in the presence of 20 μM TPM plus 10 μM OXO-M. The observed effects of TPM were fully reversed following 40 minutes washout.

6.5 Carbamazepine

Carbamazepine (CBZ; 50 μM; n=9; Section 3.5.4) exerts its anticonvulsant effect by preferentially binding to Na^+ channels in their inactive state (Schacter, 1995). CBZ (50 μM) did not affect subthreshold EPSPs elicited following either L1 or intrinsic fibre stimulation (not shown). However, suprathreshold EPSPs elicited following either L1 (Fig. 6.2B; left panel) or intrinsic (not shown) fibre stimulation were consistently inhibited, such that an action potential could not be elicited (even with increased stimulus intensities; Fig. 6.2B; middle panel) in the presence of 50 μM CBZ. This effect was reversible on drug washout (Fig. 6.2; right panel) and was likely to be due to the blockade of pre- and/or postsynaptic voltage-dependent sodium channels, preventing action potential firing. In the presence of 10 μM OXO-M plus 50 μM CBZ, suprathreshold EPSPs elicited following L1 or intrinsic fibre stimulation were again inhibited and presented as subthreshold responses (not shown). Subthreshold EPSPs elicited following L1 fibre stimulation, in 10 μM OXO-M plus 50 μM CBZ, were unaffected whilst those elicited following intrinsic fibre stimulation were significantly inhibited (27 ± 6.2%; P<0.05 compared with controls) by the same degree as seen in the presence of 10 μM OXO-M alone. The observed effects of CBZ were fully reversed following 40 minutes washout.

6.6 Felbamate

Felbamate (FBM; 300 μM; n=5; Section 3.5.5) is thought to exert its anticonvulsant effects primarily via NMDA receptor blockade. However other mechanisms of action have been proposed, such as the blockade of Na^+ channels, Ca^{2+} channels, potentiation of GABA-mediated inhibition, inhibition of carbonic anhydrase and adenosine uptake (Burdette & Sackellares, 1994; Pisani *et al.*, 1995). Subthreshold EPSPs evoked in the presence of 300 μM FBM were significantly inhibited compared to controls whether they were evoked following L1 (57 ± 6.1%; P<0.05 *vs.* control; not shown) or intrinsic

(41 ± 4.8%; P<0.05 *vs.* control; Fig. 6.3A) fibre stimulation. The different degrees of suppression shown by the two inputs were found to be slightly, but significantly different from one another (P<0.05). When subthreshold EPSPs were evoked in the presence of 10 μM OXO-M plus 300 μM FBM, the inhibition of intrinsically evoked EPSPs was significantly increased (79 ± 9.1% compared to controls; P<0.05 *vs.* in 300 μM FBM alone; Fig 6.3A), whilst the degree of suppression found in L1 fibre-evoked EPSPs was reduced (35 ± 7.5%; P<0.05 *vs.* in 300 μM FBM alone; not shown). The observed effects of FBM were fully reversed after 40 minutes washout.

6.7 Phenobarbitone

Phenobarbitone sodium (PBN; 50 μM; n=7; Section 3.6.6), binds to GABA-mediated Cl^- channels in an '*open*' state, thereby prolonging channel lifetime (Upton, 1994) and therefore enhancing inhibition. Interestingly, sub- and suprathreshold EPSPs evoked following L1 fibre stimulation in the presence of PBN (50 μM) were unchanged in magnitude and appearance from those elicited in control conditions. However, subthreshold EPSPs elicited following intrinsic fibre stimulation in the presence of 50 μM PBN were slightly, but significantly inhibited (11 ± 6.1%; P<0.05 *vs.* controls) and further inhibited (21 ± 7.2%; P<0.05 *vs.* PBN alone and *vs.* controls) in the presence of 10 μM OXO-M plus 50 μM PBN (Fig. 6.3B). Contrastingly, EPSPs elicited following L1 fibre stimulation, in the presence of 10 μM OXO-M plus 50 μM PBN were unaffected. The observed effects of PBN were fully reversed after 40 minutes washout.

6.8 Discussion

In chapter 3 the postsynaptic effects of a range of anticonvulsants upon OXO-M-induced epileptiform bursting activity were examined in immature rat piriform cortical slices (Section 3.5) and the implications of these results on our understanding of the bursting phenomenon and the types of epilepsy this model might best represent, where discussed. In order to gain further insight into these mechanisms, the effects of these anticonvulsants upon excitatory (afferent and intrinsic) synaptic transmission, in both control conditions and in the presence of 10 μM OXO-M (in neurones displaying established bursting characteristics) were also examined. A summary of the data are presented in Table 6.1.

6.8.1 Gabapentin

Gabapentin alone, suppressed intrinsic fibre-elicited excitatory synaptic transmission but had no effect upon L1 fibre-elicited EPSPs (Table 6.1). This selective suppression of intrinsic fibre-mediated transmission was increased in the presence of OXO-M, probably due to the additional suppression of transmission via presynaptic mAChRs (Chapter 4). GPN has been shown to bind with high affinity to the alpha(2)delta-1 subunit of voltage-dependent Ca^{2+} channels in certain subgroups of excitatory and inhibitory neurones, thereby inhibiting the release of neurotransmitter and (dependent upon the neurones type inhibited) suppressing excitatory or inhibitory synaptic transmission (van Hooft *et al.*, 2002). This selective presynaptic action of GPN, previously demonstrated in the rat hippocampus and neocortex has here been demonstrated in the piriform cortex by the clearly observed difference in afferent and intrinsic fibre sensitivity to GPN-induced suppression of excitatory transmission.

6.8.2 Lamotrigine

The presynaptic effects of lamotrigine (LTG) have been shown to be produced by the inhibition of voltage-gated Na^{+} channels, thereby reducing neurotransmitter release (Upton, 1994). However, like GPN, LTG affects neurotransmitter release from both excitatory (Calabresi *et al.*, 1999; Calabresi *et al.*, 2000; Wang *et al.*, 1996) and inhibitory (Braga *et al.*, 2002; Cunningham & Jones, 2000) presynapses, consequently making its efficacy difficult to predict since its specificity for particular synapse types (excitatory or inhibitory) varies from tissue to tissue (Braga *et al.*, 2002; Leach *et al.*, 1986). In the present study, LTG inhibited excitatory synaptic transmission following either L1 or intrinsic fibre stimulation equally, although in the presence of 10 μM OXO-M, L1-elicted EPSPs were less inhibited by LTG than in control, whilst intrinsic fibre-

elicited EPSPs were more inhibited (Table 6.1). This disparity in effect was most likely to be due to the difference in the effect of OXO-M upon L1 and intrinsic fibre-mediated transmission (OXO-M potentiated L1 fibre transmission whilst inhibiting intrinsic fibre transmission; Chapter 4), rather than a true difference in the specificity of LTG for different terminals in the presence of OXO-M. The results presented here are consistent with the overall effects of LTG described in previous reports (Calabresi *et al.*, 1999; Cunningham & Jones, 2000) and suggest that it has an equal inhibitory effect upon either L1 or intrinsic fibre mediated excitatory synaptic transmission in the piriform cortex.

6.8.3 Topiramate

Topiramate (TPM) has previously been shown to inhibit AMPAR- and NMDAR-mediated excitatory synaptic transmission (DeLorenzo *et al.*, 2000; White, 1999) and the results of this present study correlated with these prior results. In a manner similar to LTG, both L1 (21 ± 7.2%) and intrinsic (26 ± 5.3%) fibre-elicited EPSPs were comparably suppressed by 20 μM TPM alone. In OXO-M plus TPM, EPSPs elicited following L1 fibre stimulation (9 ± 6.1%) were significantly less suppressed than those elicited following intrinsic fibre stimulation (44 ± 8.9%; $P<0.01$ *vs.* L1 fibre-elicited EPSPs; Table 6.1). This would confirm that the observed effect of TPM upon synaptic responses did not appear to be selective for either of the two primary excitatory inputs of the piriform cortex.

6.8.4 Carbamazepine

Carbamazepine (CBZ) acts as an anticonvulsant primarily by binding to and prolonging the inactive state of voltage-dependent Na^+ channels, thereby inhibiting conduction. However, some reports have suggested that CBZ may also inhibit NMDAR-mediated synaptic transmission (Cunha *et al.*, 2002; Gean *et al.*, 1993). In the present study, although CBZ prevented the firing of action potentials following *suprathreshold* synaptic stimulation (via either L1 or intrinsic fibres), no observable inhibitory (or potentiating) effects were observed following *subthreshold* synaptic stimulation. This would suggest that the inhibition of suprathreshold EPSPs was solely due to the inhibition of pre- and/or postsynaptic Na^+ channels preventing action potential firing, rather than a direct presynaptic inhibitory effect of the drug (Table 6.1).

6.8.5 Felbamate

Felbamate (FBM) is known to exert its anticonvulsant effects through a number of mechanisms (Section 3.6.5 for postsynaptic effects), with the principal mechanism affecting synaptic transmission being the blockade of NMDARs (Libri *et al.*, 1996; Pisani *et al.*, 1995). The results of the present study found that responses elicited following L1 fibre stimulation were more inhibited by FBM than those elicited following intrinsic fibre stimulation (Table 5.3). This would suggest a specificity of felbamate for L1 over intrinsic fibre synapses that may be related to the NMDAR-blocking effect of this drug. However, FBM has also been shown to potentiate GABA-ergic transmission and affect both voltage-dependent Na^+ and Ca^{2+} channels (Burdette & Sackellares, 1994), effects that clearly have the potential to reduce excitatory transmission and consequently should not be discounted.

6.8.6 Phenobarbitone

Phenobarbitone (PBN) has been shown to bind to an allosteric binding site on the $GABA_AR$ complex to affect channel opening time, permitting more Cl^- to flow across the membrane and therefore enhance hyperpolarization (Macdonald & Kelly, 1995). PBN also affects AMPAR-mediated transmission and may inhibit Ca^{2+} channels although these are considered minor effects by comparison with the modulation of GABAergic responses (Schacter, 1995). The pharmacological effects of PBN have been previously investigated in the guinea pig piriform cortex where it was found to produce a ten-fold increase in the fast, $GABA_AR$-mediated inhibitory postsynaptic conductance (Scholfield, 1978a; Scholfield, 1980). However, this earlier study did not attempt to isolate synaptic events in response to stimulation of separate excitatory inputs. In the present study, PBN alone did not affect synaptic responses elicited following L1 fibre stimulation, but was found to slightly suppress EPSPs elicited following intrinsic fibre stimulation. This PBN-mediated suppression of intrinsic transmission was increased in the presence of OXO-M, an effect that was again, probably a cumulative effect of the intrinsic fibre synaptic transmission inhibiting properties of OXO-M and PBN (Table 6.1). Therefore, PBN selectively inhibited intrinsic over L1 fibre transmission, a specificity that has been previously unreported in this brain area. This specificity may also account for the limited ability of PBN to abolish OXO-M-induced epileptiform bursting since inhibition of the already inhibited (by OXO-M) intrinsic fibre transmission is less likely to be effective in abolishing burst firing that inhibition of the potentiated (by OXO-M) L1 fibre inputs.

6.8.7 Summary of AED effects

The relative order of potency of the anticonvulsants tested, based upon their postsynaptic effectiveness (determined by speed of abolition of burst firing and degree of I_{ADP} inhibition; Section 3.8.7) was found to be (in descending order of potency): TPM > CBZ > FBM = GPN > LTG > PBN. By comparing the effects of these anticonvulsants upon excitatory synaptic transmission, a similar order of effectiveness was drawn up. The order of effectiveness was based upon the ability of the test compound to inhibit excitatory synaptic transmission. Particular emphasis was placed upon ability to inhibit L1 fibre-elicited excitatory transmission since it has been shown to be significantly potentiated in our OXO-M-induced model of epileptiform activity and is therefore likely to contribute significantly to the bursting phenomenon (Chapter 4). Consequently, a simple decreasing order of effectiveness was derived from the accumulated data (Table 6.1) FBM > LTG > TPM > GPN = PBN. CBZ was not included in the list since although its effects on suprathreshold EPSPs were most likely due to generalised blockade of pre- and/or postsynaptic Na^+ channels rather than a specific effect upon synaptic transmission. From these two lists of potency order (synaptic and non-synaptic), the proportion of a given drug's anticonvulsant activity that was due to either postsynaptic or synaptic transmission blocking mechanisms might be proposed. From this mechanistic comparison of potency, it is clear that the anticonvulsants that possessed both pre- and post synaptic mechanisms of action (e.g. FBM and TPM) were most successful in abolishing epileptiform activity in our model. Finally, these results have clearly demonstrated the importance of the delicate balance between the muscarinic potentiation of L1 fibre-mediated excitatory synaptic transmission and the inhibition of intrinsic fibre-mediated excitatory synaptic transmission to the expression of epileptiform bursting seen in this mAChR agonist-induced model of epilepsy.

6.9 Summary

1. The effects of a range of anticonvulsants upon afferent and intrinsic excitatory synaptic transmission in control conditions and in the presence of 10 μM OXO-M were investigated.
2. AEDs that were shown to have a significant inhibitory effect upon *afferent* excitatory synaptic transmission (*e.g.* felbamate, lamotrigine, topiramate) were found to be the most effective in inhibiting OXO-M-induced bursting.
3. The order of effectiveness in inhibiting excitatory synaptic transmission (in descending order of potency) was found to be: FBM > LTG > TPM > GPN > PBN.

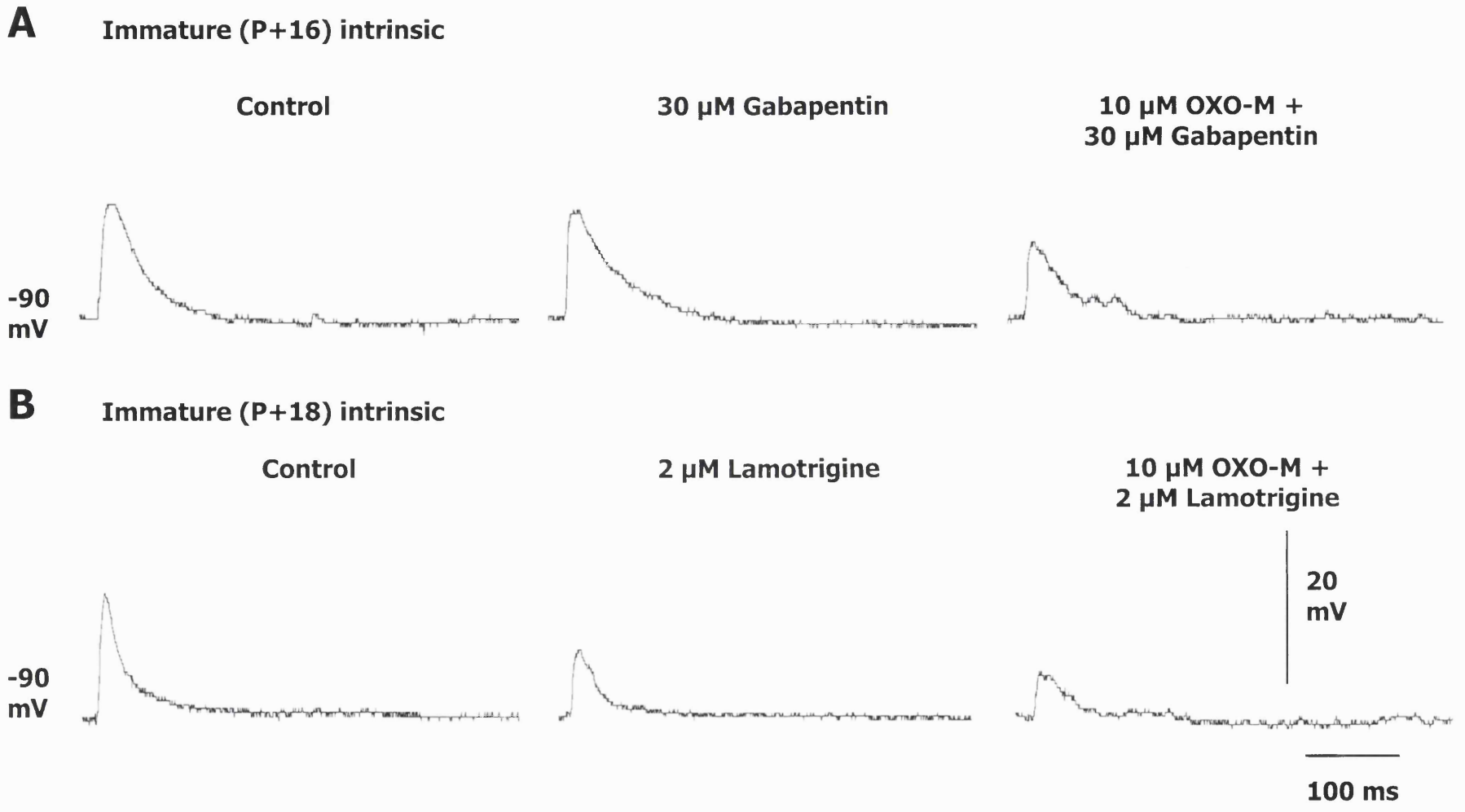
A
Immature (P+16) intrinsic
Control
30 µM Gabapentin
10 µM OXO-M +
30 µM Gabapentin
-90
mV
B
Immature (P+18) intrinsic
Control
2 µM Lamotrigine
10 µM OXO-M +
2 µM Lamotrigine
-90
mV
20
mV
100 ms

Figure 6.1

Figure 6.1

Subthreshold EPSPs elicited following the stimulation of intrinsic fibres and recorded from immature presumed deep pyramidal neurones. **A.** Recordings made from an immature (P+16) presumed deep pyramidal neurone in control conditions (**left panel**), in 30 μM gabapentin (**middle panel**) and in 10 μM OXO-M *plus* 30 μM gabapentin (**right panel**). Control resting potential=-82 mV in control conditions. Stimulus strength=4 V; 0.2 ms. The effects of both gabapentin and OXO-M were fully reversible upon washout (not shown). Note the small suppression of intrinsic fibre excitatory transmission by gabapentin and further suppression in the presence of OXO-M *plus* gabapentin. **B.** Recordings made from an immature (P+18) presumed deep pyramidal neurone in control (**left panel**), in 2 μM lamotrigine (**middle panel**) and in 10 μM OXO-M *plus* 2 μM lamotrigine (**right panel**). Control resting potential=-82 mV. Stimulus strength=7 V; 0.2 ms. The effects of both lamotrigine and OXO-M were fully reversible upon washout (not shown). Note the strong suppression of intrinsic fibre excitatory transmission by lamotrigine and the further suppression in the presence of OXO-M *plus* lamotrigine. Cells were held at -90 mV throughout by negative current injection.

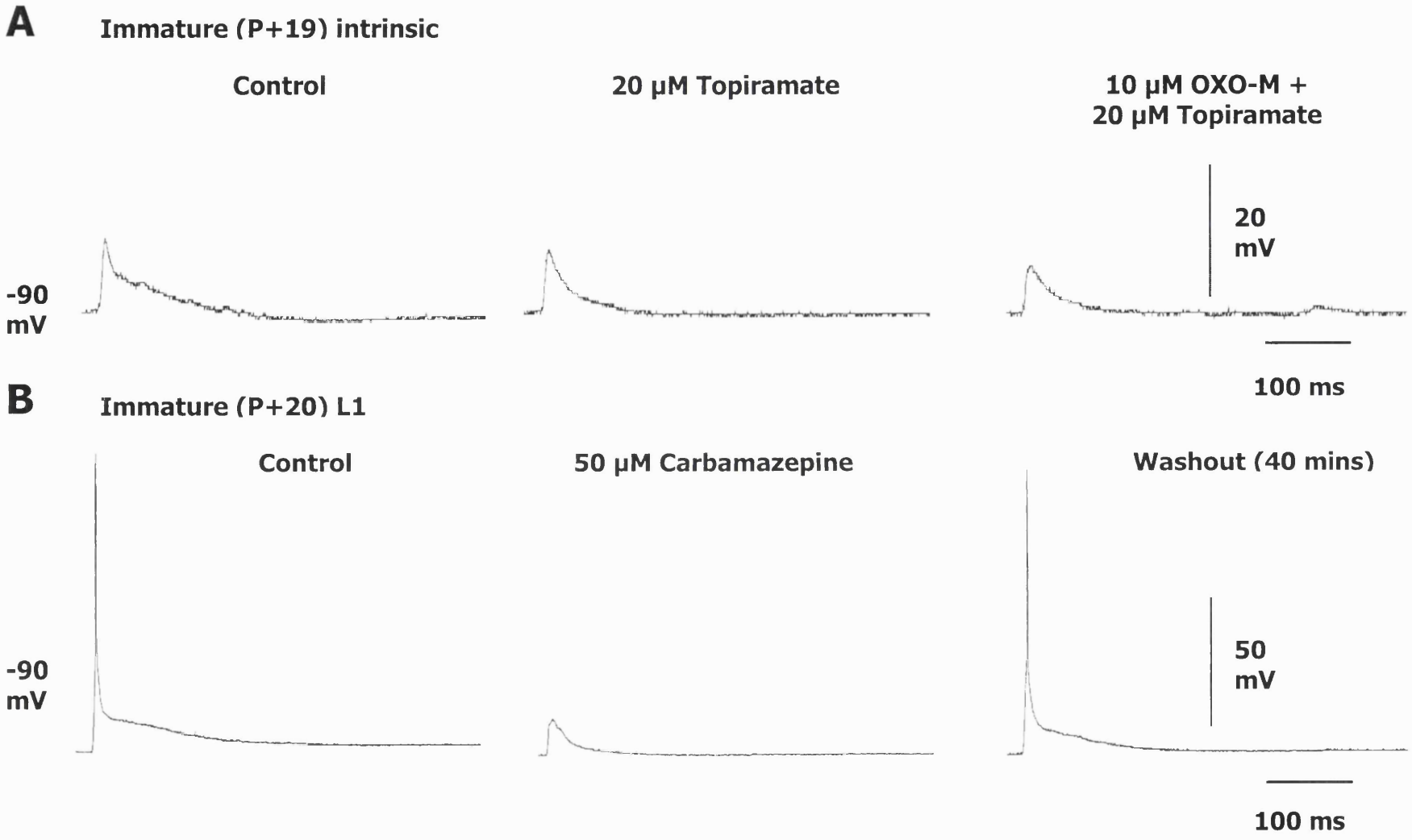
A
Immature (P+19) intrinsic
Control
20 µM Topiramate
10 µM OXO-M +
20 µM Topiramate
-90
mV
20
mV
100 ms
B
Immature (P+20) L1
Control
50 µM Carbamazepine
Washout (40 mins)
-90
mV
50
mV
100 ms

Figure 6.2

Figure 6.2

Subthreshold EPSPs elicited following the stimulation of L1 or intrinsic fibres and recorded from immature presumed deep pyramidal neurones. **A.** Recordings made following intrinsic fibre stimulation from an immature (P+19) presumed deep pyramidal neurone in control conditions (**left panel**), in 20 μM topiramate (**middle panel**) and in 10 μM OXO-M *plus* 20 μM topiramate (**right panel**). Control membrane potential=-83 mV. Stimulus strength=5 V; 0.2 ms. The effects of both topiramate and OXO-M were fully reversed on washout (not shown). Note the weak suppression of intrinsic fibre excitatory transmission by topiramate and further suppression in the presence of OXO-M *plus* topiramate. **B.** Recordings made following L1 fibre stimulation from an immature (P+20) presumed deep pyramidal neurone in control conditions (**left panel**), in 50 μM carbamazepine (**middle panel**) and following 40 minutes washout (**right panel**). Control membrane potential=-82 mV. Stimulus strength=8 V; 0.2 ms. Note the reversible suppression of afferent fibre excitatory transmission by carbamazepine. Cells were held at -90 mV throughout by steady negative current injection.

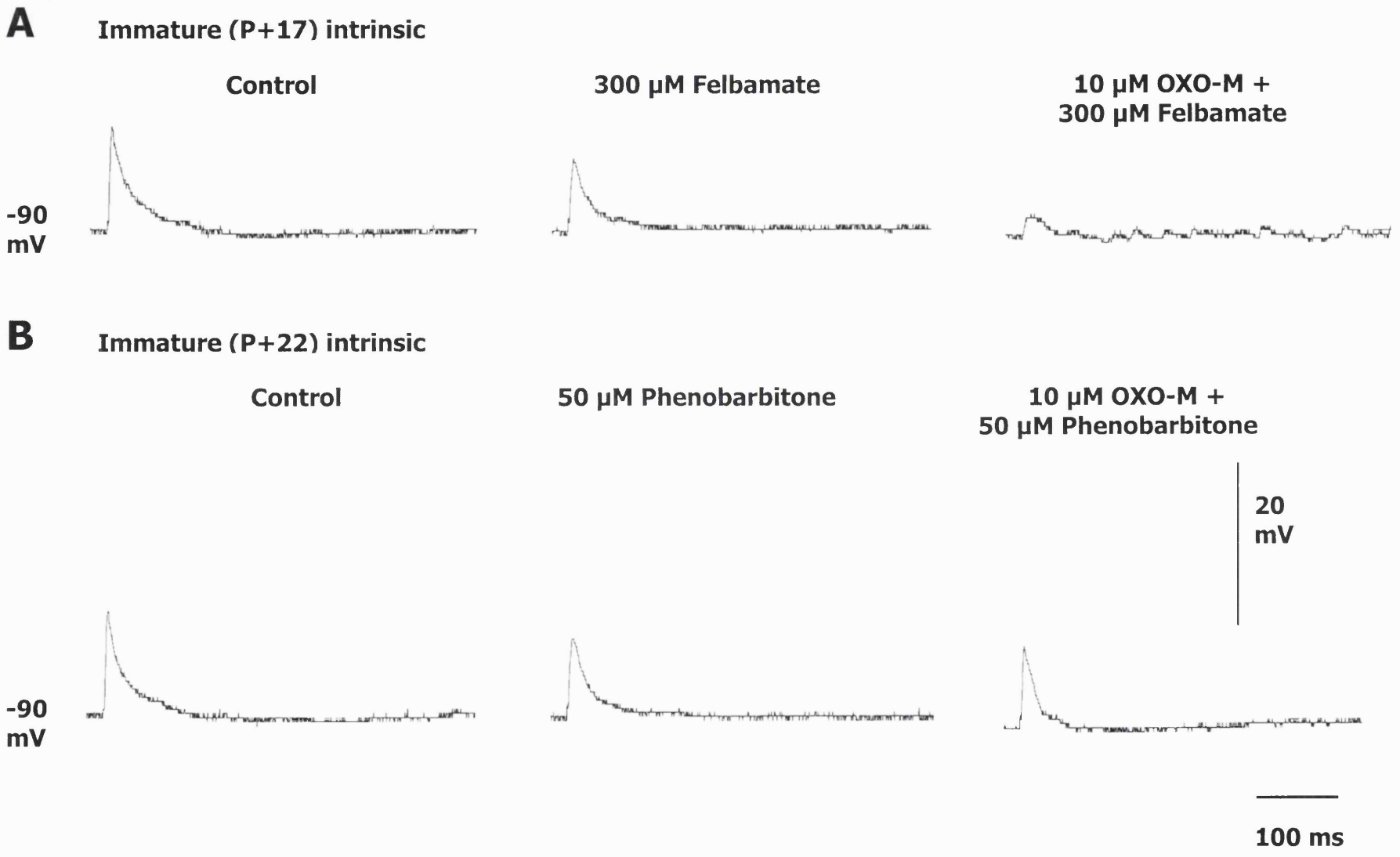
A
Immature (P+17) intrinsic
Control
300 µM Felbamate
10 µM OXO-M +
300 µM Felbamate
-90
mV
B
Immature (P+22) intrinsic
Control
50 µM Phenobarbitone
10 µM OXO-M +
50 µM Phenobarbitone
20
mV
-90
mV
100 ms

Figure 6.3

Figure 6.3

Subthreshold EPSPs elicited following stimulation of intrinsic fibres and recorded from presumed deep pyramidal neurones. **A.** Recordings made from an immature (P+17) presumed deep pyramidal neurone in control conditions (**left panel**), in 300 μM felbamate (**middle panel**) and in 10 μM OXO-M *plus* 300 μM felbamate (**right panel**). Control resting potential=-81 mV. Stimulus strength=4.5 V; 0.2 ms. The effects of both felbamate and OXO-M were fully reversed on washout (not shown). Note the suppression of intrinsic fibre excitatory transmission by felbamate and further suppression in the presence of OXO-M *plus* felbamate. **B.** Recordings made from an immature (P+22) presumed deep pyramidal neurone in control conditions (**left panel**), in 50 μM phenobarbitone (**middle panel**) and in 10 μM OXO-M plus 50 μM phenobarbitone (**right panel**). Control resting potential=-83 mV. Stimulus strength=5 V; 0.2 ms. The effects of both phenobarbitone and OXO-M were fully reversible upon washout (not shown). Note the slight suppression of intrinsic fibre excitatory transmission by phenobarbitone and slight further suppression in the presence of OXO-M *plus* phenobarbitone. Cells were held at -90 mV throughout by negative current injection.

Table 6.1

Anticonvulsant	Suppression of subthreshold L1 fibre elicited EPSPs (%)		Suppression of subthreshold intrinsic fibre elicited EPSPs (%)	
	AED	AED plus 10 μM OXO-M	AED	AED plus 10 μM OXO-M
Felbamate (300 μM; n=5)	57 ± 6.1	35 ± 7.5	41 ± 4.8	79 ± 9.1
Lamotrigine (2 μM; n=5)	48 ± 4.2	24 ± 8.2	51 ± 5.7	71 ± 8.7
Topiramate (20 μM; n=7)	21 ± 7.2	9 ± 6.1	26 ± 5.3	44 ± 8.9
Gabapentin (30 μM; n=10)	None	None	22 ± 5.7	36 ± 8.4
Phenobarbitone (50 μM; n=7)	None	None	11 ± 6.1	21 ±7.2
Carbamazepine (50 μM; n=9)	None*	None*	None*	None*

Table 6.1

The effect of antiepileptic drugs (AEDs) upon subthreshold EPSPs elicited following either L1 or intrinsic fibre stimulation in control conditions and in the presence of 10 μM OXO-M. In all cases, recordings were made from presumed deep pyramidal neurones from immature (P+14 to P+24) transverse piriform cortical brain slices. * Carbamazepine did not affect the amplitude of subthreshold EPSPs however it did abolish all suprathrehold responses (likely due to the blockade of pre- and/or postsynaptic Na^+ channels). Data are means ± SEM. n=number of neurones.

Chapter 7:

The effects of rostro-caudal lesions and gap junction-blockade upon OXO-M-induced epileptiform bursting in immature piriform cortical brain slices

7.1 Introduction

7.1.1 Rostro-caudal lesions in the transverse piriform cortical brain slice preparation

The piriform cortex has long been recognised as being highly susceptible to the generation and propagation of epileptiform activity (Section 1.3) (Loscher & Ebert, 1996; McIntyre & Kelly, 2000; Pelletier & Carlen, 1996). The present investigation of both the post- (Chapter 3) and presynaptic (Chapters 4 & 5) mechanisms that underlie the epileptiform bursting phenomenon produced following mAChR activation in the immature transverse piriform cortical brain slice preparation has provided a greater understanding of this phenomenon. However, a number of previous studies have suggested that the epileptiform activity seen in the piriform cortex, *in vivo* may have originated in other brain areas such as the endopiriform nucleus (Hoffman & Haberly, 1996a), the horizontal limb of the diagonal band of broca (Linster *et al.*, 1999) or the hippocampus (Bertram, 1997; Kelly *et al.*, 2002), since the transverse slice preparation used in the present study is likely to contain the deeper endopiriform nucleus region that may contribute to epileptiform burst generation in OXO-M. Consequently, in order to determine whether the mAChR agonist-induced epileptiform activity seen in the immature slice preparation originated within the piriform cortical network itself or was generated by the endopiriform nucleus (or other areas) acting as pacemaker regions (Loscher & Ebert, 1996), layer-specific rostro-caudal lesions were made in slices prepared from both adult and immature tissue (Section 2.6) in order to either separate specific inputs into the piriform cortex or isolate the piriform cortex from other brain areas. This technique has previously been used to determine the origins and spread of epileptiform activity in the piriform cortex (Demir *et al.*, 2001; Haberly & Bower, 1984; Hori *et al.*, 1988) and a number of other brain areas including the hippocampal CA3 region (Barbarosie *et al.*, 2000), entorhinal cortex (Calcagnotto *et al.*, 2000) and neocortex (Hoffman *et al.*, 1994). Two types of lesion were made (only one lesion per experiment) in the present study: either between layers I and II (Fig. 2.9A), thereby severing the apical dendrites of deep and superficial pyramidal neurones and effectively removing the afferent LOT input, or along the boundary of layer III and the deeper endopiriform nucleus (Fig. 2.9B), thereby severing the deep pyramidal basal dendrites and axons and separating the piriform cortex from this brain area. It was hoped that this approach might also provide some information on whether the mAChR agonist-induced sADP (a characteristic response of deep piriform cortical pyramidal neurones to

mAChR activation (Constanti *et al.*, 1993) had a specific somatic or distal dendritic origin.

7.1.2 Gap junction blockade and epileptiform burst firing

The possibility than non-synaptic means of inter-cellular communication might be involved in the generation and maintenance of the OXO-M-induced epileptiform bursting phenomenon was also investigated by examining the effect of two well-recognised gap junction blockers upon mAChR agonist-induced bursting activity in the immature piriform cortical brain slice preparation. Gap junctions have been shown to exist in adult and immature rat olfactory bulbs (Reyher *et al.*, 1991) and guinea pig cortices (de Curtis *et al.*, 1998; Micevych & Abelson, 1991). They have also been demonstrated to play a significant role in high-frequency network oscillations (a requirement for associative memory) (Maier *et al.*, 2002) and the onset and maintenance of epileptiform activity in a number of brain areas, such as the adult guinea pig piriform cortex (de Curtis *et al.*, 1998), immature rat hippocampus (Traub *et al.*, 2002; Uusisaari *et al.*, 2002), immature rat dentate gyrus (Schweitzer *et al.*, 2000) and immature rat amygdala (Elisevich *et al.*, 1998). Additionally, in humans, changes in neuronal gap junction behaviour have been linked to complex partial seizures (Elisevich *et al.*, 1997a) and their upregulation to intractable (Lee *et al.*, 1995), mesial temporal lobe (Fonseca *et al.*, 2002) and other seizure types (Li *et al.*, 2001; Naus *et al.*, 1991). Consequently, gap junction blockers have been proposed as potential antiepileptic drugs (Margineanu & Klitgaard, 2001). Interestingly, the gene coding for the neuronal gap junction protein, connexin-36, assigned it to band 15q14, an area that has been linked to a form of familial epilepsy (Belluardo *et al.*, 1999).

7.2 Apical lesions in the adult and immature piriform cortical brain slice preparations

Transverse piriform cortical brain slices were prepared from adult and immature rats, as previously described and mounted in the recording bath in the usual manner. A single rostro-caudal lesion was then made, using a microscalpel, along the length of each slice (adult: n=5; immature: n=8) as previously described (Section 2.6; Fig. 2.9A), effectively severing layer I from the remainder of the slice preparation (apical lesion). One bipolar stimulating electrode was then placed in layers II/III, as previously described (Chapter 4) in order to stimulate intrinsic excitatory fibres, whilst another stimulating electrode was placed in layer I in order to confirm the effectiveness of the lesion; if stimuli

applied through the electrode in layer I elicited no response from the recorded cell then the lesioning was known to be successful and was found to be the case in all experiments. The electrode in layer I also served to anchor the lesioned tissue during the experiment. The slices were then left to recover from the lesioning procedure for a minimum of 45 minutes before intracellular recordings were made. In recordings from both adult and immature presumed deep pyramidal neurones, no notable differences in the responses of the recorded cells to depolarizing and hyperpolarizing electrotonic stimuli were seen, in control conditions or in the presence of 10 μM OXO-M, (Table 7.1) compared to the same responses elicited from non-lesioned slices (Chapter 3; Figs. 3.7 and 3.13). Additionally, sub- and suprathreshold EPSPs, elicited in control conditions and following stimulation in layers II/III (not shown), were not found to differ from controls elicited from non-lesioned slices, in control conditions or in the presence of 10 μM OXO-M (Chapter 4; Figs. 4.1 and 4.2). Finally, in control solution, neither the time courses nor the peak amplitudes of the sAHP (or underlying hybrid I_{AHP} tail current) elicited from apically-lesioned, adult or immature deep pyramidal piriform cortical neurones held at -70 mV and following a long (+2 nA; 1.6s) depolarizing stimulus train were found to differ significantly from the responses of non-lesioned cells recorded in control conditions (Fig. 7.1; Table 7.2). However, rather surprisingly, when the same stimulus was applied to adult deep pyramidal neurones recorded from apically-lesioned slices in the presence of 10 μM OXO-M, the sADP that was typically evoked in non-lesioned slices consistently failed to be generated. Instead, the sAHP that was present in control was reduced in the usual manner. The magnitude (8 ± 1.1 mV; $P<0.05$; Fig. 7.1; Table 7.2) and time course (2.1 ± 1.2 mV; $P<0.05$; Fig. 7.1; Table 7.2) of the sAHP, evoked in the presence of 10 μM OXO-M, in apically lesioned slices, was found to be significantly smaller than those elicited from either apically lesioned or non-lesioned slices in control conditions. In contrast, in apically-lesioned *immature* piriform cortical slices, in the presence of 10 μM OXO-M, a long depolarizing stimulus elicited a typical sADP and underlying I_{ADP} tail current. The magnitude and time course of these responses were not found to be significantly different from those elicited from non-lesioned slices (Table 7.2). Finally, the frequency of incidence (~60%; n=8) of the characteristic OXO-M-induced epileptiform burst firing phenomenon seen in the immature preparation was unaffected by apical lesioning when compared with results from non-lesioned slices (Chapter 3).

7.3 Basal lesions in the adult and immature piriform cortical brain slice preparations

The same experimental protocols described above were also applied to both adult (n=6) and immature (n=10) transverse piriform cortical brain slices that had been lesioned between layer III and the underlying endopiriform nucleus (also sometimes referred to as piriform cortical layer IV (Tseng & Haberly, 1989b)). This cut (termed here a basal lesion) was intended to sever connections, not only with the endopiriform nucleus, an area that has previously been proposed as the source of some epileptiform activity observed in the piriform cortex (Hoffman & Haberly, 1991a; Loscher & Ebert, 1996), but with all other surrounding brain areas remaining on the slice. Consequently, by isolating layers I to III of the piriform cortex with this basal lesion, the important question of whether the OXO-M-induced epileptiform bursting phenomenon seen in the immature preparation did in fact originate from within these layers or whether it had spread to this area from an outlying region could be addressed. Confirmation that the lesioning technique used had electrically isolated layers I to III of the slice preparation from the remainder of the slice was obtained by the absence of any response from the recorded cell in layer III to electrical stimulation from an electrode placed in the endopiriform nucleus.

In control conditions, responses elicited from both adult and immature basally-lesioned slices following either electrotonic stimuli (+1.2 to -1.2 nA; 160 ms; delivered through the recording microelectrode) or following the stimulation of afferent (layer I) or intrinsic (Layers II/III) excitatory fibres were found to be indistinguishable from responses elicited under the same conditions from non-lesioned or apically-lesioned slices (Table 7.3). Additionally, when the same stimuli were applied to basally-lesioned immature piriform cortical slices, in the presence of 10 μM OXO-M, responses were not found to differ from the responses elicited from unlesioned or apically-lesioned slices under the same conditions (Table 7.3). By contrast, the sAHP (and underlying I_{AHP} tail current) elicited from basally-lesioned *adult* slices in control conditions was *not* replaced by a sADP (or underlying I_{ADP}) in OXO-M as was the case with the immature preparation. Instead, a diminished sAHP (77 ± 11.3%; $P<0.05$ *vs.* controls; Fig. 7.2A) and underlying slow outward tail current (I_{AHP}; Fig. 7.2B) were elicited. Additionally, the magnitude of the sAHP elicited from adult basally-lesioned slices in OXO-M was found to be significantly smaller than the sAHP elicited from apically-lesioned adult slices in OXO-M (mean apically-lesioned sAHP amplitude=8 ± 1.1 mV; n=5; mean basally-lesioned sAHP amplitude=3 ± 1.5 mV; n=6; $P<0.05$). Finally, the frequency of

incidence (~60%) of the characteristic OXO-M-induced epileptiform burst firing phenomenon seen in the immature preparation was, like the apically-lesioned slices, found to be unaffected by basal lesioning when compared with results from non-lesioned slices (Chapter 3). These results clearly show that the OXO-M-induced bursting seen in immature slices originates and is maintained by neuronal circuitry present solely within piriform cortical layers I to III. Consequently, although some forms of epileptiform activity observed in the piriform cortex have been shown to originate from other brain areas such as the endopiriform nucleus (the principal source of cholinergic input to the piriform cortex) (Hoffman & Haberly, 1996a), the horizontal limb of the diagonal band of Broca (Linster *et al.*, 1999) and the hippocampus (Bertram, 1997; Kelly *et al.*, 2002), the present work has demonstrated that our cortical seizure model of epilepsy triggered by mAChR activation was initiated and maintained solely by the neuronal circuitry intrinsic to this brain area. Additionally, the results from this section and section 7.2 provide further evidence of a close link between the induced sADP and the epileptiform activity seen in the immature slice preparation. The implications of these results are discussed in Section 7.5.1.

7.4 The effect of gap junction blockers upon mAChR agonist-induced burst firing in immature rat piriform cortex

The present study has investigated, in detail, age-related changes in both the postsynaptic and synaptic responses of deep pyramidal neurones of the piriform cortex, in order to better understand the mechanism of OXO-M-induced epileptiform bursting in the immature slices. However, the possibility that non-synaptic mechanisms of inter-cellular communication (*i.e.* gap junctions) might be involved in the generation and maintenance of the observed bursting phenomenon could not be discounted. Since gap junctions (Section 1.8) have previously been shown to exist in the adult piriform cortex (de Curtis *et al.*, 1998) (see also (Micevych & Abelson, 1991); gap junction mRNA), any role they might have in the generation and/or maintenance of the OXO-M-induced bursting warranted investigation. Consequently, the effects of two known gap junction blockers, carbenoxolone (100 μM; n=10) (Ross *et al.*, 2000) and octanol (280 μM; n=8) (Kohling *et al.*, 2001) upon synaptic and postsynaptic responses elicited from immature presumed deep pyramidal neurones already displaying established OXO-M-induced bursting were investigated. When carbenoxolone (n=3) or octanol (n=3) were applied alone, neuronal responses (spike firing frequency, cell input resistance, resting membrane potential) were not found to differ in any way from controls (not shown).

Carbenoxolone has also been shown to be a mineralocorticoid agonist (Ross *et al.*, 2000) and consequently, the mineralocorticoid antagonist, spironolactone (100 nM) was applied alone (n=2) and with carbenoxolone (n=2) to ensure none of the effects observed, in the presence of OXO-M, were due to a (non-genomic) mineralocorticoid agonist action. Spironolactone was found not to inhibit the effects of carbenoxolone described below and had no observable effects when applied alone.

7.4.1 The effects of gap junction blockers upon excitatory synaptic (afferent and intrinsic) transmission and postsynaptic muscarinic responsiveness in immature presumed deep pyramidal neurones

Neither octanol (280 μM; n=8) nor carbenoxolone (100 μM; n=10) were found to have any significant effect upon sub- or suprathreshold EPSPs elicited, as previously described (Chapter 4), following the stimulation of either afferent (layer I) or intrinsic (layer II/III) fibres in the immature piriform cortical slice preparation in the presence of 10 μM OXO-M. EPSPs elicited following suprathreshold afferent fibre stimulation in the presence of 10 μM OXO-M plus either gap junction blocker were still potentiated (not shown) in the same way as previously described (Fig. 4.5) in the presence of OXO-M alone. However, unlike these latter responses, a suprathreshold response never initiated a period of burst firing (see below and Section 4.3.2). The routinely observed OXO-M-induced inhibition of EPSPs elicited following stimulation in layers II/III, in the presence of OXO-M was not significantly influenced by gap junction blockers (mean inhibition in octanol=22 ± 5.4%; carbenoxolone=29 ± 6.8%; not significantly different from mean inhibition in OXO-M alone: 25 ± 5.4%; $P>0.05$ for both agents; Fig. 4.6; Table 7.4). Finally, cellular responses to injected depolarizing and hyperpolarizing current stimuli (+1.2 to -1.2 nA; 160 ms) in the presence of OXO-M plus a gap junction blocker (not shown) were indistinguishable from those elicited in the presence of OXO-M alone, demonstrating no observable changes in either postsynaptic cellular excitability or input resistance or degree of OXO-M-induced depolarisation (Table 7.4).

7.4.2 The effects of gap junction blockers upon OXO-M-induced epileptiform bursting behaviour recorded in immature slices

In order to determine the effects following gap junction blockade, upon the OXO-M-induced epileptiform bursting seen in immature slices, carbenoxolone (100 μM; n=6) or octanol (280 μM; n=5) were applied to cells already showing established bursting behaviour in OXO-M alone. Both carbenoxolone (5/6 cells) and octanol (4/5 cells)

abolished epileptiform burst firing ~15 minutes following addition to the bathing medium (Fig. 7.3A). The large paroxysmal depolarizing shifts (PDS) that characterised the bursting phenomenon in slices prepared from younger animals (P+14 to P+18; mean amplitude=27 ± 4.2 mV; Section 3.8.5) were replaced with significantly smaller variations in resting membrane potential (PDS in carbenoxolone=4.3 ± 3.1 mV; PDS in octanol=5.8 ± 2.6 mV; $P<0.05$ for both agents *vs.* controls; Table 7.4) measured from a resting potential equivalent to the most hyperpolarized potential the cell reached in the presence of OXO-M alone. Additionally, the rapid, repetitive firing displayed by the cell during the depolarized period of the bursting cycle was replaced with occasional single spikes at the peak of the small PDS (Fig. 7.3). In recorded cells that did not exhibit the behaviour detailed above the established epileptiform bursting activity was replaced by regular repetitive firing in the presence of either carbenoxolone (1/6 cells) or octanol (1/5 cells) that was indistinguishable from the repetitive firing recorded in adult deep pyramidal neurones in response to OXO-M alone.

7.4.3 The effects of gap junction blockers upon the OXO-M-induced slow afterdepolarization (sADP) and underlying slow inward tail current (I_{ADP}) recorded in immature presumed deep pyramidal neurones

During the course of examining the effects of carbenoxolone and octanol upon the OXO-M-induced model of epileptiform behaviour in immature slices, their effects upon the induced sADP (and the I_{ADP} tail current) were also investigated. Interestingly, sADPs evoked at –70 mV following a long depolarizing stimulus (+2 nA; 1.6 s) in OXO-M alone (mean=12 ± 1.2 mV; n=18; Fig. 7.3A) were significantly diminished (62 ± 7.2%; $P<0.05$ *vs.* control) following the addition of either carbenoxolone (5 ± 0.9 mV; 100 μM; n=10) or octanol (4 ± 1.1 mV; 280 μM; n=8) to the bathing medium. Additionally, the sADP elicited in OXO-M plus either carbenoxolone or octanol displayed a fast hyperpolarizing component directly following the end of the stimulus train (Fig. 7.3C) prior to expression of the sADP. This modification of the sADP was also reflected by the changes in the underlying hybrid I_{ADP} current. Thus, the I_{ADP} seen in OXO-M alone (mean=0.51 ± 0.03 nA; n=18; Fig. 7.3D) was significantly diminished (67 ± 5.6%; $P<0.05$ *vs.* control) in OXO-M plus carbenoxolone (0.21 ± 0.06 nA; 100 μM; n=10) or octanol (0.19 ± 0.03 nA; 280 μM; n=8) and displayed a fast outward component directly after the stimulus train (Fig. 7.3E; 1) immediately followed by a diminished slow inward component (Fig. 7.3E; 2; Table 7.4). These results clearly show

that gap junctions linking neurones in the immature piriform cortex are able to affect the OXO-M-induced epileptiform bursting.

7.5 Discussion

The results presented in this chapter have described the effects produced following rostro-caudal lesioning or gap junction blockade, upon the mAChR-mediated epileptiform bursting seen in immature piriform cortical slices. These data have a number of important implications upon our current understanding of the mechanisms underlying the initiation and maintenance of this bursting behaviour. These implications and incidences of similar findings in other brain areas and models of epileptiform behaviour are discussed below.

7.5.1 The implications of rostro-caudal lesioning upon OXO-M-induced epileptiform bursting and sADP generation in the immature piriform cortical brain slice preparation

The present results have clearly demonstrated that both the OXO-M-induced epileptiform bursting and the sADP elicited in immature preparations were unaffected by either apical or basal lesions to the slice. A number of previous studies have examined the effects of lesions in layer I of the olfactory cortex both *in vitro* (Motokizawa & Ino, 1981; Shepherd & Haberly, 1970) and *in vivo* (Haberly & Bower, 1984); however, in these cases, the technique was used as a means of isolating synaptic inputs and to elucidate the synaptic circuitry of the piriform cortex rather than to investigate epileptiform activity. These studies also noted that apical lesioning would sever a significant number of the apical dendrites belonging to both superficial and deep pyramidal neurones within the slice preparation (Hori *et al.*, 1988), suggesting that any differences seen in our results between apically-lesioned and non-lesioned slices may be attributable to the absence of a dendritic influence present in the intact slice. Consequently, it was of particular interest to note that no differences were seen in the amplitude of sAHPs elicited from either adult or immature apically lesioned slices and intact slices but, following the application of OXO-M, the sADP that would normally be evoked from the intact *adult* preparation was abolished, whilst the sADP evoked from the immature preparation was unaffected by the apical lesion. From these novel observations it could be suggested that the ion channels (proposed to be Ca^{2+}-activated K^{+}-channels (Constanti & Sim, 1987a; Postlethwaite *et al.*, 2000)) mediating sAHPs in both the both the adult and immature preparations and those underlying the sADP (Constanti *et al.*, 1993) evoked from the immature preparation were situated closer to the soma, whilst conversely, the sADP evoked from the adult preparation has a predominantly dendritic origin. Additionally, lesions made between layer III and the

endopiriform nucleus would have severed a significant number of basal dendrites (Hori *et al.*, 1988) that form the excitatory association fibres arising from the superficial and deep pyramidal neurones. Once again, the adult and immature sAHPs and the immature sADP were unaffected by basal lesioning, but the *adult* sADP was abolished. This too suggested a causal relationship between the adult (but not the immature) sADP and the basal dendritic lesion. This result further strengthens the likelihood of a link between the observed OXO-M-induced epileptiform bursting phenomenon seen in the immature slice and sADP generation, since a clear difference between the possible location of adult and immature sADPs has now been demonstrated.

Slow afterdepolarizations (also called plateau potentials) have all been shown to have dendritic origins in a number of preparations such as the adult rat neocortex (Mittmann *et al.*, 1997), entorhinal cortex (Jahromi *et al.*, 1999), rat sensorimotor cortex (Schwindt & Crill, 1999), spiny motoneurones (Booth *et al.*, 1997), Purkinje cells of cat cerebellar cortex (Ekerot & Oscarsson, 1981) and rat dentate gyrus neurones (Godfraind, 1985). This dendritic origin has been shown to maintain cortical oscillations in thalamic neurones (Jahnsen & Llinas, 1984) and abducens motoneurones (Korogod *et al.*, 1996), a requirement recognised as essential to the function of associative memory (Claverol *et al.*, 2002; Hasselmo *et al.*, 2000) and the predisposition of a brain area to epileptogenesis (Bragin *et al.*, 2002; Draguhn *et al.*, 2000). Interestingly, the amplitude and time course of Ca^{2+}-mediated plateau potentials elicited in striatal neurones were found to decrease with increasing age (Dunia *et al.*, 1996) showing a clear link between sADP properties and ageing, an observation of particular significance to this present study. A study of epileptiform bursting induced in the adult hippocampal subiculum demonstrated that the sADP elicited from pyramidal neurones in this area plays a central role in bursting behaviour within this neuronal population and, most significantly, the reason for this critical role was the somatic location of the ion channel type responsible for the sADP (Jung *et al.*, 2001). Finally, in an interesting parallel to the OXO-M-induced epileptiform behaviour reported in this present report, a study of OXO-M-induced plateau potentials in CA1 pyramidal neurones in the adult rat hippocampus concluded that not only were they critical to epileptogenesis in this brain area, but also $GABA_AR$- and $GABA_BR$-mediated inhibition of excitatory synaptic transmission was responsible for preventing epileptogenic states from arising under normal conditions (Fraser *et al.*, 2001).

These results clearly parallel a number of the results in this present report where expression of the sADP in the immature piriform cortex has been shown to differ in a

number of critical ways from its expression in the adult preparation (Chapter 3) alongside a number of developmental changes in excitatory and inhibitory synaptic transmission that have all been shown to result in a heightened state of excitability in the immature preparation (Chapters 4 and 5). When this is considered in conjunction with the fact that the piriform cortex is one of the areas of the cortex most densely innervated with cholinergic fibres (Eckenstein *et al.*, 1988) the OXO-M-induced epileptiform activity observed in the immature slice preparation becomes even more physiologically relevant as a useful model of temporal lobe epilepsy. When the demonstration, in this present report, that there is a definite age-dependent variation in sADP magnitude following apical or basal lesioning *and* the results of previous investigations, discussed above, are considered together, it seems reasonable to suggest that the ion channels responsible for the sADP in the piriform cortical brain slice preparation, whilst initially located in or near the soma in the immature animal, may migrate towards the apical and basal dendrites as the animal ages. In light of the results discussed above, particularly those of Fraser *et al.* (2001) and Dunia *et al.* (1998), it also seems likely that the somatic location of the channels in the immature animal increase the propensity of the preparation to exhibit epileptiform behaviour. Alternatively, the sADP channels may in fact be uniform in distribution, but the sites of Ca^{2+} entry may differ with age in the same manner described above.

In a previous study of kindling behaviour, the endopiriform nucleus, located below layer III of the piriform cortex (Behan & Haberly, 1999), was identified as being responsible for the initiation of epileptiform events that consequently spread to the piriform cortex (Hoffman & Haberly, 1993b; Hoffman & Haberly, 1996b). Epileptiform bursting in the endopiriform nucleus was found to precede activity in the piriform cortex (spread by AMPA-mediated EPSPs; a phenomenon also seen in kindled seizures initiated in the olfactory bulb that spread to the reciprocally connected piriform cortex (Haberly & Sutula, 1992; Racine *et al.*, 1991)) and attributed to *'a regenerative buildup in synaptically mediated transmission in the endopiriform nucleus'* (Hoffman & Haberly, 1996b) arising from the dense formation of intrinsic fibres in this area. Interestingly, the reasons proposed for this *'regenerative buildup'* were a reduction in $GABA_AR$-mediated inhibition (*cf.* Chapter 5) and a concomitant increase in intrinsic excitatory transmission (*cf.* Chapter 4) (Hoffman & Haberly, 1996b). The causes of epileptiform activity in the endopiriform nucleus described above show a clear parallel with the developmental changes in synaptic transmission described in this present report investigating the OXO-M-induced epileptiform bursting phenomenon seen in immature

slices. This present study showed that immature slices exhibited potentiated afferent excitatory synaptic transmission, reduced OXO-M-mediated inhibition of intrinsic excitatory transmission and reduced $GABA_AR$- and presynaptic $GABA_BR$-mediated inhibitory synaptic transmission, all of which result in raised levels of excitability within the slice preparation. Given the high density of intrinsic fibres (which may be considered analogous to the intrinsic fibres of the endopiriform nucleus in this situation) found in layer III of the piriform cortex (Datiche *et al.*, 1996) and the developmental synaptic changes described previously (that may be considered analogous to a *'regenerative buildup in synaptically mediated transmission'*), the similarities between these two brain areas are quite clear. Consequently, it is reasonable to propose that, although Hoffman *et al.* (1998) clearly showed epileptiform activity, initiated in the endopiriform nucleus to spread to the piriform cortex, this does not preclude the piriform cortex form possessing the requisite neuronal circuitry to initiate similar epileptiform activity itself, as has been demonstrated by the continued appearance of OXO-M-induced epileptiform activity in basally-lesioned slices. Encouragingly, the fact that our OXO-M-induced *in vitro* model of epileptiform activity shares many of the characteristics and mechanisms of the *in vivo* model described by Hoffman *et al.* (1998) provides convincing evidence that the *in* vitro model we investigated retains substantial physiological relevance and consequently further validates its role as a useful model of temporal lobe epilepsy. Finally, given the reciprocal connectivity that has been demonstrated between the piriform cortex and the endopiriform nucleus (Haberly & Price, 1978), it would be of considerable interest to determine whether epileptiform activity induced by OXO-M in the immature piriform cortex would spread to the endopiriform nucleus in a similar manner to that described, from the endopiriform nucleus to the piriform cortex, above. This would be especially interesting since the intrinsic fibres of the piriform cortex have not only been shown to excite the endopiriform nucleus (Tseng & Haberly, 1989c) but have here been shown to be less inhibited following mAChR activation in the immature animal.

7.5.2 A possible role for gap junctions in OXO-M-induced epileptiform bursting and sADP generation in the immature piriform cortical brain slice preparation

The present chapter has also described the effects following gap junction blockade by 100 μM carbenoxolone and 280 μM octanol upon the OXO-M-induced epileptiform burst firing phenomenon and the sADP seen in immature piriform cortical slices. Both gap junction blockers tested were found to abolish epileptiform burst firing without any

apparent modification of the postsynaptic effects of OXO-M (*e.g.* depolarisation, increased cellular excitability, increased membrane input resistance). Additionally, the post-stimulus sADP and underlying I_{ADP} tail current, normally recorded from deep pyramidal cells held at –70 mV in OXO-M was significantly diminished and acquired an early hyperpolarizing aspect (Fig. 7.3C & E). mRNA coding for gap junction proteins have been known to exist in the piriform cortex for some time (Micevych & Abelson, 1991) and gap junctions have also been implicated in the initiation and maintenance of epileptiform bursting behaviour in a number of adult brain areas (including the piriform cortex) (de Curtis *et al.*, 1998; Elisevich *et al.*, 1998; Schweitzer *et al.*, 2000; Traub *et al.*, 2002; Uusisaari *et al.*, 2002). Interestingly, a study of bicuculline-induced spontaneous interictal spike (sIS) generation in an *in vitro* preparation of the adult piriform cortex demonstrated that sIS generation was closely linked to gap junction coupling, most probably as a result of bursting-induced intracellular acidification causing increased gap junction connectivity (de Curtis *et al.*, 1998). The same effect has also been demonstrated in an *in vitro* model of 4-AP-induced epileptiform bursting in CA1 hippocampal slices where gap junction blockers reduced epileptiform burst firing and intracellular alkalosis reduced burst rate, whilst acidosis increased burst rate. An increase in dye-coupling was also seen following the induction of bursting behaviour indicating increased gap junction coupling (Ross *et al.*, 2000). The similiarities between the results described above and the replacement of bursting behaviour seen in the OXO-M-induced epileptiform model (examined in this present report) with occasional spikes (analogous to the interictal spikes seen by deCurtis *et al.* (1998)) in the presence of gap junction blockers clearly demonstrate a link between gap junction-mediated intercellular communication and epileptiform burst firing in the piriform cortex and would suggest that an investigation of the effects of pH-mediated modulation of gap junctional coupling upon OXO-M-induced epileptiform bursting would be a most useful exercise. It has also been proposed that gap junctions have little effect upon the initial spontaneous burst generated as a result of the intrinsic properties of a single cell (primary epileptiform discharges) (Ross *et al.*, 2000) but, in fact aid or complement the spread of epileptiform behaviour to other cells by synaptic and non-synaptic mechanisms (secondary epileptiform discharges) (Kohling *et al.*, 2001). This holds particular relevance in our OXO-M-induced seizure model of epilepsy, since the phenomenon has here been shown to arise as a result of distinct developmental changes in synaptic transmission (Chapters 4 & 5) although synaptic transmission in the slice preparation was unaffected by the gap junction blockers used.

Additionally, secondary discharges have also previously been shown to be dependent upon sustained depolarizations (Traub *et al.*, 1993; Traub *et al.*, 1996), such as the sADP described here, activating other cellular mechanisms. The reduction of the sADP magnitude observed in the presence of OXO-M plus carbenoxolone (Fig. 7.3) was unexpected and suggests a clear link between the appearance of this sustained depolarization and gap junction function. Thus, the sADP may not be solely modulated by mechanisms intrinsic to the individual neurone exhibiting it, but dependent upon intercellular oscillatory synaptic connections mediated by gap junctions, further developing our understanding of this curious muscarinic phenomenon. Additionally, gap junctions have been shown to be present in larger numbers in the brain tissue of the immature rat compared with the adult (Rorig *et al.*, 1996), whilst other studies have shown an upregulation of gap junction connectivity in intractable human epilepsies (Lee *et al.*, 1995) and *in vitro* hippocampal (Li *et al.*, 2001) and amygdala (Elisevich *et al.*, 1997b) preparations. When these observations are considered in tandem, the appearance of OXO-M-induced bursting only in immature animal slices makes it probable that the increased gap junction connectivity in such slices contributes significantly to the incidence of bursting behaviour seen in the present study.

7.6 Summary

1. Rostro-caudal lesioning between layers I and II (apical) or layer III and the deeper endopiriform cortex (basal) had no effect upon postsynaptic depolarisation, excitability, membrane input resistance or evoked afferent or intrinsic excitatory synaptic transmission in control conditions or the in the presence of 10 μM OXO-M recorded from adult or immature piriform cortical brain slices.
2. OXO-M-induced epileptiform bursting behaviour and sADP/I_{ADP} generation were unaffected by apical or basal lesioning in the immature slice preparation.
3. The OXO-M-induced sADP and underlying slow inward tail current (I_{ADP}), normally elicited from deep pyramidal neurones was absent following apical or basal lesioning in adult *but not immature slices.*
4. Gap junction blockade by 100 μM carbenoxolone or 280 μM octanol disrupted OXO-M-induced epileptiform burst firing and significantly diminished the evoked sADP (and underlying I_{ADP} tail current) in the immature slice preparation.

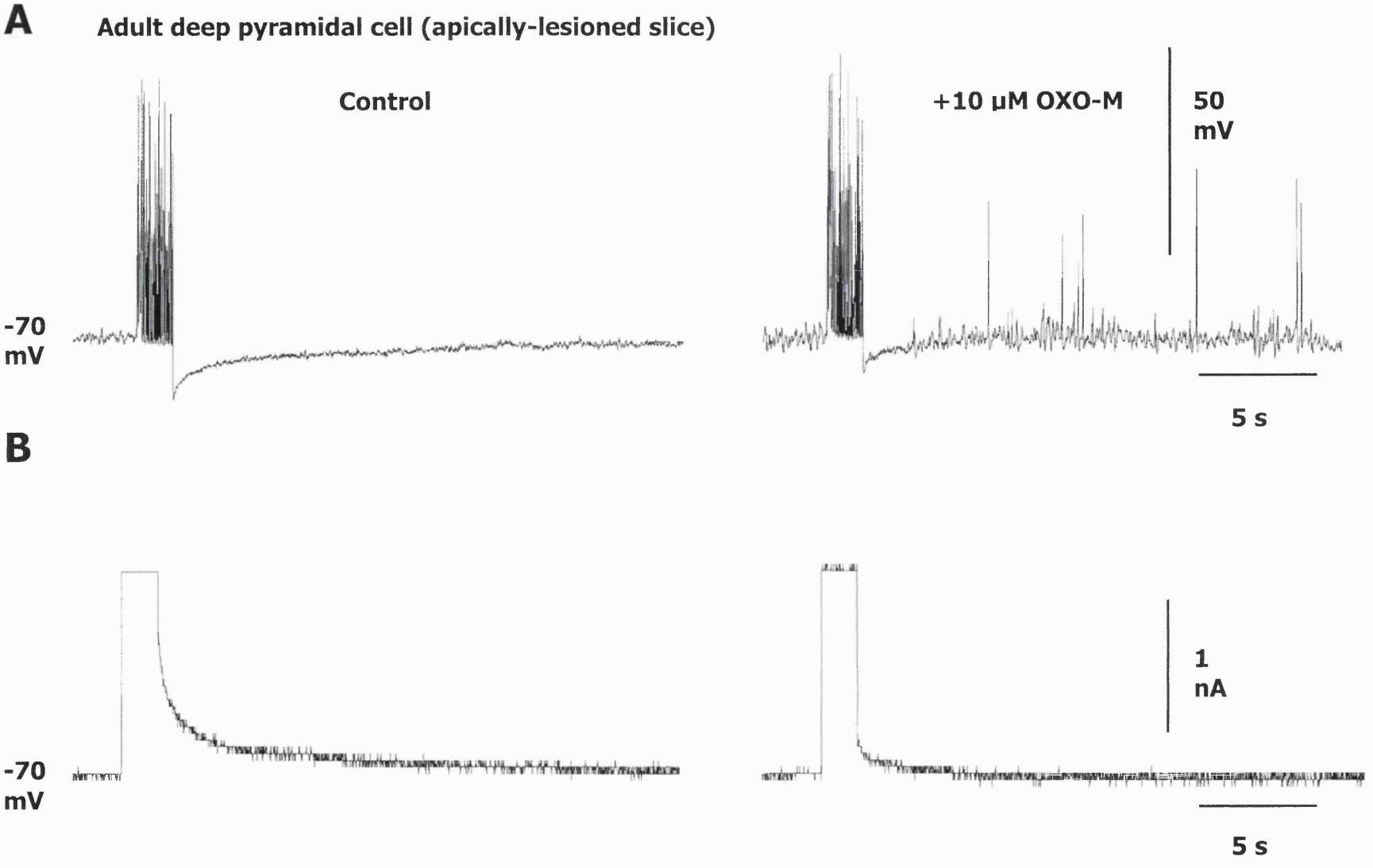
A
Adult deep pyramidal cell (apically-lesioned slice)
Control
+10 µM OXO-M
50
mV
-70
mV
5 s
B
1
nA
-70
mV
5 s

Figure 7.1

Figure 7.1

Slow after-hyperpolarizations (sAHPs) and their underlying slow outward tail currents (I_{AHP}) elicited following a long stimulus train (+2 nA; 1.6 s) applied to an adult presumed deep pyramidal neurone in a transverse piriform cortical brain slice preparation that had been apically-lesioned between layers I and II of the slice. Recordings of sAHPs (**A**) were made in DCC mode in control conditions (**left panel**) and in the presence of 10 μM OXO-M (**right panel**). Recordings of I_{AHP}s (**B**) were made in 'hybrid' clamp mode in control (**left panel**) and in OXO-M (**right panel**). The resting potential was held at -70 mV by the application of positive current passed through the recording microelectrode. Control membrane potential=-82 mV. sAHPs and I_{AHP}s elicited in control conditions were not significantly different in magnitude or time course from those elicited in non-lesioned slices. However, in OXO-M, no sADP (or underlying slow inward tail current, I_{ADP}) that were routinely generated in non-lesioned adult slices were observed. Instead, a diminished sAHP and I_{AHP} were seen.

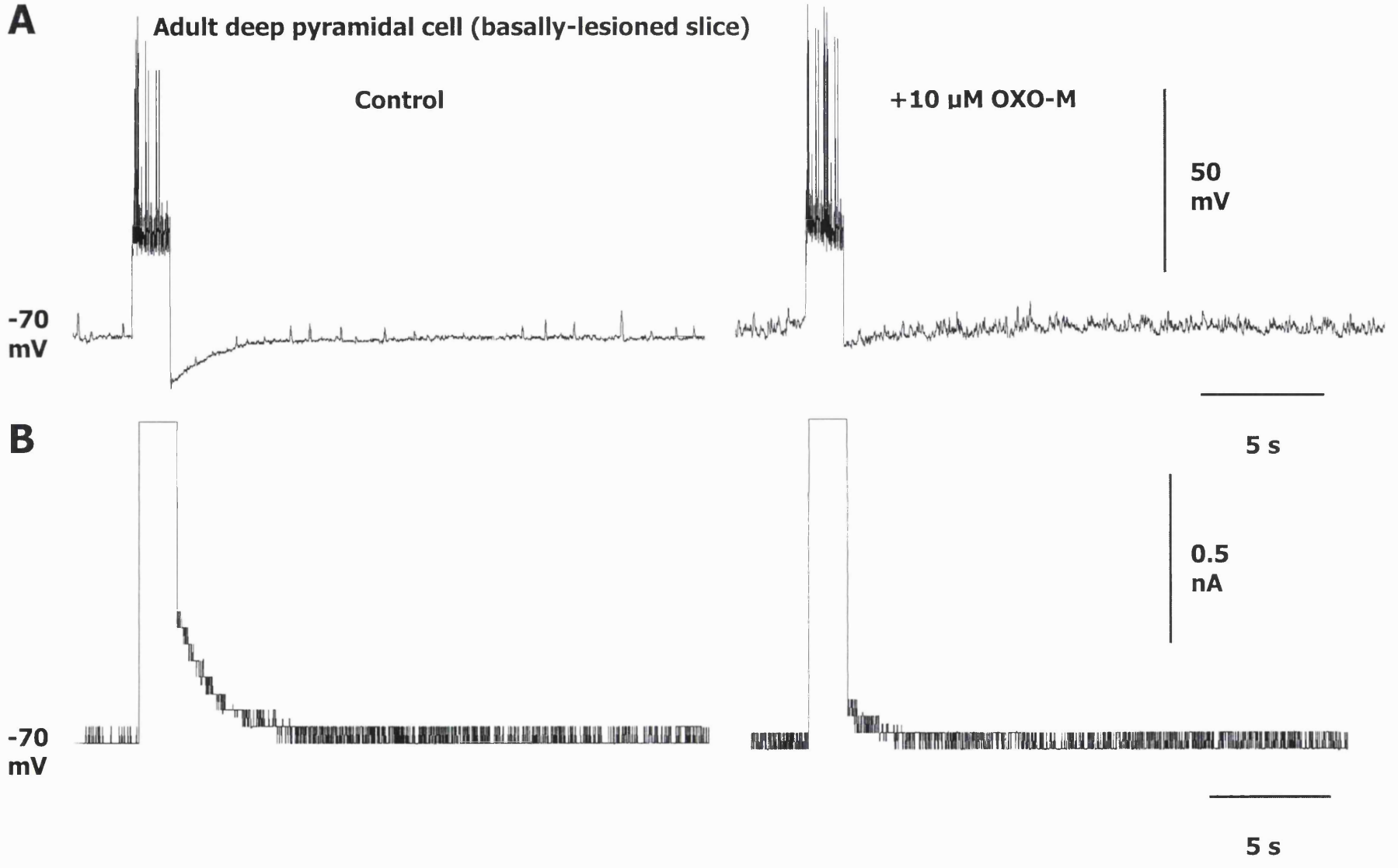
A
Adult deep pyramidal cell (basally-lesioned slice)
Control
+10 µM OXO-M
50
mV
-70
mV
5 s
B
0.5
nA
-70
mV
5 s

Figure 7.2

Figure 7.2

Slow after-hyperpolarizations (sAHPs) and their underlying slow outward tail currents (I_{AHP}) elicited following a long stimulus train (+2 nA; 1.6 s) applied to an adult presumed deep pyramidal neurone in a transverse piriform cortical brain slice preparation that had been basally-lesioned between layer III and the underlying endopiriform nucleus. Recordings of sAHPs (**A**) were made in current clamp mode in control (**left panel**) and in OXO-M (**right panel**). Recordings of I_{AHP}s (**B**) were made in 'hybrid' clamp mode in control (**left panel**) and in OXO-M (**right panel**). The cell was maintained at -70 mV by positive current injection. Control resting membrane potential=-83 mV. sAHPs and I_{AHP}s elicited in control conditions were not significantly different in magnitude or time course from those elicited in non-lesioned slices. However, as with apical lesions (Fig. 7.1), in OXO-M, no sADP or underlying I_{ADP} tail current were generated. Only a depressed sAHP and I_{AHP} were seen (*cf.* Fig. 7.1).

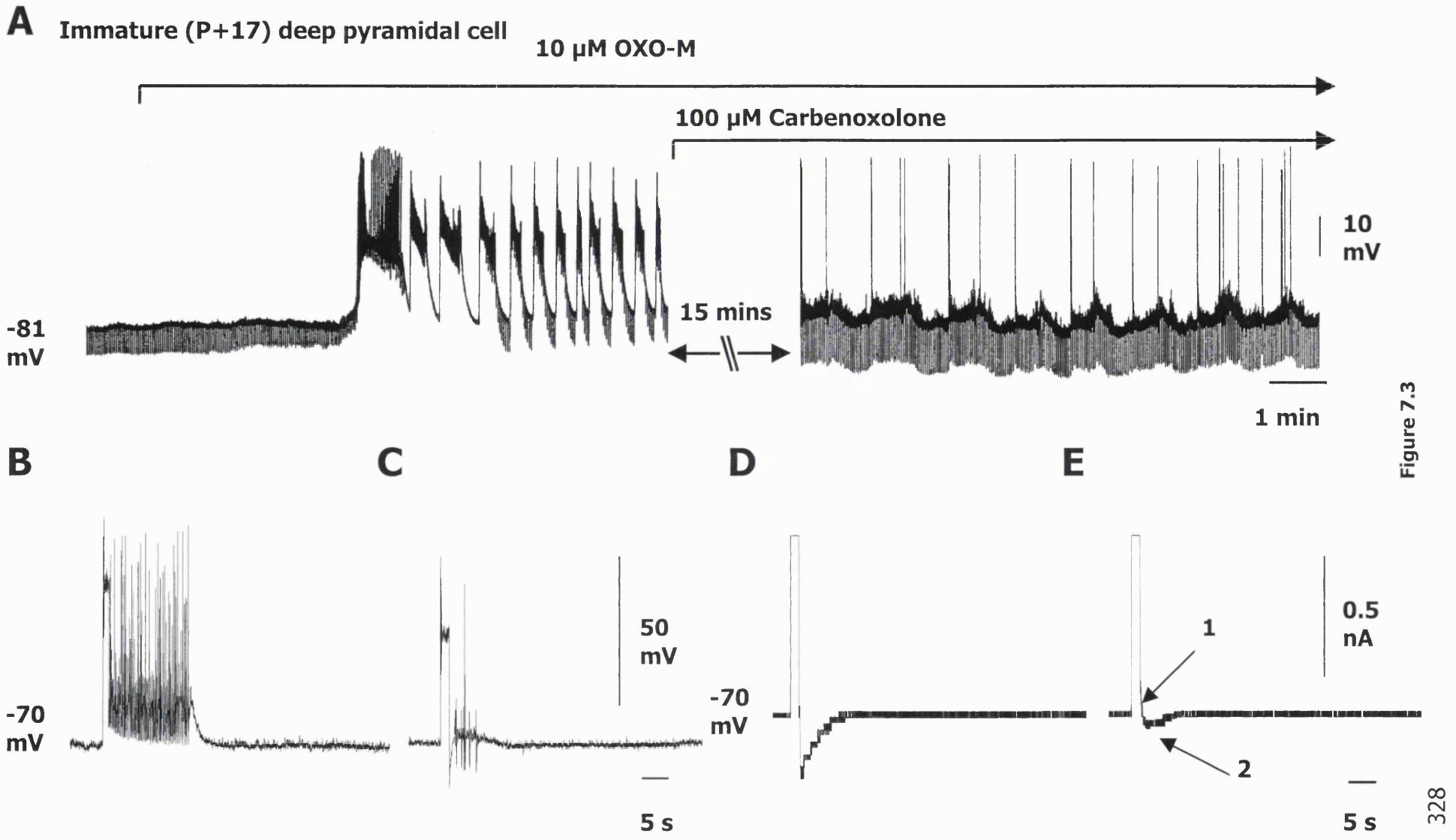
A
Immature (P+17) deep pyramidal cell
10 μM OXO-M
100 μM Carbenoxolone
-81
mV
15 mins
10
mV
1 min
B
C
D
E
-70
mV
50
mV
5 s
-70
mV
1
2
0.5
nA
5 s

Figure 7.3

Figure 7.3

A. Chart trace showing 10 μM OXO-M-induced spontaneous epileptiform burst firing in an immature (P+17) presumed deep pyramidal neurone and the abolition of burst firing by the gap junction blocker, carbenoxolone (100 μM). Control resting membrane potential=-81 mV. Note that although epileptiform burst firing was abolished, the recorded cell still remained depolarized and highly excitable. The OXO-M-induced increase in membrane input resistance was not reversed and the cell continued to fire spontaneously (not seen in control). **B.** A sADP elicited in the presence of 10 μM OXO-M following a long depolarizing stimulus train (+2 nA for 1.6 s) applied to the same neurone as **A**, maintained at –70 mV (close to threshold potential) in current clamp (CC) mode. **C.** A diminished sAHP/sADP complex elicited by the same stimulus as **B**, in the presence of OXO-M plus 100 μM carbenoxolone. **D.** The underlying I_{ADP} recorded at –70 mV in 'hybrid' voltage clamp (VC) mode in OXO-M. **E.** I_{ADP} in OXO-M plus carbenoxolone. Note the initial outward (**1**), then inward (**2**) complex tail current (I_{AHP}/I_{ADP}) revealed (same stimulus parameters as in **D**).

Table 7.1

	Control adult deep pyramidal cells (n=44)	Control immature deep pyramidal cells (n=176)	Basally lesioned adult deep pyramidal cells (n=6)	Basally lesioned immature deep pyramidal cells (n=10)	Apically lesioned adult deep pyramidal cells (n=5)	Apically lesioned immature deep pyramidal cells (n=8)
Resting input resistance (MΩ)	44 ± 2.1	46 ± 1.8	45 ± 2.6	44 ± 2.0	47 ± 2.5	42 ± 2.8
Input resistance in 10 μM OXO-M	49 ± 3.6	56 ± 2.7	51 ± 2.6	58 ± 3.1	48 ± 2.9	57 ± 4.0
Depolarization induced by 10 μM OXO-M	11 ± 0.8	12 ± 0.7	11 ± 0.9	13 ± 0.9	12 ± 1.1	12 ± 0.6

Table 7.1

Table 7.1

The effect of lesions made between layers I and II (apical) or between layer III and the endopiriform nucleus (basal) upon a number of responses elicited from adult and immature deep pyramidal piriform cortical neurones in control conditions and in 10 μM OXO-M. Data are means ± SEM. n=number of neurones. Spike amplitude was measured from resting potential to peak. Resting input resistance (R_{in}) was calculated from -70 mV resting membrane potential (achieved by application of positive holding current) using the steady-state electrotonic response (≤10 mV) to a -0.25 nA current pulse. No significant differences ($P>0.05$; Students t-tests) were found between the results obtained for unlesioned and either type (apical or basal) of lesioned slice.

Table 7.2

	sAHP		I_{AHP}	
	Peak amplitude (mV)	Time course (s)	Peak amplitude (nA)	Time course (s)
Non-lesioned slices; control conditions				
Adult (n=86)	13 ± 1.4	3.9 ± 1.7	0.81 ± 0.07	4.1 ± 1.5
Immature (n=266)	12 ± 1.2	5.0 ±1.7	0.76 ± 0.05	4.8 ± 1.6
Apically-lesioned slices; control conditions				
Adult (n=5)	12 ± 1.2	4.2 ± 1.8	0.77 ± 0.06	4.2 ± 1.6
Immature (n=8)	14 ± 1.7	4.6 ±1.2	0.79 ± 0.05	4.5 ± 1.2
	sADP		I_{ADP}	
Non-lesioned slices + 10 μM OXO-M				
Adult (n=44)	11 ± 1.4	32 ± 3.2	0.51 ± 0.04	32 ± 4.1
Immature (n=176)	12 ± 1.2	36 ± 5.3	0.53 ± 0.03	35 ± 4.9
Apically-lesioned slices + 10 μM OXO-M				
	sAHP		I_{AHP}	
Adult (n=5)	8 ± 1.1*	2.1 ± 1.2*	0.52 ± 0.06*	2.2 ± 1.4*
	sADP		I_{ADP}	
Immature (n=8)	12 ± 1.7	31 ± 5.8	0.49 ± 0.07	34 ± 4.6

Table 7.2

The effect of lesions made between layers I and II (apical) of adult and immature transverse piriform cortical brain slice preparations upon the sAHP and underlying slow outward tail current, I_{AHP}, in control conditions and upon the sADP and underlying slow inward tail current, I_{ADP} in the presence of 10 μM OXO-M, elicited following a long (+2 nA; 1.6 s) depolarizing stimulus recorded in current clamp and 'hybrid' clamp modes. Note that apical lesioning had no significant effect on the magnitude or time course of the sAHP (or I_{AHP} tail current) in the adult or immature preparations. However, in the presence of 10 μM OXO-M, the sADP (and underlying I_{ADP} tail current) typically recorded in adult neurones was absent and replaced by a diminished I_{AHP}. The magnitude and time course of the adult sAHPs evoked in the presence of 10 μM OXO-M in apically lesioned slices were found to be significantly ($P<0.05$) smaller than those elicited from either apically lesioned or non-lesioned slices in control conditions. Contrastingly, in OXO-M, the long depolarizing stimulus elicited the expected sADP (and I_{ADP}) in the apically-lesioned immature slices. The magnitude and time course of the sADP did not differ significantly from sADPs evoked in non-lesioned slices. * indicates results significantly different ($P<0.05$) from control. Data are means ± SEM. n=number of neurones.

Table 7.3

	sAHP		I_{AHP}	
	Peak amplitude (mV)	Time course (s)	Peak amplitude (nA)	Time course (s)
Non-lesioned slices; control conditions				
Adult (n=86)	13 ± 1.4	3.9 ± 1.7	0.81 ± 0.07	4.1 ± 1.5
Immature (n=266)	12 ± 1.2	5.0 ±1.7	0.76 ± 0.05	4.8 ± 1.6
Basally-lesioned slices; control conditions				
Adult (n=6)	13 ± 1.6	5.1 ± 1.9	0.73 ± 0.07	3.8 ± 1.6
Immature (n=10)	13 ± 1.4	4.8 ±1.1	0.79 ± 0.08	4.9 ± 1.2
	sADP		I_{ADP}	
Non-lesioned slices + 10 μM OXO-M				
Adult (n=44)	11 ± 1.4	32 ± 3.2	0.51 ± 0.04	32 ± 4.1
Immature (n=176)	12 ± 1.2	36 ± 5.3	0.53 ± 0.03	35 ± 4.9
Bsally-lesioned slices + 10 μM OXO-M				
	sAHP		I_{AHP}	
Adult (n=6)	3 ± 1.5*	2.3 ± 1.6*	0.21 ± 0.09*	2.5 ± 1.1*
	sADP		I_{ADP}	
Immature (n=10)	13 ± 1.4	35 ± 6.2	0.52 ± 0.06	32 ± 5.7

Table 7.3

The effect of lesions made between layer III and the underlying endopiriform nucleus (basal lesions) of adult and immature transverse piriform cortical brain slice preparations upon the sAHP and underlying I_{AHP} tail current, in control conditions and upon the sADP and underlying slow inward tail current (I_{ADP}) in the presence of 10 μM OXO-M, elicited following a long (+2 nA; 1.6 s) depolarizing stimulus in current clamp and 'hybrid' clamp modes. Note that basal lesioning had no effect on the magnitude or time course of the sAHP (or the underlying I_{AHP}) in the adult or immature preparations. However, in OXO-M, the sADP (and I_{ADP}) typically evoked from recorded adult neurones was replaced by a depressed sAHP (and I_{AHP}). The magnitude and time course of the adult sAHPs evoked in the presence of 10 μM OXO-M in basally lesioned slices were found to be significantly ($P<0.05$) smaller than those elicited from either basally lesioned or non-lesioned slices in control conditions. Contrastingly, in the presence of 10 μM OXO-M, the long depolarizing stimulus elicited the expected sADP (and underlying slow inward tail current) in the basally lesioned immature slice preparation. The magnitude and time course of the sADP evoked did not differ significantly from sADPs evoked in non-lesioned slices. * indicates results significantly different ($P<0.05$) from control. Data are means ± SEM. n=number of neurones.

Table 7.4

Elicited Response	10 μM OXO-M (n=18)	10 μM OXO-M plus 100 μM carbenoxolone (n=10)	10 μM OXO-M plus 280 μM octanol (n=8)
Suppression of excitatory intrinsic fibre synaptic transmission (%; *vs.* control)	25 ± 5.4	29 ± 6.8	22 ± 5.4
OXO-M-induced increase in membrane input resistance (%; *vs.* control)	20 ± 2.1	23 ± 1.8	20 ± 2.3
Magnitude of paroxysmal depolarizing shift (mV)	27 ± 4.2	4.3 ± 3.1*	5.8 ± 2.6*
sADP magnitude (mV)	12 ± 1.2	5 ± 0.9*	4 ± 1.1*
I_{ADP} magnitude (nA)	0.51 ± 0.03	0.21 ± 0.06*	0.19 ± 0.03*
OXO-M-induced depolarisation (mV)	12 ± 0.7	11 ± 0.9	12 ± 0.7

Table 7.4

The effect of the gap junction blockers, carbenoxolone (100 μM) and octanol (280 μM) upon a number of established OXO-M-induced effects recorded from presumed deep pyramidal neurones in immature (P+14 to P+28) piriform cortical brain slices. Intrinsic excitatory synaptic transmission, OXO-M-induced increases in membrane input resistance and OXO-M-induced depolarisation were all unaffected by either gap junction blocker. However the magnitude of, the epileptiform paroxysmal depolarizing shifts, sADP and underlying tail current (I_{ADP}) were all significantly ($P<0.05$) diminished in the presence of 10 μM OXO-M plus either gap junction blocker compared with the same responses elicited in the presence of 10 μM OXO-M alone. * indicates results significantly different ($P<0.05$) from control. Data are means ± SEM. n=number of neurones.

Chapter 8:
General Discussion
and
Conclusions

8.1 General Discussion and Conclusions

The principal aims of the present work were to characterise in detail, and attempt a determination of the mechanisms underlying, mAChR agonist-induced epileptiform bursting recorded from deep pyramidal neurones in immature rat piriform cortex slices, *in viitro*. The only extant work previously describing this phenomenon (Postlethwaite *et al.*, 1998a), whilst characterising some of its principal characteristics and responses to some pharmacological tools, left a number of mechanistic and phenomenological questions unanswered.

The present work has demonstrated an apparently linear decrease in epileptogenic susceptibility with increasing age that was not previously noted, an observation that may explain the higher frequency of burst incidence seen in the present work (~63%) compared to that of Postlethwaite et al. (1998)(~40%). Further age-dependent characterisation of the bursting phenomenon, by measurement and comparison of paroxysmal depolarising shift magnitude, inter-burst interval and variation in burst incidence along the rostro-caudal length of the slice has now further defined the phenomenon.

Having extensively characterised the phenomenon in this manner, further pharmacological tests were performed using subtype-specific mAChR antagonists (see below) and a range of anti-epileptic drugs in order to permit categorisation of this phenomenon by seizure type. Consequently, this immature model of piriform cortical activity was found to be most like *in vivo*, kindling-induced, piriform cortical seizure models (Kalimullina *et al.*, 2000)) or drug-induced picrotoxin or pentylenetetrazol (PTZ) animal seizure models (Macdonald & Kelly, 1995; Ramsay & Slater, 1993; Schacter, 1995) that have been likened to 'real-life' epileptiform events that manifest as generalised tonic-clonic seizures and thus, have allowed us to classify this phenomenon amongst comparable models of epileptiform behaviour (Section 1.5).

The viability of epileptiform seizure induction utilising *endogenous* ACh was also investigated by raising endogenous ACh levels in the slice using the anticholinesterase, neostigmine. Although overall cellular excitability was significantly increased, epileptiform bursting, of the type seen following mAChR agonist application, was never observed. These findings led us to the conclusion that, for epileptiform activity of this type to occur spontaneously *in vivo*, an increase in cellular excitability, independent of the cholinergic system (*e.g.* an increase in glutamatergic tone) would be required to raise piriform cortical excitation to a level where the increase in ACh-mediated excitability and ACh-mediated decrease in inhibition seen in the immature

preparation (see below) would be sufficient to initiate and maintain epileptiform bursting.

Subsequently, having characterised the bursting phenomenon in a principally empirically manner and determined that postsynaptic cholinergic modulation was mediated by the M1 mAChR subtype in both immature and adult slices, our attention was turned to which mAChR subtypes, if any, modulated presynaptic activity in this system. It was here that the principal differences between the immature and adult preparations were found. In summary, presynaptic mAChR activation (by an mAChR agonist or, to a lesser degree, neostigmine) prolonged afferent excitatory synaptic transmission and inhibited fast $GABA_A$-mediated synaptic transmission to a greater degree in the immature than the adult preparation, whilst mAChR-mediated inhibition of intrinsic excitatory synaptic transmission was significantly reduced in the immature preparation. These findings clearly demonstrated a heightened excitability in the immature preparation that not only manifested as epileptiform acitivity, but also as increased *'all or nothing'* firing, superimposed spike firing upon EPSPs and sustained post-stimulus depolarisations, all of which are known to be characteristics not only of seizure-prone systems, but also of associative memory processes.

The underlying reason for the observed differences between the responses of adult and immature preparations was found to be due to a change in the mAChR subtype responsible for presynaptic modulation, from the M2 subtype in the immature preparation to the M1 subtype in the adult. Consequently, we proposed that the gradual decrease in bursting incidence with increasing age was primarily due to this progressive change in mAChR subtype from M2 to M1. However, a significant question that remains is how can the M2 subtype in the immature preparation be more effective at inhibiting fast inhibitory synaptic transmission than the M1 subtype in the adult, whilst the reverse is true of intrinsic excitatory transmission? Whether this is due to either differential coupling mechanisms between inhibitory and excitatory control systems or a variation in presynaptic mAChR numbers remains to be determined.

The final series of experiment in the present work addressed the fact that a number of reports (Hoffman & Haberly, 1996a) (Bertram, 1997; Kelly *et al.*, 2002; Linster *et al.*, 1999) have suggested that epileptiform activity recorded in the piriform cortex may in fact originate from outside the piriform cortex region. Consequently, lesioning techniques were used that demonstrated that, in *this model* of piriform cortical epilepsy, epileptiform bursting *did* originate from within the piriform cortex itself. Interestingly, these experiments also revealed that the ability of deep pyramidal piriform

cortical neurones to exhibit a slow post-stimulus afterdepolarization (sADP) in the presence of a mAChR agonist was abolished in the adult, but not the immature preparation following apical *or* basal lesioning. This would suggest that structures critical for sADP generation in the adult preparation may be located on distal dendrites whilst the same structures may be more proximally located in the immature preparation.

Finally, gap junction blockers were used to investigate whether electrotonic transmission was in any way responsible for the initiation and maintenance of the mAChR agonist-induced burst firing. It was found that gap junction blockade not only disrupted epileptiform activity, but also significantly diminished the sADP thereby, in conjunction with the lesioning experiments, demonstrating a clear link between gap junction activity, epileptiform bursting and sADP generation.

In conclusion, the present work has not only extensively characterised and determined many of the underlying mechanistic and phenomenological aspects of mAChR agonist-induced epileptiform bursting activity in the immature rat piriform cortical slice preparation, but also demonstrated a clear causal link between the sADP, gap junction functionality and burst firing in this brain area and a variety of consequences that arise as a result of the developmental mAChR subtype *'switch'*.

These results show the piriform cortex to be a brain area that is not only ripe for further neuronal, developmental, pathological and aetiological investigation, but also that the immature slice preparation is a valuable model of both sustained epileptiform behaviour and associative memory processes.

References

1. ADAMS, P. R., BROWN, D. A. & CONSTANTI, A. (1982). Pharmacological inhibition of the M-current. *J. Physiol,* **332**, 223-262.

2. ALLEN, T. G. & BROWN, D. A. (1993). M2 muscarinic receptor-mediated inhibition of the Ca2+ current in rat magnocellular cholinergic basal forebrain neurones. *J. Physiol,* **466**, 173-189.

3. ANDRADE, R. (1991). Cell excitation enhances muscarinic cholinergic responses in rat association cortex. *Brain Res.,* **548**, 81-93.

4. ANDREASEN, M., LAMBERT, J. D. & JENSEN, M. S. (1989). Effects of new non-N-methyl-D-aspartate antagonists on synaptic transmission in the in vitro rat hippocampus. *J. Physiol,* **414**, 317-336.

5. APPLEGATE, C. D. & SAMORISKI, G. M. (1993). Mechanisms of kindling: an evaluation of single trial seizure induction procedures for use as controls. *Epilepsy Res.,* **15**, 201-205.

6. ARAKI, T., KATO, H., FUJIWARA, T. & ITOYAMA, Y. (1995). Age-related changes in bindings of second messengers in the rat brain. *Brain Res.,* **704**, 227-232.

7. ARAKI, T., KATO, H., FUJIWARA, T. & ITOYAMA, Y. (1996). Regional age-related alterations in cholinergic and GABAergic receptors in the rat brain. *Mech. Ageing Dev.,* **88**, 49-60.

8. ARAMAKIS, V. B., BANDROWSKI, A. E. & ASHE, J. H. (1997). Muscarinic reduction of GABAergic synaptic potentials results in disinhibition of the AMPA/kainate-mediated EPSP in auditory cortex. *Brain Res.,* **758**, 107-117.

9. ARANEDA, R. & ANDRADE, R. (1991). 5-Hydroxytryptamine2 and 5-hydroxytryptamine 1A receptors mediate opposing responses on membrane excitability in rat association cortex. *Neuroscience,* **40**, 399-412.

10. BAGETTA, G. & CONSTANTI, A. (1991). Muscarinic inhibition of excitatory neurotransmission in guinea-pig olfactory cortex slices: weak antagonism by M3-muscarinic receptor antagonists. *Eur. J. Pharmacol.,* **198**, 69-75.

11. BARBAROSIE, M., LOUVEL, J., KURCEWICZ, I. & AVOLI, M. (2000). CA3-Released entorhinal seizures disclose dentate gyrus epileptogenicity and unmask a temporoammonic pathway. *J. Neurophysiol.,* **83**, 1115-1124.

12. BARKAI, E., BERGMAN, R. E., HORWITZ, G. & HASSELMO, M. E. (1994). Modulation of associative memory function in a biophysical simulation of rat piriform cortex. *J. Neurophysiol.,* **72**, 659-677.

13. BARKAI, E. & HASSELMO, M. E. (1994). Modulation of the input/output function of rat piriform cortex pyramidal cells. *J. Neurophysiol.,* **72**, 644-658.

14. BARKAI, E. & HASSELMO, M. H. (1997). Acetylcholine and associative memory in the piriform cortex. *Mol. Neurobiol.,* **15**, 17-29.

15. BARKAI, E. & SAAR, D. (2001). Cellular correlates of olfactory learning in the rat piriform cortex. *Rev. Neurosci.,* **12**, 111-120.

16. BEHAN, M. & HABERLY, L. B. (1999). Intrinsic and efferent connections of the endopiriform nucleus in rat. *J. Comp Neurol.,* **408**, 532-548.

17. BELLUARDO, N., TROVATO-SALINARO, A., MUDO, G., HURD, Y. L. & CONDORELLI, D. F. (1999). Structure, chromosomal localization, and brain expression of human Cx36 gene. *J. Neurosci. Res.,* **57**, 740-752.

18. BERTRAM, E. H. (1997). Functional anatomy of spontaneous seizures in a rat model of limbic epilepsy. *Epilepsia,* **38**, 95-105.

19. BIEDENBACH, M. A. & STEVENS, C. F. (1969). Synaptic organization of cat olfactory cortex as revealed by intracellular recording. *J. Neurophysiol.,* **32**, 204-214.

20. BIELLA, G, FORTI, M. & DE CURTIS, M (1996). Propagation of epileptiform potentials in the guinea-pig piriform cortex is sustained by associative fibres. Epilepsy Research 24, 137-146.
Ref Type: Generic

21. BIRNBAUMER, L., ABRAMOWITZ, J. & BROWN, A. M. (1990). Receptor-effector coupling by G proteins. *Biochim. Biophys. Acta,* **1031**, 163-224.

22. BLOMS-FUNKE, P., GERNERT, M., EBERT, U. & LOSCHER, W. (1999). Extracellular single-unit recordings of piriform cortex neurons in rats: influence of different types of anesthesia and characterization of neurons by pharmacological manipulation of serotonin receptors. *J. Neurosci. Res.,* **55**, 608-619.

23. BOCTI, C., ROBITAILLE, Y., DIADORI, P., LORTIE, A., MERCIER, C., BOUTHILLIER, A. & CARMANT, L. (2003). The pathological basis of temporal lobe epilepsy in childhood. *Neurology,* **60**, 191-195.

24. BOOTH, V., RINZEL, J. & KIEHN, O. (1997). Compartmental model of vertebrate motoneurons for Ca2+-dependent spiking and plateau potentials under pharmacological treatment. *J. Neurophysiol.,* **78**, 3371-3385.

25. BOWER, J. M. & HABERLY, L. B. (1986). Facilitating and nonfacilitating synapses on pyramidal cells: a correlation between physiology and morphology. *Proc. Natl. Acad. Sci. U. S. A.,* **83**, 1115-1119.

26. BRAGA, M. F., ARONIADOU-ANDERJASKA, V., POST, R. M. & LI, H. (2002). Lamotrigine reduces spontaneous and evoked GABAA receptor-mediated synaptic transmission in the basolateral amygdala: implications for its effects in seizure and affective disorders. *Neuropharmacology,* **42**, 522-529.

27. BRAGIN, A., MODY, I., WILSON, C. L. & ENGEL, J., JR. (2002). Local generation of fast ripples in epileptic brain. *J. Neurosci.,* **22**, 2012-2021.

28. BROWN, D. A. (1990). G-proteins and potassium currents in neurons. *Annu. Rev. Physiol,* **52**, 215-242.

29. BROWN, D. A. & ADAMS, P. R. (1980). Muscarinic suppression of a novel voltage-sensitive K^+ current in a vertebrate neurone. *Nature,* **283**, 673-676.

30. BROWN, D. A., FORWARD, A. & MARSH, S. (1980). Antagonist discrimination between ganglionic and ileal muscarinic receptors. *Br. J. Pharmacol.,* **71**, 362-364.

31. BROWN, D. A., FORWARD, A. & MARSH, S. (1997). Antagonist discrimination between ganglionic and ileal muscarinic receptors. 1980. *Br. J. Pharmacol.,* **120**, 447-449.

32. BROWNING, R., MAGGIO, R., SAHIBZADA, N. & GALE, K. (1993). Role of brainstem structures in seizures initiated from the deep prepiriform cortex of rats. *Epilepsia,* **34**, 393-407.

33. BRUZZONE, R. (2001). Learning the language of cell-cell communication through connexin channels. *Genome Biol.,* **2**, REPORTS4027.

34. BUCKLEY, N. J. (1990). In *Intracellular messengers and implications for drug development.* pp. 11-30. Publisher: Wiley, New York.

35. BUCKLEY, N. J., BONNER, T. I. & BRANN, M. R. (1988). Localization of a family of muscarinic receptor mRNAs in rat brain. *J. Neurosci.,* **8**, 4646-4652.

36. BURDETTE, D. & SACKELLARES, J. (1994). Felbamate pharmacology and use in epilepsy. *Clinical Neuropharmacology,* **17(5)**, 389-402.

37. CALABRESI, P., CENTONZE, D., MARFIA, G. A., PISANI, A. & BERNARDI, G. (1999). An in vitro electrophysiological study on the effects of phenytoin, lamotrigine and gabapentin on striatal neurons. *Br. J. Pharmacol.,* **126**, 689-696.

38. CALABRESI, P., PICCONI, B., SAULLE, E., CENTONZE, D., HAINSWORTH, A. H. & BERNARDI, G. (2000). Is pharmacological neuroprotection dependent on reduced glutamate release? *Stroke,* **31**, 766-772.

39. CALCAGNOTTO, M. E., BARBAROSIE, M. & AVOLI, M. (2000). Hippocampus-entorhinal cortex loop and seizure generation in the young rodent limbic system. *J. Neurophysiol.,* **83**, 3183-3187.

40. CARMICHAEL, S. T., CLUGNET, M. C. & PRICE, J. L. (1994). Central olfactory connections in the macaque monkey. *J. Comp Neurol.,* **346**, 403-434.

41. CAULFIELD, M. P. (1993). Muscarinic receptors--characterization, coupling and function. *Pharmacol. Ther.,* **58**, 319-379.

42. CAULFIELD, M. P. & BROWN, D. A. (1991). Pharmacology of the putative M4 muscarinic receptor mediating Ca- current inhibition in neuroblastoma x glioma hybrid (NG 108-15) cells. *Br. J. Pharmacol.,* **104**, 39-44.

43. CHABAUD, P., RAVEL, N., WILSON, D. & GERVAIS, R. (1999). Functional coupling in rat central olfactory pathways: a coherence analysis. *Neuroscience Letters*, **276**, 17-20.

44. CHU, S. & DOWNES, J. J. (2000). Long live Proust: the odour-cued autobiographical memory bump. *Cognition,* **75**, B41-B50.

45. CLAVEROL, E. T., BROWN, A. D. & CHAD, J. E. (2002). A large-scale simulation of the piriform cortex by a cell automaton-based network model. *IEEE Trans. Biomed. Eng,* **49**, 921-935.

46. COLE, A. E. & NICOLL, R. A. (1984). Characterization of a slow cholinergic post-synaptic potential recorded in vitro from rat hippocampal pyramidal cells. *J. Physiol,* **352**, 173-188.

47. COLLINS, G., ANSON, J. & KELLY, E. (1982). Baclofen: effects on evoked field potentials and amino acid neurotransmitter release in the rat olfactory cortex slice. *Brain Research*, **238**, 371-383.

48. COLLINS, G. & HOWLETT, S. (1988). The pharmacology of excitatory neurotransmission transmission in the rat olfactory cortex slice. *Neuropharmacology*, **27**, 697-705.

49. CONDORELLI, D. F., PARENTI, R., SPINELLA, F., TROVATO, S. A., BELLUARDO, N., CARDILE, V. & CICIRATA, F. (1998). Cloning of a new gap junction gene (Cx36) highly expressed in mammalian brain neurons. *Eur. J. Neurosci.,* **10**, 1202-1208.

50. CONSTANTI, A. & BAGETTA, G. (1991). Muscarinic receptor activation induces a prolonged post-stimulus afterdepolarization with a conductance decrease in guinea-pig olfactory cortex neurones in vitro. *Neurosci. Lett.*, **131**, 27-32.

51. CONSTANTI, A., BAGETTA, G. & LIBRI, V. (1993). Persistent muscarinic excitation in guinea-pig olfactory cortex neurons: involvement of a slow post-stimulus afterdepolarizing current. *Neuroscience,* **56**, 887-904.

52. CONSTANTI, A. & GALVAN, M. (1983). Fast inward-rectifying current accounts for anomalous rectification in olfactory cortex neurones. *J. Physiol,* **335**, 153-178.

53. CONSTANTI, A., GALVAN, M., FRANZ, P. & SIM, J. A. (1985). Calcium-dependent inward currents in voltage-clamped guinea-pig olfactory cortex neurones. *Pflugers Arch.,* **404**, 259-265.

54. CONSTANTI, A. & LIBRI, V. (1992). Trans-ACPD induces a slow post-stimulus inward tail current (IADP) in guinea-pig olfactory cortex neurones in vitro. *Eur. J. Pharmacol.,* **216**, 463-464.

55. CONSTANTI, A. & SIM, J. A. (1987a). Calcium-dependent potassium conductance in guinea-pig olfactory cortex neurones in vitro. *J. Physiol,* **387**, 173-194.

56. CONSTANTI, A. & SIM, J. A. (1987b). Muscarinic receptors mediating suppression of the M-current in guinea-pig olfactory cortex neurones may be of the M2-subtype. *Br. J. Pharmacol.,* **90**, 3-5.

57. COWAN, L. D. (2002). The epidemiology of the epilepsies in children. *Ment. Retard. Dev. Disabil. Res. Rev.,* **8**, 171-181.

58. CUNHA, R. A., COELHO, J. E., COSTENLA, A. R., LOPES, L. V., PARADA, A., DE MENDONCA, A., SEBASTIAO, A. M. & RIBEIRO, J. A. (2002). Effects of carbamazepine and novel 10,11-dihydro-5H-dibenz[b,f]azepine-5-carboxamide derivatives on synaptic transmission in rat hippocampal slices. *Pharmacol. Toxicol.,* **90**, 208-213.

59. CUNNINGHAM, M. O. & JONES, R. S. (2000). The anticonvulsant, lamotrigine decreases spontaneous glutamate release but increases spontaneous GABA release in the rat entorhinal cortex in vitro. *Neuropharmacology,* **39**, 2139-2146.

60. DADE, L. A., ZATORRE, R. J. & JONES-GOTMAN, M. (2002). Olfactory learning: convergent findings from lesion and brain imaging studies in humans. *Brain,* **125**, 86-101.

61. DATICHE, F. & CATTARELLI, M. (1996a). Catecholamine innervation of the piriform cortex: a tracing and immunohistochemical study in the rat. *Brain Res.*, **710**, 69-78.

62. DATICHE, F. & CATTARELLI, M. (1996b). Reciprocal and topographic connections between the piriform and prefrontal cortices in the rat: a tracing study using the B subunit of the cholera toxin. *Brain Res. Bull.*, **41**, 391-398.

63. DATICHE, F., LITAUDON, P. & CATTARELLI, M. (1996). Intrinsic association fiber system of the piriform cortex: a quantitative study based on a cholera toxin B subunit tracing in the rat. *J. Comp Neurol.*, **376**, 265-277.

64. DE CURTIS, M., BIELLA, G. & FORTI, M. (1996). Epileptiform activity in the piriform cortex of the in vitro isolated guinea pig brain preparation. *Epilepsy Res.*, **26**, 75-80.

65. DE CURTIS, M., MANFRIDI, A. & BIELLA, G. (1998). Activity-dependent pH shifts and periodic recurrence of spontaneous interictal spikes in a model of focal epileptogenesis. *J. Neurosci.*, **18**, 7543-7551.

66. DEISZ, R. A. (1999). GABA(B) receptor-mediated effects in human and rat neocortical neurones in vitro. *Neuropharmacology,* **38**, 1755-1766.

67. DELORENZO, R. J., SOMBATI, S. & COULTER, D. A. (2000). Effects of topiramate on sustained repetitive firing and spontaneous recurrent seizure discharges in cultured hippocampal neurons. *Epilepsia,* **41 Suppl 1**, S40-S44.

68. DEMIR, R., HABERLY, L. B. & JACKSON, M. B. (2000). Characteristics of plateau activity during the latent period prior to epileptiform discharges in slices from rat piriform cortex. *J. Neurophysiol.*, **83**, 1088-1098.

69. DEMIR, R., HABERLY, L. B. & JACKSON, M. B. (2001). Epileptiform discharges with in-vivo-like features in slices of rat piriform cortex with longitudinal association fibers. *J. Neurophysiol.*, **86**, 2445-2460.

70. DICKSON, C. T., MAGISTRETTI, J., SHALINSKY, M. H., FRANSEN, E., HASSELMO, M. E. & ALONSO, A. (2000). Properties and role of I(h) in the pacing of subthreshold oscillations in entorhinal cortex layer II neurons. *J. Neurophysiol.*, **83**, 2562-2579.

71. DODGSON, S., SHANK, R. & MARYANOFF, B. (2000). Topiramate as an inhibitor of carbonic anhydrase isozymes. *Epilepsia,* **41 (Suppl. 1)**, S35-S39.

72. DOHERTY, J., GALE, K. & EAGLES, D. A. (2000). Evoked epileptiform discharges in the rat anterior piriform cortex: generation and local propagation. *Brain Res.*, **861**, 77-87.

73. DORJE, F., WESS, J., LAMBRECHT, G., TACKE, R., MUTSCHLER, E. & BRANN, M. R. (1991). Antagonist binding profiles of five cloned human muscarinic receptor subtypes. *J. Pharmacol. Exp. Ther.*, **256**, 727-733.

74. DRAGUHN, A., TRAUB, R. D., BIBBIG, A. & SCHMITZ, D. (2000). Ripple (approximately 200-Hz) oscillations in temporal structures. *J. Clin. Neurophysiol.*, **17**, 361-376.

75. DUNIA, R., BUCKWALTER, G., DEFAZIO, T., VILLAR, F. D., MCNEILL, T. H. & WALSH, J. P. (1996). Decreased duration of Ca(2+)-mediated plateau potentials in striatal neurons from aged rats. *J. Neurophysiol.*, **76**, 2353-2363.

76. DUTAR, P. & NICOLL, R. A. (1988b). A physiological role for GABAB receptors in the central nervous system. *Nature,* **332**, 156-158.

77. DUTAR, P. & NICOLL, R. A. (1988a). Stimulation of phosphatidylinositol (PI) turnover may mediate the muscarinic suppression of the M-current in hippocampal pyramidal cells. *Neurosci. Lett.*, **85**, 89-94.

78. EBERT, U., RUNDFELDT, C. & LOSCHER, W. (1995). Development and pharmacological suppression of secondary afterdischarges in the hippocampus of amygdala-kindled rats. *Eur. J. Neurosci.*, **7**, 732-741.

79. ECKENSTEIN, F. P., BAUGHMAN, R. W. & QUINN, J. (1988). An anatomical study of cholinergic innervation in rat cerebral cortex. *Neuroscience,* **25**, 457-474.

80. EGAN, T. M. & NORTH, R. A. (1985). Acetylcholine acts on m2-muscarinic receptors to excite rat locus coeruleus neurones. *Br. J. Pharmacol.*, **85**, 733-735.

81. EGOZI, Y., SOKOLOVSKY, M., SCHEJTER, E., BLATT, I., ZAKUT, H., MATZKEL, A. & SOREQ, H. (1986). Divergent regulation of muscarinic binding sites and acetylcholinesterase in discrete regions of the developing human fetal brain. *Cell Mol. Neurobiol.*, **6**, 55-70.

82. EKEROT, C. F. & OSCARSSON, O. (1981). Prolonged depolarization elicited in Purkinje cell dendrites by climbing fibre impulses in the cat. *J. Physiol,* **318**, 207-221.

83. EKSTRAND, J. J., DOMROESE, M. E., FEIG, S. L., ILLIG, K. R. & HABERLY, L. B. (2001a). Immunocytochemical analysis of basket cells in rat piriform cortex. *J. Comp Neurol.*, **434**, 308-328.

84. EKSTRAND, J. J., DOMROESE, M. E., JOHNSON, D. M., FEIG, S. L., KNODEL, S. M., BEHAN, M. & HABERLY, L. B. (2001b). A new subdivision of

anterior piriform cortex and associated deep nucleus with novel features of interest for olfaction and epilepsy. *J. Comp Neurol.*, **434**, 289-307.

85. ELISEVICH, K., REMPEL, S. A., SMITH, B. & ALLAR, N. (1997b). Connexin 43 mRNA expression in two experimental models of epilepsy. *Mol. Chem. Neuropathol.*, **32**, 75-88.

86. ELISEVICH, K., REMPEL, S. A., SMITH, B. & HIRST, K. (1998). Temporal profile of connexin 43 mRNA expression in a tetanus toxin-induced seizure disorder. *Mol. Chem. Neuropathol.*, **35**, 23-37.

87. ELISEVICH, K., REMPEL, S. A., SMITH, B. J. & EDVARDSEN, K. (1997a). Hippocampal connexin 43 expression in human complex partial seizure disorder. *Exp. Neurol.*, **145**, 154-164.

88. FALLON, J. H., HICKS, R. & LOUGHLIN, S. E. (1983). The origin of cholecystokinin terminals in the basal forebrain of the rat: evidence from immunofluorescence and retrograde tracing. *Neurosci. Lett.*, **37**, 29-35.

89. FELDER, C. C., POULTER, M. O. & WESS, J. (1992). Muscarinic receptor-operated Ca2+ influx in transfected fibroblast cells is independent of inositol phosphates and release of intracellular Ca2+. *Proc. Natl. Acad. Sci. U. S. A*, **89**, 509-513.

90. FERRIS, C. D. & SNYDER, S. H. (1992). Inositol 1,4,5-trisphosphate-activated calcium channels. *Annu. Rev. Physiol*, **54**, 469-488.

91. FISHER, R. S. (1989). Animal models of the epilepsies. *Brain Res. Brain Res. Rev.*, **14**, 245-278.

92. FONSECA, C. G., GREEN, C. R. & NICHOLSON, L. F. (2002). Upregulation in astrocytic connexin 43 gap junction levels may exacerbate generalized seizures in mesial temporal lobe epilepsy. *Brain Res.*, **929**, 105-116.

93. FORTI, M., BIELLA, G., CACCIA, S. & DE CURTIS, M. (1997). Persistent excitability changes in the piriform cortex of the isolated guinea-pig brain after transient exposure to bicuculline. *Eur. J. Neurosci.*, **9**, 435-451.

94. FRASER, D. D., DOLL, D. & MACVICAR, B. A. (2001). Serine/threonine protein phosphatases and synaptic inhibition regulate the expression of cholinergic-dependent plateau potentials. *J. Neurophysiol.*, **85**, 1197-1205.

95. FURSHPAN, E. & POTTER, D. (1959). Transmission at the giant motor synapses of the crayfish. *J. Physiol. (Lond.)*, **145**, 289-325.

96. GAHWILER, B. H. (1984). Facilitation by acetylcholine of tetrodotoxin-resistant spikes in rat hippocampal pyramidal cells. *Neuroscience*, **11**, 381-388.

97. GAHWILER, B. H. & BROWN, D. A. (1987). Muscarine affects calcium-currents in rat hippocampal pyramidal cells in vitro. *Neurosci. Lett.*, **76**, 301-306.

98. GAIARSA, J. L., MCLEAN, H., CONGAR, P., LEINEKUGEL, X., KHAZIPOV, R., TSEEB, V. & BEN ARI, Y. (1995). Postnatal maturation of gamma-aminobutyric acidA and B-mediated inhibition in the CA3 hippocampal region of the rat. *J. Neurobiol.*, **26**, 339-349.

99. GAIARSA, J. L., ZAGREAN, L. & BEN ARI, Y. (1994). Neonatal irradiation prevents the formation of hippocampal mossy fibers and the epileptic action of kainate on rat CA3 pyramidal neurons. *J. Neurophysiol.*, **71**, 204-215.

100. GALLIGAN, J. J., NORTH, R. A. & TOKIMASA, T. (1989). Muscarinic agonists and potassium currents in guinea-pig myenteric neurones. *Br. J. Pharmacol.*, **96**, 193-203.

101. GALVAN, M., FRANZ, P. & CONSTANTI, A. (1985). Spontaneous inhibitory postsynaptic potentials in guinea pig neocortex and olfactory cortex neurones. *Neurosci. Lett.*, **57**, 131-135.

102. GEAN, P. W., HUANG, C. C., KUO, J. R., LIN, J. H., YI, P. L. & TSAI, J. J. (1993). Analysis of carbamazepine's anticonvulsant actions in hippocampal and amygdaloid slices of the rat. *Chin J. Physiol,* **36**, 199-204.

103. GERNERT, M., BLOMS-FUNKE, P., EBERT, U. & LOSCHER, W. (2000). Kindling causes persistent in vivo changes in firing rates and glutamate sensitivity of central piriform cortex neurons in rats. *Neuroscience,* **99**, 217-227.

104. GERNERT, M., THOMPSON, K. W., LOSCHER, W. & TOBIN, A. J. (2002). Genetically engineered GABA-producing cells demonstrate anticonvulsant effects and long-term transgene expression when transplanted into the central piriform cortex of rats. *Exp. Neurol.*, **176**, 183-192.

105. GIL, Z., CONNORS, B. W. & AMITAI, Y. (1997). Differential regulation of neocortical synapses by neuromodulators and activity. *Neuron,* **19**, 679-686.

106. GIRGIS, M. (1978). Neostigmine activated epileptiform discharge in the amygdala: electrographic-behavioral correlations. *Epilepsia,* **19**, 521-530.

107. GIRGIS, M. (1981). Neuronal hypersensitivity to acetylcholinesterase inhibitors induced by a kindling stimulus in the rabbit brain. *Brain Res.*, **208**, 379-386.

108. GODDARD, G. V. (1967). Development of epileptic seizures through brain stimulation at low intensity. *Nature,* **214**, 1020-1021.

109. GODFRAIND, J. M. (1985). Intrasomatic and intradendritic recordings of plateau potentials in slices of the dentate gyrus maintained in vitro. *Exp. Brain Res.*, **57**, 233-238.

110. GONZALES, R. A. & CREWS, F. T. (1984). Characterization of the cholinergic stimulation of phosphoinositide hydrolysis in rat brain slices. *J. Neurosci.*, **4**, 3120-3127.

111. GOTTFRIED, J. A., DEICHMANN, R., WINSTON, J. S. & DOLAN, R. J. (2002). Functional heterogeneity in human olfactory cortex: an event-related functional magnetic resonance imaging study. *J. Neurosci.*, **22**, 10819-10828.

112. GRAYBIEL, A. M., PICKEL, V. M., JOH, T. H., REIS, D. J. & RAGSDALE, C. W. (1981). Direct demonstration of a correspondence between the dopamine islands and acetylcholinesterase patches in the developing striatum. *Proc. Natl. Acad. Sci. U. S. A*, **78**, 5871-5875.

113. GRUSLIN, E., DESCOMBES, S. & PSARROPOULOU, C. (1999). Epileptiform activity generated by endogenous acetylcholine during blockade of GABAergic inhibition in immature and adult rat hippocampus. *Brain Res.*, **835**, 290-297.

114. HABERLY, L. & BEHAN, M. (1983). Structure of the piriform cortex of the opossum. III. Ultrastructural characterization of synaptic terminals of association and olfactory bulb afferent fibers. *J. Comp Neurol.*, **219**, 448-460.

115. HABERLY, L. B. (1973). Unitary analysis of opossum prepyriform cortex. *J. Neurophysiol.*, **36**, 762-774.

116. HABERLY, L. B. (1983). Structure of the piriform cortex of the opossum. I. Description of neuron types with Golgi methods. *J. Comp Neurol.*, **213**, 163-187.

117. HABERLY, L. B. & BOWER, J. M. (1984). Analysis of association fiber system in piriform cortex with intracellular recording and staining techniques. *J. Neurophysiol.*, **51**, 90-112.

118. HABERLY, L. B. & BOWER, J. M. (1989). Olfactory cortex: model circuit for study of associative memory? *Trends Neurosci.*, **12**, 258-264.

119. HABERLY, L. B. & FEIG, S. L. (1983). Structure of the piriform cortex of the opossum. II. Fine structure of cell bodies and neuropil. *J. Comp Neurol.*, **216**, 69-88.

120. HABERLY, L. B., HANSEN, D. J., FEIG, S. L. & PRESTO, S. (1987). Distribution and ultrastructure of neurons in opossum piriform cortex displaying

immunoreactivity to GABA and GAD and high-affinity tritiated GABA uptake. *J. Comp Neurol.*, **266**, 269-290.

121. HABERLY, L. B. & PRESTO, S. (1986). Ultrastructural analysis of synaptic relationships of intracellularly stained pyramidal cell axons in piriform cortex. *J. Comp Neurol.*, **248** , 464-474.

122. HABERLY, L. B. & PRICE, J. L. (1977). The axonal projection patterns of the mitral and tufted cells of the olfactory bulb in the rat. *Brain Res.*, **129**, 152-157.

123. HABERLY, L. B. & PRICE, J. L. (1978). Association and commissural fiber systems of the olfactory cortex of the rat. *J. Comp Neurol.*, **178**, 711-740.

124. HABERLY, L. B. & SUTULA, T. P. (1992). Neuronal processes that underlie expression of kindled epileptiform events in the piriform cortex in vivo. *J. Neurosci.*, **12**, 2211-2224.

125. HAGA, K. & HAGA, T. (1990). Dual regulation by G proteins of agonist-dependent phosphorylation of muscarinic acetylcholine receptors. *FEBS Lett.*, **268**, 43-47.

126. HAJ-DAHMANE, S. & ANDRADE, R. (1998). Ionic mechanism of the slow afterdepolarization induced by muscarinic receptor activation in rat prefrontal cortex. *J. Neurophysiol.*, **80**, 1197-1210.

127. HAJ-DAHMANE, S. & ANDRADE, R. (1999). Muscarinic receptors regulate two different calcium-dependent non-selective cation currents in rat prefrontal cortex. *Eur. J. Neurosci.*, **11**, 1973-1980.

128. HAMMER, R., BERRIE, C. P., BIRDSALL, N. J., BURGEN, A. S. & HULME, E. C. (1980). Pirenzepine distinguishes between different subclasses of muscarinic receptors. *Nature,* **283**, 90-92.

129. HARVEY, J. A., SCHOLFIELD, C. N. & BROWN, D. A. (1974). Evoked surface-positive potentials in isolated mammalian olfactory cortex. *Brain Res.*, **76**, 235-245.

130. HASSELMO, M. E., ANDERSON, B. P. & BOWER, J. M. (1992). Cholinergic modulation of cortical associative memory function. *J. Neurophysiol.*, **67**, 1230-1246.

131. HASSELMO, M. E. & BARKAI, E. (1995). Cholinergic modulation of activity-dependent synaptic plasticity in the piriform cortex and associative memory function in a network biophysical simulation. *J. Neurosci.*, **15**, 6592-6604.

132. HASSELMO, M. E. & BOWER, J. M. (1990). Afferent and association fiber differences in short-term potentiation in piriform (olfactory) cortex of the rat. *J. Neurophysiol.*, **64**, 179-190.

133. HASSELMO, M. E. & BOWER, J. M. (1991). Selective suppression of afferent but not intrinsic fiber synaptic transmission by 2-amino-4-phosphonobutyric acid (AP4) in piriform cortex. *Brain Res.*, **548**, 248-255.

134. HASSELMO, M. E. & BOWER, J. M. (1992). Cholinergic suppression specific to intrinsic not afferent fiber synapses in rat piriform (olfactory) cortex. *J. Neurophysiol.*, **67**, 1222-1229.

135. HASSELMO, M. E. & BOWER, J. M. (1993). Acetylcholine and memory. *Trends Neurosci.*, **16**, 218-222.

136. HASSELMO, M. E., FRANSEN, E., DICKSON, C. & ALONSO, A. A. (2000). Computational modeling of entorhinal cortex. *Ann. N. Y. Acad. Sci.*, **911**, 418-446.

137. HASSELMO, M. E., WILSON, M. A., ANDERSON, B. P. & BOWER, J. M. (1990). Associative memory function in piriform (olfactory) cortex: computational modeling and neuropharmacology. *Cold Spring Harb. Symp. Quant. Biol.*, **55**, 599-610.

138. HASUO, H. & GALLAGHER, J. P. (1990). Facilitatory action of muscarine on the slow afterdepolarization of rat dorsolateral septal nucleus neurons in vitro. *Neurosci. Lett.*, **112** , 234-238.

139. HENZI, V. & MACDERMOTT, A. B. (1992). Characteristics and function of Ca(2+)- and inositol 1,4,5- trisphosphate-releasable stores of Ca2+ in neurons. *Neuroscience,* **46**, 251-273.

140. HOFFMAN, S. N., SALIN, P. A. & PRINCE, D. A. (1994). Chronic neocortical epileptogenesis in vitro. *J. Neurophysiol.*, **71**, 1762-1773.

141. HOFFMAN, W. H. & HABERLY, L. B. (1989b). Bursting induces persistent all-or-none EPSPs by an NMDA-dependent process in piriform cortex. *J. Neurosci.*, **9**, 206-215.

142. HOFFMAN, W. H. & HABERLY, L. B. (1989a). Bursting induces persistent all-or-none EPSPs by an NMDA-dependent process in piriform cortex. *J. Neurosci.*, **9**, 206-215.

143. HOFFMAN, W. H. & HABERLY, L. B. (1991b). Bursting-induced epileptiform EPSPs in slices of piriform cortex are generated by deep cells. *J. Neurosci.*, **11**, 2021-2031.

144. HOFFMAN, W. H. & HABERLY, L. B. (1991a). Bursting-induced epileptiform EPSPs in slices of piriform cortex are generated by deep cells. *J. Neurosci.*, **11**, 2021-2031.

145. HOFFMAN, W. H. & HABERLY, L. B. (1993b). Role of synaptic excitation in the generation of bursting-induced epileptiform potentials in the endopiriform nucleus and piriform cortex. *J. Neurophysiol.*, **70**, 2550-2561.

146. HOFFMAN, W. H. & HABERLY, L. B. (1993a). Role of synaptic excitation in the generation of bursting-induced epileptiform potentials in the endopiriform nucleus and piriform cortex. *J. Neurophysiol.*, **70**, 2550-2561.

147. HOFFMAN, W. H. & HABERLY, L. B. (1996b). Kindling-induced epileptiform potentials in piriform cortex slices originate in the underlying endopiriform nucleus. *J. Neurophysiol.*, **76**, 1430-1438.

148. HOFFMAN, W. H. & HABERLY, L. B. (1996a). Kindling-induced epileptiform potentials in piriform cortex slices originate in the underlying endopiriform nucleus. *J. Neurophysiol.*, **76**, 1430-1438.

149. HOHMANN, C. F., PERT, C. C. & EBNER, F. F. (1985). Development of cholinergic markers in mouse forebrain. II. Muscarinic receptor binding in cortex. *Brain Res.*, **355**, 243-253.

150. HOLLIDAY, J. & SPITZER, N. C. (1990). Spontaneous calcium influx and its roles in differentiation of spinal neurons in culture. *Dev. Biol.*, **141**, 13-23.

151. HORI, N., AKAIKE, N. & CARPENTER, D. O. (1988). Piriform cortex brain slices: techniques for isolation of synaptic inputs. *J. Neurosci. Methods,* **25**, 197-208.

152. HULME, E. C., BIRDSALL, N. J. & BUCKLEY, N. J. (1990). Muscarinic receptor subtypes. *Annu. Rev. Pharmacol. Toxicol.*, **30**, 633-673.

153. ILLIG, K. R. & HABERLY, L. B. (2003). Odor-evoked activity is spatially distributed in piriform cortex. *J. Comp Neurol.*, **457**, 361-373.

154. JAHNSEN, H. & LLINAS, R. (1984). Ionic basis for the electro-responsiveness and oscillatory properties of guinea-pig thalamic neurones in vitro. *J. Physiol,* **349**, 227-247.

155. JAHROMI, B. S., ZHANG, L., CARLEN, P. L. & PENNEFATHER, P. (1999). Differential time-course of slow afterhyperpolarizations and associated Ca2+ transients in rat CA1 pyramidal neurons: further dissociation by Ca2+ buffer. *Neuroscience,* **88**, 719-726.

156. JOHNSON, D. M., ILLIG, K. R., BEHAN, M. & HABERLY, L. B. (2000). New features of connectivity in piriform cortex visualized by intracellular injection of pyramidal cells suggest that "primary" olfactory cortex functions like "association" cortex in other sensory systems. *J. Neurosci.,* **20**, 6974-6982.

157. JOHNSTON, M. V. (1996). Developmental aspects of epileptogenesis. *Epilepsia,* **37 Suppl 1**, S2-S9.

158. JUNG, H. Y., STAFF, N. P. & SPRUSTON, N. (2001). Action potential bursting in subicular pyramidal neurons is driven by a calcium tail current. *J. Neurosci.,* **21**, 3312-3321.

159. KALIMULLINA, L. B., BIKBAEV, A. F., KARPOVA, A. V., CHEPURNOVA, N. E., SAAKIAN, S. A. & CHEPURNOV, S. A. (2000). [The piriform cortex and the cortical nucleus of the amygdala in epileptogenesis--the role of the rostrocaudal gradient]. *Usp. Fiziol. Nauk,* **31**, 63-74.

160. KANTER, E. D. & HABERLY, L. B. (1993). Associative long-term potentiation in piriform cortex slices requires GABAA blockade. *J. Neurosci.,* **13**, 2477-2482.

161. KAPUR, A., LYTTON, W. W., KETCHUM, K. L. & HABERLY, L. B. (1997b). Regulation of the NMDA component of EPSPs by different components of postsynaptic GABAergic inhibition: computer simulation analysis in piriform cortex. *J. Neurophysiol.,* **78**, 2546-2559.

162. KAPUR, A., PEARCE, R. A., LYTTON, W. W. & HABERLY, L. B. (1997a). GABAA-mediated IPSCs in piriform cortex have fast and slow components with different properties and locations on pyramidal cells. *J. Neurophysiol.,* **78**, 2531-2545.

163. KATZ, A., WU, D. & SIMON, M. I. (1992). Subunits beta gamma of heterotrimeric G protein activate beta 2 isoform of phospholipase C. *Nature,* **360**, 686-689.

164. KELLAWAY, P., HRACHOVY, R. A., FROST, J. D., JR. & ZION, T. (1979). Precise characterization and quantification of infantile spasms. *Ann. Neurol.,* **6**, 214-218.

165. KELLY, M. E., STAINES, W. A. & MCINTYRE, D. C. (2002). Secondary generalization of hippocampal kindled seizures in rats: examining the role of the piriform cortex. *Brain Res.,* **957**, 152-161.

166. KETCHUM, K. L. & HABERLY, L. B. (1993b). Membrane currents evoked by afferent fiber stimulation in rat piriform cortex. II. Analysis with a system model. *J. Neurophysiol.*, **69**, 261-281.

167. KETCHUM, K. L. & HABERLY, L. B. (1993a). Synaptic events that generate fast oscillations in piriform cortex. *J. Neurosci.*, **13**, 3980-3985.

168. KIMURA, F. & BAUGHMAN, R. W. (1997). Distinct muscarinic receptor subtypes suppress excitatory and inhibitory synaptic responses in cortical neurons. *J. Neurophysiol.*, **77**, 709-716.

169. KIMURA, F., FUKUDA, M. & TSUMOTO, T. (1999). Acetylcholine suppresses the spread of excitation in the visual cortex revealed by optical recording: possible differential effect depending on the source of input. *Eur. J. Neurosci.*, **11**, 3597-3609.

170. KISS, J. & PATEL, A. J. (1992). Development of the cholinergic fibres innervating the cerebral cortex of the rat. *Int. J. Dev. Neurosci.*, **10**, 153-170.

171. KLEIN, P., PASSEL-CLARK, L. M. & PEZZULLO, J. C. (2003). Onset of epilepsy at the time of menarche. *Neurology*, **60**, 495-497.

172. KOBAYASHI, I., SHIBASAKI, H., TAKAHASHI, K., TOHYAMA, K., KURACHI, Y., ITO, H., UI, M. & KATADA, T. (1990). Purification and characterization of five different alpha subunits of guanine-nucleotide-binding proteins in bovine brain membranes. Their physiological properties concerning the activities of adenylate cyclase and atrial muscarinic K+ channels. *Eur. J. Biochem.*, **191**, 499-506.

173. KOHLING, R., GLADWELL, S. J., BRACCI, E., VREUGDENHIL, M. & JEFFERYS, J. G. (2001). Prolonged epileptiform bursting induced by 0-Mg(2+) in rat hippocampal slices depends on gap junctional coupling. *Neuroscience*, **105**, 579-587.

174. KOROGOD, S. M., KOPYSOVA, I. L., BRAS, H., GOGAN, P. & TYC-DUMONT, S. (1996). Differential back-invasion of a single complex dendrite of an abducens motoneuron by N-methyl-D-aspartate-induced oscillations: a simulation study. *Neuroscience*, **75**, 1153-1163.

175. KRNJEVIC, K. (1986). The future of neuroscience. *Clin. Invest Med.*, **9**, 296-300.

176. KRNJEVIC, K., PUMAIN, R. & RENAUD, L. (1971). The mechanism of excitation by acetylcholine in the cerebral cortex. *J. Physiol*, **215**, 247-268.

177. KUHAR, M. J., BIRDSALL, N. J., BURGEN, A. S. & HULME, E. C. (1980). Ontogeny of muscarinic receptors in rat brain. *Brain Res.*, **184**, 375-383.

178. LACEY, M. G., CALABRESI, P. & NORTH, R. A. (1990). Muscarine depolarizes rat substantia nigra zona compacta and ventral tegmental neurons in vitro through M1-like receptors. *J. Pharmacol. Exp. Ther.,* **253**, 395-400.

179. LAIDLAW, J., RICHENS, A. & OXLEY, J. (1988). In *Textbook Of Epilepsy.* Publisher: Churchill Livingstone, Edinburgh, U.K.

180. LANCASTER, B. & ADAMS, P. R. (1986). Calcium-dependent current generating the afterhyperpolarization of hippocampal neurons. *J. Neurophysiol.,* **55**, 1268-1282.

181. LARGE, T. H., LAMBERT, M. P., GREMILLION, M. A. & KLEIN, W. L. (1986). Parallel postnatal development of choline acetyltransferase activity and muscarinic acetylcholine receptors in the rat olfactory bulb. *J. Neurochem.,* **46**, 671-680.

182. LARGE, T. H., RAUH, J. J., DE MELLO, F. G. & KLEIN, W. L. (1985). Two molecular weight forms of muscarinic acetylcholine receptors in the avian central nervous system: switch in predominant form during differentiation of synapses. *Proc. Natl. Acad. Sci. U. S. A,* **82**, 8785-8789.

183. LEACH, M. J., MARDEN, C. M. & MILLER, A. A. (1986). Pharmacological studies on lamotrigine, a novel potential antiepileptic drug: II. Neurochemical studies on the mechanism of action. *Epilepsia,* **27**, 490-497.

184. LEE, S. H., MAGGE, S., SPENCER, D. D., SONTHEIMER, H. & CORNELL-BELL, A. H. (1995). Human epileptic astrocytes exhibit increased gap junction coupling. *Glia,* **15**, 195-202.

185. LEE, W., NICKLAUS, K. J., MANNING, D. R. & WOLFE, B. B. (1990). Ontogeny of cortical muscarinic receptor subtypes and muscarinic receptor-mediated responses in rat. *J. Pharmacol. Exp. Ther.,* **252**, 482-490.

186. LESTER, R., HERRON, C., COAN, E. & COLLINGRIDGE, D. (1988). In *Excitatory amino acids in health and disease.* pp. 64-67. Publisher: Wiley, Chichester.

187. LEVEY, A., WEINER, D. M., ELLIS, J., NOVOTNY, E., YU, S., DORJE, F., WESS, J. & BRANN, M. R. (1992). In *Molecular Biology of G-protein Coupled Receptors.* pp. 170-197. Publisher: Birkhauser, Boston, U.S.A.

188. LEVEY, A. I., KITT, C. A., SIMONDS, W. F., PRICE, D. L. & BRANN, M. R. (1991). Identification and localization of muscarinic acetylcholine receptor proteins in brain with subtype-specific antibodies. *J. Neurosci.,* **11**, 3218-3226.

189. LI, J., SHEN, H., NAUS, C. C., ZHANG, L. & CARLEN, P. L. (2001). Upregulation of gap junction connexin 32 with epileptiform activity in the isolated mouse hippocampus. *Neuroscience,* **105**, 589-598.

190. LIAN, J., BIKSON, M., SHUAI, J. & DURAND, D. M. (2001). Propagation of non-synaptic epileptiform activity across a lesion in rat hippocampal slices. *J. Physiol,* **537**, 191-199.

191. LIBRI, V., CONSTANTI, A., CALAMINICI, M. & NISTICO, G. (1994). A comparison of the muscarinic response and morphological properties of identified cells in the guinea-pig olfactory cortex in vitro. *Neuroscience,* **59**, 331-347.

192. LIBRI, V., CONSTANTI, A., POSTLETHWAITE, M. & BOWERY, N. G. (1998). Blockade of GABA(B) receptors facilitates muscarinic agonist-induced epileptiform activity in immature rat piriform cortex in vitro. *Naunyn Schmiedebergs Arch. Pharmacol.,* **358**, 168-174.

193. LIBRI, V., CONSTANTI, A., ZIBETTI, M. & NISTICO, S. (1996). Effects of felbamate on muscarinic and metabotropic-glutamate agonist- mediated responses and magnesium-free or 4-aminopyridine-induced epileptiform activity in guinea pig olfactory cortex neurons in vitro. *J. Pharmacol. Exp. Ther.,* **277**, 1759-1769.

194. LIBRI, V., CONSTANTI, A., ZIBETTI, M. & POSTLETHWAITE, M. (1997). Metabotropic glutamate receptor subtypes mediating slow inward tail current (IADP) induction and inhibition of synaptic transmission in olfactory cortical neurones. *Br. J. Pharmacol.,* **120**, 1083-1095.

195. LILJENSTROM, H. & HASSELMO, M. E. (1995). Cholinergic modulation of cortical oscillatory dynamics. *J. Neurophysiol.,* **74**, 288-297.

196. LIN, Y. & PHILLIS, J. W. (1991). Muscarinic agonist-mediated induction of long-term potentiation in rat cerebral cortex. *Brain Res.,* **551**, 342-345.

197. LINSTER, C., WYBLE, B. P. & HASSELMO, M. E. (1999). Electrical stimulation of the horizontal limb of the diagonal band of broca modulates population EPSPs in piriform cortex. *J. Neurophysiol.,* **81**, 2737-2742.

198. LITAUDON, P. & CATTARELLI, M. (1994). Multi-site optical recording of the rat piriform cortex activity. *Neuroreport,* **5**, 743-746.

199. LITAUDON, P. & CATTARELLI, M. (1995). Piriform cortex late activity revealed functional spatial heterogeneity. *Neuroreport,* **6**, 1377-1380.

200. LITAUDON, P., DATICHE, F. & CATTARELLI, M. (1997). Optical recording of the rat piriform cortex activity. *Prog. Neurobiol.,* **52**, 485-510.

201. LONDONG, W. (1986). Present status and future perspectives of muscarinic receptor antagonists. *Scand. J. Gastroenterol. Suppl,* **125:55-60.**, 55-60.

202. LOSCHER, W. & EBERT, U. (1996). The role of the piriform cortex in kindling. *Prog. Neurobiol.,* **50**, 427-481.

203. LOSCHER, W., EBERT, U., WAHNSCHAFFE, U. & RUNDFELDT, C. (1995). Susceptibility of different cell layers of the anterior and posterior part of the piriform cortex to electrical stimulation and kindling: comparison with the basolateral amygdala and "area tempestas". *Neuroscience,* **66**, 265-276.

204. LOSCHER, W., LEHMANN, H. & EBERT, U. (1998). Differences in the distribution of GABA- and GAD-immunoreactive neurons in the anterior and posterior piriform cortex of rats. *Brain Res.,* **800**, 21-31.

205. LUO Z.D., CALCUTT N.A., HIGUERA E.S., VALDER C.R., SONG Y.H., SVENSSON C.I. & MYRES R.R. (2003). Injury type-specific calcium channel alpha 2 delta-1 subunit up-regulation in rat neuropathic pain models correlates with antiallodynic effects of gabapentin. *J. Pharmacol. and Exp. Ther.* **303(3)**, 1199-1205.

206. LUSKIN, M. B. & PRICE, J. L. (1983). The laminar distribution of intracortical fibers originating in the olfactory cortex of the rat. *J. Comp Neurol.,* **216**, 292-302.

207. LUTHI, A. & MCCORMICK, D. A. (1998). H-current: properties of a neuronal and network pacemaker. *Neuron,* **21**, 9-12.

208. LUTHI, A. & MCCORMICK, D. A. (1999). Modulation of a pacemaker current through Ca(2+)-induced stimulation of cAMP production. *Nat. Neurosci.,* **2**, 634-641.

209. MACDONALD, R. L. & KELLY, K. M. (1993). Antiepileptic drug mechanisms of action. *Epilepsia,* **34 Suppl 5**, S1-S8.

210. MACDONALD, R. L. & KELLY, K. M. (1995). Antiepileptic drug mechanisms of action. *Epilepsia,* **36 Suppl 2**, S2-12.

211. MACRIDES, F. (1977). Dynamic aspects of central olfactory processing. In *Chemical Signals in Vertebrates.* Publisher: Wiley, New York.

212. MACRIDES, F., DAVIS, B. J., YOUNGS, W. M., NADI, N. S. & MARGOLIS, F. L. (1981). Cholinergic and catecholaminergic afferents to the olfactory bulb in the hamster: a neuroanatomical, biochemical, and histochemical investigation. *J. Comp Neurol.,* **203**, 495-514.

213. MAGGIO, R., LANAUD, P., GRAYSON, D. R. & GALE, K. (1993). Expression of c-fos mRNA following seizures evoked from an epileptogenic site in the

deep prepiriform cortex: regional distribution in brain as shown by in situ hybridization. *Exp. Neurol.*, **119**, 11-19.

214. MAIER, N., GULDENAGEL, M., SOHL, G., SIEGMUND, H., WILLECKE, K. & DRAGUHN, A. (2002). Reduction of high-frequency network oscillations (ripples) and pathological network discharges in hippocampal slices from connexin 36-deficient mice. *J. Physiol,* **541**, 521-528.

215. MALCANGIO, M., LIBRI, V., TEOH, H., CONSTANTI, A. & BOWERY, N. G. (1995). Chronic (-)baclofen or CGP 36742 alters GABAB receptor sensitivity in rat brain and spinal cord. *Neuroreport,* **6**, 399-403.

216. MALINOW, R., MADISON, D. V. & TSIEN, R. W. (1988). Persistent protein kinase activity underlying long-term potentiation. *Nature,* **335**, 820-824.

217. MARCHI, M. & RAITERI, M. (1989). Interaction acetylcholine-glutamate in rat hippocampus: involvement of two subtypes of M-2 muscarinic receptors. *J. Pharmacol. Exp. Ther.*, **248** , 1255-1260.

218. MARCHI, M. & RAITERI, M. (1996). Nicotinic autoreceptors mediating enhancement of acetylcholine release become operative in conditions of "impaired" cholinergic presynaptic function. *J. Neurochem.*, **67**, 1974-1981.

219. MARCHI, M., RUELLE, A., ANDRIOLI, G. C. & RAITERI, M. (1990). Pirenzepine-insensitive muscarinic autoreceptors regulate acetylcholine release in human neocortex. *Brain Res.*, **520**, 347-350.

220. MARGINEANU, D. G. & KLITGAARD, H. (2001). Can gap-junction blockade preferentially inhibit neuronal hypersynchrony vs. excitability? *Neuropharmacology,* **41**, 377-383.

221. MARK, G. P. & FINN, D. A. (2002). The relationship between hippocampal acetylcholine release and cholinergic convulsant sensitivity in withdrawal seizure-prone and withdrawal seizure-resistant selected mouse lines. *Alcohol Clin. Exp. Res.*, **26**, 1141-1152.

222. MAYER M.L. & WESTBROOK A (1983). A voltage clamp analysis of inward (anomalous) rectification in mouse spiny sensory ganglion neurones. *J. Physiol.* **340**, 19-45.

223. MCCARREN, M. & ALGER, B. E. (1985). Use-dependent depression of IPSPs in rat hippocampal pyramidal cells in vitro. *J. Neurophysiol.*, **53**, 557-571.

224. MCCORMICK, D. A. & PRINCE, D. A. (1985). Two types of muscarinic response to acetylcholine in mammalian cortical neurons. *Proc. Natl. Acad. Sci. U. S. A,* **82**, 6344-6348.

225. MCCORMICK, D. A. & PRINCE, D. A. (1986). Mechanisms of action of acetylcholine in the guinea-pig cerebral cortex in vitro. *J. Physiol,* **375**, 169-194.

226. MCINTYRE, D. C. & KELLY, M. E. (2000). The parahippocampal cortices and kindling. *Ann. N. Y. Acad. Sci.,* **911**, 343-354.

227. MELCHIORRE, C., ANGELI, P., LAMBRECHT, G., MUTSCHLER, E., PICCHIO, M. T. & WESS, J. (1987). Antimuscarinic action of methoctramine, a new cardioselective M-2 muscarinic receptor antagonist, alone and in combination with atropine and gallamine. *Eur. J. Pharmacol.,* **144**, 117-124.

228. MELDRUM, B., MILLAN, M., PATEL, S. & DE SARRO, G. (1988). Anti-epileptic effects of focal micro-injection of excitatory amino acid antagonists. *J. Neural Transm.,* **72**, 191-200.

229. MELDRUM, B. S., NAQUET, R. & BALZANO, E. (1970). Effects of atropine and eserine on the electroencephalogram, on behaviour and on light-induced epilepsy in the adolescent baboon (Papio papio). *Electroencephalogr. Clin. Neurophysiol.,* **28**, 449-458.

230. MICEVYCH, P. E. & ABELSON, L. (1991). Distribution of mRNAs coding for liver and heart gap junction proteins in the rat central nervous system. *J. Comp Neurol.,* **305**, 96-118.

231. MILBURN, C. M. & PRINCE, D. A. (1993). Postnatal development of cholinergic presynaptic inhibition in rat hippocampus. *Brain Res. Dev. Brain Res.,* **74**, 133-137.

232. MILLAN, M. H., PATEL, S., MELLO, L. M. & MELDRUM, B. S. (1986). Focal injection of 2-amino-7-phosphonoheptanoic acid into prepiriform cortex protects against pilocarpine-induced limbic seizures in rats. *Neurosci. Lett.,* **70**, 69-74.

233. MITCHELSON, F. (1988). Muscarinic receptor differentiation. *Pharmacol. Ther.,* **37**, 357-423.

234. MITTMANN, T., LINTON, S. M., SCHWINDT, P. & CRILL, W. (1997). Evidence for persistent Na+ current in apical dendrites of rat neocortical neurons from imaging of Na+-sensitive dye. *J. Neurophysiol.,* **78**, 1188-1192.

235. MOSH, S. & LUDVIG, N. (1988). In *Recent Advances in Epilepsy, Vol. 4.* pp. 64-72. Publisher: Churchill Livingstone, Edinburgh, U.K.

236. MOTOKIZAWA, F. & INO, Y. (1981). A search for olfactory receiving areas in the cerebral cortex of cats. *Neuroscience,* **6**, 39-46.

237. MOULY, A., FORT, A., BEN-BOUTAYAB, N. & GERVAIS, R. (2001). Olfactory learning induces differential long-lasting changes in rat central olfactory cortical pathways. *Neuroscience*, **102(1)**, 11-21.

238. NAGATA, K., HUANG, C. S., SONG, J. H. & NARAHASHI, T. (1997). Direct actions of anticholinesterases on the neuronal nicotinic acetylcholine receptor channels. *Brain Res.*, **769**, 211-218.

239. NAUS, C. C., BECHBERGER, J. F. & PAUL, D. L. (1991). Gap junction gene expression in human seizure disorder. *Exp. Neurol.*, **111**, 198-203.

240. NORTH, R. A. (1989a). In *Muscarinic cholinergic receptor regulation of ion channels*. pp. 341-347. Publisher: Humana Press, Clifton.

241. NORTH, R. A. (1989b). In *Muscarinic Receptor Subtypes*. pp. 341-373. Publisher: Humana Press, Clifton.

242. OLDS, R. (1979). In *A colour atlas of the rat : dissection guide*. pp. 87-88. Publisher: Wolfe Medical.

243. OROZCO-SUAREZ, S., BRUNSON, K. L., FERIA-VELASCO, A. & RIBAK, C. E. (2000). Increased expression of gamma-aminobutyric acid transporter-1 in the forebrain of infant rats with corticotropin-releasing hormone-induced seizures but not in those with hyperthermia-induced seizures. *Epilepsy Res.*, **42**, 141-157.

244. PAPATHEODOROPOULOS, C. & KOSTOPOULOS, G. (1996). Age-related changes in excitability and recurrent inhibition in the rat CA1 hippocampal region. *Eur. J. Neurosci.*, **8**, 510-520.

245. PARKER, E. M., KAMEYAMA, K., HIGASHIJIMA, T. & ROSS, E. M. (1991). Reconstitutively active G protein-coupled receptors purified from baculovirus-infected insect cells. *J. Biol. Chem.*, **266**, 519-527.

246. PATIL, M. M. & HASSELMO, M. E. (1999). Modulation of inhibitory synaptic potentials in the piriform cortex. *J. Neurophysiol.*, **81**, 2103-2118.

247. PATIL, M. M., LINSTER, C., LUBENOV, E. & HASSELMO, M. E. (1998). Cholinergic agonist carbachol enables associative long-term potentiation in piriform cortex slices. *J. Neurophysiol.*, **80**, 2467-2474.

248. PELLETIER, M. R. & CARLEN, P. L. (1996). Repeated tetanic stimulation in piriform cortex in vitro: epileptogenesis and pharmacology. *J. Neurophysiol.*, **76**, 4069-4079.

249. PINA-GARZA, J. & MCLEAN, M. (1996). Different effects of topiramate and phenytoin on mouse seizures and responses of cultyred neurones to excitatory amino acids. *Epilepsia*, **37 (Suppl. 5)**, S26-S26.

250. PIREDDA, S & GALE, K. (1985). A crucial epileptogenic site in the deep prepiriform cortex. *Nature*, **317**, 623-625.

251. PISANI, A., STEFANI, A., SINISCALCHI, A., MERCURI, N. B., BERNARDI, G. & CALABRESI, P. (1995). Electrophysiological actions of felbamate on rat striatal neurones. *Br. J. Pharmacol.*, **116**, 2053-2061.

252. PITLER, T. A. & ALGER, B. E. (1990). Activation of the pharmacologically defined M3 muscarinic receptor depolarizes hippocampal pyramidal cells. *Brain Res.*, **534**, 257-262.

253. POSTLETHWAITE, M., CONSTANTI, A. & LIBRI, V. (1998). Muscarinic agonist-induced burst firing in immature rat olfactory cortex neurons In vitro. *J. Neurophysiol.*, **79**, 2003-2012.

254. POSTLETHWAITE, M., CONSTANTI, A. & LIBRI, V. (2000). Investigation of the role of intracellular Ca(2+) stores in generation of the muscarinic agonist-induced slow afterdepolarization (sADP) in guinea-pig olfactory cortical neurones in vitro. *Br. J. Pharmacol.*, **129**, 1447-1457.

255. POTIER, S. & PSARROPOULOU, C. (2001). Endogenous acetylcholine facilitates epileptogenesis in immature rat neocortex. *Neurosci. Lett.*, **302**, 25-28.

256. PRICE, J. L. (1973). An autoradiographic study of complementary laminar patterns of termination of afferent fibers to the olfactory cortex. *J. Comp Neurol.*, **150**, 87-108.

257. PRICE, J. L. & SPRICH, W. W. (1975). Observations on the lateral olfactory tract of the rat. *J. Comp Neurol.*, **162**, 321-336.

258. PROTOPAPAS, A. D. & BOWER, J. M. (2000). Physiological characterization of layer III non-pyramidal neurons in piriform (olfactory) cortex of rat. *Brain Res.*, **865**, 1-11.

259. PUTNEY, J. W., JR., TAKEMURA, H., HUGHES, A. R., HORSTMAN, D. A. & THASTRUP, O. (1989). How do inositol phosphates regulate calcium signaling? *FASEB J.*, **3**, 1899-1905.

260. RACINE, R. J., MOORE, K. A. & EVANS, C. (1991). Kindling-induced potentiation in the piriform cortex. *Brain Res.*, **556**, 218-225.

261. RAITERI, M., LEARDI, R. & MARCHI, M. (1984). Heterogeneity of presynaptic muscarinic receptors regulating neurotransmitter release in the rat brain. *J. Pharmacol. Exp. Ther.*, **228**, 209-214.

262. RAITERI, M., MARCHI, M., PAUDICE, P. & PITTALUGA, A. (1990). Muscarinic receptors mediating inhibition of gamma-aminobutyric acid release in rat

corpus striatum and their pharmacological characterization. *J. Pharmacol. Exp. Ther.*, **254**, 496-501.

263. RAMSAY, R. E. (1993). Advances in the pharmacotherapy of epilepsy. *Epilepsia,* **34 Suppl 5**, S9-16.

264. RAMSAY, R. E. & SLATER, J. D. (1993). Antiepileptic drugs in clinical development. *Epilepsy Res. Suppl,* **10**, 45-67.

265. REITSTETTER, R., HE, D. S. & GRUENER, R. (1994). Oxotremorine-M activates single nicotinic acetylcholine receptor channels in cultured Xenopus myocytes. *Eur. J. Pharmacol.*, **264**, 27-32.

266. REYHER, C. K., LUBKE, J., LARSEN, W. J., HENDRIX, G. M., SHIPLEY, M. T. & BAUMGARTEN, H. G. (1991). Olfactory bulb granule cell aggregates: morphological evidence for interperikaryal electrotonic coupling via gap junctions. *J. Neurosci.,* **11**, 1485-1495.

267. RICHARDS, C. D. & SERCOMBE, R. (1968). Electrical activity observed in guinea-pig olfactory cortex maintained in vitro. *J. Physiol,* **197**, 667-683.

268. RODRIGUEZ, R. & HABERLY, L. B. (1989). Analysis of synaptic events in the opossum piriform cortex with improved current source-density techniques. *J. Neurophysiol.,* **61**, 702-718.

269. ROGAWSKI, M. & PORTER, R. (1990). Antiepileptic drugs: pharmacological mechanisms and clinical efficacy with consideration of promising developmental stage compounds. *Pharmacological Reviews*, **42**, 223-286.

270. RORIG, B., KLAUSA, G. & SUTOR, B. (1996). Intracellular acidification reduced gap junction coupling between immature rat neocortical pyramidal neurones. *J. Physiol,* **490 (Pt 1)**, 31-49.

271. ROSIN, J. F., DATICHE, F. & CATTARELLI, M. (1999). Modulation of the piriform cortex activity by the basal forebrain: an optical recording study in the rat. *Brain Res.,* **820**, 105-111.

272. ROSS, F. M., GWYN, P., SPANSWICK, D. & DAVIES, S. N. (2000). Carbenoxolone depresses spontaneous epileptiform activity in the CA1 region of rat hippocampal slices. *Neuroscience,* **100**, 789-796.

273. ROTTER, A., FIELD, P. M. & RAISMAN, G. (1979). Muscarinic receptofs in the central nervous system of the rat. III. Postnatal development of binding of [3H]propylbenzilylcholine mustard. *Brain Res.,* **180**, 185-205.

274. RUSSO, E. & CONSTANTI, A. (2002). Topiramate enhances and prolongs the slow post-stimulus afterhyperpolarization (sAHP) in rat olfactory cortical neurones in vitro. *Br. J. Pharmacol.*, **81P**, 135-135.

275. SAAR, D., GROSSMAN, Y. & BARKAI, E. (1999). Reduced synaptic facilitation between pyramidal neurons in the piriform cortex after odor learning. *J. Neurosci.*, **19**, 8616-8622.

276. SAAR, D., GROSSMAN, Y. & BARKAI, E. (2001). Long-lasting cholinergic modulation underlies rule learning in rats. *J. Neurosci.*, **21**, 1385-1392.

277. SAPER, C. B. (1985). Organization of cerebral cortical afferent systems in the rat. II. Hypothalamocortical projections. *J. Comp Neurol.*, **237**, 21-46.

278. SATOU, M., MORI, K., TAZAWA, Y. & TAKAGI, S. F. (1982). Two types of postsynaptic inhibition in pyriform cortex of the rabbit: fast and slow inhibitory postsynaptic potentials. *J. Neurophysiol.*, **48**, 1142-1156.

279. SATOU, M., MORI, K., TAZAWA, Y. & TAKAGI, S. F. (1983a). Interneurons mediating fast postsynaptic inhibition in pyriform cortex of the rabbit. *J. Neurophysiol.*, **50**, 89-101.

280. SATOU, M., MORI, K., TAZAWA, Y. & TAKAGI, S. F. (1983b). Neuronal pathways for activation of inhibitory interneurons in pyriform cortex of the rabbit. *J. Neurophysiol.*, **50**, 74-88.

281. SCANZIANI, M., GAHWILER, B. H. & THOMPSON, S. M. (1995). Presynaptic inhibition of excitatory synaptic transmission by muscarinic and metabotropic glutamate receptor activation in the hippocampus: are Ca2+ channels involved? *Neuropharmacology*, **34**, 1549-1557.

282. SCHACTER, S. (1995). Review of the mechanisms of action of antiepileptic drugs. *Pharmacol. & Ther.*, **4(6)**, 469-477.

283. SCHOLFIELD, C. N. (1978a). A barbiturate induced intensification of the inhibitory potential in slices of guinea-pig olfactory cortex. *J. Physiol*, **275**, 559-566.

284. SCHOLFIELD, C. N. (1978b). A depolarizing inhibitory potential in neurones of the olfactory cortex in vitro. *J. Physiol*, **275**, 547-557.

285. SCHOLFIELD, C. N. (1978c). Electrical properties of neurones in the olfactory cortex slice in vitro. *J. Physiol*, **275**, 535-546.

286. SCHOLFIELD, C. N. (1980). Potentiation of inhibition by general anaesthetics in neurones of the olfactory cortex in vitro. *Pflugers Arch.*, **383**, 249-255.

287. SCHOLZ, K. P. & MILLER, R. J. (1992). Inhibition of quantal transmitter release in the absence of calcium influx by a G protein-linked adenosine receptor at hippocampal synapses. *Neuron,* **8**, 1139-1150.

288. SCHWEITZER, J. S., WANG, H., XIONG, Z. Q. & STRINGER, J. L. (2000). pH Sensitivity of non-synaptic field bursts in the dentate gyrus. *J. Neurophysiol.,* **84**, 927-933.

289. SCHWINDT, P. & CRILL, W. (1999). Mechanisms underlying burst and regular spiking evoked by dendritic depolarization in layer 5 cortical pyramidal neurons. *J. Neurophysiol.,* **81** , 1341-1354.

290. SCHWINDT, P. C., SPAIN, W. J., FOEHRING, R. C., CHUBB, M. C. & CRILL, W. E. (1988). Slow conductances in neurons from cat sensorimotor cortex in vitro and their role in slow excitability changes. *J. Neurophysiol.,* **59**, 450-467.

291. SCIANCALEPORE, M. & CONSTANTI, A. (1998). Inward-rectifying membrane currents activated by hyperpolarization in immature rat olfactory cortex neurones in vitro. *Brain Res.,* **814**, 133-142.

292. SHANK, R., GARDOCKI, J., STREETER, A. & MARYANOFF, B. (2000). An overview of the preclinical aspects of topiramate: pharmacology, pharmacokinetics and mechanism of action. *Epilepsia*, **41 (Suppl. 1)**, S3-S9.

293. SHANK, R. P., GARDOCKI, J. F., VAUGHT, J. L., DAVIS, C. B., SCHUPSKY, J. J., RAFFA, R. B., DODGSON, S. J., NORTEY, S. O. & MARYANOFF, B. E. (1994). Topiramate: preclinical evaluation of structurally novel anticonvulsant. *Epilepsia,* **35**, 450-460.

294. SHEPHERD, G. M. & HABERLY, L. B. (1970). Partial activation of olfactory bulb: analysis of field potentials and topographical relation between bulb and lateral olfactory tract. *J. Neurophysiol.,* **33**, 643-653.

295. SOREQ, H., GURWITZ, D., ELIYAHU, D. & SOKOLOVSKY, M. (1982). Altered ontogenesis of muscarinic receptors in agranular cerebellar cortex. *J. Neurochem.,* **39**, 756-763.

296. SPERBER, E. F., VELISKOVA, J., BENENATI, B. & MOSHE, S. L. (1998). Enhanced epileptogenicity of area tempestas in the immature rat. *Dev. Neurosci.,* **20**, 540-545.

297. STANFORD, I. M., WHEAL, H. V. & CHAD, J. E. (1995). Bicuculline enhances the late $GABA_B$ receptor-mediated paired-pulse inhibition observed in rat hippocampal slices. *Eur. J. Pharmacol.,* **277**, 229-234.

298. STARKE, K., GOTHERT, M. & KILBINGER, H. (1989). Modulation of neurotransmitter release by presynaptic autoreceptors. *Physiol Rev.*, **69**, 864-989.

299. STUART, G. J. & REDMAN, S. J. (1991). Mechanisms of presynaptic inhibition studied using paired-pulse facilitation. *Neurosci. Lett.*, **126**, 179-183.

300. SUSSKAND, K. & SEWING, K. F. (1979). Anticholinergic effects of pirenzepine on the guinea-pig isolated atrium. *Pharmacology*, **19**, 163-164.

301. TAMAS, G., BUHL, E. H. & SOMOGYI, P. (1997). Fast IPSPs elicited via multiple synaptic release sites by different types of GABAergic neurone in the cat visual cortex. *J. Physiol*, **500 (Pt 3)**, 715-738.

302. TAN, X. X. & COSTA, L. G. (1995). Postnatal development of muscarinic receptor-stimulated phosphoinositide metabolism in mouse cerebral cortex: sensitivity to ethanol. *Brain Res. Dev. Brain Res.*, **86**, 348-353.

303. TANG, A. C. & HASSELMO, M. E. (1994). Selective suppression of intrinsic but not afferent fiber synaptic transmission by baclofen in the piriform (olfactory) cortex. *Brain Res.*, **659**, 75-81.

304. TERRY, B. (1922). Journal of Laboratory and Clinical Medicine TEUBNER B., DEGEN J., SOHL G., GULDENAGEL M., BUKAUSKAS F.F., TREXLER E.B., VERSELIS V.K., DE ZEEUW C.I., LEE C.G., KOZAK C.A., PETRASCH-PARWEZ E., DERMIETZEL R., WILLECKE K. (2000). Functional expression of the murine connexin 36 gene coding for a neuron-specific gap junctional protein. *J Membr Biol.* **176(3)**, 249-62.

305. THOMSON, A. M., WEST, D. C., HAHN, J. & DEUCHARS, J. (1996). Single axon IPSPs elicited in pyramidal cells by three classes of interneurones in slices of rat neocortex. *J. Physiol*, **496 (Pt 1)**, 81-102.

306. TICE, M. A., HASHEMI, T., TAYLOR, L. A. & MCQUADE, R. D. (1996). Distribution of muscarinic receptor subtypes in rat brain from postnatal to old age. *Brain Res. Dev. Brain Res.*, **92**, 70-76.

307. TRAUB, R. D., BORCK, C., COLLING, S. B. & JEFFERYS, J. G. (1996). On the structure of ictal events in vitro. *Epilepsia*, **37**, 879-891.

308. TRAUB, R. D., DRAGUHN, A., WHITTINGTON, M. A., BALDEWEG, T., BIBBIG, A., BUHL, E. H. & SCHMITZ, D. (2002). Axonal gap junctions between principal neurons: a novel source of network oscillations, and perhaps epileptogenesis. *Rev. Neurosci.*, **13**, 1-30.

309. TRAUB, R. D., KNOWLES, W. D., MILES, R. & WONG, R. K. (1987). Models of the cellular mechanism underlying propagation of epileptiform activity in the CA2-CA3 region of the hippocampal slice. *Neuroscience,* **21**, 457-470.

310. TRAUB, R. D., MILES, R. & JEFFERYS, J. G. (1993). Synaptic and intrinsic conductances shape picrotoxin-induced synchronized after-discharges in the guinea-pig hippocampal slice. *J. Physiol,* **461**, 525-547.

311. TSENG, G. F. & HABERLY, L. B. (1988). Characterization of synaptically mediated fast and slow inhibitory processes in piriform cortex in an in vitro slice preparation. *J. Neurophysiol.,* **59**, 1352-1376.

312. TSENG, G. F. & HABERLY, L. B. (1989a). Deep neurons in piriform cortex. I. Morphology and synaptically evoked responses including a unique high-amplitude paired shock facilitation. *J. Neurophysiol.,* **62**, 369-385.

313. TSENG, G. F. & HABERLY, L. B. (1989b). Deep neurons in piriform cortex. II. Membrane properties that underlie unusual synaptic responses. *J. Neurophysiol.,* **62**, 386-400.

314. TURSKI, L., IKONOMIDOU, C., TURSKI, W. A., BORTOLOTTO, Z. A. & CAVALHEIRO, E. A. (1989). Review: cholinergic mechanisms and epileptogenesis. The seizures induced by pilocarpine: a novel experimental model of intractable epilepsy. *Synapse,* **3**, 154-171.

315. UCHIMURA, N. & NORTH, R. A. (1990). Muscarine reduces inwardly rectifying potassium conductance in rat nucleus accumbens neurones. *J. Physiol,* **422**, 369-380.

316. UPTON, N. (1994). Mechanims of action of new antiepileptic drugs: rational design and serendipitous findings. *Trends in Pharmacological Sciences*, **15**, 456-463.

317. UUSISAARI, M., SMIRNOV, S., VOIPIO, J. & KAILA, K. (2002). Spontaneous epileptiform activity mediated by GABA(A) receptors and gap junctions in the rat hippocampal slice following long-term exposure to GABA(B) antagonists. *Neuropharmacology,* **43**, 563-572.

318. VALVERDE, F. & SANTACANA, M. (1994). Developmental and early postnatal maturation of the primary olfactory cortex. *Developmental Brain Research*, **80**, 96-114.

319. VAN HOOFT, J. A., DOUGHERTY, J. J., ENDEMAN, D., NICHOLS, R. A. & WADMAN, W. J. (2002). Gabapentin inhibits presynaptic Ca(2+) influx and

synaptic transmission in rat hippocampus and neocortex. *Eur. J. Pharmacol.,* **449**, 221-228.

320. VELISEK, L., VELISKOVA, J. & MOSHE, S. L. (1995). Developmental seizure models. *Ital. J. Neurol. Sci.,* **16**, 127-133.

321. VILARO, M. T., PALACIOS, J. M. & MENGOD, G. (1990b). Localization of m5 muscarinic receptor mRNA in rat brain examined by in situ hybridization histochemistry. *Neurosci. Lett.,* **114**, 154-159.

322. VILARO, M. T., PALACIOS, J. M. & MENGOD, G. (1990a). Localization of m5 muscarinic receptor mRNA in rat brain examined by in situ hybridization histochemistry. *Neurosci. Lett.,* **114**, 154-159.

323. VU, E. T. & KRASNE, F. B. (1992). Evidence for a computational distinction between proximal and distal neuronal inhibition. *Science,* **255**, 1710-1712.

324. WAELBROECK, M., TASTENOY, M., CAMUS, J. & CHRISTOPHE, J. (1990). Binding of selective antagonists to four muscarinic receptors (M1 to M4) in rat forebrain. *Mol. Pharmacol.,* **38** , 267-273.

325. WANG, S. J., HUANG, C. C., HSU, K. S., TSAI, J. J. & GEAN, P. W. (1996). Presynaptic inhibition of excitatory neurotransmission by lamotrigine in the rat amygdalar neurons. *Synapse,* **24**, 248-255.

326. WASHBURN, M. S. & MOISES, H. C. (1992). Muscarinic responses of rat basolateral amygdaloid neurons recorded in vitro. *J. Physiol,* **449**, 121-154.

327. WEINSTOCK, M. (1997). Possible role of the cholinergic system and disease models. *J. Neural Transm. Suppl,* **49**, 93-102.

328. WENK, H., MEYER, U. & BIGL, V. (1977). Centrifugal cholinergic connections in the olfactory system of rats. *Neuroscience,* **2**, 797-800.

329. WHALLEY, B. & CONSTANTI, A. (2003) Developmental change in inhibitory presynaptic muscarinic receptor subtypes in rat olfactory cortex. *Br. J. Pharmacol.,* **135**, 355P.

330. WHITE, H. S. (1999). Comparative anticonvulsant and mechanistic profile of the established and newer antiepileptic drugs. *Epilepsia,* **40 Suppl 5**, S2-10.

331. WILLIAMS, S. H. & CONSTANTI, A. (1988). Quantitative effects of some muscarinic agonists on evoked surface- negative field potentials recorded from the guinea-pig olfactory cortex slice. *Br. J. Pharmacol.,* **93**, 846-854.

332. WILSON, M. & BOWER, J. M. (1989). In *The Simulation of Large-Scale Neural Networks.* pp. 171-194. Publisher: MIT Press.

333. WOMBLE, M. D. & MOISES, H. C. (1992). Muscarinic inhibition of M-current and a potassium leak conductance in neurones of the rat basolateral amygdala. *J. Physiol,* **457**, 93-114.

334. YAMAMOTO, C. & MCILWAIN, H. (1966). Electrical activities in thin sections from the mammalian brain maintained in chemically-defined media in vitro. *J. Neurochem.,* **13**, 1333-1343.

335. YAMAUCHI, T., KUDO, T. & KATAOKA, N. (1989). Studies on mechanisms of initiation and propagation of seizure activity following penicillin application. *Jpn. J. Psychiatry Neurol.,* **43**, 445-449.

336. ZHOU F-M & HABLITZ J.J. (1996). Postnatal development of membrane properties of layer I neurons in rat neocortex. *J. Neurosci.,* **16**, 1131-1139.

337. ZIMMER, L. A., ENNIS, M. & SHIPLEY, M. T. (1999). Diagonal band stimulation increases piriform cortex neuronal excitability in vivo. *Neuroreport,* **10**, 2101-2105.

338. ZINYUK, L. E., DATICHE, F. & CATTARELLI, M. (2001). Cell activity in the anterior piriform cortex during an olfactory learning in the rat. *Behav. Brain Res.,* **124**, 29-32.

339. ZUCKER, R. S. & REGEHR, W. G. (2002). Short-term synaptic plasticity. *Ann. Rev. Physiol,* **64**, 355-405.